Queen Mary
University of London

Characterisation of a novel therapeutic peptide derived from Syndecan-2

William Harvey Research Institute, Centre for Microvascular Research

Student name: **Michaela Balderstone**
Student number: 150183606
Supervisors: **Dr James Whiteford** (primary)
Dr Tom Nightingale (secondary)

Statement of Originality

I, Michaela Joan Margaret Balderstone, confirm that the research included within this thesis is my own work or that where it has been carried out in collaboration with, or supported by others, that this is duly acknowledged below and my contribution indicated. Previously published material is also acknowledged below.

I attest that I have exercised reasonable care to ensure that the work is original, and does not to the best of my knowledge break any UK law, infringe any third party's copyright or other Intellectual Property Right, or contain any confidential material.

I accept that the College has the right to use plagiarism detection software to check the electronic version of the thesis.

I confirm that this thesis has not been previously submitted for the award of a degree by this or any other university.

The copyright of this thesis rests with the author and no quotation from it or information derived from it may be published without the prior written consent of the author.

Signature:

Date: 20th January 2023

Details of collaboration and publications:

Aspects of this thesis have been previously presented at:

British Society for Matrix Biology Autumn Meeting (poster), Norwich, September 2019

British Society for Matrix Biology Spring Meeting (online; poster), April 2021

William Harvey PhD Symposium (online; oral presentation), January 2021

Acknowledgements

Firstly, I am grateful to everyone in the Centre for Microvascular Research, both past and present members. However, a special mention goes to a few members in particular: my secondary supervisor, Tom Nightingale, for both his academic input and his sense of humour. Also to Laura Deelen, my desk buddy; Tom Mitchell, my fellow Midlandser; and Faheem Shaik for coaching me through the thesis process. Finally, to my primary supervisor, mentor and friend, James Whiteford, who believed in me and my abilities from the beginning, even on days that I didn't believe in myself.

I am massively thankful for my family and friends for their endless love, support and encouragement. I am especially grateful to the best people in my life: my mum, my dad, Xen and Leon. Also to my oldest friend (regarding the length of the friendship, not her age), Katie, for cheering me on from afar, always. Finally to Becky for her unwavering support, particularly since moving in together.

Without further ado, time for the ol' razzle dazzle…

Abstract

Angiogenesis, the formation of new blood vessels from pre-existing vasculature, is a feature of a number of pathologies, including neovascular eye diseases such as diabetic retinopathy. A key pro-angiogenic signalling pathway is the vascular endothelial growth factor (VEGF) system and current therapeutic options for the treatment of pathological angiogenesis target VEGF, blocking its binding and subsequent activation of VEGF receptors to prevent downstream pro-angiogenic signalling. These therapies have significant drawbacks and so in this thesis, we propose an alternative treatment option, in the form of a therapeutic peptide derived from human syndecan-2 (SDC2).

Previous work by our group has provided evidence of an inhibitory role for SDC2 in angiogenesis, a signalling pathway in which the protein tyrosine phosphatase receptor (PTPR), CD148, has been implicated as a binding target of SDC2. Angiogenesis is inhibited upon SDC2 interaction with CD148. Building on this, I have produced a body of work that characterises our therapeutic peptide, regarding its stability and detectability, through novel *in vitro* stability assays. Furthermore, I have accumulated preliminary evidence for its inhibition of angiogenesis and, for the first time, provided insight into its mode of action. This was completed primarily through optimisation of solid phase binding assays, with miniaturisation of binding proteins to determine the specific site responsible for the interaction.

In addition, we have explored the anti-angiogenic activity of CD148 short form (CD148SF), an endogenous protein translated from a CD148 splice variant. The data in this thesis provides evidence that CD148SF inhibits angiogenesis, demonstrated across a variety of *in vitro* and *ex vivo* angiogenesis models. As well as using established angiogenesis assays, I developed a novel angiogenesis model and used it to show CD148SF inhibitory effects.

Together, the work contained in this thesis provides novel understanding into the activity of our therapeutic peptide, specifically regarding its binding and stability, and delivers preliminary insight into the role of CD148SF.

Contents

List of tables

List of figures

Abbreviations

Akt	Protein kinase B
AMD	Age-related macular degeneration
Ang	Angiopoietin
BCA	Bicinchoninic acid
BCR	Breakpoint cluster region
BSA	Bovine serum albumin
Cdc42	Cell division cycle 42
CD148CT	CD148 C-terminus
CD148SF	CD148 short form
CD148NT	CD148 N-terminus
DEP1	Density-enhanced phosphatase 1
dH_2O	Deionised water
Dll4	Delta-like-4
EC	Endothelial cell
EGF	Epidermal growth factor
ELISA	Enzyme-linked immunosorbent assay
Fab	Fragment antigen-binding
FAS pathway	Fatty acid synthase pathway
FBS	Fetal bovine serum
FGFR	Fibroblast growth factor receptor
FGF2	Fibroblast growth factor 2
FNIII	Fibronectin type III
GAG	Glycosaminoglycan
GLUT2	Glucose transporter 2
HEKs	Human embryonic kidney
HIF1	Hypoxia inducible factor 1
HS	Heparan sulphate

HSPG	Heparan sulphate proteoglycan
IGF1R	Insulin like growth factor receptor 1
ILK	Integrin-linked kinase
KD	Knockdown
KO	Knockout
MAPK	Mitogen-activated protein kinase
MMP	Matrix metalloproteinase
MODY	Maturity-onset diabetes of the young
NOS	Nitric oxide synthase
PBS	Phosphate-buffered saline
PCR	Polymerase chain reaction
PDGF	Platelet-derived growth factor
PDGFR	Platelet-derived growth factor receptor
PFA	Paraformaldehyde
PlGF	Placental growth factor
PI3K	Phosphoinositide 3-kinase
PKC	Protein kinase C
PLC-γ1	Phospholipase C-γ1
PMA	Phorbol 12-myristate 13-acetate
PRP	Panretinal photocoagulation
P/S	Penicillin/ Streptomycin
PTK	Protein tyrosine kinase
PTP	Protein tyrosine phosphatase
ROS	Reactive oxygen species
sENDs	Skin endothelial cells
WHO	World Health Organisation

Chapter 1

1. Introduction

1.1. The eye

The human eye is a specialised sense organ that receives visual images and relays them to the brain. It is an assemblage of a number of tissues consisting of a variety of cell types (Fig. 1.1). The cornea is the clear window at the front of the eye and is the main refractive surface for light waves entering the eye [1]. The anterior chamber, located between the cornea and iris, contains the aqueous humour: a transparent fluid, not unlike plasma, but containing low protein concentrations [2]. The iris itself is a muscle [1], which is heavily pigmented due to a high melanin content, which varies amongst individuals; the more melanin present the darker the individual's eye colour [2]. The iris surrounds the pupil, an opening through which light travels, and controls the size of it to adjust the amount of light entering the eye [3]. As light travels through the eye, it is focused by the lens onto the retina [1]. The lens is a multi-layered transparent body consisting of proteins and water [2], whose shape is dictated by the ciliary body, a circular muscle that contracts or relaxes to adjust the shape of the lens in order to accurately focus the light [3].

The vitreous humour is a clear gelatinous body, which fills the space between the lens and retina, in order to maintain the shape of the eye [3]. The eye receives its blood supply from two main sources: the ophthalmic artery and, branching off this, the central retinal artery [4]. Corresponding veins are also present.

Located at the back of the eye is the retina, a light-sensitive tissue that contains two types of photoreceptors: rods, which are more abundant and are active at low light levels, and cones, which are responsible for colour vision

[1, 2]. Photoreceptors carry out photo-transduction, whereby light is absorbed and converted into electrochemical signals to be transported along the optic nerve to the brain. At the centre of the retina is the macula, responsible for central vision [1, 3]. Behind this is the choroid, a vascular layer that provides oxygen and other nutrients to outer retina layers. The sclera is the final layer at the back of the eye [3] and is commonly called the "white of the eye". It functions as a connective tissue coat for the eye [2].

The conjunctiva, seen in Fig. 1.1 at the front of the eye, forms a transparent mucous membrane and has a rich vascular supply [4]. Finally, the optic nerve is comprised of axons from ganglion cells as they exit the eye [4]. At the back of the eye, the optic disc represents the location where the optic nerve is bundled and leaves the retina [3]. There are no photoreceptors here, hence there is a "blind spot" or scotoma [1].

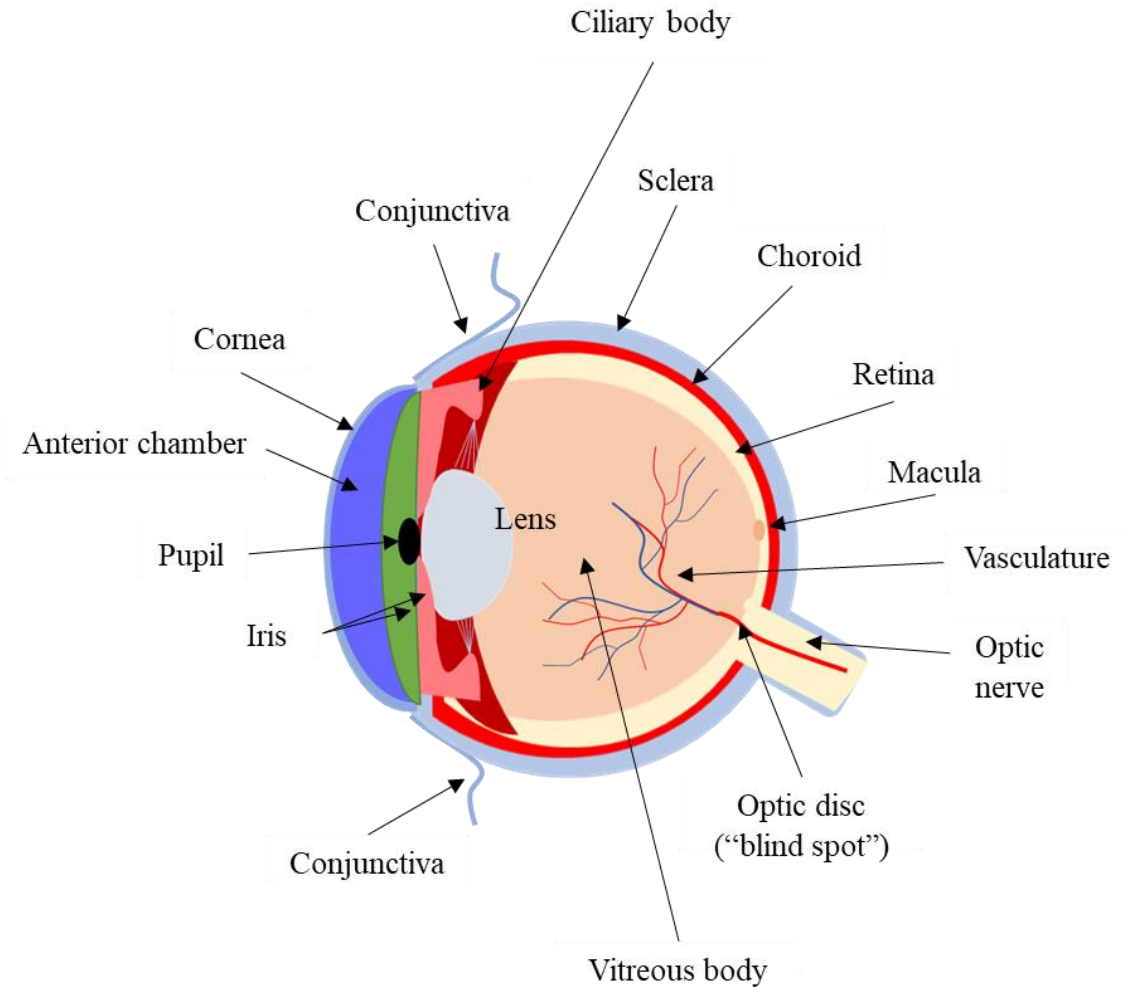

Figure 1.1. **Anatomy of the eye.** Adapted from: *Willoughby, C.E., et al. 2010*.

1.1.1. Common eye diseases

Due to the complexity of the eye, a variety of diseases can develop which affect different parts of the eye. Less severe afflictions include allergies (most commonly caused by pollen) which cause inflammation in the cornea and conjunctiva, resulting in watery, itchy eyes [5]. In addition, refractive errors in the lens can lead to hyperopia and myopia, colloquially referred to as “long-” and “short-sightedness”, respectively [6]. The causes of refractive errors are poorly understood, although hyperopia seems to have a genetic link and could be caused by the lenses becoming stiffer with age, as it generally presents in older individuals [7]. Myopia onset is also linked with genetic factors, although it also appears to be more common in children who spend long periods of time focusing on near objects, activities such as reading or looking at a computer screen [7]. Prescriptive corrective eyeglasses or contact lenses manage refractive errors, and corrective surgery may be an option for some patients.

Also affecting the lens are cataracts, the most common cause of blindness worldwide. These are protein ‘clumps’ that appear as cloudy areas on the normally clear lens and interfere with patients’ vision [6], caused by age- or injury-related breakdown of proteins and fibres in the lens of the eye [8]. Risk factors for cataracts include ageing, family history, diabetes and smoking, among others [8]. The only established treatment for severe cataracts is surgery to replace the cloudy lens [9].

Glaucoma refers to a group of diseases whose onset is brought about by an increase in fluid pressure, causing damage to the optic nerve and ultimately resulting in blindness [10]. There are two major categories of glaucoma: “open angle”, which is chronic and develops slowly over time, presenting with late-stage symptoms, and “closed angle”, referring to glaucoma where painful symptoms appear suddenly and visual loss can happen rapidly (without treatment) [6]. Risk factors include ageing, family

history and having pre-existing medical conditions, including diabetes and hyperopia or myopia [11].

1.1.2. Neovascular eye disease

As mentioned previously, the two major groups of blood vessels supplying the eye are the ophthalmic and central retinal vessels. The central retinal artery branches off the ophthalmic artery, as do the posterior and anterior ciliary arteries. The central retinal vein and ophthalmic (vortex) vein provide drainage for the eye. In the case of neovascular eye diseases, the central retinal vasculature is damaged and the subsequent neovascular repair mechanisms that are employed by the body affect the central retinal vasculature [12].

Neovascularisation, the formation of new blood vessels, is a physiological phenomenon that is crucial in processes such as embryonic development, wound healing and at stages in the female reproductive cycle. However, in certain diseases neovascularisation perpetuates symptoms – for example, dysregulated growth of new blood vessels within the eye contributes to visual loss in a number of ocular diseases [13]. There are various types of neovascularisation, with the most common being angiogenesis (the formation of new blood vessels from pre-existing vasculature): this is often observed in diseases where neovascularisation is a feature. Vasculogenesis, in contrast, is the origin of *de novo* (new) vasculature.

The most common neovascular eye diseases are proliferative diabetic retinopathy, wet age-related macular degeneration and retinopathy of prematurity.

1.1.3. Diabetic retinopathy

Diabetic retinopathy is the most common microvascular complication of diabetes mellitus. According to the World Health Organisation (WHO), it is thought that 422 million individuals globally have diabetes mellitus (also referred to as solely "diabetes") [14, 15]. There are a number of types of diabetes, with the most commonly recognised forms being Type 1, Type 2, and gestational diabetes, which occurs in pregnant women [16, 17]. Of these, the most prevalent is Type 2 diabetes; an estimated 90% of all diabetes cases are diagnosed with Type 2 diabetes, while the remaining 10% are Type 1 [14, 16, 18].

1.1.3.1. Type 1 diabetes mellitus

Type 1 diabetes is a chronic autoimmune condition, whereby the ability of the pancreas to produce insulin is impaired. The Islets of Langerhans are clusters of cells within the pancreas. The two main cell types within the Islets are α- and β-cells, responsible for producing hormones to maintain glucose homeostasis [19-21]. In order to sense the level of glucose present in the vasculature, the Islets of Langerhans form dense clusters supplied by fenestrated capillaries, enhancing permeability and blood supply to allow rapid exchange of glucose molecules and quick response to changing states [19, 22]. β-cells express several glucose transporter molecules, which act as glucose sensors. Glucose transporter 2 (GLUT2) facilitates diffusion of glucose into β-cells until equilibrium is reached, whereupon glucokinase phosphorylates glucose molecules as the first stage of glucose metabolism [23]. Later stages of glucose metabolism are coupled to adenosine triphosphate (ATP)-sensitive potassium channel-dependent insulin secretion. As glucose metabolism continues, intracellular ATP increases until these potassium channels close, depolarising the plasma membrane and causing voltage-dependent calcium channels to open. This initiates a calcium

influx, which activates the exocytosis of insulin granules and the secretion of insulin into the vasculature [22, 24, 25]. β-cells produce and secrete insulin in response to elevated blood glucose levels by promoting glycogenesis in adipose, hepatic and muscle tissues, converting glucose to glycogen for storage [23]. In those with Type 1 diabetes, however, these cells have a reduced ability to make insulin and ultimately stop manufacturing it altogether. This leads to chronically elevated blood glucose levels [21]. The other major cell type within the Islets of Langerhans, α-cells, secrete the hormone glucagon, to elevate the blood glucose levels in response to low levels. Transmembrane ATP-dependent potassium channels found on the α-cells generate action potentials of sodium and calcium at low glucose levels, triggering the exocytosis of glucagon granules and therefore the secretion of glucagon [26]. In cases of high blood glucose levels, these channels are blocked, preventing action potentials from activating glucagon secretion [26, 27].

Type 1 diabetes is a multifactorial disease and numerous genetic mutations are associated with the destruction of β-cells [22]. There is strong evidence to suggest that, in the majority of cases, disease onset is initiated by viral infection [28-30]. Immune cells recognise autoantigens on β-cell surfaces, including macrophages, dendritic cells, and B and T lymphocytes, all of which have been found to be involved in the pathogenesis of Type 1 diabetes mellitus [31-33]. It is usually an inherited condition: if an individual has a close relative with the condition, they have approximately a 6% chance of developing it themselves. Type 1 diabetes was historically called "Juvenile-onset diabetes" due to its high incidence in children; diabetes diagnoses in adulthood were thought not to be Type 1 diabetes mellitus. This has been revised in latter years following the discovery that not all childhood diagnoses of "diabetes" meant Type 1 and vice versa [18]. There is increasing research and evidence into the role of the gut microbiome in Type

1 diabetes onset, due to the link between biome and immunity becoming ever clearer [34, 35]. Ongoing research suggests that dysbiosis, or an imbalance between the different floras in the gut, may disrupt homeostasis and trigger autoimmune diseases [30, 34, 36, 37].

Diabetes UK, one of the leading charities involved in diabetes research, created a new campaign in 2012, the "4Ts campaign", to increase awareness of the symptoms of diabetes and allow swifter diagnoses before further complications arise [38]. These four "Ts" align with the major indicators of diabetes onset, which are "Toilet, Thirsty, Tired, Thinner" [38]. The decreased production of insulin in those individuals with Type 1 diabetes prevents the absorption of glucose from the blood, leading to hyperglycaemia (high blood glucose levels). This causes excessive thirst ("Thirsty") and as a result, increased frequency of urination ("Toilet"). Due to the dysregulation of glucose homeostasis and the lack of glycogenesis, muscle tissues fatigue, causing individuals to feel exhausted and lethargic ("Tired"). Finally, muscle and adipose tissues start to breakdown as gluconeogenesis is triggered to compensate for the low availability of glucose from the diet as an energy source. This process generates glucose from non-carbohydrate carbon substrates, including lipid and protein substrates. The breakdown of body tissues as a source of energy leads to weight loss ("Thinner") [39, 40]. Due to the absence of insulin in the blood, this breakdown also causes ketone bodies to form, which unbalance the electrolyte system as they alter the pH of the blood to become acidic [40, 41]. This, in combination with high levels of glucose in the blood, can lead to diabetic ketoacidosis, which is life threatening if not treated rapidly [39-41].

Treatment for Type 1 diabetes is a life-long undertaking. The overall aim is blood glucose management, through glucose testing and regular injections or infusions of insulin to replace that which the body is unable to

produce. This aims to keep the blood glucose levels stable [42]. Glucose levels have previously been measured by finger prick testing, where a small amount of blood is used to determine the amount of glucose present. However, novel approaches use subcutaneous methods to measure interstitial glucose levels, which reduces the number of finger prick tests a patient needs to perform [43]. Testing glucose levels allows individuals with diabetes to react to any changes, imitating the function of β-cells in a healthy pancreas. This involves the delivery of insulin in response to high glucose readings, or in preparation for increasing glucose levels due to consumption of carbohydrates.

With regard to insulin delivery, there are a variety of therapies available to patients. Primarily, these are insulin injections, administered at least four times per day, and pump therapy, where an insulin pump is attached to the individual and continually delivers insulin subcutaneously in small doses throughout the day. Pump therapy reduces the need for multiple injections and provides the user with the ability to make smaller and more accurate adjustments to insulin delivery [44, 45]. Diet and exercise are also important factors for glucose management; exercise increases the sensitivity of body tissues to insulin, causing it to be used more efficiently [46] and thus reducing the volume required to stabilise blood glucose levels. Carbohydrate is the main source of glucose in humans and therefore it is imperative that this is regulated in the diet. Reducing the amount of carbohydrate consumed decreases the volume of insulin required and improves glucose control over time. This is due to fewer incidences of rapid increases and decreases in blood glucose levels, aiding their stabilisation and avoiding the resulting damage from rapid changes in glucose amounts.

Maintaining stable glucose levels has been shown to reduce the risk of developing further complications associated with having diabetes;

therefore, this is the ultimate aim of diabetes treatment, including for Type 1.

1.1.3.2. Type 2 diabetes mellitus

It is estimated that 90% of patients with diabetes mellitus have Type 2 diabetes [47], which was approximately 380 million globally as of 2012 [15]. In 2019, it was thought that 3.9 million individuals in the UK had a diabetes diagnosis and at least 90% were Type 2 diabetes mellitus: this makes at least 3.5 million in the UK [47]. Type 2 diabetes mellitus is a metabolic disorder resulting in hyperglycaemia. This is due to either insulin resistance, where the body of the individual uses the insulin produced ineffectively, or the inability of the pancreas to produce enough inulin [48, 49]. Previously, it has been referred to as "adult-onset diabetes" as its diagnosis was most commonly in those over the age of forty years. Currently, however, its occurrence in children and young people is rapidly increasing; this is thought to be a consequence of increasing incidences of obesity. Risk factors associated with developing Type 2 include being overweight or obese, consumption of an unhealthy diet and a lack of physical activity [50, 51]. There is also a strong association with family history: if an individual has a first-degree family member with Type 2 diabetes, their risk of developing it themselves increases to 15%. If both of an individual's parents have it, their risk increases to 75% [52]. The symptoms experienced prior to diagnosis can be similar to Type 1 diabetes: excessive thirst, frequent urination, increased hunger, fatigue and the rapid loss of muscle mass. This is a consequence of hyperglycaemia [47-49].

Initial treatment involves increasing participation in physical activity and modifications to the diet, primarily to decrease the amount of carbohydrate consumed, as carbohydrate increases the need for insulin. Low calorie and low carbohydrate diets are often prescribed for patients who are

overweight or obese, as this lowers the requirement for insulin in the body, reducing the demand on the pancreas [51]. Drugs such as metformin are frequently prescribed to increase patients' sensitivity to insulin. Metformin is a biguanide, a group of drugs which inhibit the production of glucose in the liver. This leads to a reduction of insulin levels in the body and improves the body's sensitivity to insulin, as well as reducing the amount of sugar absorbed by the intestines. Metformin, and other "diabetes medications" help to maintain healthy blood glucose levels in diabetic patients [51]. Insulin injections are sometimes recommended for Type 2 diabetic patients, particularly those who have lived with the disease for an extended period, or those for whom metformin has little or no effect.

1.1.3.3. Other types of diabetes

A number of other types of diabetes have been identified, though these comprise the smallest percentage of the overall number of cases. The most common of these is gestational diabetes, which presents in pregnant women: hyperglycaemia develops usually during the second or third trimester, caused by the pancreas's inability to produce sufficient insulin to meet additional needs of the body during pregnancy. Usually this is rectified after pregnancy.

Maturity onset diabetes of the young (MODY) makes up 1-2% of all diabetes cases in the UK and is often mistaken initially for Type 1 or Type 2 diabetes mellitus. It is caused by a single gene mutation and does not necessarily result in the need for insulin injections.

1.1.3.4. Main complications of diabetes

There are a number of complications associated with having diabetes, however, although it is common for individuals with diabetes to develop co-morbidities, it is not inevitable and there are factors that increase an

individual's risk of developing them. These include having diabetes for twenty years or more and poor glycaemic control (indicated by inconsistent, out-of-range blood glucose levels).

The most common complications are diabetic nephropathy, which is the deterioration of kidney function, diabetic neuropathy (damage to the nerves), and diabetic retinopathy, caused by damage to the microvasculature supplying the eye. All can be considered a direct consequence of chronically elevated blood glucose volumes [53].

Nephropathy is a macrovascular complication caused by exposure of the kidneys to elevated blood glucose levels, which causes increased hypertension and damage to the kidneys through reactive oxygen species (ROS) production and oxidative stress [54]. High blood pressure within the kidneys causes damage to the filtration units (nephrons) over time, resulting in their loss of ability to adequately filter the blood.

Diabetic neuropathy is nerve damage caused by diabetes through various mechanisms. Predominantly, damage occurs via the direct impact of hyperglycaemia and reduced blood flow to nerves, caused by injury to small blood vessels. Consequently, patients can suffer from sensory damage in their extremities, in the form of numbness or pain, depending on which nerves are affected. The impairment to nerves is especially prevalent in the feet, where decreased sensation leads to patients' inability to recognise cuts or blisters, often leading to the formation of ulcers and foot infections [55].

Hyperglycaemia is a common consequence of having diabetes and an indicator that an individual has diabetes, prior to diagnosis. Over time, chronic hyperglycaemia contributes to atherosclerosis and this injury to the vessels promotes initiation of repair processes, increasing cellular energy demand. Oxidative stress is another result of persistent hyperglycaemia, due to elevated concentrations of sugars and lipids present in the blood. This causes a surge in oxygen-derived free radicals, which damage blood vessels

and cause the pro-oxidant and antioxidant systems to become unbalanced [56]. ROS are formed as a result of normal oxygen metabolism and their production is an essential feature of wound healing and tissue repair. The presence of ROS causes the oxidative degeneration of proteins and lipids (peroxidation), which can affect their functions *in vivo*. This includes lipids comprising plasma cell membranes, promoting the creation of damaging secondary compounds due to the oxidation process, which induce damage in addition to that caused by ROS [57].

The damage caused is exhibited as inflammation; nitric oxide synthase (NOS) is secreted, to induce production of nitric oxide to help attenuate the inflammation. NOS functions by binding to the endothelium via palmitate molecules. One pathway which produces palmitate is the fatty acid synthase (FAS) pathway. FAS is an enzyme regulated by insulin and individuals with diabetes have low levels of FAS due to impaired insulin function, either as a result of insulin deficiency or resistance to it [58, 59]. As such, it has been proposed that those with diabetes may be more prone to develop vascular damage, as NOS does not function as effectively in these patients.

Patients with all types of diabetes are subject to an increased risk of stroke and heart attack, although Type 2 has a stronger causal association with an unhealthy diet and sedentary lifestyle, which also increases an individual's risk for these [15, 60, 61].

The most common microvascular complication that occurs in Type 1 and Type 2 diabetic patients is diabetic retinopathy, which is initiated by damage to the blood vessels supplying the back of the eye; chiefly, those supplying the retina (light-sensitive tissue). It develops as a result of oxidative stress caused by chronic hyperglycaemia; the type of injury observed is identical to that observed in inflammation. Vessels become permeable, causing leakage of fluids and lipids. The macula, located at the centre of the retina, swells when the blood vessels that supply it become permeable, resulting in

blurred vision. This is known as macula oedema, also referred to as diabetic maculopathy, and is thought to affect half of diabetic retinopathy patients. In response to microvascular damage in the eye, repair mechanisms, most notably angiogenesis, are initiated to replace the defective and damaged blood vessels. The disease develops progressively; the main stages are outlined in Table 1.1 [62] (see Fig. 1.2 also). “Diabetic retinopathy” generally refers to both diabetic maculopathy and proliferative retinopathy [63].

Table 1.1. An outline of each progressive disease stage found in diabetic retinopathy.

Disease stage	Main features	Consequence	Treatment
Background retinopathy	Micro-aneurysms in retinal microvasculature, blood vessels rupture and leak blood into surrounding tissues	Eyesight unaffected, risk of future blindness is increased	Lifestyle changes: optimal control of blood glucose, blood pressure and cholesterol levels
Pre-proliferative retinopathy	Severe changes to the retinal microvasculature: retinal occlusions and increased vascular permeability causing bleeding into the retina	Areas of the retina become ischaemic as they are starved of oxygen and nutrients, pro-angiogenic factors stimulated, such as VEGF	Lifestyle changes
Proliferative retinopathy	Vision loss due to angiogenesis and scar tissue formation on retina. New blood vessels are fragile and leaky, blood leakage into the retina	New vessels grow into vitreous body, retinal detachment as the leaked blood and micro vessels push it into the vitreous body, blindness	Anti-VEGF medication and, in the most advanced cases, surgical procedures, such as retinal reattachment

Diabetic retinopathy is the leading cause of blindness globally: approximately one third of people with diabetes present with signs of retinopathy. Of these, a further one third have vision-threatening retinopathy [64, 65]. Any individual with diabetes is at risk of developing diabetic retinopathy, though a patient's chance of developing the disease is increased by a number of factors, including hypertension, high cholesterol levels and a high body mass index. Non-modifiable risk factors include 20 or more years since diabetes onset and pregnancy [66]. Patients with diabetes who are over the age of 12 years in the UK are screened annually for any signs of retinopathy: early detection is imperative to prevent loss of vision and permanent blindness.

Prevention is preferable to treatment – therefore, reducing the risk of developing diabetic retinopathy to begin with is crucial. The most effective way to do this is intensive glycaemic control, whereby patients keep their blood glucose within optimal range (for insulin-dependent diabetes, this is between 4.0 and 7.0mmol/ L [66]). Keeping blood glucose, blood pressure and blood cholesterol levels within range can help to reduce the chance of retinopathy development. Both the Diabetes Control and Complications Trial [67] and the UK Prospective Diabetes Study [68] showed that intensive glycaemic control reduced the risk of developing diabetic macula oedema by approximately 25%.

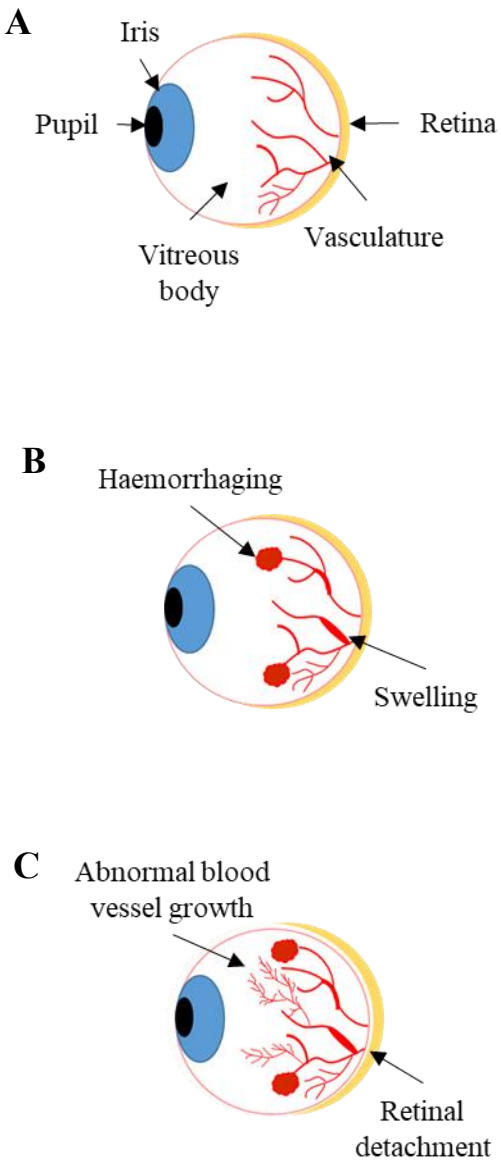

Figure 1.2. **The major stages of progressing diabetic retinopathy. (A)** A healthy eye, before onset of diabetic retinopathy. **(B)** Early-stage diabetic retinopathy, usually eyesight is unaffected at this stage. **(C)** Proliferative retinopathy, where neovascularisation is a prominent feature and eyesight is very poor.

Current treatment options include surgical and drug-based therapies. The first-line therapy used to treat diabetic maculopathy is laser treatment: the laser creates small burns on the retina to offset the leakage of blood from the damaged vessels and reduce macula oedema. For proliferative retinopathy, panretinal photocoagulation (PRP) is required, a procedure that shrinks and seals new blood vessels that have formed already and prevents additional new vasculature from growing on the retina. This in turn reduces the risk of haemorrhaging and further leakage. By using PRP, patients are prevented from losing their remaining eyesight and the chance of developing retinal detachment is reduced [69]. Other surgical procedures that are used in treating diabetic retinopathy include vitrectomy and retinal re-attachment. Pars plana vitrectomy is performed when a patient develops vitreous haemorrhage (VH), or retinal detachment with or without VH. VH develops as a consequence of angiogenesis; as the vessels proliferate into the vitreous body and along the retina, they eventually cause its detachment. As they grow into the vitreous body, the blood vessels rupture and cause recurrent haemorrhages. As blood leaks into the vitreous humour, patients suffer pain and loss of vision. Pars plana vitrectomy involves removing some or all of the gel from the vitreous humour and potentially replacing it with, for example, saline. This removes the blood from the vitreous body, which attenuates some vision loss and pain. It can also be employed when performing a retinal reattachment operation [69].

In diabetic retinopathy, tears in the retina combined with fluid leakage and build up can cause the retina to become detached, which results in patient blindness. Retinal re-attachment can be performed, using a gas bubble and post-operative positioning to maintain the placement of the bubble. This procedure first requires laser photocoagulation or cryotherapy (freezing treatment) to stabilise the haemorrhaging blood vessels; this is followed by

injection of an intraocular gas, for example SF_6, to form a small bubble that covers the pathology.

Drug-based therapy options include corticosteroids and anti-VEGF (vascular endothelial growth factor) drugs, described later in section 1.4., via intra-vitreal injection. Corticosteroids are used to inhibit VEGF expression; they act to down-regulate platelet-derived growth factor (PDGF, see section 1.2.4.), which reduces new blood vessel formation by angiogenesis [70, 71]. The adverse effects associated with long-term steroid use have been well established, such as development of cataracts that further impair patients' vision; therefore, they cannot be used indefinitely to treat diabetic retinopathy.

1.1.4. Age-related macular degeneration

Age-related macular degeneration (AMD) is a progressive disease involving degeneration of the macula, an area of tissue in the centre of the retina at the back of the eye, resulting in the loss of central vision [72]. Globally, AMD is the leading cause of central visual loss in those over the age of 65 years, and the third most common cause of blindness (following cataracts and glaucoma) [73], affecting 10% of those over 65 years and more than 25% of individuals aged 75 years [74]. It has two forms; dry, which is more common, and wet AMD, which develops from the dry form, usually developing more rapidly. The main feature of the wet form is neovascularisation within the macula, which is absent in dry AMD.

Human retinal pigment epithelium (RPE) is a complex tissue made up of a monolayer of non-dividing pigmented cells present at the neuroretina and choroid interface. It has a number of functions imperative for maintaining photoreceptor cells but can undergo various changes during the aging process, which can lead to the formation of drusen [72]. These are yellow deposits located beneath the retina, between the RPE and Bruch's

membrane, comprising lipids and proteins [72, 75]. There are different types of drusen: small, hard drusen may not affect patients' vision, whereas presence of large, soft drusen is a known risk factor for, and a hallmark of, AMD [76-78]. The formation of drusen is indicative of RPE dysfunction and promotes loss of RPE and photoreceptor death [79]. Some of the key constituents of drusen are vitronectin and apolipoprotein E (apoE) [80]. Vitronectin is a glycoprotein found abundantly in serum, extracellular matrix (ECM) and bone. It binds with various integrin molecules to play a role in tissue remodelling by cell adhesion regulation [81]. ApoE is a protein involved in fat metabolism by binding lipids to form lipoproteins, with its predominant role being to transport cholesterol [82]. Both of these molecules have been found to accumulate in drusen, which reflects the protein profile of RPE cells as well [80].

The soluble glycoprotein, complement factor H, has also been isolated from ocular drusen. It has a protective effect as it regulates the alternative complement pathway activation to ensure the complement system targets pathogens and not self-cells. It is mainly produced by the liver and circulates in the plasma; however, it can be synthesised by RPE cells and has been found to accumulate in drusen where it prevents degradation of drusen by the alternative complement pathway [83]. Degeneration of RPE leads to progressive damage to the Bruch's membrane that, in combination with the upregulation of pro-angiogenic factors like VEGF, promotes growth of abnormal blood vessels from the choroid beneath the RPE. As the disease advances, these vessels also grow under the retina. Vision loss can develop as a consequence of choroidal neovascularisation, as blood vessels grow into the macula and, due to their fragility, are prone to haemorrhaging and so leak blood into the retina and surrounding tissues. Macula oedema also contributes to vision loss and occurs when fluid builds up in the back of the eye, distorting the vision or causing complete vision loss.

End-stage wet AMD results in the permanent loss of central vision, causing blurred vision or a blind spot in the visual field [84]. Wet AMD is distinct to other neovascular eye diseases in that aberrant angiogenesis occurs in the choroidal and not the retinal vasculature [62]. In those for whom central vision loss has developed as a consequence of wet AMD, the risk of depression increases as their ability to participate in various social activities is compromised. Charles Bonnet syndrome, wherein patients experience visual hallucinations, has also been linked with profound vision loss in patients with wet AMD. Up to 50% of individuals with macular degeneration experience this, though it is more likely to occur in those with loss of vision in both eyes, and the onset of hallucinations commonly happens after a sudden worsening of eyesight [85].

There is no obvious cause of wet AMD, although it has been noted that it develops from the dry form. The risk factors are numerous; twin studies have established that family history is a risk factor as the disease has a hereditary component [86], however the greatest risk factor is age: this disease is rare in those under 50 and most common in people over 75 [87-91]. The prevalence of advanced AMD, including the wet form, increases with each decade after the age of 50 years. The highest prevalence is after the age of 80 years [72, 73]. Race is another risk factor, as there is a higher disease prevalence in Caucasian individuals. These are referred to as personal risk factors. Environmental risk factors for AMD include smoking, high blood pressure and cardiovascular disease, since conditions which affect the heart and vasculature may increase risk of other vascular conditions developing [72, 73, 87-91].

Prevention of wet AMD is crucial to prevent vision impairment: therefore, patients over the age of 60 years receive free routine eye examinations to identify early signs of AMD. Early detection and treatment of wet AMD can help to reduce loss of vision. Managing medical conditions,

such as cardiovascular disease, can also help to reduce the risk of AMD development, along with avoiding smoking and maintaining a healthy weight through regular exercise and a healthy diet [73, 92]. Despite a lack of treatment available for dry AMD, central vision may not be affected at early stages of this disease. As wet AMD progresses, however, anti-VEGF drugs may be administered to prevent vision from worsening in 90% of patients, however, restoration of normal visual acuity occurs in considerably fewer (30%) [93].

1.1.5. Retinopathy of prematurity

Retinopathy of prematurity (ROP) is a vasoproliferative disorder, in which there is abnormal growth of blood vessels at the back of the eye [94]. Normally, the retina becomes completely vascularised at full term, however in the premature baby, the retina remains incompletely vascularised at the time of birth. Thus, neovascularisation becomes disrupted and retinopathy occurs [62]. It develops in a two-phase process; the first phase occurs when a preterm neonate (defined as babies born alive before the completion of 37 weeks of pregnancy) begins to breathe. The immature retinas become hyperoxic (a state of excess oxygen supply to the tissues [95]), which leads to suppression of growth factors such as VEGF and insulin-like growth factor-1. Due to the low-level presence of these factors, retinal blood vessel growth is attenuated [96].

Consequently, the retina becomes hypoxic, as it becomes more metabolically active but poorly vascularised; this stimulates the release of an abundance of growth factors to induce vasoproliferation [94, 96]. This is the second phase of the disease development, characterised by the consequential disorganised retinal vascular growth, plus oxidative damage to endothelial cells (ECs) [96]. As the vasculature develops, this can cause retinal detachment. Controlled administration of oxygen to these neonates can

reduce retinopathy of prematurity, though this cannot eliminate it altogether [97]. There are five disease stages, outlined in Table 1.2. [94, 96].

In 2010, it was estimated that the number of premature neonates who developed severe ROP worldwide was 53,000, with 20,000 becoming blind or severely visually impaired [98, 99]. In developed countries, the incidence of blindness in infants with ROP is low at 3-13%, although the overall incidence of ROP is increasing in these countries on account of advances in neonatal management that allow the survival of more premature infants [98, 100, 101]. Generally, around 90% of infants with ROP are in stages I and II, the milder disease categories, in which they do not experience long-lasting damage nor impaired vision [102].

The two greatest risk factors for ROP development are gestational age and birth weight, which are inversely proportional to the risk. This means the lower the birth weight and the earlier the gestational age of a neonate, the more likely they are to develop ROP. Another key factor is the use of supplemental oxygen, received in neonatal intensive care; however, the use of this for preterm neonates decreases the risk of systemic injury. Other risk factors include sepsis, blood transfusion and intraventricular haemorrhage [96, 102].

Table 1.2. An outline of each progressive disease stage found in retinopathy of prematurity.

Disease stage	Main features	Consequence
I	Mild abnormal blood vessel growth	Resolves without treatment and children develop normal vision
II	Moderate abnormal blood vessel growth	Usually resolves without treatment and children develop normal vision
III	Severe abnormal blood vessel growth; vessels grow towards the centre of the eye, instead of normal growth pattern along retina surface	Various: some infants improve without treatment, develop normal vision. Others develop "plus disease" (disease worsens as retinal blood vessels become enlarged and twisted) so treatment is considered, which should prevent retinal detachment
IV	Partially detached retina	Traction from the scar produced by bleeding, abnormal vessel growth pulls retina away from the eye wall; treatment considered
V	Completely detached retina and disease end stage	Treatment given to prevent severe visual impairment and blindness

With regard to treatment options, laser therapy and cryotherapy are both used to destroy the periphery of the retina, to slow or reverse the abnormal blood vessel growth. Although they preserve the crucial part of our sight, the central vision, these treatments do impair peripheral vision and the long-term side effects are not known. Thus, they are only performed on infants with advanced retinopathy: stage III with “plus disease” or more [96, 102].

Later disease stages, primarily stages IV and V, can also require a scleral buckle, where a silicone band is placed around the eye to tighten it and prevent the vitreous gel from pulling on scar tissue, in order for the retina to flatten against the wall of the eye. The band is removed after a few months or a year, as the eye continues to grow. The final treatment option for stage V ROP is a vitrectomy, where the vitreous humour is removed, either fully or partially, and replaced with saline solution. Following the extraction of the vitreous humour, the scar tissue on the retina can be removed, allowing the retina to flatten against the eye wall and preventing complete blindness [96, 102].

Retinal detachment can develop if infants do not respond to treatments for ROP. If there is only a partial detachment, classified as stage IV, no further treatment is given, as the retina may remain the same or reattach without treatment. However, in some instances additional treatment is offered to avoid further advancement of the retinal detachment (stage V). If the centre of the retina, or the entire retina, detaches, central vision is threatened: at this point, surgery may be recommended to reattach the retina [96, 102]. It is worth noting that surgical interventions to treat retinal detachment have limited success due to the small size of their eyes and the firm vitreoretinal attachments found in neonates [62].

1.2. What is angiogenesis?

1.2.1. The circulatory system

The human circulatory system comprises two distinct networks: the cardiovascular system, responsible for the transport of blood, and the lymphatic system, which transports lymph. Both systems consist of a series of branching vessels that supply body tissues to deliver necessary components (such as oxygen) to body tissues, and to remove waste products [103].

Major blood components include plasma, erythrocytes, immune cells and platelets. Primarily, plasma contains water, proteins (including antibodies, hormones, enzymes and other factors such as chemokines and cytokines) and salts [104]. Put simply, the human heart pumps blood to the lungs where haemoglobin is oxygenated (this is the pulmonary circulation) before the blood returns to the heart to be transported to the body tissues (systemic circulation).

1.2.2. Blood vessels

There are three major types of blood vessel – arteries, which have thick muscular vessel walls and transport blood at a high pressure; veins, which transport blood at a lesser pressure and therefore have thinner walls; and the smallest vessels, capillaries, which make up vascular beds to directly supply blood to tissues.

In the pulmonary circuit, pulmonary arteries transport blood with low oxygen content to the lungs, which is returned to the heart, where systemic arteries transport oxygenated blood to body tissues. Artery walls comprise three key layers. The outermost layer, the tunica adventitia, connects the artery to surrounding tissues as part of the ECM [105]. Consequently, this layer is made up of connective tissue and elastic and collagenous fibres. The

next layer is the tunica media, which is composed of smooth muscle and provides support for the cells and allows alterations in vessel diameter as part of blood pressure and blood flow regulation [105]. Finally, surrounding the vessel lumen is the tunica intima, the inside layer, which is the endothelial layer. This consists of a single EC layer attached to a basement membrane (simple squamous epithelium), surrounded by fibro-elastic connective tissue and elastic fibres, to provide flexibility and stability for the ECs [104, 105]. Blood flows through the entire network of arteries, from the largest arteries into smaller arteries, to arterioles, which play a key role in regulation of blood flow into the capillaries that supply the tissues, aided by the smooth muscle cells in arteriole walls [104, 105].

Capillaries directly supply body tissues and are the connecting vessels between arteries and veins. They form vascular beds allowing efficient exchange of materials between the blood and tissues. Tissues with greater metabolic activity demand more oxygen and a rapid removal of metabolic waste products, therefore the capillary network is more extensive to maintain the blood supply [104].

Systemic veins return blood to the heart from capillaries, via venules, the smallest veins, which connect to increasingly larger veins until the blood enters the heart. This blood has a reduced oxygen content due to oxygen having been used for metabolic activities in cells throughout the body. On the other hand, pulmonary veins carry blood with a high oxygen content to the heart from the lungs, where it is pumped through systemic arteries to body tissues. Venular walls have the same layered structure as arteries, though blood is not transported at such a high pressure, hence they contain less smooth muscle and connective tissue, meaning the walls are ultimately thinner [105]. A prominent feature of veins is that they contain valves to help maintain blood flow in the direction of the heart, which is particularly

important in the arms and legs where venous valves prevent the backflow of blood in response to gravity [104].

1.2.3. Cells of the vasculature

1.2.3.1. Endothelial cells

ECs are a flattened cell type that line the lumen of all blood vessels on a basement lamina, therefore lining the entire vascular system. Their remodelling ability, whereby they adjust their number and arrangement in response to local requirements, allows them to supply every region of the body and adapt constantly as needed for growth and tissue repair [106]. During embryonic growth, the development of arteries and veins derives from small vessels consisting only of ECs and the basal lamina. Other blood vessel components are recruited by EC signals, where required, demonstrating the fundamental role of ECs in blood vessel formation.

Upon vessel maturation, interactions between ECs and surrounding connective tissue and smooth muscle is integral in regulation of the blood vessel's function and structure. One example of this is mechanoreceptors on ECs, which allow them to detect shear stress caused by blood flow over their cell surface, information that they communicate to surrounding cells to enable adjustment of blood vessel lumen diameter to accommodate blood flow. Another is that ECs release nitric oxide to initiate smooth muscle relaxation in vessel walls and cause blood vessel dilation, allowing increased blood flow where necessary.

ECs are critical for tissue homeostasis and form a direct contact with the blood in vessel lumen. They regulate vascular tone, via interactions with the peripheral nervous system, and partake in both coagulation and thrombolysis processes [107, 108]. Furthermore, they are involved in

inflammatory and immunological pathways mediated by a layer of surface glycoproteins [109].

ECs can be characterised by a number of cell markers; for example, the transmembrane glycoprotein, CD31, is expressed by a number of vascular cells, including ECs, platelets and macrophages. It has been implicated in integrin activation, angiogenesis and leukocyte transmigration [110-112]. CD34 is another EC marker – it is a cell surface glycoprotein, with roles in cell-cell adhesion and cell proliferation and differentiation [111, 112].

EC markers can change during angiogenesis, as ECs differentiate during blood vessel formation. CD105, for instance, is a homodimeric transmembrane glycoprotein which is usually expressed at low levels in resting ECs. However, during neoangiogenesis, as ECs become more active in sites of vascular injury or inflammation, or in tumour vasculature, CD105 is upregulated to fulfil its role as an auxiliary receptor for the TGF-β receptor complex, involved in cell proliferation and differentiation.

The VEGF receptor (VEGFR) family is central to angiogenesis, with VEGFR1 and -2 expressed on ECs (more information on this is available in chapter 1.2.4). ECs are directly involved in physiological and pathological angiogenesis, as new blood vessels sprout and grow from existing vasculature and ECs line the entire vascular system. This is explained in full in chapter 1.2.5. and Fig. 1.5.

1.2.3.2. Pericytes

Pericytes are a type of mesenchymal cell, with the potential to differentiate into a multitude of different cell types, such as fibroblasts, osteoblasts, adipocytes and chondrocytes. [113-116]. Traditionally, pericyte cell markers are CD146, CDPG4 and PDGFRb, however they are not unique to pericytes

as they also expressed on other mesenchymal cell types, including smooth muscle cells and ECs [117-119].

Therefore, pericytes are distinguishable from other vascular cells chiefly by their distinct morphology: an oval cell body and long cytoplasmic processes that surround neighbouring ECs [108, 117, 120]

One of the main roles of pericytes is to provide ECs with a balanced microenvironment. They are embedded in the basement membrane alongside ECs, allowing them to communicate by means of direct cell-cell contact and paracrine signalling [108, 120, 121].

Microvascular pericytes, present in capillaries, communicate with ECs via gap junctions and aid ECs with proliferation and selective inhibition, as they differentiate as part of the angiogenic process (Fig. 1.5). Pericytes have also been shown to protect ECs from cell death by apoptosis or cytotoxic processes. They have been shown *in vivo* to release pericytic aminopeptidase hormone, which, when secreted in the presence of ECs and astrocytes, caused pericytes to group into structures resembling capillaries. In this experiment, when the pericytes were removed, ECs underwent apoptosis. This provides more evidence for pericyte involvement in both EC survival and angiogenesis [122]. Furthermore, pericytes have been found to contribute to EC survival through production of Bcl-w during cellular crosstalk, a protein that is instrumental in VEGFA expression and downregulating apoptosis [123].

In diabetic retinopathy, patients' retinas often exhibit loss of pericytes – this is a characteristic factor in early disease stages. As pericytes are essential for EC and retinal capillary protection, this loss contributes to microaneurysm formation in the capillaries and leads to an increase in vascular permeability, macular oedema, and formation of new blood vessels that ultimately can lead to reduced or complete loss of vision [124].

1.2.3.3. Smooth muscle cells

Vascular smooth muscle cells, specifically, are defined based on their anatomical localisation (in the vasculature) and functionality. They are located in the medical layer and are responsible for arterial contraction to aid blood flow, and production of many key ECM components, including proteoglycans, collagen and elastin, and numerous proteins responsible for ECM synthesis and degradation, such as lysyl oxidase and metalloproteinases [125, 126]. These cells are spindle-shaped (round in the centre and tapering at each end), with an elongated nucleus, and their membrane configuration changes during contraction and relaxation – such as in arterial wall remodelling, to enable the diameter of the vessel lumen to change in response to blood flow [125]. Their cytoplasm contains large amounts of actin (thin) and myosin (thick) filaments, which act as the main proteins involved in muscle contraction [125, 127].

Smooth muscle cells are characterised by these contractile filaments, particularly the thin filaments as they fill most of the cytoplasm, connecting with "dense bodies", electron-rich areas anchored to the plasma membranes, to link actin with the membranes to allow cell contractility [125]. Cell markers for smooth muscle cells include ACTA2 (an actin protein) and CNN1 (calponin 1, a protein with a role in contraction) [128].

During angiogenesis, smooth muscle cells help to stabilise the new vessel following EC migration and proliferation. They also aid myogenesis (formation of new muscular tissue) around the newly formed blood vessel by inhibiting further EC migration and proliferation, and by stimulating ECM production [129].

1.2.4. Vascular endothelial growth factor

Angiogenesis is initiated by pro-angiogenic factors, the most well documented of which is vascular endothelial growth factor (see Figs. 1.3 and 1.4), which modulates a range of cellular processes (including angiogenesis and lymphangiogenesis), through binding homo- or heterodimeric transmembrane receptor tyrosine kinases (VEGFR1, -2 and -3, Fig. 1.4). Some isoforms also bind neuropilin co-receptors (NRP1 and NRP2, see section 1.2.6.1.) that contribute to modulation of cellular responses to the VEGFRs [130-132]. The VEGF subfamily makes up a supergene family, along with the PDGF subfamily [130, 131]. PDGF is a pro-inflammatory cytokine which induces the expression of the VEGF gene [133]. VEGFA is the most abundant member of the VEGF family; VEGFA-null mice die during embryonic development due to angiogenic defects, indicating the necessity of VEGFA production for complete vascular development [134, 135].

1.2.4.1. Family and isoforms

The VEGF family consists of five structurally related secreted glycoproteins: VEGFs A, B, C, D and placental growth factor (PlGF) [136]. The role of VEGFB is poorly understood, although it is known to be essential for blood vessel survival. It consists of two isoforms, $VEGFB_{167}$ and $VEGFB_{186}$, which bind only to VEGFR1 [137]. VEGFC and VEGFD, which have integral roles in lymphangiogenesis, have no known isoforms [138]. PlGF, predominantly expressed in placental tissues, has four isoforms in humans: PlGF1 ($PlGF_{131}$), PlGF2 ($PlGF_{152}$), PlGF3 ($PlGF_{203}$) and PlGF4 ($PlGF_{224}$) [138]. PlGF has clear roles in angiogenesis: all isoforms recognise and bind to VEGFR1 [139, 140] and deletion of the human *PlGF* gene results in impairment of angiogenesis, inflammation and wound healing [139, 141].

However, the consequence of PlGF upregulation is pathological angiogenesis [142].

VEGFA is the most well characterised family member, with established roles in angiogenesis and lymphangiogenesis. It is the most potent pro-angiogenic growth factor compared to other VEGFs [136, 143]. It is usually found as a homodimer, although it can form heterodimers with VEGFB and PlGF [144]. VEGFA specifically binds to VEGFR1 and VEGFR2 (Figs. 1.3 and 1.4) on ECs, but can also bind with lower affinity to co-receptors NRP1 and NRP2, expressed on the vascular endothelium and neurons [145]. There are 16 known isoforms of VEGFA, with the two major isoforms being $VEGFA_{121}$ and $VEGFA_{165}$. $VEGFA_{165}$ was the first isoform to be characterised and remains the most highly investigated isoform, with regard to its function, signalling, expression and pathological roles [146]. As a potent stimulator of angiogenesis, $VEGFA_{165}$ is considered the original pro-angiogenic VEGFA isoform [136]. VEGFR tyrosine kinase activity is stimulated by all VEGFA isoforms, except for $VEGFA_{165B}$, which appears to negatively regulate VEGFR activity [138, 147].

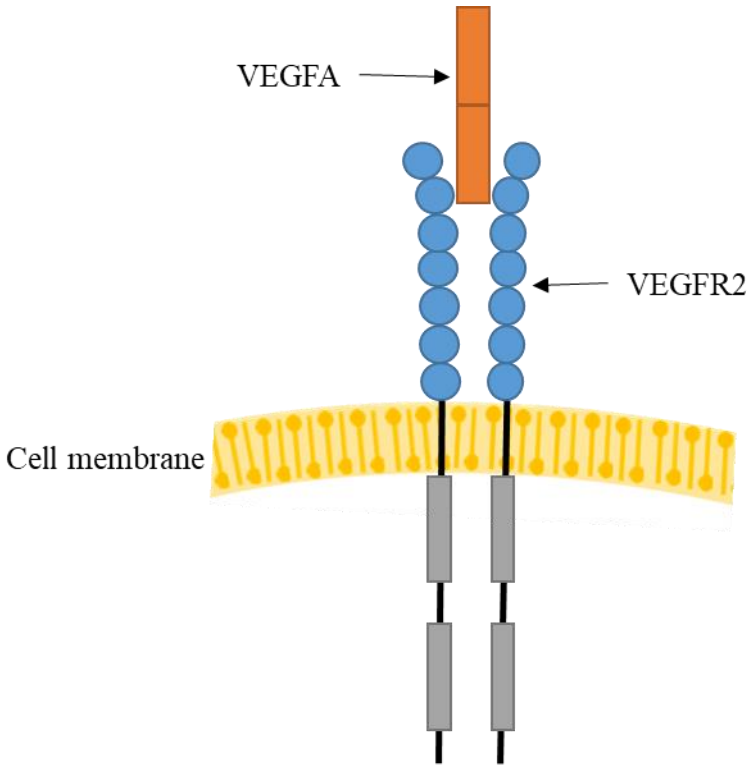

Figure 1.3. **Binding of VEGFA with its receptor.** Upon ligand binding, the VEGF receptor dimerises, initiating tyrosine kinase activity. This leads to the autophosphorylation of intracellular domains and activates signalling pathways.

1.2.4.2. Receptors

There are three VEGF receptors: VEGFR1, VEGFR2 and VEGFR3 (Fig. 1.4). As stated previously, they can form homodimers or heterodimers and are involved in both angiogenesis and lymphangiogenesis. In angiogenesis, VEGFR1 and VEGFR2 homodimers are both integral; however, VEGFR2 forms a heterodimer with either VEGFR1 or VEGFR3 as well, both of which are also involved in angiogenesis. The VEGFR3 homodimer and VEGFR2/ VEGFR3 heterodimer both facilitate lymphangiogenesis [138].

All isoforms of VEGFA, VEGFB and PlGF are ligands for VEGFR1 and although VEGFA binds with VEGFR2, it binds more strongly with VEGFR1 [148]. This receptor is crucial for blood vessel formation and for mediating EC proliferation [149]. Its expression is upregulated under hypoxic conditions with involvement from HIF1 (hypoxia inducible factor 1): this is the central mediator of hypoxic response, with the ability to regulate numerous genes, including VEGF [150]. The VEGFR1 promoter contains a hypoxia-responsive element sequence, which enables HIF1 binding and leads to stimulation of VEGFR1 locus transcription [151]. VEGFR1 also has an alternative spice variant, which produces a soluble form of the receptor that acts as a decoy receptor for VEGFA and, consequently, negatively regulates VEGFR2 [147, 152].

VEGFR2 is expressed on endothelial and lymphatic cells and binds with VEGFA, C and D. Although its binding affinity for VEGFA is less than that of VEGFR1 [148], the relative abundance of VEGFR2 is greater [153]. It does preferentially form heterodimers with VEGFR1 rather than homodimers, although VEGFR2 homodimers are functionally necessary [154-156]. Binding of VEGFA to VEGFR2 causes the autophosphorylation of specific tyrosine residues in VEGFR2's cytoplasmic domain. Phosphorylated VEGFR2 promotes downstream pro-angiogenic signalling pathways and generates several EC responses, such as a strong mitogenic

signal and survival signal, necessary for angiogenesis. VEGFA-VEGFR1 binding does not evoke this strong mitogenic signal [157, 158]. This, combined with the relative abundance of VEGR2 versus that of VEGFR1, supports the idea that VEGFR2 homodimers are the main signal transducers in the angiogenic process [153]. Although a soluble form of this VEGF receptor has been identified in mice and humans, its function has yet to be determined [138, 159].

The final VEGF receptor is VEGFR3, which binds VEGFC and D to induce signalling pathways promoting lymphangiogenesis. There are two splice variants, one long and one short, both expressed on lymphatic ECs [160]. There is also a soluble variant of VEGFR3, which has been identified in corneal ECs and has anti-lymphangiogenic properties, though it also binds VEGFC and D [161]. Based on this information, it has been proposed that soluble VEGFR3 functions as a decoy receptor for these VEGF ligands, thus preventing VEGFR3-induced pro-lymphangiogenesis signal transduction [161, 162]. VEGFR3 also forms heterodimers with VEGFR2, but not VEGFR1 [157], providing unique signalling outcomes in both lymphangiogenesis and angiogenesis [163].

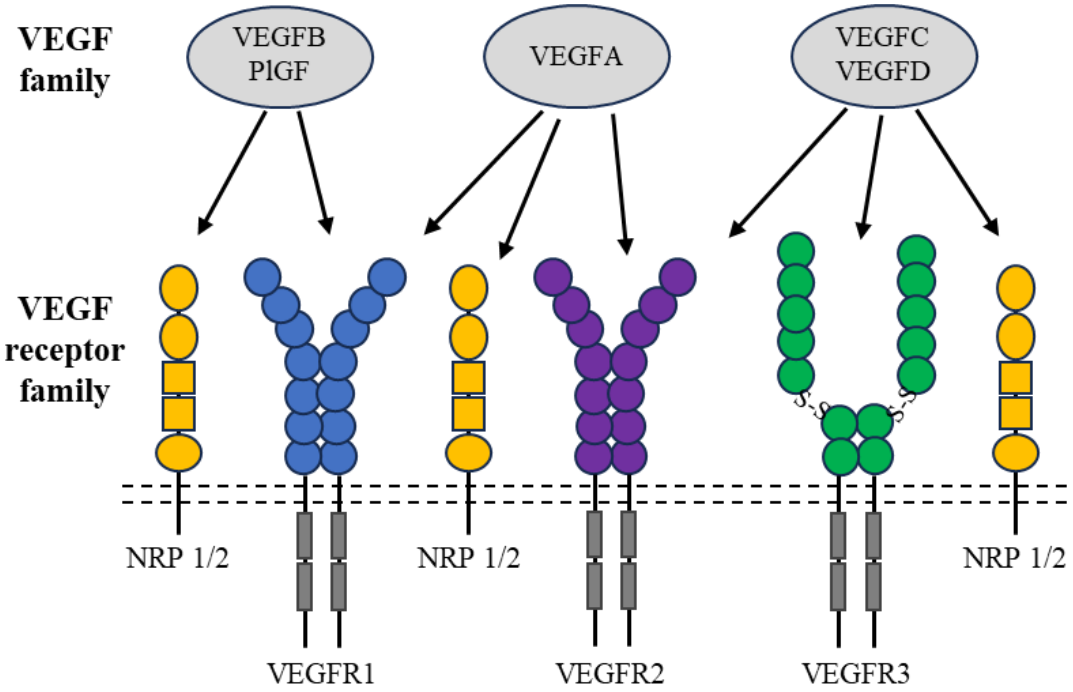

Figure 1.4. **Schematic of the VEGF family.** Shown are family members with their respective receptors and associated neuropilin co-receptors. In the VEGFRs: coloured circles in extracellular regions represent Ig-like domains; black rectangles represent intracellular tyrosine kinase domains. In neuropilin co-receptors: membrane-distal brown ovals represent two extracellular domain tandem complement binding factor domains; brown squares represent two tandem Factor V/ VIII homology domains; and membrane-proximal brown oval represents single MAM domain. Redrawn from: *Cao, Y., Positive and Negative Modulation of Angiogenesis by VEGFR1 Ligands. 2009. 2(59): p. re1-re1.*

1.2.5. Types of angiogenesis

Angiogenesis is the sprouting of new blood vessels from those that are already present (angiogenesis overview shown in Fig. 1.5). This is a physiological response to injury in wound healing, as well as a feature of processes such as embryonic development, tissue development and organ regeneration [145]. During wound healing in adults, angiogenesis occurs in response to tissue demands for oxygen, which results in a cycle of hypoxia and re-oxygenation, promoting ROS formation and, in turn, stimulating angiogenesis. Therefore, the angiogenic process accelerates with increased ROS formation.

There are two types of angiogenesis, which occur both in adults and *in utero*: sprouting and intussusceptive angiogenesis. Sprouting angiogenesis comprises several well-characterised stages, including enzymatic degradation of the capillary basement membrane, proliferation and migration of ECs, endothelial tube formation, vessel fusion and pruning, and pericyte stabilisation (Fig. 1.5) [164]. This type of angiogenesis originates in body tissues with poor perfusion; when hypoxia is detected, oxygen demands increase and new blood vessel formation is necessary to meet this requirement. Parenchymal cells in a hypoxic environment generally secrete VEGFA to initiate angiogenesis [164]. ECs that comprise an angiogenic sprout can be subdivided into tip cells and stalk cells. Tip cells are characterised by their localisation at the forefront of blood vessel branches and numerous filopodia that probe the environment during migration towards angiogenic stimuli. They are also characterised by the expression of VEGF receptors 2 and 3, platelet-derived growth factor, Delta-like ligand 4 (Dll4) and NRP1, allowing tip cells to detect and respond to gradients of angiogenic stimuli, such as VEGFA [165-170]. Stalk cells follow tip cells and produce fewer filopodia, are highly proliferative and form tight junctions to ensure angiogenic sprout stability [165, 171-174].

An important component of sprout formation is cell-cell communication via the Delta-Notch signalling pathway. Notch is a cell surface receptor with a key role in vascular development [175] and a downstream target of VEGFA [176]. Its transmembrane ligand, Dll4, is expressed on arterial blood vessels and endothelial tip cells [175, 177-179]. The Notch pathway regulates cell proliferation and differentiation, cell fate and cell death [175]. Upon ligand interaction, the ligand-receptor complex undergoes endocytosis and causes unfolding of the juxtamembrane negative control region of the Notch protein. This allows cleavage of the intracellular domain, which can then travel to the cell nucleus to regulate transcription [175]. VEGFA induces tip cell production of Dll4, causing Notch receptor activation in stalk cells, and suppressing VEGFR2 production in these same cells by way of inhibiting transcription [175, 180]. This reduces their migratory behaviour compared to tip cells and as a result, ECs that are exposed to the highest VEGFA concentration are the most likely to develop into tip cells [170, 180, 181]. This way, the Delta-Notch pathway controls which cells become angiogenic [170, 175].

Despite tip cell exposure to the highest VEGFA concentration, their rate of proliferation is less than the rate of stalk cell proliferation. Production of viable vasculature is dependent on VEGFA concentration. Evidence for this includes embryonic lethality following a 50% reduction of VEGFA, due to vascular defects [143, 182]. Also, in the presence of excess VEGFA, tumours overproduce tip cells, leading to disorganised vasculature [183].

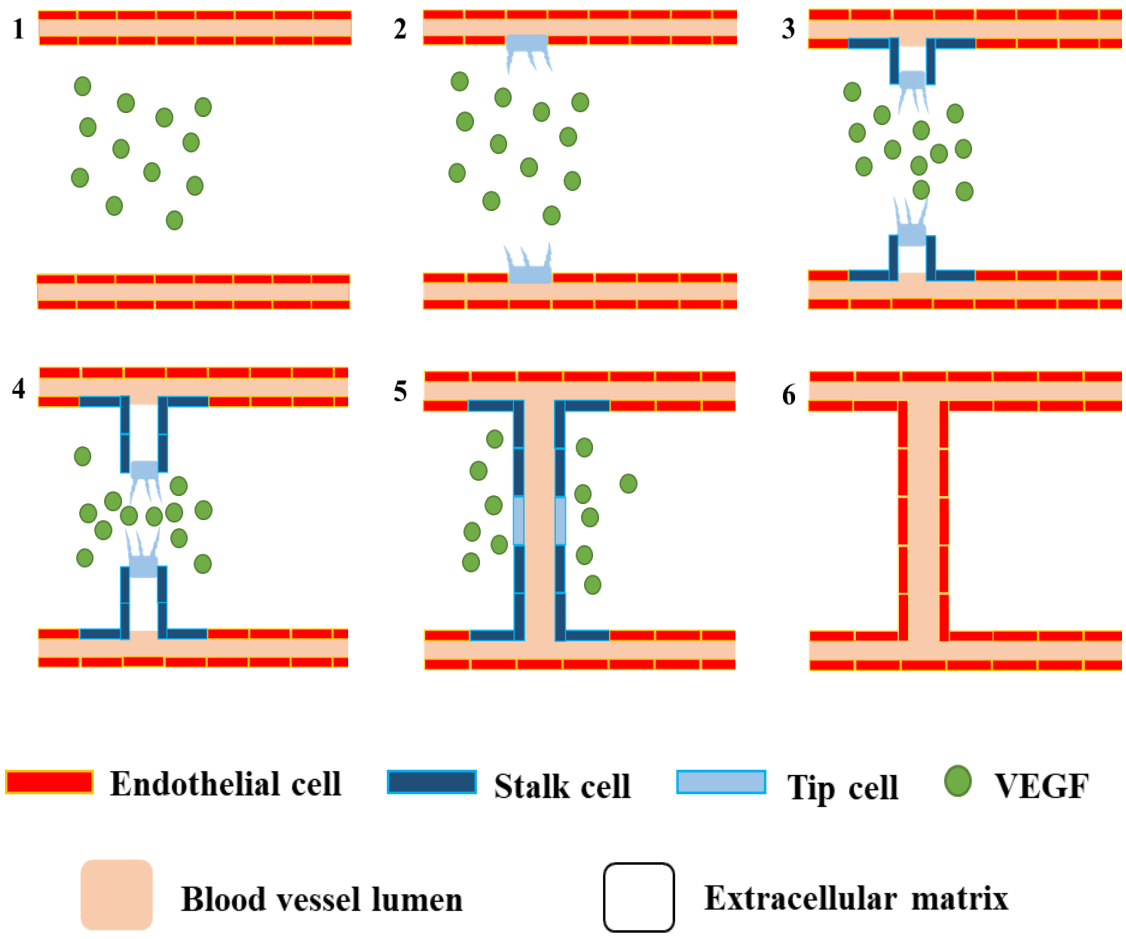

Figure 1.5. **Overview of the angiogenesis process.** (1) Endothelial cells are exposed to a high concentration of VEGFA; those exposed to the highest concentration become tip cells. (2) Tip cells lead the developing blood vessel sprout by extending filopodia. (3) The sprout lengthens as endothelial stalk cells, following the tip cells, proliferate. (4) The tip cells from two different sprouts fuse to create a new lumen. (5) This fusion enables blood flow through the new capillary, oxygenating the tissues and reducing VEGFA secretion. (6) The newly developed capillary is stabilised. Redrawn from: *Carmeliet, P., F. De Smet, and S.e.a. Loges, Branching morphogenesis and antiangiogenesis candidates: tip cells lead the way. Nat Rev Clin Oncol 2009. 6: p. 315-326.*

Intussusceptive angiogenesis (also known as splitting angiogenesis) is the formation of a new blood vessel by splitting an existing blood vessel into two [184]. Compared with sprouting angiogenesis, this type of angiogenesis is more rapid and efficient, as it does not require EC proliferation and migration; rather it relies on the reorganising of already established ECs [164], therefore allowing a vast increase in the number of capillaries without a corresponding increase in the number of ECs [185]. *In utero*, resources are limited, rendering it impossible to create a rich microvasculature with new cells every time a new vessel develops [185-188]. For this reason, intussusceptive angiogenesis is especially important in embryonic development, although it does occur throughout life, mainly promoting new capillary growth where capillaries already exist. It has been established in human postnatal lungs, along with other tissues and organs in capillary networks that border an epithelial surface, including the choroid of the eye, kidney, ovary and uterus [184, 189]. It has also been found to occur in skeletal muscle, heart and the brain [164].

In summary, the main phases of intussusceptive angiogenesis are as follows: the capillary walls make contact, EC junctions are reorganised and the vessel bilayer is perforated, allowing growth factors (such as VEGFA [184, 186]) and cells to enter the lumen. Following this, a core is formed between the two new blood vessels at the point of contact. This contains pericytes and myofibroblasts, which start to lay collagen fibres to provide ECM for the vessel lumen to develop. More cells accumulate to allow the new blood vessel to expand [184, 185].

Neoangiogenesis refers to a newly made vasculature and is a hallmark of cancer. This new vascular supply allows the tumour cells to grow, as it provides a method by which their metabolic substrates can be removed, and to metastasise, encouraging the growth of the tumour and therefore aiding cancer progression.

1.2.5.1. Vascular permeability

Vascular permeability results from acute exposure to vascular permeabilising factors, such as VEGFA, histamine and serotonin. Response to these factors results in a rapid influx of plasma into the tissues [190, 191]. A low level of vascular permeability for molecular exchange is essential for maintaining tissue homeostasis: this is referred to as basal vascular permeability, where the fluid transported from the circulation into body tissues is called plasma filtrate. Capillaries provide molecular exchange throughout the vascular system, including exchange of gases, water and small molecules (like salt and sugars) in major organs like the heart, lungs and kidneys. In basal vascular permeability, small volumes of plasma proteins may also be exchanged [192]. However, vascular permeability is also one of the cardinal features of pathological angiogenesis [193].

VEGFA has two main functions in angiogenesis: as well as stimulating EC proliferation and migration, it causes the walls of blood vessels in microvasculature to become hyperpermeable, resulting in the leakage of fluid containing large amounts of plasma proteins. For this reason, VEGFA has historically been referred to as vascular permeability factor [194]. In cases of acute vascular hyperpermeability, seen in pathological angiogenesis where vascular permeability is increased as part of the angiogenic process, among the plasma proteins contained in the spilled fluid (referred to as an “exudate”) are fibrinogen and members of the blood clotting cascade. Tissue factor protein, expressed by interstitial cells, interacts with these plasma proteins and activates the clotting system, which in turn causes the exudate to clot to deposited fibrin [195, 196]. This is essential for formation of new vasculature, as extravascular fibrin provides an initial matrix to support the growth of new blood vessels and to help establish new stroma [194].

Despite the necessity of vascular permeability in angiogenesis, vascular permeability can become pathological. The interaction of tissue factor protein with plasma proteins forms a gel, trapping water and other solutes to prevent their clearance by either the circulatory or lymphatic system, which ultimately causes oedema [192]. In the absence of the permeability stimulus, fibrin deposits are degraded without consequence, however in cases of pathological angiogenesis, the permeability stimulus is consistently present. Some of the exudate in this case is derived from the new, developing vasculature, which is characterised by fragile vessels that are inevitably leaky [197]. Therefore, the accumulation of more permeable blood vessels results in more plasma protein leakage; as a result, tissues can become oedematous [193]. In the case of neovascular eye diseases, the accumulation of fluid in the eye compounds issues that are already suffered as a result of the disease, such as acceleration of retinal detachment.

1.2.6. Other pro-angiogenic factors

1.2.6.1. Neuropilins

As well as stimulating VEGF receptors, VEGF molecules signal through neuropilins (NRPs), a family of transmembrane glycoproteins with short cytoplasmic domains [198]. There are two major family members, NRP1 and NRP2, and these are further subdivided into 8 sub-family members in humans [199]. They are expressed on a broad range of cell types, including neuronal cells, immune cells, epithelial cells and ECs [200, 201], on which they are differentially expressed: NRP1 is located on arterial endothelium, while NRP2 is expressed on venous and lymphatic endothelium [198].

There is a multitude of evidence for NRP involvement in angiogenesis. NRP1 KO mouse models result in embryonic lethality,

associated with vascular dysfunction [202, 203], whereas NRP2 KO mice show normal vasculature but with defects in neuronal guidance and defective lymphangiogenesis [204, 205]. However, in dual KO models, where both neuropilins are knocked out, the vascular defects observed are severe, suggesting that NRP2 partially compensates for loss of NRP1 [206]. Further evidence for this is that when NRP2 is over-expressed in ECs, an increase in VEGFR2 phosphorylation is observed, as well as pro-migratory and pro-survival effects of VEGFA [199, 207].

Both NRP1 and NRP2 have been implicated in vascular development, primarily as VEGFR co-receptors, thought to enhance the angiogenic and lymphangiogenic roles of VEGFR2 (NRP1/ NRP2) or VEGFR3 (NRP2) [199, 208, 209]. For the VEGFR2/ NRP1 interaction, VEGFA binds to both receptors forming a heterotrimeric complex [210]. When this complex is formed from receptors expressed on the same cell (in *cis*) the outcome is pro-angiogenic; however, when the complex forms with NRP1 on adjacent cells (in *trans*), angiogenesis is inhibited, likely by retaining VEGFR2 at the cell surface [211]. NRP2 binds as a VEGFR2 co-receptor to $VEGFA_{165}$ and VEGFC, promoting EC survival and migration [207]. Although it has not been proven, it is assumed that NRP2 also forms a heterotrimeric complex with VEGFR2 and $VEGFA_{165}$, in both *cis* and *trans* conformations [199].

1.2.6.2. Integrins

The integrins are a family of homologous type I transmembrane cell adhesion molecules, integral in cell mobility and at cell-cell contacts in blood cells, aiding their binding to one another, and with the ECM [212].

Integrins are comprised of two noncovalently-bound transmembrane glycoprotein subunits, alpha (α) and beta (β), arranged in different dimeric complexes, which have varying affinities to extracellular ligands [213]. Integrins bind their ligand with lower affinity and are present in higher

numbers at the cell surface than other cell-surface receptors. This is in order to prevent cells from adhering permanently to the ECM: if attachment of cells to matrix proteins depends upon large numbers of weaker binding points, this is less likely to occur (known as the "Velcro principle") [214]. Integrins have also been found to activate intracellular signalling pathways to communicate to the cell which matrix protein it is bound to, allowing the cell to respond to the ECM [214].

Despite finding the same integrin molecule across different cell types, the ligand-binding specificities can vary between them. This strongly implies that there are additional factors, specific to the cell type where the integrins are present, which can interact with integrins to modulate their activity [213].

Structure

Both α and β integrin subunits consist of a large multi-domain extracellular region, a transmembrane helix and a short cytoplasmic domain. The extracellular portions, more than ten times larger than the cytoplasmic domain, interact with ligands in the ECM, while the cytoplasmic domains mediate integrin interactions with intracellular proteins, including those involved with the cytoskeleton and in signalling [213, 215].

In their active state, integrins have a high affinity for ligand binding. However, in their inactive, low affinity state, integrins present in a closed conformation, where they appear "bent" or "folded" (Fig. 1.6). In this state, their affinity for ligand binding is low, thus they are inactive [213]. Integrin activation, in response to intra- or extracellular stimuli, initially occurs by ligand binding to its extracellular domains or by changes on cytoplasmic tails, causing the molecule to elongate and its legs to separate. This allows the integrin to mediate bi-directional signalling: inside-out signalling, where integrin ligand binding function is initiated by activators such as talin, and outside-in signalling, where the integrin interacts with signal transduction

and cytoskeletal molecules to produce cellular responses induced by ligand binding. These responses lead to cell spreading, retraction, migration and proliferation [212].

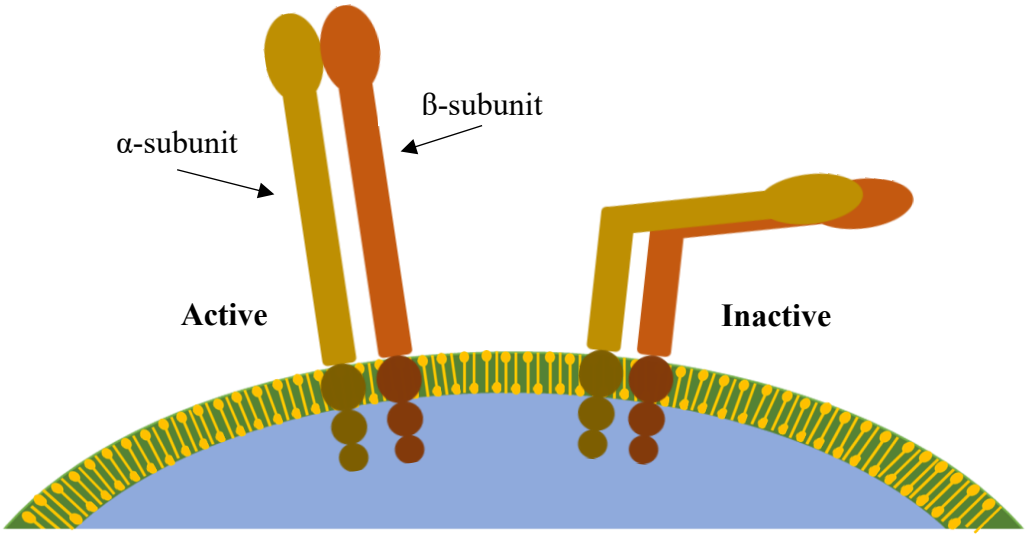

Figure 1.6. **Integrin conformation.** Integrins exist on the cell surface in two distinct states: they appear straight in their active conformation, exposing their extracellular domain and so allowing them to bind extracellular matrix ligands. In their inactive conformation, they appear bent.

Integrin behaviour

The presence of divalent-cation-binding domains in the extracellular parts of both integrin subunits is evident, as the binding between integrins and their ligands is dependent on extracellular divalent cations: either Ca^{2+} or Mg^{2+}, depending on the integrin [214]. The type of cation can influence both the affinity of an integrin for its ligand and the binding specificity.

Multiple integrins can recognise a number of matrix proteins – for example, there are at least eight integrins known to bind fibronectin (a large matrix glycoprotein, which also binds other matrix proteins, like collagen, and heparan sulphate proteoglycans, including syndecans) [216]. At least 24 human integrin heterodimers can be formed from 18 varieties of α subunit and eight types of β subunit and this diversity is further perpetuated by alternative splicing of some integrin RNA [213, 214]. These αβ pairings provide specificity of integrin to ligand, as well as modulating formation of intracellular adhesion complexes and regulating downstream signalling [217].

The most promiscuous integrin heterodimer is β_1 integrin, which can pair with at least 12 α subunits to create numerous distinct integrin heterodimers [214]. β_1 integrins are present on most vertebrate cells and their importance has been demonstrated in multiple mouse models: a mutant mouse model where β_1 integrins cannot be synthesised results in embryonic lethality.

It is known that β_2 subunits form dimers with four different α subunits and are expressed exclusively on white blood cells, in order to fulfil their role in enabling cells to combat infection [214]. These integrins generally mediate cell-cell interactions, rather than participating in cell-matrix interaction, binding ligands on other cells, such as ECs at infection sites. Humans with leukocyte adhesion deficiency do not express β_2 subunits; consequently, their immune cells lack these receptors and they are

susceptible to repeated bacterial infections [214]. β_3 integrins are found on several different cell types, including platelets in the blood. They bind multiple matrix proteins, including fibrinogen: platelets interact with fibrinogen during blood clotting. Individuals who are genetically deficient in β_3 integrins, a condition known as Glanzmann's disease, bleed excessively [213, 214].

Examples of the best-studied integrins include $\alpha_5\beta_1$, ubiquitously expressed and known to bind fibronectin and $\alpha_7\beta_1$, present on muscle cells and found to bind laminin (a large ECM protein, which influences cell differentiation, migration and adhesion). Also, $\alpha_2\beta_3$, which is expressed on platelets and binds fibrinogen, a glycoprotein complex that circulates in the blood and is enzymatically converted, by thrombin, to fibrin for clotting [214, 217].

Integrins in angiogenesis

Integrins are a major driving force behind EC migration, a key component of angiogenesis. β_1 and β_3 work with receptor tyrosine kinases (RTKs) to regulate angiogenesis. Growth factors are, of course, also integral in angiogenesis: for example, VEGFA acts through the RTK, VEGFR2, expressed specifically on ECs, to drive angiogenesis [218, 219].

The most common β subunit in integrin heterodimers is β_1, whose key roles in angiogenesis are well established. *In vivo* models have shown embryonic lethality in mouse models where β_1 is absent, due to their inability to form the more elaborate vasculature necessary for further development. This indicates the integral role for β_1 integrins in EC function in vascular development β_1 *in utero* [220].

An important angiogenesis integrin is α_v integrin, which forms heterodimers with at least five β subunits, providing each with its own unique ligand-binding profile. Importantly, $\alpha_v\beta_3$ and $\alpha_v\beta_5$ have integral roles in

angiogenesis [217]. The endothelial integrin, $\alpha_v\beta_5$, is key in angiogenesis. It is highly upregulated at active angiogenesis sites, such as sites of tissue regeneration, inflammation and tumours: when $\alpha_v\beta_5$ is inhibited, tumour angiogenesis is potently inhibited *in vivo* [221, 222]. It is not highly expressed on vasculature in healthy human tissues, except in chronic disease states where angiogenesis is generally persistent and abnormal when compared with physiological angiogenesis (such as in wound healing), as the process is highly regulated and self-limiting.

There is clear interplay between $\alpha_v\beta_3$ and VEGFR2, evidence for which includes an observed increase in VEGFA-induced mitogenesis during human umbilical vein endothelial cell (HUVEC) attachment to $\alpha_v\beta_3$-specific ligands and ECM ligands, including vitronectin and fibrinogen. Furthermore, there is evidence of interplay between common signalling pathways: ILK (integrin-linked kinase), an adhesion-complex protein, binds cytoplasmic domains of both β_1 and β_3 integrins and is associated with VEGF-induced capillary formation [219, 223]. ILK contributes to Akt activation and, as VEGF activation of protein kinase B/ Akt is integral in angiogenesis, there may also be downstream co-operation through this signal integrator [219, 223, 224].

Expression of $\alpha_v\beta_3$ integrin on ECs is stimulated by angiogenic growth factors, such as FGF2 (fibroblast growth factor 2), TNFα and IL-8. As previously mentioned, it is upregulated on the endothelium in tumours and at sites of inflammation and wound healing. It is required for vascular development, as shown by the lethality of β_3-null mouse models [225], and plays a prominent role in EC survival and migration during angiogenesis [226-229].

The $\alpha_v\beta_5$ integrin promotes a separate angiogenic pathway to that regulated by $\alpha_v\beta_3$ [230, 231]. The $\alpha_v\beta_5$-initiated pathway is dependent on Src kinase and protein kinase c. It is also required for TGFα- and VEGF-

mediated angiogenesis, as evidenced by *in vivo* assays. The conclusion drawn from this is that different angiogenic pathologies may depend on different integrin-mediated pathways [217].

Numerous other cell surface receptors interact with ECM ligands to alter the activation state of integrins; one such example is the syndecan family. Syndecan-2 (SDC2)'s ectodomain core protein is shed from the cell surface under inflammatory conditions and ultimately deactivates β_1 integrin [218].

1.2.6.3. Tie-2 and angiopoietin-2

The angiopoietins are a group of vascular growth factors with key roles in embryonic and postnatal angiogenesis. There are four family members, angiopoietin (Ang)-1 – 4, and roles for Ang-1 and Ang-2 have been identified in angiogenesis. Tie-1 and Tie-2 are RTKs, specifically expressed on the vascular endothelium [232]. Angiopoietins are Tie ligands and, along with VEGFs and their receptors, they form two signalling pathways with the Tie receptors. Upon binding with Tie-2, angiopoietins induce phosphorylation of specific tyrosine residues on the Tie-2 receptor to mediate cell signals. Under basal conditions, the Ang-1/ Tie-2 signalling axis is active, maintaining EC quiescence by stimulating β1-integrin and N-cadherin, and promoting vessel maturation, cell adhesion and survival [233, 234]. However, during angiogenesis, Ang-2 expression is increased and functions as an autocrine-acting ligand of vessel maturation, binding Tie-2 to negatively regulate the Ang-1/ Tie-2 signalling. Working in conjunction with VEGFA, Ang-2 destabilises quiescent blood vessels and allows VEGFA to drive EC proliferation and chemotactic migration, ultimately stimulating angiogenesis [233, 234]. Crucially, the role of Ang-2 is context-dependent; in the absence of Ang-1, it is in fact a weak agonist of Tie-2 [234, 235]. It is thought that this agonistic effect relies on Tie-1, whose mode of

action is not well understood, although it has been shown to be integral in vascular structural integrity [236, 237]. In one study, following Tie-1 cleavage from inflamed epithelium, Ang2 activity switched from agonistic to antagonistic [238, 239], while in another, Ang-2 antagonistic activity was absent in mice deficient in Tie-1 [239, 240].

Currently, therapeutics to attenuate pathological angiogenesis target the VEGFA pathway (detailed in 1.4). Another approach currently being explored is to target the angiopoietin-Tie pathway. Ang-2 blockers have been explored as a treatment option for tumour angiogenesis, however these have limited efficacy beyond this (for example, in advanced metastasis), with no plans for their use in neovascular eye diseases [234]. A number of small-molecule tyrosine kinase inhibitors that inhibit Tie-2 are currently used in the clinic. However, many have multiple targets, also inhibiting VEGFR2 and other tyrosine kinase molecules, meaning it is not possible to determine the specific contribution of Tie-2 inhibition to the efficacy of these drugs [234, 241-243]. Moreover, studies comparing Ang-2 inhibitors with Tie-2 inhibitors have reported similar efficacy in tumour models, determining that there is no superiority of Tie-2 inhibitors to Ang-2 inhibitors [234, 244, 245].

1.2.6.4. Fibroblast growth factor

The fibroblast growth factor family comprises at least 20 cell signalling molecules [246] involved in a number of physiological processes, including angiogenesis [247]. FGF1 and FGF2, have been shown to induce angiogenesis in a number of tissues, including retinal, corneal and choroidal in the eye [248], and in different diseases (such as colon cancer) [249] and endometriosis [250]. One of their defining properties is that they bind with high affinity to heparin and to heparan sulphate proteoglycans (HSPGs), such as syndecans, located on the surface of most cells and within the ECM [246, 251]. This creates a reservoir of FGFs secreted by ECs, macrophages

and fibroblasts that can be released locally in a regulated manner – such as by the action of heparanases [246]. HSPGs serve as co-receptors for FGF, shown to modulate the effects of FGF *in vitro* and *in vivo* [252], and several studies have shown that heparin is required for high affinity binding of FGF to FGF receptors (FGFRs) in cells without HSPGs [246, 253, 254].

FGFRs are four structurally related RTKs (FGFR1, FGFR2, FGFR3 and FGFR4). FGF1 binds to all FGFRs, while FGF2 binds only to FGFR1, FGFR2 and FGFR4. FGF activation of these transmembrane tyrosine kinases and their coupled intracellular signalling pathways stimulates downstream signalling through phospholipase C-γ1 (PLC-γ1), Ras-mitogen-activated protein kinase (MAPK) and phosphoinositide 3-kinase-Akt (PI3K-Akt) pathways [255-257]. To initiate signalling, FGF2 interacts with cell surface HSPGs and FGFRs in a ternary complex, causing FGFRs to dimerise and changing the receptor's structural conformation. This will then allow transphosphorylation of multiple cytoplasmic tyrosine residues, leading to activation of downstream signalling pathways that lead to cell proliferation, survival and differentiation [257, 258]. FGFRs mediate the stimulation of cellular metabolism by FGFs, and so many FGFR isoforms bind several FGFs, with HSPG receptors providing further specificity [255]. FGF1 is less well characterised than FGF2, though it has been implicated in cell survival [246]. FGF2 possesses mitogenic and cell survival actions and elevated levels have been detected in serum from cancer patients, indicating its involvement in angiogenesis in tumour development [246, 259].

1.3. Angiogenesis in disease

Angiogenesis is a characteristic of a number of pathologies: as well as macular degeneration and diabetic retinopathy, excessive angiogenesis can contribute to cancer, rheumatoid arthritis and idiopathic lung fibrosis. Insufficient angiogenesis can lead to impaired tissue repair, for example in ischaemic tissues [260, 261].

1.3.1. Cancer

Neovascularisation is a key feature in solid tumour formation, as tumours require a blood supply to grow and metastasise. Solid tumours can produce VEGFA, among other pro-angiogenic growth factors, to initiate angiogenesis and they can stimulate other neighbouring cells to produce their own pro-angiogenic factors [262]. Lymphangiogenesis is also a feature of cancer, to enable solid tumour growth and metastasis [263]. When a cancerous tumour reaches 1-2mm in diameter, it requires its own vascular supply to continue its growth. Anti-angiogenesis therapies are used to slow cancer growth and shrink tumours [264], in conjunction with chemotherapies.

Commonly used anti-angiogenesis therapies in cancer treatment include anti-VEGF antibody therapies and tyrosine kinase inhibitors. Bevacizumab is the most widely used anti-VEGF drug, administered by intravenous injection and targeting VEGFA directly [265]. This is used in combination with chemotherapy treatments for many types of cancer, including metastatic colon cancer, non-squamous, non-small cell lung cancer and breast cancer [266].

Protein tyrosine kinase (PTK) inhibitors are a form of targeted therapy, used to block downstream signalling of VEGFR, preventing angiogenesis initiation. A commonly used inhibitor is sunitinib, a treatment for kidney cancer, neuroendocrine tumour of the pancreas and

gastrointestinal stromal tumour, a rare form of stomach cancer [267]. Other anti-angiogenesis drugs include thalidomide and its derivative, lenalidomide (brand name Revlimid), which interfere with cell-cell signalling to prevent neovascularisation. These drugs are used in multiple myeloma and lymphoma: "blood cancers" [268].

1.3.2. Rheumatoid arthritis

Rheumatoid arthritis is an inflammatory autoimmune disease affecting the joints. This disease also requires a vascular supply, to allow for the excessive migration of circulating leukocytes to patients' joints [269]. Synovial tissue fibroblasts in rheumatoid arthritis that become exposed to toll-like receptor endogenous ligands and pro-inflammatory cytokines, produced by neighbouring macrophages, transform into "tumour like" cells [270]. Thus, in the active state of the disease, these fibroblasts are activated by inflammatory mediators to secrete a range of pro-angiogenic factors [271]. This includes chemokines and cytokines, as well as adhesion molecules and matrix metalloproteinase, plus growth factors, with VEGFA being a key one [272].

VEGFA-mediated angiogenesis plays a crucial role in the early stage of arthritis disease development [273], while the combination of all of these factors results in angiogenesis in the joints, exacerbating disease severity. Although anti-VEGF biologicals are not commonly used in rheumatoid arthritis treatment, anti-TNF-α biologicals (such as infliximab) are routinely used immunosuppressants, which help to prevent further damage to joints caused by the immune system. TNF-α is a promoter of angiogenesis and cell proliferation [274], thus the use of anti-TNF-α therapies could also suppress angiogenesis [275].

1.3.3. Idiopathic pulmonary fibrosis (IPF)

Idiopathic pulmonary or lung fibrosis is an interstitial lung disease, characterised by progressive scarring of the lung tissue and associated loss of pulmonary function, resulting in respiratory failure due to reduced gas exchange capacity [276-278] and, ultimately, death [279, 280]. Repetitive epithelial microinjury leads to myofibroblast activation and the underlying pathology is known to involve numerous cells of the vasculature, whose interaction is regulated by angiogenic promoters and inhibitors, along with growth factors [279]. Pulmonary hypertension is an established factor for overall prognosis in patients with lung fibrosis [279].

Angiogenesis and vasculogenesis both feature in this disease and VEGFA is involved in both processes [281-283]. VEGFA promotes fibrosis through angiogenesis and works in collaboration with TGF-β to increase ECM production by fibroblasts [284]. Although the bleomycin model of pulmonary fibrosis differs from human idiopathic lung fibrosis, in that the epithelial injury in rodents results in differing vascular changes (neovascularisation rather than angiogenesis), it has been used to show that inhibition of VEGFA reduces fibrosis [276, 284].

The two main drug treatment options for idiopathic pulmonary fibrosis are PTK inhibitors, nintedanib (a multiple tyrosine kinase inhibitor) and pirfenidone, both of which have antifibrotic and antiangiogenic properties, downstream of VEGFA and other growth factors [285]. Although these therapies slow disease progression [280, 285], they are not a cure and lung transplant is recommended for all patients [286].

1.4. Current anti-angiogenic therapies

1.4.1. Targeting VEGFA

Anti-VEGF therapies are commonly used in treating wet-AMD and diabetic retinopathy (outlined in Table 1.3). This type of therapy overcomes adverse effects like irreparable retinal tissue damage from laser treatments and glaucoma or cataract occurrence as a result of corticosteroid intravitreal injections. The most commonly used anti-VEGF drugs are ranibizumab (trade name: Lucentis), aflibercept (also known as Eylea) and bevacizumab (or Avastin). Ranibizumab is a monoclonal antibody fragment (Fab, fragment antigen-binding) which directly inhibits human VEGFA by binding to the receptor binding sites on biologically active forms of VEGFA. This prevents interaction of VEGFA with VEGFRs on ECs, inhibiting VEGFA activity and reducing angiogenesis, cell proliferation and vascular permeability. Bevacizumab is a recombinant humanised monoclonal antibody (full length) which is effective against all isoforms of VEGFA. This antibody also binds directly to the VEGFA molecule, preventing receptor binding and therefore VEGFA-driven pro-angiogenic effects. Aflibercept is a recombinant protein, comprising of two VEGFRs and a human Fc region. It acts as a decoy receptor for VEGFA, preventing it from binding with VEGFR1 or VEGFR2 on EC surfaces, therefore suppressing vascular permeability and angiogenesis.

In the case of each therapy, VEGFA binding with its receptors is prevented and the pro-angiogenic effects of VEGFA are suppressed. As the main pathway responsible for angiogenesis in diabetic retinopathy and wet AMD, down-regulation of the VEGFA pathway can be very effective in preventing disease progression and help to delay vision loss in patients with either of these diseases.

Table 1.3. Summary of most commonly used anti-VEGF medications in the UK and USA.

Drug/ trade name	Type of drug	Indication(s)	Cost per injection (GBP)
Ranzibizumab/ Lucentis	Humanised antibody Fab fragment	Wet AMD, Diabetic retinopathy	551
Aflibercept/ Eyelea	Soluble decoy receptor	Wet AMD, Diabetic retinopathy	816
Bevacizumab/ Avastin	Human monoclonal IgG1 antibody	Colorectal cancer, Wet AMD (off-label), Diabetic retinopathy (off-label)	20
Brolucizumab/ Beovu	Humanised single-chain antibody fragment	Wet AMD	816

1.4.2. Limitations of current therapies

There is no universal definition for non-responsiveness to anti-VEGF medications – however, if successful, they should prevent further vision loss in patients since eyesight generally cannot be restored at this point in disease progression. A major drawback of anti-VEGF therapies is the lack of patient response; the response rate is approximately 50%, meaning that at least half of treated patients see no improvement in their condition.

Furthermore, because anti-VEGF treatments do not modify the underlying disease, neovascularisation that has been initiated in response to this underlying disease is still upregulated by the immune system. This means that during the time between anti-VEGF treatments, angiogenesis is promoted and although most anti-VEGF therapies block VEGFA binding with VEGFR2, there is an upregulation of other pro-angiogenic factors, resulting in new blood vessel formation [287, 288].

These other pro-angiogenic factors can be other VEGF family members, though it has also been found that despite the VEGFA-induced signalling cascade being the primary mechanism of angiogenesis in diabetic retinopathy, other VEGFA-independent pathways have been identified. For example, the pathway involving synthesis of lipid oxidation products [56]. Consequently, blocking VEGFA-induced angiogenesis may lead to the up-regulation of other pro-angiogenic pathways and therefore therapies will not attenuate the disease in patients.

Tolerance also becomes a problem for many patients, as these drugs must be administered long-term. The result is that the effects of the drugs are reduced in patients, meaning they require a higher dosage over time, which increases the risk of adverse effects associated with these therapies.

Patient perception and compliance is also a factor in why anti-VEGF therapies fail. If patients deem that there is no improvement in their condition, this can affect them returning for further treatment. Although this

is not a direct failure of the therapy, it perhaps does suggest that patients would be more likely to adhere to a treatment regime if there was a treatment that was more efficacious and resulted in improvements to vision more quickly [289].

The high cost of these drugs presents another problem. On average, each dose of anti-VEGFA drug costs approximately 750 GBP and patients generally require 12 doses to complete a treatment course. Furthermore, specialist ophthalmologists must administer the treatments to patients, rather than a general practitioner, which is an additional cost. Therefore, this is not a widely-available treatment due to its inaccessibility to some patients [290].

The significant problems associated with anti-VEGF therapies clearly demonstrate a niche in the market for a novel therapeutic, with an alternative target, which will be effective against numerous pro-angiogenic factors and not only against VEGFA.

1.4.2.1. Cilengitide

It is worth mentioning a failed therapeutic intended to treat glioblastoma by inhibiting $\alpha_v\beta_3$ and $\alpha_v\beta_5$ integrins (discussed in 1.2.6.2), cilengitide. Integrins are a family of molecules implicated in a number of processes, including tumour angiogenesis and invasion [291, 292]. Many integrin receptors are active in both normal and cancerous cells, making integrins difficult to target. The $\alpha_v\beta_3$ integrin is involved in angiogenesis and cell migration and proliferation. It is expressed at low levels in normal cells and overexpressed in various cancer cells, including glioblastoma. Preclinical *in vitro* and *in vivo* studies showed cilengitide to be a potent inhibitor of angiogenesis and an inducer of EC apoptosis, by inhibiting interaction between $\alpha_v\beta_3$ and its ECM ligands [293], although its value of adding cilengitide to radiotherapy and temozolomide was inconsistent [294, 295]. In its phase 3 clinical trial, cilengitide was found to not improve survival in patients compared to the control group, leading the drug manufacturer to stop further development of it as a cancer treatment [293].

There are very few integrin antagonists available clinically, due to the aforementioned difficulties with targeting integrins. In this case, targeting of $\alpha_v\beta_3$ integrin is complex due to opposing effects of cilengitide according to its dose; it was been reported that low doses stimulate blood vessel growth and tumour angiogenesis, whereas higher doses have an inhibitory effect [291, 296]. Only two different dosages were offered in the phase 3 trial, which may not fully display the duality effect of the compound [291]. Furthermore, although it has been determined (by way of metabolic imaging and tissue analysis), that cilengitide reaches its target, analysis of patients with glioblastoma treated with radiotherapy, temozolomide and cilengitide did not see a change in progression pattern compared with historical controls, suggesting the drug lacks anti-invasive properties [297]. Cilengitide also produces unfavourable pharmacokinetics: its short half-life (2-4 hours) and

twice-weekly administration make it unsuitable for long-term administration to patients, especially as a first-line treatment.

1.5. Other forms of neovascularisation

1.5.1. Vasculogenesis

Vasculogenesis is a form of neovascularisation, defined as the *de novo* formation of ECs from progenitor cells [298]. The angiogenic process generally follows this, though can sometimes can take place alongside vasculogenesis [299]. The key feature of vasculogenesis is that, unlike in angiogenesis, blood vessels do not form from pre-existing vasculature. They form when endothelial precursor cells (angioblasts) migrate and differentiate into ECs in response to growth factor secretion, establishing new vessels in blood islands during embryonic development [300, 301]. These islands extend into vascular trees and are then modified by angiogenesis [299]. Vasculogenesis can also occur in adults, for example during tumour growth, neovascularisation after trauma (such as cardiac or retinal ischaemia) and, determined more recently, in endometriosis [301, 302].

Genetic studies demonstrate the necessity of VEGF and VEGF receptors in vasculogenesis: embryos that lack VEGFR2 die early in development due to an inability to form vessels and blood cells and therefore to initiate vasculogenesis and haematopoiesis [303, 304]. Embryos that are deficient in VEGF also suffer severe vascular defects and so do not survive; even deletion of one VEGF allele results in embryonic lethality [143, 182]. In embryos lacking VEGFR1, vascular defects are also evident, resulting in lethality. In this model, instead of angioblasts localising to the periphery, they congregate in central regions of the blood islands [305], suggesting there is EC overgrowth rather than inhibition.

1.5.2. Lymphangiogenesis

The lymphatic system is involved in physiological processes such as homeostasis, metabolism and immunity. Issues with lymphatic vessel

formation, by way of impaired or excessive formation, is associated with oedema, rheumatoid arthritis, psoriasis and impaired wound healing [306].

Lymphangiogenesis is the formation of new lymphatic vessels from pre-existing ones. The establishment of lymphatic vasculature arises after the cardiovascular system has developed, approximately at embryonic weeks 6-7 [307, 308]. Similarly to angiogenesis, it occurs physiologically in embryonic development and wound healing, and also appears in certain pathologies, including cancer [309]. Like angiogenesis it involves cell proliferation, sprouting, migration and tube formation. VEGFC is predominantly responsible for lymphangiogenesis, with its closest relative (structurally and functionally) being VEGFD, also implicated in lymphangiogenesis [310]. Lymphatic ECs, upon which lymphangiogenesis relies, depend on VEGFR2 and VEGFR3 signalling, driven by pro-lymphangiogenic factors VEGFC [311] and VEGFD [310]. Upon stimulation by mature VEGFC, VEGFR3 can form a homodimer to activate ERK1 and ERK2 pathways [306]. Alternatively, VEGFR3 can form a heterodimer complex with VEGFR2, which activates AKT signalling [144, 306]. The role of NRP2 in lymphangiogenesis has been linked specifically to the growth of small lymphatic vessels during development, where it regulates vessel sprouting following generation of large lymphatic vessels from veins [199, 209, 312]. Here, NRP2 acts as a co-receptor for VEGFR3 binding [209], either with VEGFC in a heparin-independent manner, or with VEGFD in a heparin-dependent manner [146].

VEGFR3 is expressed on all endothelia during the early developmental stages and is necessary for the formation of the cardiovascular system [307, 313]. After this, when the lymphatic system begins to develop, VEGFR3 is exclusively expressed on lymphatic ECs and fenestrated blood vessels present in endocrine organs (the thyroid, adrenal glands and pancreas) [314]. The lymphangiogenic process is comparable to

that of angiogenesis, regulated by VEGFA through its activation of VEGFR2 and NRP1 [260], as are the cellular events that are characteristic of angiogenesis, including differentiation of ECs into tip and stalk cells [315]. However, the molecular mechanisms involved in lymphangiogenesis are less well-characterised [209] and there are clear differences between vascular ECs and lymphatic ECs, illustrated by their distinct gene expression and functional characteristics [316], plus their independent specification and development during embryonic growth [317].

1.6. Syndecans

Heparan sulphate proteoglycans are a class of glycoproteins comprising a core protein with linear glycosaminoglycan (GAG) chains attached. They are ubiquitously expressed across all tissue types in animals that display true tissues (eumetazoa) [318]. The syndecan family are type-I transmembrane HSPGs: cell surface proteins covalently coupled via serine residues to GAG chains, HS or chondroitin-sulphate, and linked to a short cytoplasmic domain by a single transmembrane domain (Fig. 1.7) [319]. GAG chains comprise repetitions of disaccharides (anywhere between 50 and 200 repetitions), the composition of which differ between HS and chondroitin-sulphate chains. An important characteristic of GAG chains is that they can be sulphated, providing them with a negative charge, which is key to syndecan functions and structure. The extent and type of sulphation depends on the identity of the core protein and the cell type expressing it. The negative charge of the chains means that they repulse each other and so can extend into space, increasing their area of action. They can also interact and bind a large range of positively charged molecules, including matrix proteins, growth factors, chemokines and cytokines [320]. Syndecan cytoplasmic domains also interact with a number of cytoskeletal proteins [321-323]. Syndecan transmembrane domains are necessary for some syndecan functions, which depend on syndecan transmembrane self-association [324]. The single-pass transmembrane domain of all syndecans contains a conserved motif, GxxxG, implicated in syndecan homodimerisation at the cell surface, and in retaining cholesterol in lipid rafts [321, 325].

The short cytoplasmic domains of the syndecan family members are divided into three identifiable regions: the membrane-proximal C1 and membrane-distal C2 regions are highly conserved across the family members and flank a central variable region (V), which lacks the homology seen in the C regions [326, 327]. This homology across both family members and

species makes invertebrate syndecan molecules recognisable by these two regions alone [326].

Although the syndecan cytoplasmic domains lack fundamental enzymatic activity, the C regions have been implicated in cell trafficking: syndecans can both interact with the actin cytoskeleton and signal through binding of specific proteins [326]. Their C2 regions allow binding with PDZ-containing proteins (like synbindin, synectin, syntenin) [328-330], while their C1 region interacts particularly with actin-binding proteins (such as ezrin and moesin) [331]. Less is known about the V region, although its diversity between family members is clear across species.

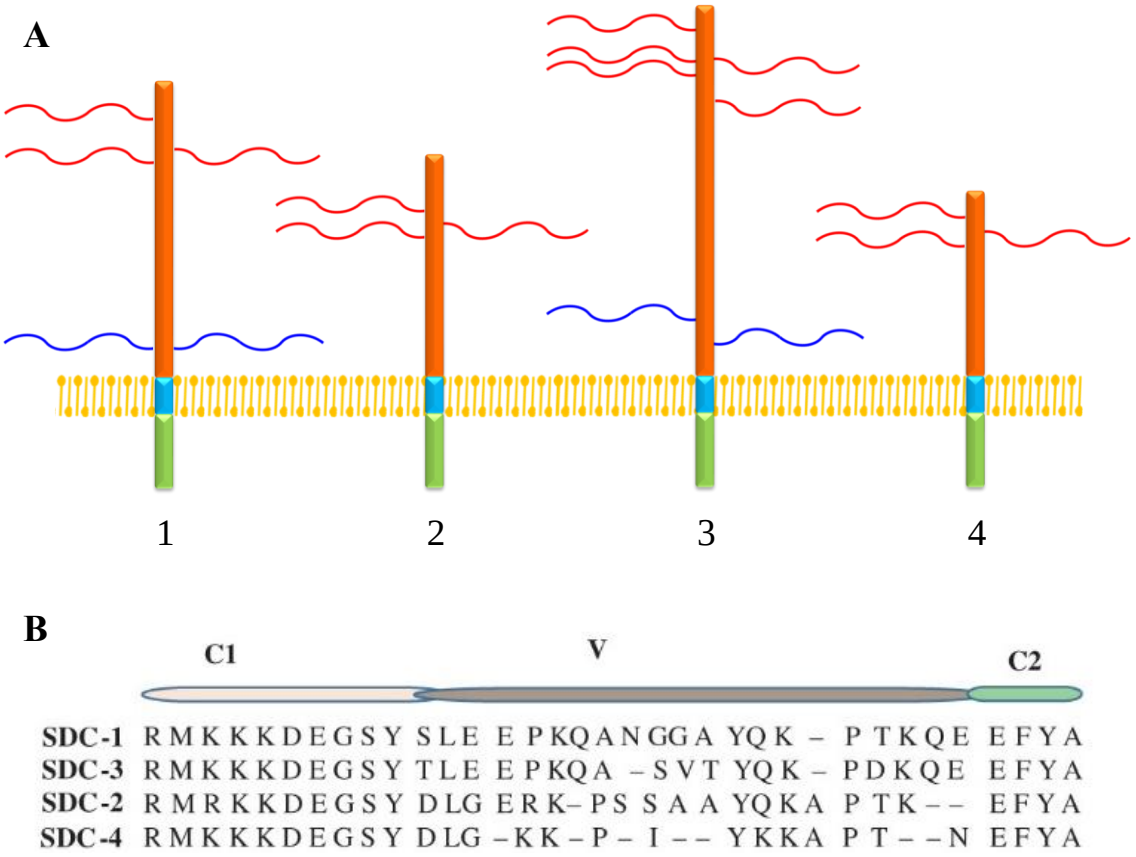

Figure 1.7: **The syndecan family. (A)** Shown in orange are the syndecan ectodomains, projecting outside the cellular space. These molecules are composed of a core protein bound to HS chains (shown in red) and, in the case of syndecan-1 and -3, chondroitin-sulphate chains (shown in blue). In light blue are shown the transmembrane domains and in green, the cytoplasmic domains. **(B)** Amino acid sequences of the human syndecan cytoplasmic domains. The C1 and C2 regions are highly conserved across all syndecans; the variable (V) regions are specific to each different syndecan molecule. Taken from: *Gopal, S., et al., Syndecan receptors: pericellular regulators in development and inflammatory disease. Open biology, 2021. 11(2): p. 200377-200377.*

Each member of the syndecan family has a distinctive expression pattern. SDC1 is primarily expressed on epithelial and plasma cells; SDC2 is expressed on ECs, fibroblasts, neurons and smooth muscle cells; SDC3 is expressed mainly on cells of the nervous system and chondrocytes; SDC4 is ubiquitously expressed. Family members can be grouped based on their primary structure into syndecan-1 and -3, or -2 and -4, wherein each pair shares a large amount of homology [332]. SDC2 and -4 have a shorter polypeptide chain compared to -1 and -3, and are substituted by HS chains only, while SDC1 and -3 can possess chondroitin-sulphate chains in addition to HS chains. Syndecans are involved in various physiological processes, including tumour development, cell migration and wound healing (SDC1); cell adhesion (SDC2); angiogenesis and feeding behaviour (SDC3); wound healing, directional cell migration and cytoskeleton assembly (SDC4).

1.6.1.1. Syndecan shedding

As with other proteoglycans, syndecan core proteins are thought to have distinct binding abilities and engage in specific protein–protein interactions, thus determining functional specificity of various syndecan-dependent biological processes [333, 334]. At the cell surface, syndecans can undergo proteolytic cleavage, or “shedding”, where they are enzymatically cleaved from the cell surface at a juxtamembrane region by enzymes known as sheddases [335]. In the case of syndecans, this cleavage is matrix metalloproteinase-dependent [336, 337]. A number of intracellular signalling pathways are involved in syndecan shedding, including the protein kinase C (PKC), PTK and MAPK pathways [336]. Activation of epidermal growth factor (EGF)- and thrombin receptor-mediated shedding aligns with the MAPK signalling cascade; on the other hand, PMA- and cellular stress-inducing shedding initiate the PKC pathway [338]. PTK contribution has been determined through both chemical inhibitor studies, where tyrosine

kinase inhibition prevents syndecan shedding, and through bacterial virulence studies. A number of pathogens have been found to stimulate their own pathogenesis by causing excessive syndecan shedding, through virulence factors such as α- and β-toxins that cause the activation of syndecan shedding through PTK-dependent intracellular signalling pathways [338, 339].

1.6.1.2. Syndecans in angiogenesis

Roles for all members of the SDC family have been identified in angiogenesis, particularly SDC1, -2 and -4. SDC1 has been shown in a variety of cell types to associate directly via its ectodomain with $\alpha_V\beta_3$ and $\alpha_V\beta_5$ integrins, leading to their activation [340-342]. In human microvascular ECs, immunoprecipitation experiments showed co-precipitation of β_3 and β_5 integrins with SDC1, and that by silencing SDC1 expression, these cells were unable to spread on vitronectin (a ligand of $\alpha_V\beta_3$) [343]. Previously, the same group showed that fibroblasts seeded on SDC1 antibody would spread and activate $\alpha_V\beta_3$ and $\alpha_V\beta_5$, even in the absence of integrin ligands [341]. Subsequently, this group determined the mechanism through which SDC1 activates $\alpha_V\beta_3$ and $\alpha_V\beta_5$ integrins. SDC1 was co-precipitated with $\alpha_V\beta_3$ and IGF1R (insulin like growth factor receptor 1) from ECs in a way that suggested the integrin and SDC1 were acting as a docking site for IGFR1. Furthermore, they showed this ternary complex was present on focal contacts when cells were plated on vitronectin [344]. The proposed model to explain this is that during the early phase of angiogenesis, SDC1 is necessary for VEGF-induced integrin activation, in its ternary complex with $\alpha_V\beta_3$ and IGFR1 [345].

SDC2 is essential for developmental angiogenesis, demonstrated by Chen *et al.* in 2004, wherein SDC2 knockdown (KD) resulted in significant impairment of developmental angiogenesis. Angiogenic sprouting could be

restored following injection of exogenous SDC2 cDNA, either zebrafish or human, demonstrating functional conservation across species [346]. Although the exact mechanism behind SDC2's pro-angiogenic function is not clear, the cytoplasmic domain was clearly shown in this study to be important. Following this, Whiteford *et al.* have provided compelling evidence that the SDC2 ectodomain is shed from the cell surface and interacts with the PTPR, CD148, to regulate angiogenesis [218, 347]. SDC2 may also play a role in pathological angiogenesis, as it was found to be upregulated on blood vessels in gliomas and from normal brain, despite not being present in the surrounding parenchyma [348]. While this study showed that SDC2 KD in murine vein ECs caused a decrease in cell migration on fibronectin and in tube formation on matrigel, indicative of SDC2 involvement in angiogenesis, pro-angiogenic factors known to be upregulated in gliomas (EGF, bFGF and VEGF) were shown to promote SDC2 shedding from these cells [348]. Further studies have shown shed SDC2 to promote angiogenesis in murine vein ECs [348]. Approximately 80% of all HSPGs expressed on the cell surface of human microvascular ECs are SDC2, and this expression increases in response to angiogenic stimuli and is dependent on the type of matrix on which cells are seeded. In another study, downregulation of SDC2 resulted in increased cell migration, while also impairing the ECs' ability to form capillary structures on matrigel [349], suggesting an integral role for SDC2 in angiogenesis. Together, the evidence suggests that the vascular function of SDC2 results from a complicated balance of its functions on the cell surface, the regulation of its shedding and a possible autocrine or paracrine role as a shed molecule [320, 348, 349].

Most investigations into SDC3 focus on its effect on behaviour, due to its presence in the nervous system. However, it is also expressed on the endothelium of various vascular beds, including joints, dermis and the cremaster muscle [350]. Regarding its role in angiogenesis, SDC3 knockout

(KO) mice are viable and develop normally, and the Whiteford group completed a study wherein SDC3's extracellular core protein (lacking GAG chains) can produce potentially therapeutic effects in pathologies where angiogenesis is increased. Recombinant bacterially-derived SDC3 extracellular domain protein was shown to significantly inhibit angiogenesis in the *ex vivo* aortic ring assay, and to inhibit skin and brain EC tube formation and cell migration through collagen in 2D and 3D [351]. These data support the idea that shed syndecan core proteins can act as important effectors of cell behaviour.

The first clear evidence of a functional role of SDC4 in angiogenesis came from the work of Echtermeyer *et al.* in 2001. They generated a SDC4 KO mouse that showed significant delays in wound healing in a model of skin injury. Although the number of newly generated vessels populating the healing tissue was unaffected by the lack of SDC4, the vessels were smaller compared to wild-type mice [352]. SDC4 is essential in mediating the pro-angiogenic effects of thrombospondin-1; a 2008 study proposed a model whereby two heparin-binding sequences contained within thrombospondin-1 can compete with fibronectin for interaction with SDC4, resulting in interference with SDC4-mediated EC adhesion [353]. *In vitro* experiments have also implicated SDC4 in signalling of pro-angiogenic molecules [354-356], such as FGF. As well as facilitating the FGF2/ FGFR1 interaction, the SDC4 ectodomain seems to have a key role, as deletion mutants of this portion (lacking the V or the C2 regions) fail to promote an effective intracellular response to FGF2 [356-359].

Together, the evidence suggests pro-angiogenic roles for full-length extracellular domains of SDC1, -2 and -4, while the core proteins of SDC2 and SDC3 demonstrate inhibitory effects.

1.7. Receptor-type protein tyrosine phosphatases

Reversible protein tyrosine phosphorylation is a key regulatory mechanism controlling a range of processes, including cell proliferation, differentiation, communication and adhesion [360]. Two major families control tyrosine phosphorylation: PTKs and protein tyrosine phosphatases (PTPs), and these families can each be sub-divided into receptor and non-receptor subtypes. The PTK family is made up of cell surface proteins that bind extracellular ligands (such as growth factors and cytokines) to initiate intracellular tyrosine phosphorylation-dependent signal transduction. Similarly, PTPRs possess intracellular domains with phosphatase activity that facilitates downstream signalling. Of the 37 classical human PTPs, 21 are receptor-like transmembrane proteins and 16 are intracellular non-transmembrane proteins [361-363]. PTPRs have a single transmembrane spanning domain, variable N-terminal extracellular regions (which display sequence homology to cell adhesion molecules [364]), and either a single or tandem intracellular phosphatase domain. They are grouped into eight sub-families (R1-8) as shown in Fig. 1.8.

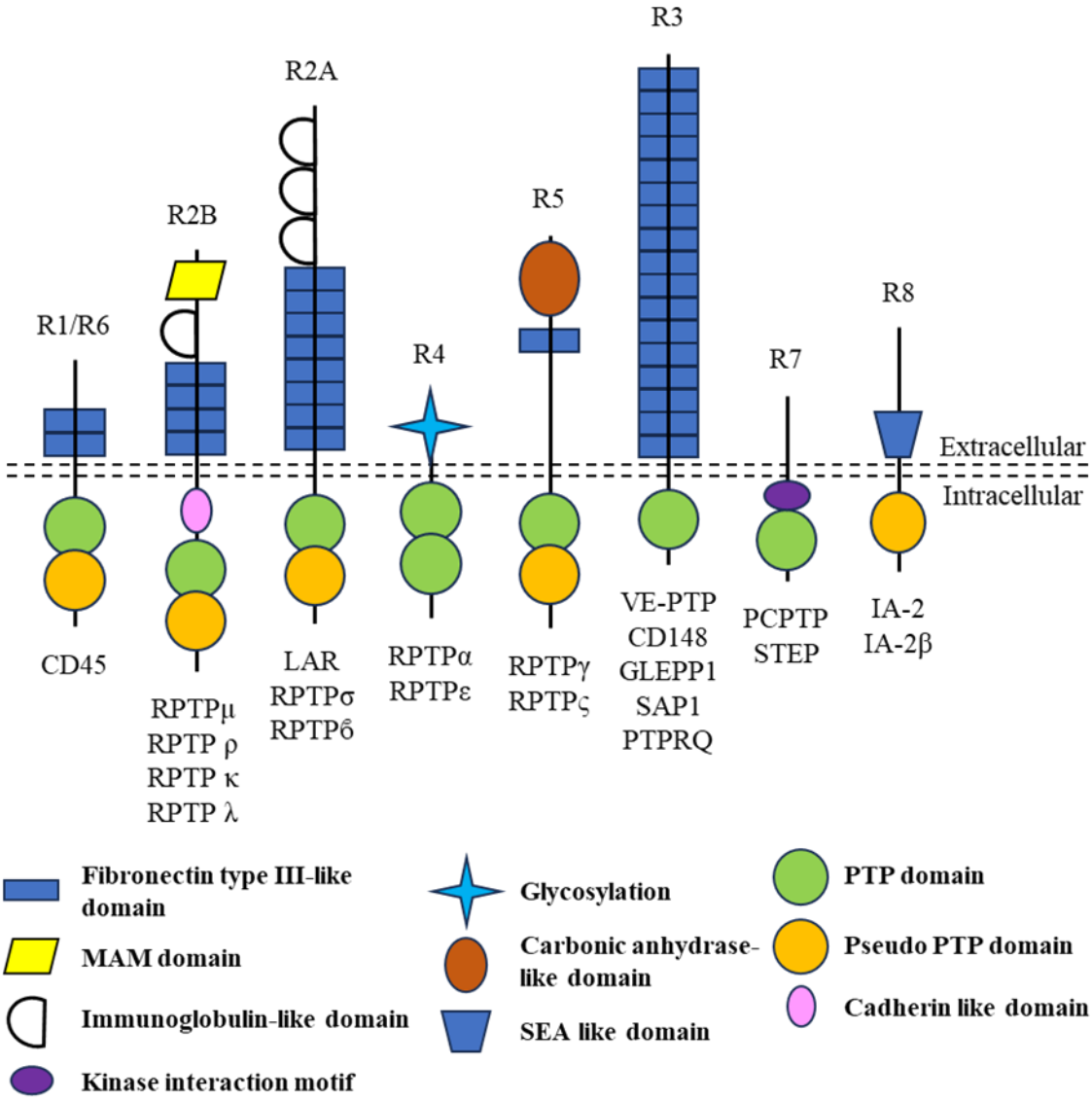

Figure 1.8. **Schematic diagram of the eight PTPR subfamilies.** Redrawn from: *Johnson, K. and D. Vactor, Receptor Protein Tyrosine Phosphatases in Nervous System Development. Physiological reviews, 2003. 83: p. 1-24.*

The structural features determining this grouping include presence of a fibronectin type-III (FNIII) domain and an Ig domain, and number of PTP domains [364], among others. R3 subfamily members, specifically, exhibit various numbers of FNIII domains and contain a single intracellular phosphatase domain. Briefly, type I PTPRs contain a single extracellular FNIII domain and two cytoplasmic phosphatase domains. Type IIa subfamily members have large extracellular domains made up of three NH_2-terminal Ig domains and eight FNIII domains, while type IIb members have an extracellular meprin-A5-PTP (MAM) domain, a single Ig domain, and multiple FNIII domains. Members of the type III subfamily have multiple extracellular FNIII domains but with only one cytoplasmic phosphatase domain. Type IV PTPRs have the shortest, often highly glycosylated, extracellular domains. Type V extracellular domains have a carbonic anhydrase domain, linked to one FNIII domain. Type VII PTPRs have a single cytoplasmic domain and a short extracellular domain. PTPRs in the type VIII subfamily contain a RDGS adhesion recognition motif, and are thought to be catalytically inactive [365].

1.7.1. CD148

The PTPR, CD148 (PTPRJ; density enhanced phosphatase-1, DEP1 [366]) is a member of the R3 subfamily of PTPRs, expressed across a broad range of vascular cells, including ECs, fibroblasts and platelets (on which it is the only RPTP expressed). It is made up of 3 distinct domains (as shown in Fig. 1.9); its extracellular domain consists of 9 FNIII repeats and within the first 5 repeats resides the binding domain for CD148 ligands, such as shed SDC2 and thrombospondin, suggestive of roles for CD148 in angiogenesis, platelet activation and thrombosis [367]. The cytoplasmic domain contains the single catalytic phosphatase domain, giving CD148 its phosphatase activity.

With regard to its function, CD148 is associated with contact inhibition of VEGF-induced EC growth [368] and has been implicated in angiogenesis, as disruption of the *PTPRJ* gene in transgenic mice results in embryonic lethality with severe defects in vascular organisation and increased EC proliferation leading to enlarged vessels [369]. Expression of wild-type CD148 inhibits cell proliferation in HeLa cell lines, while mutations in its extracellular domain impair its dimerisation in the plasma membrane and prevent its inhibition of cell proliferation, despite its catalytic activity remaining intact [370]. CD148 regulates density-dependent inhibition of cell growth, demonstrated by its increased expression with increasing cell density observed in WI-38 human embryonic lung fibroblasts [366]. There is mounting evidence that CD148 functions as a tumour suppressor: deletions and mutations in *PTPRJ* have been identified in a number of human cancers [371, 372] and its expression is down-regulated in many cancer cells, while its forced expression inhibits their malignant phenotype [373-375]. This anti-proliferative activity is likely due to CD148's direct negative regulation of kinases such as platelet-derived growth factor receptor (PDGFR) [376], Src [377], VEGFR2 [378] and the p85 subunit of PI3 kinase [379].

cDNA encoding CD148 was isolated from a HeLa cell library. It was found to have two splice variants; one encoding the full length molecule and a shorter variant comprising the first five fibronectin repeats from the extracellular domain (Fig. 1.9), discussed at length in Chapter 5, Fig. 5.1 [380]. The shorter variant (termed CD148 short form, CD148SF) is expressed by WI-38 human embryonic lung fibroblasts and is an inhibitor of angiogenesis [347, 366].

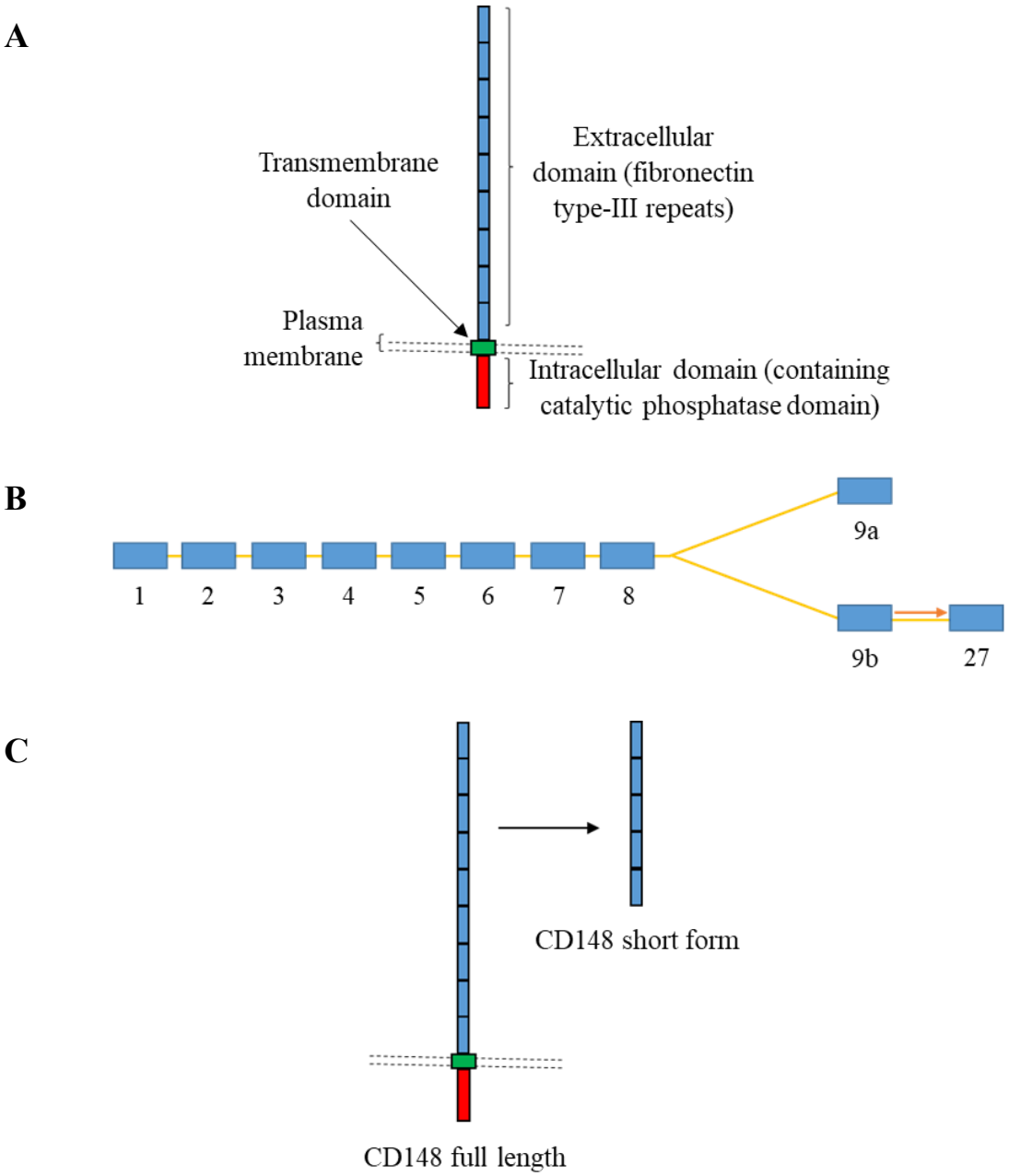

Figure 1.9. **Schematic diagram of CD148, showing its overall structure. (A)** Full-length CD148 is made up of three distinct parts: the intracellular, transmembrane and extracellular domains. **(B)** The two mRNA variants of CD148 produced by alternative exons (9a/ b). 9a encodes the spliced variant (3193bp), 9b encodes full-length CD148 (7854bp). Redrawn from: *Bilotta, A., et al., A novel splice variant of the protein tyrosine phosphatase PTPRJ that encodes for a soluble protein involved in angiogenesis. Oncotarget, 2017.* ***8****(6): p. 10091-10102*. **(C)** Splice variants give rise to the full-length molecule and the first five fibronectin type-III repeats from the extracellular domain, termed the "short form" (SF).

1.8. Interaction between CD148 and Syndecan 2

The PI3K cascade is integral in the regulation of numerous essential cellular functions, including cell growth and survival [381], cell proliferation, motility, apoptosis and in vesicular trafficking [382, 383]. Abnormal activation of this pathway has been implicated in increased cell growth and tumour malignancy [381, 384]. The best-characterised PI3Ks are those in class I – heterodimers composed of separate regulatory and catalytic subunits. RTKs and Rho family GTPases activate class IA PI3Ks [383, 385, 386]. Multiple isoforms have been described for class IA regulatory and catalytic subunits and these are ubiquitous [382, 383].

A well-characterised heterodimeric PI3K is made up of a 110 kDa catalytic and 85 kDa regulatory subunit: p110 and p85, respectively [379]. The p85 regulatory subunit contains distinct modular domains that mediate signalling protein interactions. These domains comprise a single SH3 (Src homology 3) domain and 2 proline-rich domains, supporting the SH3 domain binding with other proteins, demonstrated *in vitro* [387]. The BCR (breakpoint cluster region) homology domain is homologous with a domain of the BCR gene product [388], binding to the Rho GTP, Rac and Cdc42 (cell division cycle 42) [386]. Finally, p85 contains two SH2 domains that bind with high affinity to tyrosine-phosphorylated receptor YXXM motifs (where X is any amino acid) [379, 389], and the region between these domains (the inter-SH2 domain) binds to the N-terminus of the corresponding catalytic domain (such as p110) [379]. At rest, the p85-p110 complex is stabilised by the p85 SH2 domains, and so PI3K activation is inhibited [383]. Further studies have shown that tyrosine phosphorylation of p85 can alter PI3K activity [383, 389, 390].

A 2008 study provided evidence for the first time that CD148 may interact with the p85 regulatory subunit of PI3K, modulating its level of

activity [379]. This was exhibited through a series of assays comparing the ability of wild-type CD148 with a mutated "substrate-trapping" CD148, wherein D^{1205} was substituted with A, "trapping" the substrate. In this study, CD148 was found to interact with the PI3K p85 subunit and to attenuate PI3K activity by dephosphorylating p85 [379]. Further studies have provided supporting evidence for this, including our group [218].

Previous research from our group into the syndecan family provides the foundations for this PhD project, specifically work regarding the SDC2 protein. SDC2 plays a significant role in angiogenesis and matrix deposition, demonstrated *in vitro* [391-393]. Under inflammatory conditions, the extracellular domain of SDC2 can be cleaved from the full-length molecule expressed on the cell surface. From here, shed SDC2 can have auto- or paracrine effects, one of which seems to be through binding with CD148. This interaction has been shown to stimulate cell adhesion and focal adhesion formation, potentially leading to angiogenesis inhibition by downregulation of cell proliferation and growth [218, 347]. It has been proposed that activation of CD148 by shed SDC2 leads to CD148 dephosphorylation of the p85 subunit of PI3K, a process requiring the action of Src kinase [218]. Furthermore, it was found that activation of CD148 by shed SDC2 leads to deactivation of β1 integrins [218, 347] (Fig. 1.10).

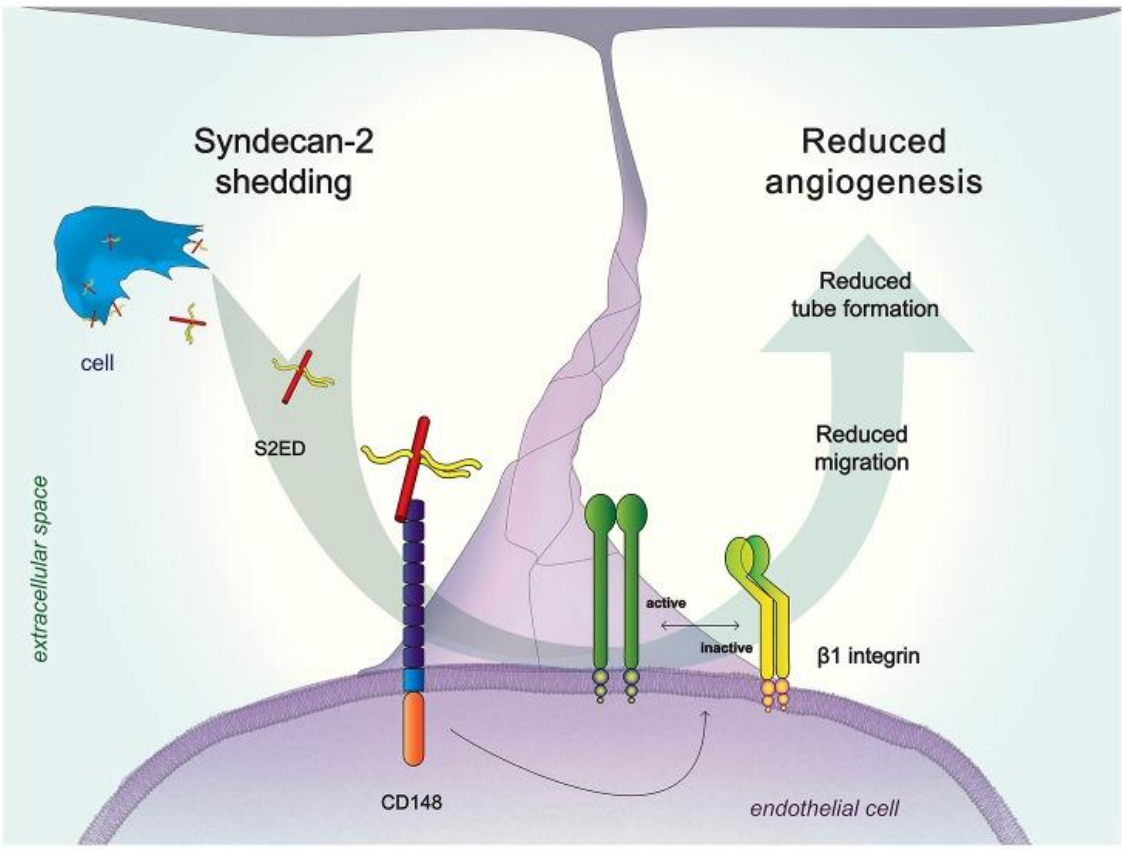

Figure 1.10. **Schematic model of syndecan-2 extracellular core protein interaction with CD148.** Shed SDC2 interacts with CD148, leading to dephosphorylation of the p85 subunit of PI3K and promoting cell adhesion via β1 integrin. Taken from: *De Rossi, G., et al., Shed syndecan-2 inhibits angiogenesis.*

1.9. Summary

Current therapeutic approaches for treating angiogenesis in diseases such as diabetic retinopathy involve intravitreal injections of anti-VEGF drugs. While these are effective for some patients, approximately half of patients who receive this treatment do not experience any benefit to their vision.

The ectodomain of SDC2 has been shown to reduce angiogenesis through its interaction with CD148. Our group has miniaturised the core protein from the SDC2 ectodomain, producing a peptide called QM107. Our proposal is that QM107 may have anti-angiogenic properties and, if this is indeed the case, these properties could be harnessed for therapeutic uses, such as treating pathological angiogenesis, therefore fulfilling a clinical niche. Furthermore, if QM107 were to be developed for clinical use, it will need to be characterised in order to determine its safety and efficacy for use in humans.

1.10. Project aims and hypothesis

Angiogenesis is the formation of new blood vessels from pre-existing vasculature and is a feature in a number of disease settings, including in neovascular eye diseases such as diabetic retinopathy and wet AMD. Current therapies to treat pathological angiogenesis target the VEGFA pathway, disrupting its pro-angiogenic signalling. However, these costly treatments are not 100% effective, meaning there remains a niche to fill in the market of anti-angiogenic therapies.

Based on the discoveries regarding SDC2 and its role in inhibiting angiogenesis via interaction with CD148, our group isolated and developed a small molecule inhibitor (developmental name: QM107), from the core protein of the SDC2 molecule. This peptide, made up of 18 amino acid residues, has been implicated in inhibition of vessel formation and vascular permeability. As a result, we are researching its therapeutic potential, with the intention of developing it as a small therapeutic peptide for treatment of neovascular eye diseases, including diabetic retinopathy and wet AMD. While current therapies aim to block the activity of VEGFA to prevent angiogenesis, QM107 seems to activate a physiological "off-switch" for angiogenesis and could be used to treat neovascular diseases, including diabetic retinopathy and wet AMD. Furthermore, the anti-angiogenic effects of the CD148SF protein determined in the aforementioned 2014 study [347] present a case for another potential alternative pathway to inhibit pathological angiogenesis.

To this end, this PhD project focuses on two main research areas: firstly, to develop methodologies to characterise QM107 and determine its mode of action in inhibition of angiogenesis; secondly, in order to further characterise CD148, the anti-angiogenic effect of CD148SF are also explored. The specific project aims are as follows:

1. Can we develop a methodology to determine QM107 stability *in vitro*?
    - Measure anti-angiogenic properties of QM107 against the SDC2 core protein using a number of angiogenesis assays
    - Raise an antibody to QM107 and determine whether this can be used to detect QM107 in *in vitro* stability assays

2. Does QM107 interact with the CD148 extracellular domain and can we map this interaction site on CD148?
    - Use ELISA techniques to measure interaction of QM107 with a variety of peptides derived from the CD148 extracellular domain sequence
    - Determine which section of the CD148 extracellular domain is the site of interaction for QM107

3. Does the CD148 short form protein, CD148SF, possess anti-angiogenic ability and can we map this inhibitory domain on the CD148SF sequence?
    - Test the ability of CD148SF to inhibit angiogenesis in a variety of *in vitro* and *ex vivo* angiogenesis assays
    - Develop a novel cell-based assay to measure angiogenesis inhibition by CD148SF

Chapter 2

2. Materials and methods

2.1. List of antibodies used

Table 2.1. List of antibodies used.

Antibody name	Epitope	Host	Dilution in PBS	Source
IgG poly-HRP	Rabbit	Goat	1:5000	Dako, Glostrup, Denmark
Anti-QM107	QM107	Rabbit	Various	CovaLab UK
Pierce™ Streptavidin Poly-HRP	Streptavidin	N/A	1:10000	Thermo Scientific™

2.2. Generation of polyclonal antibodies to QM107

Covalab UK performed immunisation of two New Zealand white rabbits (Table 2.2). Briefly, QM107 was covalently linked to carrier protein, keyhole limpet hemocyanin. This was injected in combination with Complete Freund's Adjuvant. Injections were performed on days 0, 21, 42 and 63. A pre-immune bleed was taken on day 0, to be used as a negative control for each animal, followed by subsequent test bleeds on days 53 and 74 and a final bleed on day 88. Upon receiving serum samples, purification of anti-QM107 was performed using Amicon® Pro Affinity Concentration Kit Protein G, according to manufacturer's instructions.

Table 2.2. Overview of the protocol used by CovaLabs UK to raise an antibody to QM107. Keyhole limpet hemocyanin and Freund's Adjuvant served to boost the immune responses of the rabbits to QM107, to initiate a stronger response resulting in increased antibody production. Immunopurification took place on 1 sepharose (agarose) column conjugated to the 1 peptide.

Day	Procedure
0	Pre-immune bleed
0	Injection (0.5ml antigen + 0.5ml complete Freud's Adjuvant)
21	Injection (0.5ml antigen + 0.5ml complete Freud's Adjuvant)
42	Injection (0.5ml antigen + 0.5ml complete Freud's Adjuvant)
53	Test bleed
63	Injection (0.5ml antigen + 0.5ml complete Freud's Adjuvant)
88	Test bleed
102	Final bleed

2.3. Cloning strategy of pET24 plasmid to generate CD148 variants

The coding sequences were amplified by PCR with the following reaction conditions: 5X Green GoTaq Flexi Buffer (Promega), 5mM $MgCl_2$, 0.2mM of each DNTP, 0.2µM forward and reverse primers (Table 2.3) and 5U of Taq DNA polymerase (Promega). Reactions were run on a thermocycler (30 seconds at 94°C, 30 seconds at 60°C, 60 seconds at 74°C). PCR products were precipitated using 1/10th volume 3M sodium acetate plus 1/3rd volume of 100% ethanol and run on a 1% agarose gel. Bands were excised and DNA extracted from the gel fragments using the QIAquick PCR Purification Kit (Qiagen), according to the manufacturer's instructions. PCR products were then digested with BamHI and HindIII (Promega). Following a second PCR clean-up, the digested PCR fragments were ligated into pET24 (Fig. 2.1.) using T4 DNA Ligase (Promega) and ligase buffer. Prior to ligation, pET24 vector was digested using BamHI and HindIII to generate sticky ends for ligation.

Ligations were transformed into NEB DH5-alpha Competent *E. Coli* cells, according to the New England BioLabs C2987I protocol. In brief, competent cells (25µl) were mixed with 1pg-100ng of plasmid DNA and incubated on ice for 30 minutes, followed by 30 seconds at 42°C and another 5 minutes on ice. SOC media (950µl) was added to each transformation and the cultures incubated for 1 hour at 37°C. Finally, cells were plated onto LB Agar plates containing the relevant antibiotic and, after drying, placed overnight in a 37°C incubator.

Single colonies were picked from the agar plate and cultured in LB medium containing appropriate antibiotic overnight at 37°C on an orbital shaker at 200RPM. Plasmid DNA was then isolated from cells using PureLink™ Quick Plasmid Miniprep Kit (Invitrogen) for transformation.

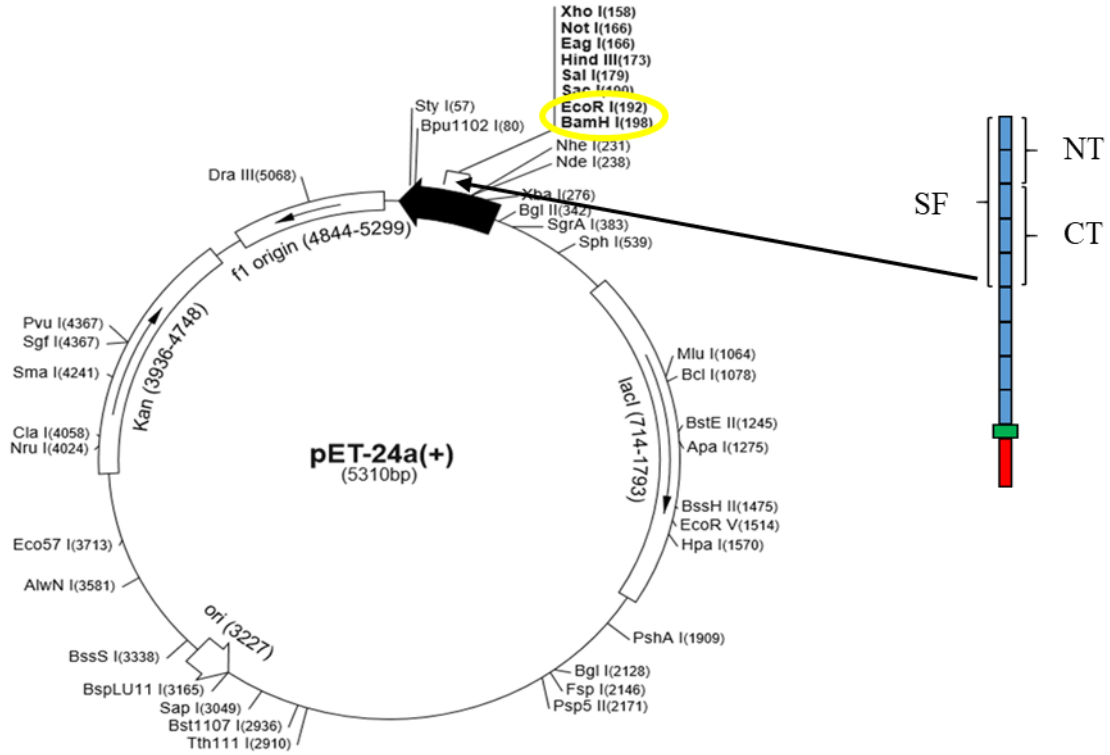

Figure 2.1. **pET24 vector map.** Vector DNA was cut at EcoR1 and BamH1 restriction sites (indicated) and plasmid DNA derived from CD148 was inserted at this site before ligation.

Table 2.3. Primer sequences used to produce DNA plasmids for all CD148-derived proteins.

Plasmid	Primer sequence
CD148 short form (CD148SF)	Forward: tatataggatccgcaggtggcacccctagt Reverse: tatataaagctttccagttctattgcaaactgtc
CD148 C-terminus (CD148CT)	Forward: ttaattaagcttttacaagccaccttctgtgccc Reverse: tatataaagctttccagttctattgcaaactgtc
CD148 N-terminus (CD148NT)	Forward: tatataggatccgcaggtggcacccctagt Reverse: tatataggatcgatgccagcaatacagagaga
Fibronectin type-III repeat 3 (FNIII3)	Forward: ttaattggatccgatgccagcaatacagagaga Reverse: tttaaaaagcttaatagcatttgtcctgaactctat
Fibronectin type-III repeat 4 (FNIII4)	Forward: ttaattggatcccaggtttttgacgtcaccg Reverse: ttaattaagctttggaacaggaggggtgtg
Fibronectin type-III repeat 5 (FNIII5)	Forward: ttaattggatccgtttctgacttccgagtgaca Reverse: tttaaaaagctttccagttctattgcaaactgt

2.4. DNA gel electrophoresis

Plasmids and PCR products were analysed on 1%-2% w/v agarose gels in 1X TAE buffer (40mM Tris pH 7.6, 20mM acetic acid, 1mM EDTA) in dH_2O, made from 50x TAE stock (Thermo Fisher Scientific). 5x DNA loading buffer (Promega) was added to each sample prior to electrophoresis at typically around 135V. Size markers used included SmartLadder Small Fragment (Eurogentec) and 1kb DNA ladder (Promega). StainIN RED (Clent Life Science) was added to gels for staining and visualisation, as per the manufacturer's instructions. Gels were imaged using the UV transilluminator on the Azure biosystems' c600 imaging system.

2.5. BL21 transformation and induction

BL21 Competent *E. Coli* cells were used for production of all recombinant proteins. Competent BL21 cells were made using the TSS method [394] and transformed using the heat shock method.

Briefly, competent cells (50µl) were mixed with 200-500ng of plasmid DNA and incubated on ice for 20 minutes, followed by 1 minute at 42°C and another 5 minutes on ice. LB media (600µl) was added to each transformation and cultures were incubated for 1 hour at 37°C. Finally, cells were plated onto LB Agar plates containing the relevant antibiotic and, after drying, placed overnight in a 37°C incubator.

Liquid cultures (5ml LB) were inoculated from single colonies of the required BL21 strain and grown overnight at 37°C on an orbital shaker (200RPM). Overnight cultures were added to inoculate fresh LB medium (same composition as previously used) in conical flasks and incubated at 37°C on an orbital shaker (overnight cultures were used at a dilution of 1 in 100). After 2 hours (OD600 of 0.4), 100µl samples were taken for later analysis and protein production was induced by the addition of 100mM IPTG to the remaining liquid cultures. These were incubated at 30°C with shaking

for a further 4 hours. After this, 100µl samples were stored for later analysis. Bacterial pellets were harvested by centrifugation at 4000xg and stored at -20°C.

2.6. Purification of CD148 recombinant proteins from BL21 cell pellets

Frozen bacterial pellets were lysed using B-PER Complete Bacterial Extraction Reagent (Thermo Fisher Scientific) according to the manufacturer's instructions. After 20 minutes of incubation at room temperature on a tube rotator, cellular debris was extracted from bacterial lysates by centrifugation at 4000xg for 15 minutes. His-tagged proteins were purified from bacterial lysates using HIS-Select® Cobalt Affinity Gel (Sigma-Aldrich), as per the manufacturer's directions. In short, resin was equilibrated in 20mM imidazole in PBS, prior to addition to bacterial lysates and incubation at room temperature on a tube rotator for 1 hour. After incubation, the resin was collected by centrifugation and washed 3x with 20mM imidazole. Proteins were eluted in 250mM imidazole in PBS. Samples were analysed using SDS-PAGE, as described in section 2.7.2.

2.6. Dialysis of protein samples

Slide-A-Lyzer™ MINI Dialysis Device from Thermo Fisher Scientific™ (pore size 10kDa cut off), was used to perform dialysis of protein samples purified from BL21 cells, in order to remove residual imidazole present in protein solutions. This was carried out using PBS, as per the manufacturer's instructions. Subsequently, a final SDS-PAGE was performed to determine the presence of recombinant proteins in the solutions after dialysis.

2.7. Protein analysis

2.7.1. BCA assay

To estimate the total protein concentration of each recombinant protein sample, bicinchoninic acid assays (BCA) were performed using the 96 well plate format from Thermo Scientific™ Pierce® BCA Protein Assay kit. This is based on colorimetric detection and quantitation of total protein and was carried out as per the manufacturer's instructions. Protein samples were added in triplicates of 25µl each. Bovine serum albumin (BSA) was used a standard protein (25-2000 ug/ ml range). After addition of BCA reagent, the plate was incubated at 37˚C for 30 minutes and then the absorbance was measured at 562nm using the Spectra MR microplate spectrophotometer (Dynex, Magellan Biosciences). Based on the BSA absorbance values, a standard curve was plotted and the protein concentrations of the test samples were determined from the equation of the line fitted to the standard values.

2.7.2. SDS-PAGE

Proteins were analysed by gel electrophoresis using standard procedures based on Laemmli [395]. Briefly, proteins were boiled in SDS loading buffer with 5µM β-mercaptoethanol (Invitrogen) and analysed on Mini-Protean TGX Stain-Free agarose gels, 4-20% (Bio-Rad), in 1X TGS buffer (192mM glycine, 25mM Tris, 0.1% w/v SDS) in dH_2O, made from 10x TGS stock from Thermo Fisher Scientific. Visualisation of proteins was performed using Coomassie brilliant blue 250, using standard procedures, on Azure biosystems' c600 imaging system. Size marker used was SeeBlue™ Plus2 Pre-stained Protein Standard (Invitrogen).

2.7.3. Western blot

Following electrophoresis, SDC2 proteins were transferred onto 45µm PVDF membranes using the Trans-Blot Turbo Transfer System (Bio-Rad), as per the manufacturer's instructions. Next, the membranes were incubated in blocking buffer (5% milk in TBST) for 1 hour at room temperature on an orbital rocker, to prevent nonspecific binding. Membranes were then incubated overnight at 4°C with primary antibody diluted 1:100 in 5% milk in TBST. Membranes were washed with TBST three times, each for 10 minutes, and incubated for 1 hour at room temperature on an orbital rocker in species-specific secondary antibody conjugated to horseradish peroxidase (HRP) at 1µg/ ml in 5% milk in TBST. After washing three times for 10 minutes with TBST, blots were developed by incubating briefly with BCL substrate to for chemiluminescence reaction. Bound antibodies were visualised using Azure biosystems' c600 imaging system.

2.8. Protein interaction assays

2.8.1. ELISA

ELISA detection of QM107 or SDC2 was performed using standard procedures. Calibrants and samples were coated onto 96 well plates overnight at 4^{o}C (for QM107 ELISA with paraformaldehyde, 4% w/v paraformaldehyde in PBS was added with QM107 calibrants). Wells were washed three times with PBS, prior to the addition of 100µl of 1% w/v BSA (Thermo Fisher Scientific) in PBS and incubation at room temperature for 30 minutes. Wells were washed as described previously and primary antibody diluted in PBS (100µl) was added and incubated for 1 hour at room temperature. Following washes, secondary antibody conjugated to HRP was applied (100µl) and plates were incubated at room temperature for 1 hour. After a final set of washes, signal detection was performed using TMB1

(Promega) as per the manufacturer's instructions, using 0.1M HCl to stop the reaction after 5 minutes. Optical density was measured at 450nm with the Spectra MR microplate spectrophotometer (Dynex, Magellan Biosciences).

2.8.2. Serum preparation for QM107 stability assays

Serum was prepared from human whole blood samples. 10ml of whole blood was obtained from each donor and incubated at room temperature for 45 minutes, followed by 5 minutes of centrifugation at 4000RPM. Serum was isolated from this and stored at -20°C. For experimental assays, it was thawed at room temperature before use.

2.8.2. Stability assays

To test whether trypsin degradation affects the ability to detect QM107 using our in-house developed polyclonal antibody, QM107 was incubated with Trypsin-EDTA (0.25%), phenol red (Thermo Fisher Scientific) at 37°C, before the reaction was stopped by the addition of 50µl of 4% w/v paraformaldehyde in PBS at various time points. Samples were then applied to 96 well plates and QM107 detection was carried out using ELISA. Stability was also assayed in vitreous humour extracted from enucleated pig eyes, which was diluted in an equal volume of PBS. Peptide samples diluted in PBS were added to an equal volume of vitreous humour and incubated at 37^{o}C for the times indicated. Reactions were stopped by the addition of 100µl of 4% w/v paraformaldehyde in PBS. Samples were then applied to 96 well plates and the peptides detected by ELISA.

2.8.3. Solid phase binding assays

All solid phase binding assays were performed using 96 well microtitre plates from Thermo Scientific^{TM}. Briefly, equimolar amounts of CD148-

derived recombinant proteins and fibronectin (200µl protein solution in PBS per well) were coated onto a 96 well plate overnight at 4°C. The following day, the plate was washed 3 times with PBS and 5µM biotinylated QM107 added (100µl per well). Following incubation for 1 hour at room temperature, the plate was washed as previously and streptavidin-HRP diluted in PBS was added (50µl), followed by a 30 minute incubation at room temperature. The plate was washed for a final time and TMB1 signal detection method was used as per manufacturer's instructions, using 0.1M HCl to stop the reaction after 5 minutes. Optical density was measured at 450nm using the Spectra MR microplate spectrophotometer (Dynex, Magellan Biosciences).

2.9. Cell culture

Brain endothelial (bEND) and skin endothelial (sEND) cell lines were obtained from HPA laboratories UK and maintained at 37°C under 10% CO_2 in DMEM (Thermo Fisher Scientific) supplemented with 10% FBS, 1% non-essential amino acids, 1% penicillin (10, 000µg/ml)/ streptomycin (10mg/ml), 5µM β-mercaptoethanol and 5µg/ml Plasmocin (Invivogen).

2.10. Angiogenesis assays

2.10.1. Scratch wound migration assay

Scratch wound migration assays were performed on confluent monolayers of ECs in 6 well tissue culture plates. Wounds were made using a pipette tip to scratch a line along one direction in the centre of the well. Medium was removed and, following a single wash with PBS, CD148-derived proteins were added to cells in fresh medium. Images were captured every 2 hours for up to 24 hours using the Olympus IX81 microscope connected to the computer and analysed using ImageJ software. The wound area between the

two cell fronts at time points 0 and 16 hours was selected and measured in pixels. Percentage wound closure was calculated.

2.10.2. Murine aortic ring assay

Angiogenic sprouts were induced from mouse or rat thoracic aortas, according to the method of Nicosia and Ottinetti [396]. 180 – 200g male Wistar rats (Harlan Laboratories) were sacrificed. Fur was sprayed with 70% ethanol and a longitudinal incision was made along the chest area using a scalpel. Skin was peeled back and pinned down with scissors and forceps to reveal the rib cage. Aortas were then dissected using forceps and micro-scissors, then placed into a 50ml pot with ice-cold PBS on ice. After an initial wash in PBS to remove the blood, the aorta was transferred into a petri dish containing fresh PBS, and fat was carefully removed using forceps, avoiding stretching the aorta, and long branches protruding from the aorta were removed using a scalpel. The aorta was then transferred to a new petri dish containing ice-cold serum-free OptiMEM (containing P/S) and cut into rings of 1mm in diameter using a scalpel. Under a tissue culture hood, rings were moved into a fresh petri dish and incubated overnight in serum-free OptiMEM (containing P/S) at 37°C. The following day, a coating gel was made by mixing type I collagen (1 mg/ml) and 10% v/v E4 media (Invitrogen) in water. 150µl of the gel was pipetted into each well of a 48 well plate (Corning) and rings were rapidly dried on the lid of the petri dish and carefully positioned in the middle of the well containing collagen. The plate was incubated at 37°C for 30 minutes to allow the collagen to polymerise, after which time wells were supplemented with OptiMEM with 1% FBS and VEGF (30 ng/ml for mouse rings, 10 ng/ml for rat rings) and incubated at 37°C, 10% CO_2. Media was changed every third day and after 1 week, angiogenic sprouts from aortic rings were counted by visualisation

under the Olympus IX81 microscope at 10x magnification, and results were expressed as the number of sprouts per ring.

2.10.3. Endothelial cell spheroid formation

To form spheroids, the "hanging drops" method was used (modified from Tetzlaff and Fischer, 2018), wherein 100,000 cells were suspended in DMEM with methylcellulose solution (1.2% w/v). A multichannel pipette was used to create 25µl droplets of cell-methylcellulose solution in a cell culture dish, which was subsequently turned upside down and incubated at 37°C under 5% CO_2 for 24 hours.

Hanging drops were washed off the plate with 10ml PBS and centrifuged for 5 minutes at 200xg, after which the pellet was re-suspended in methylcellulose solution containing 20% FBS. Spheroids were embedded in type I collagen (1mg/ ml) in E4 medium (Invitrogen) in 48 well plates, with CD148-derived proteins or QM107 incorporated into collagen matrices. Wells were further supplemented with DMEM containing CD148-derived proteins or QM107 and incubated at 37°C under 10% CO_2 to allow collagen to polymerise. Spheroids were imaged using Olympus IX81 microscope at 10x magnification and sprouting was determined by quantification of both the number of sprouts per spheroid and change in area per spheroid.

2.11. Statistical analysis

Statistical analysis was performed for stability assays, binding assays and angiogenesis assays using Dunnett's multiple comparisons test followed by one-way analysis of variance (ANOVA) using GraphPad prism software (La Jolla, CA, USA). P values of <0.05 were considered significant. For stability and binding assays, significant differences between the control and test groups were evaluated with p values less than 0.0001 (****). For the

scratch wound assay, significant differences between the control and test groups were evaluated with p values less than 0.0001 (***), indicated on the graph. For the EC spheroid assay, significant differences between the control and test groups were evaluated with p values less than 0.01 (**) and 0.5 (*), indicated on the graph. For the angiogenic sprout formation assay, significant differences between the control and test groups were evaluated with p values less than 0.0001 (****), 0.001 (***) and 0.001 (**), indicated on the graph. Error bars in graphs denote ± SEM (standard error of mean).

Chapter 3

3. QM107 stability in biological samples

3.1. Introduction

An emerging area of research relating to the syndecan family is the fact that contained within all 4 family members' extracellular core proteins are sequences that can modulate cell behaviour – in particular, angiogenesis [397]. Previous studies have shown that the extracellular core protein of SDC2 inhibits angiogenesis via an interaction with CD148 [218, 347]. In this work, it was shown that when SDC2 is shed from the cell surface, the resultant entity can block angiogenic sprout formation and inhibit EC migration. HEK293T cells constitutively expressing a shed form of SDC2 formed significantly smaller tumours when injected into the flanks of SCID mice, due to a profound lack of tumour angiogenesis. These anti-angiogenic properties of shed SDC2 are not driven by interactions with its heparan sulphate chains, since a bacterially expressed fusion protein consisting of the entire extracellular core protein of SDC2 fused at the N-terminus also exhibited strong anti-angiogenic properties. Bacteria lack the transferases necessary to synthesise heparan sulphate. Subsequent mapping via mutagenesis experiments revealed that an 18 amino acid sequence residing between P^{124} and F^{141} of murine SDC2 was required for this anti-angiogenic activity (Fig. 3.1). Following the identification of this murine sequence, we went on to map the corresponding 18 amino acid region of human SDC2 by sequence alignment to murine SDC2. Using the 'Stretcher' tool (available at https://www.ebi.ac.uk/) we found that the murine SDC2 sequence had 68% identity and 89.5% similarity to the corresponding human region (P^{123} – F^{140}, Fig. 3.2). Our group now want to determine whether the 18 amino acid peptide corresponding to the human sequence exhibits similar anti-

angiogenic properties to the murine model, which will aid us in developing a potential therapeutic peptide for neovascular eye diseases. We synthesised the human peptide sequence (QM107), which is now protected by a patent. The aim is to test QM107's efficacy in *in vitro* and *in vivo* models of angiogenesis and neovascular eye disease. Ultimately, it is envisaged that a formulation of QM107 administered via intra-vitreal injection would be used in a clinical trial, similar to anti-VEGF therapies. Choosing the human form of SDC2 (rather than murine) could potentially offset any adverse immune reactions the therapy might have, since it is expressed extensively throughout human tissues.

A

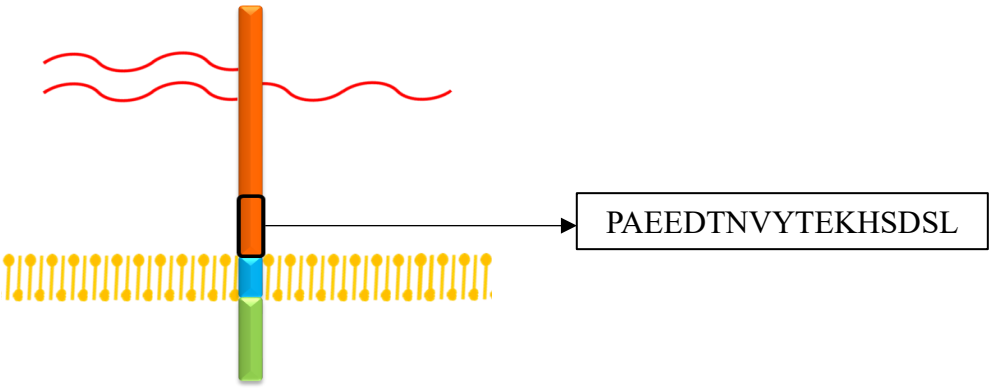

B

```
Mouse SDC2 MQRAWILLTLGLMACVSAETRTELTSDKDMYLDNSSIEEASGVYPIDDDDYSSASGSGAD   60
  Pig SDC2 MRRVWILLTLGLVACVSAESRAELTSDKDMYLDNSSIEEASGVYPIDDDDYASASGSGAD   60
Human SDC2 MRRAWILLTLGLVACVSAESRAELTSDKDMYLDNSSIEEASGVYPIDDDDYASASGSGAD   60
Rabbit SDC2 MRRAWILLTLGLVACVSAESRAELTSDKDMYLDNSSIEEASGVYPIDDDDYASASGSGAD   60
           *:*.********:******:*:*****************************:********

Mouse SDC2 EDIESPVLTTSQLIPRIPLTSAASPKVETMTLKTQSITPAQTESPEETDKEEVDISEAEE   120
  Pig SDC2 EGVESPELTTSRPLPKIPITSAAPRVETTTLDKMQNKIPAQTKSPEEIDKEKVHLSDSER   120
Human SDC2 EDVESPELTTSRPLPKILLTSAAPKVETTTLN-IQNKIPAQTKSPEETDKEKVHLSDSER   119
Rabbit SDC2 EDIESPELTTSRPFLKIPFTSAAPKVETTTLK-IQNKMPAQTKSPEEIDKEKVHLSDSER   119
           *.:*** ****: : :* :****     *     *.  ****:**** ***:*.:*::*.

Mouse SDC2 KLGPAIKSTDVYTEKHSDNLFKRTEVLAAVIAGGVIGFLFAIFLILLLVYRMRKKDEGSY   180
  Pig SDC2 KTDPAEKDTNVYTEKHSDNLFKRTEVLAAVIAGGVIGFLFAIFLILLLVYRMRKKDEGSY   180
Human SDC2 KMDPAEEDTNVYTEKHSDSLFKRTEVLAAVIAGGVIGFLFAIFLILLLVYRMRKKDEGSY   179
Rabbit SDC2 KMDPAEEGTNVFTEKHSDNLFKRTEVLAAVIAGGVIGFLFAIFLILLLVYRMRKKDEGSY   179
           * .** :.*:*:******.****************************************

Mouse SDC2 DLGERKPSSAAYQKAPTKEFYA   202
  Pig SDC2 DLGERKPSSAAYQKAPTKEFYA   202
Human SDC2 DLGERKPSSAAYQKAPTKEFYA   201
Rabbit SDC2 DLGERKPSSAAYQKAPTKEFYA   201
           **********************
```

Figure 3.1. **QM107 is derived from human syndecan-2. (A)** Human syndecan-2 (SDC2) schematic, indicating QM107's derivation from the SDC2 core protein. **(B)** Amino acid sequence of syndecan-2. Blue text indicates the extracellular portion of SDC2, with bold text highlighting heparan sulphate chain binding sites; orange text represents the transmembrane domain; green text shows the cytoplasmic domain, with the V region represented in bold text and the PDZ domain indicated by underlined text. The cleavage site for SDC2 is between the transmembrane and cytoplasmic domains (between thymine and glutamate amino acids). The yellow highlighted sequence shows the QM107 sequence in human SDC2 and how this region is conserved across species.

To achieve our objective of taking QM107 forward as a therapeutic peptide, we will need to perform pharmacokinetic studies. Pharmacokinetics is defined as "the study of the time course of drug absorption, distribution, metabolism, and excretion" [398]. This information is crucial to development of all therapeutics, as the major aim of drug development is to maximise drug efficacy while minimising toxicity. Therapeutic action sites are largely inaccessible and generally a drug's activity correlates with its concentration at sites of action [398]. To perform these studies, a robust methodology for detecting QM107 must be optimised. The ability to detect QM107 would allow us to determine the relationship between its concentration in easily obtainable biological samples, such as blood, and its therapeutic effect (termed "kinetic homogeneity") [398]. One option for this is to use mass spectrometry, but the costs of this are prohibitive. Although this would represent the 'gold standard', the purpose of this chapter is to explore an alternative methodology, in which we raise an antibody to QM107 and test whether it could be used as a tool to detect QM107 in biological samples. The use of antibodies in various research settings for detection of specific antigens has been well established, from their use in ELISAs to western blotting. They have many advantages, including their ease of production (particularly in the case of polyclonal antibodies, which are suitable for use in detection assays) and low cost, relative to mass spectrometry. The specificity of an antibody is also advantageous, particularly for use in biological samples where many proteins are present. Developing an antibody against QM107 could potentially offer a means of detecting QM107 in biological samples for pharmacokinetic studies, allowing us to continue our pursuit of developing it as a therapeutic peptide. To this end, the following aims will be addressed in this chapter:

1. Determine whether the QM107 peptide retains the same anti-angiogenic properties as the full-length extracellular SDC2 core protein

2. Generation and characterisation of an anti-QM107 antibody

3. Develop a methodology to detect QM107 in porcine vitreous humour and human serum, and use this methodology to assess QM107 stability in biological samples

3.2. Results

3.2.1. Peptide synthesis and proof of efficacy

It has been shown that a fusion protein (S2ED), consisting of Glutathione-S-transferase fused to the N-terminus of the full length murine SDC2 extracellular core protein (E^{19} – F^{141}), potently inhibited angiogenesis in a number of models [218, 347]. We set out to determine whether QM107 also exhibits inhibition of angiogenesis. Firstly, the QM107 peptide was synthesised by Bachem peptides, using a solid phase synthesis protocol (Fig. 3.2.). This was a large-scale synthesis (approximately 2g) and was assayed to have 97.7% purity by mass spectrometry. Additionally, this was an iterative step towards a GMP protocol for QM107 production.

A

```
          124                                141
Mouse PAIKSTDVYTEKHSDNLF

          123                                140
Human PAEENTNVYTEKHSDSLF
      **    * ******** **
```

B

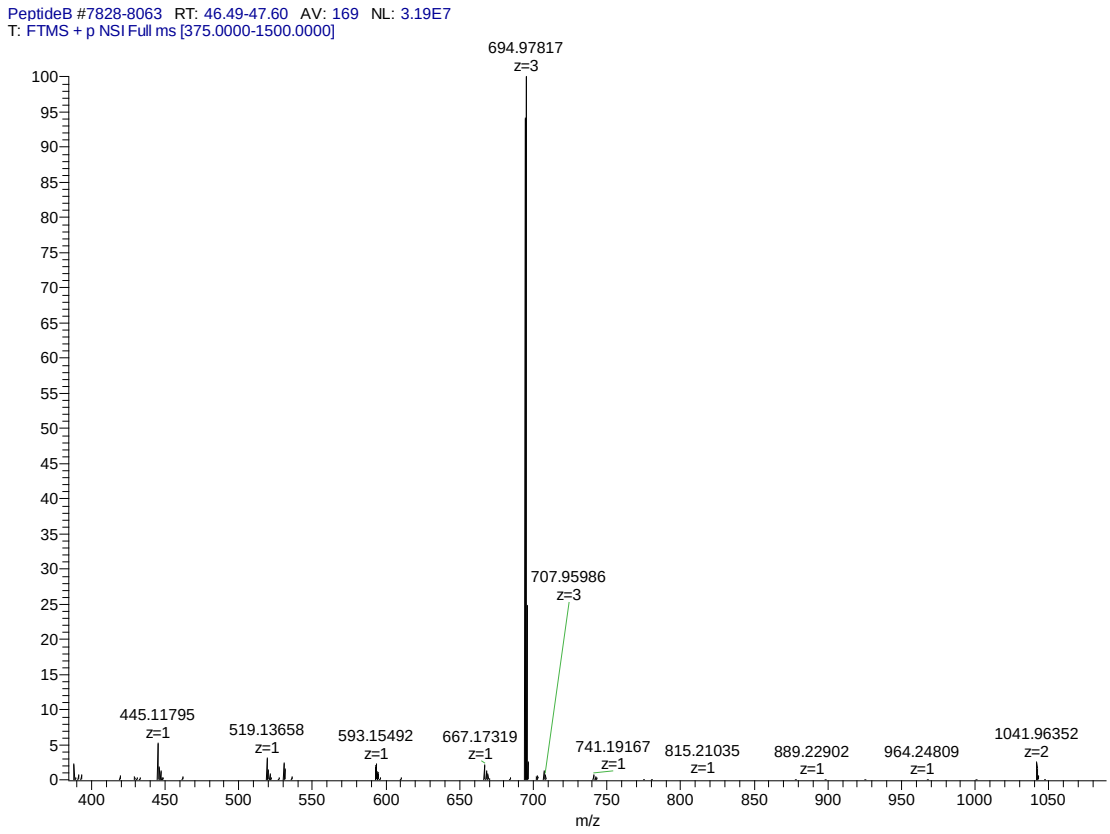

Figure 3.2. **Synthesis of QM107 peptide. (A)** Sequence comparison and homology between murine and human syndecan-2 (SDC2), that exhibit anti-angiogenic properties. In murine syndecan-2, the 18aa from P^{124} to F^{141} is shown, and the corresponding sequence in human SDC2 is from P^{123} to F^{140} (developmental name: QM107). **(B)** Mass spectrometry shows the QM107 peptide supplied by Bachem has 97.7% purity.

We compared the anti-angiogenic activity of QM107 and bacterially-expressed S2ED using aortic rings derived from rats. The results showed that sprout formation from the aortic explants was significantly inhibited by both S2ED and QM107 (0.5µM), as compared to either PBS- or GST-treated rings after 5 days. This shows that both S2ED and QM107 have anti-angiogenic activity, as they inhibited angiogenic sprout formation compared to the negative controls, indicating that the QM107 sequence was equally as effective at blocking neovascularisation as S2ED (Fig. 3.3A and B).

Inhibition of angiogenesis by S2ED occurs via inhibition of EC migration [347], so we next tested whether this was the case for QM107 using scratch wound migration assays on confluent HUVEC monolayers. We saw significant inhibition of EC migration following treatment with 0.5µM as compared to the PBS control (Fig. 3.3C). Based on this data, we determined that QM107 retains the anti-angiogenic properties of full-length shed SDC2.

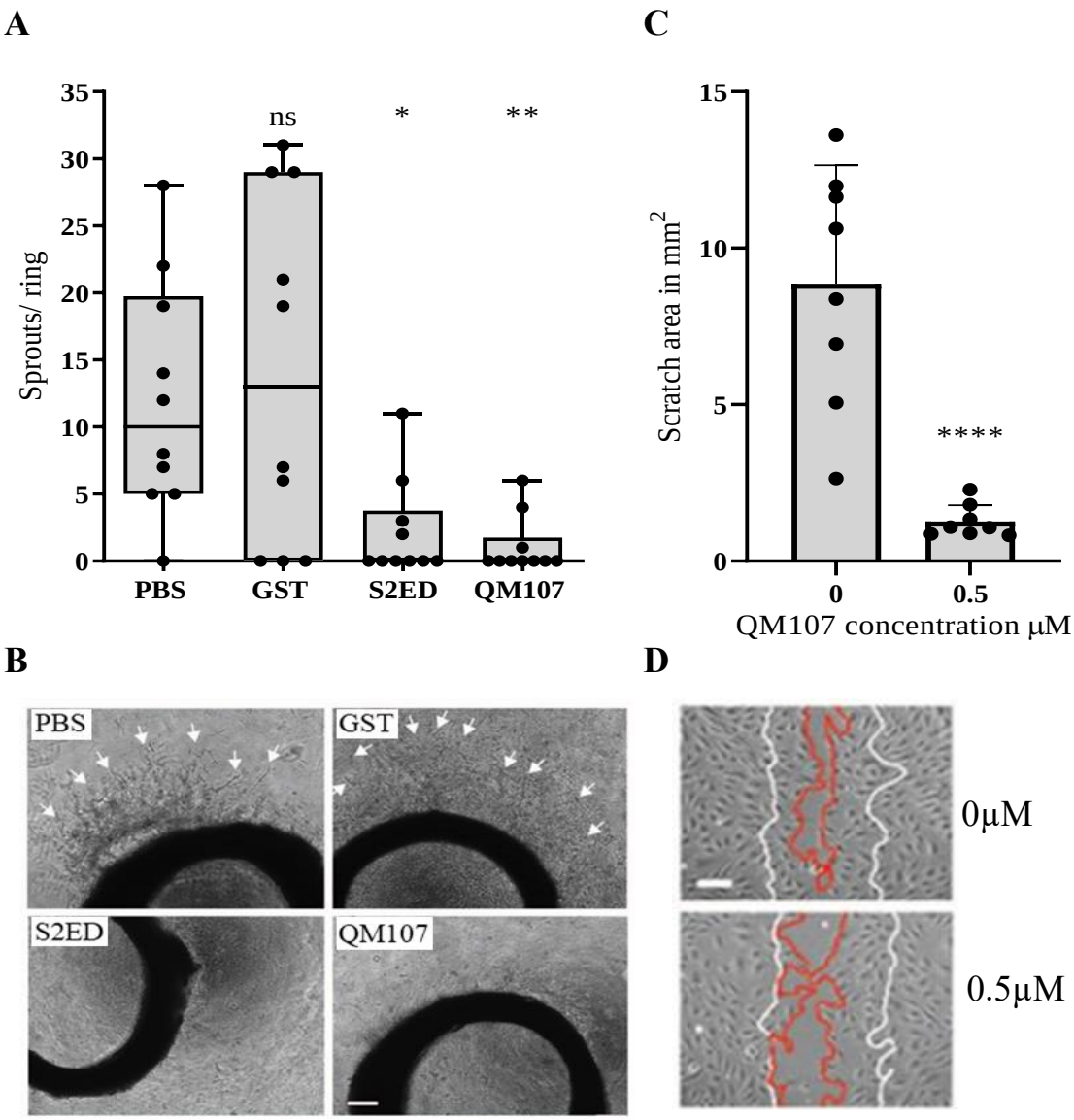
A
C
35
30
25
20
15
10
5
0
Sprouts/ ring
ns
*
**
PBS
GST
S2ED
QM107
15
10
5
0
Scratch area in mm2
****
0
0.5
QM107 concentration µM
B
D
PBS
GST
S2ED
QM107
0µM
0.5µM

Figure 3.3. **QM107, a peptide derived from syndecan-2 ectodomain, retains the same anti-angiogenic properties. (A)** Comparable inhibition of angiogenic sprout formation is observed in response to treatment with either full length SDC2 ectodomain (S2ED) or QM107. Rings were embedded in a collagen I matrix into which 0.5µM of each treatment was added. Sprouts were counted after 5 days in culture. (n=4 rats, 10 rings/ condition *p<0.05 **p<0.01) **(B)** Representative micrographs of rings from each of the conditions described in (A). Images were captured on an Olympus IX81 inverted microscope using a 4x objective, scale bar = 100µm. **(C)** QM107 inhibits HUVEC migration. Cell migration after 6 hours was quantified and expressed as migrated cell area. (n=8 experiments/ condition ****p<0.0001) **(D)** Representative micrographs of scratch wound assays performed on confluent HUVEC cultures. The initial scratch is highlighted in white and the closed area in red. Images were taken at 0 and 6 hours using an Olympus IX81 inverted microscope with a 10x objective. Cells were treated with 0.5µM QM107 (scale bar =100µm).

3.2.2. Antibody development for QM107

The next objective was to develop an antibody for QM107 detection in various applications. Rabbits were immunised with QM107 covalently linked to carrier protein keyhole limpet haemocyanin by CovalLabs UK. This was injected in combination with Complete Freund's Adjuvant to illicit an immune response in the rabbits. Injections were performed 4 times throughout the process (Table 2.2 in Materials and Methods), with a pre-immune bleed taken on day 0, to be used as a negative control for each animal, followed by 4 subsequent test bleeds throughout the process.

Following receipt of the samples and subsequent purification (section 2.2, Materials and Methods), an ELISA was carried out to determine the presence of any anti-QM107 antibody in the serum samples by coating QM107 peptide onto the plates as an antigen, followed by incubation with rabbit serum (Fig. 3.4), then probed with anti-rabbit HRP. The ELISA showed an antibody produced against QM107 in both the serum samples acquired after QM107 injection, but not in samples taken prior to QM107 injection. This is evident from the optical density presented in Fig. 3.4, where post-injection samples presented a much higher readout than pre-injection serum samples, indicating binding with QM107, and suggesting that the injection of QM107 produced an immunogenic response in the rabbits.

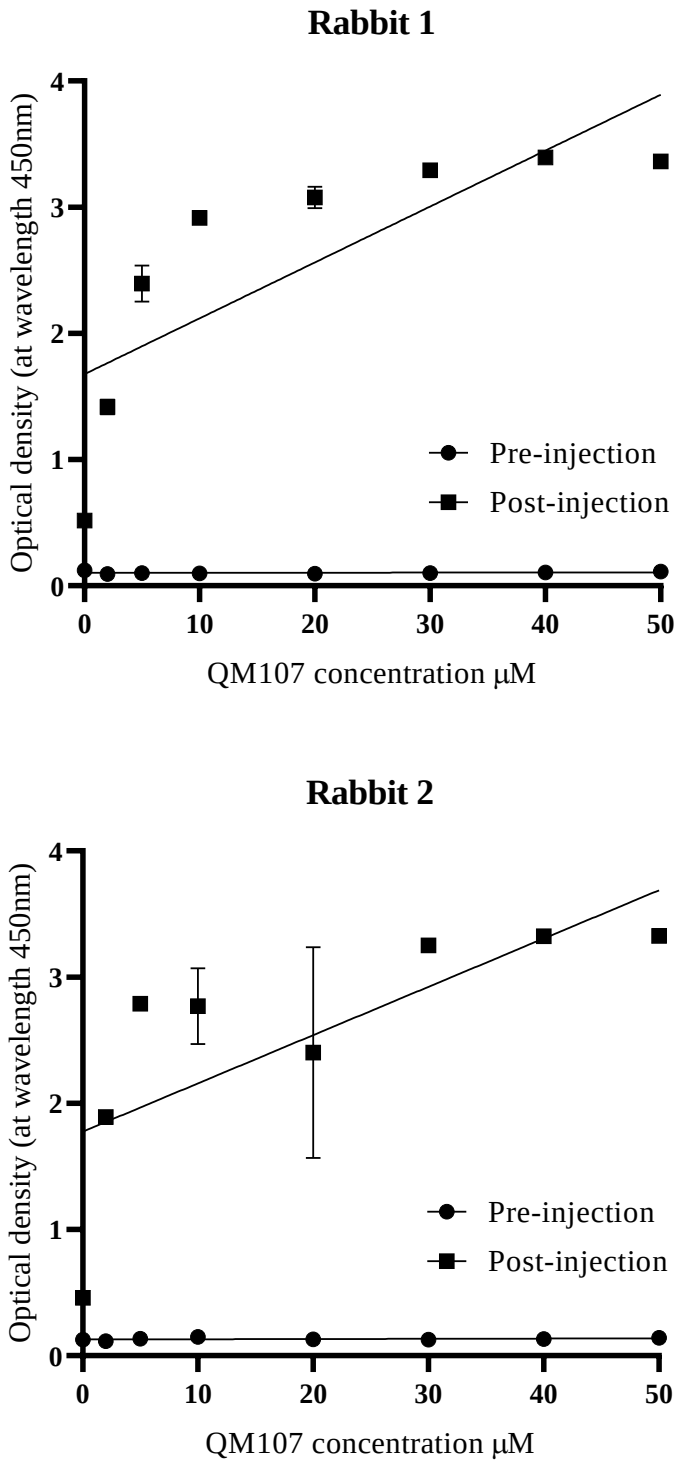

Figure 3.4. **Generation of rabbit polyclonal antibodies to QM107.** Plates were coated with QM107 and left overnight to adhere, followed by ELISA, performed using the serum samples acquired from two rabbits (n=2). A strong signal was obtained in serum from both animals, but not in serum from the pre-injection samples.

Following the detection of anti-QM107 antibody in rabbit serum, we wanted to test the specificity of the antibody. Fig. 3.5A depicts the amino acid sequences of both QM107 and scrambled QM107 (an alternative configuration of the same sequence, as shown). Using both peptides, ELISAs were performed using pre- and post-injection rabbit serum, to assess whether the antibody was able to detect the scrambled QM107 sequence. Despite the scrambled sequence containing the same amino acids, albeit in a different order, there was a distinct lack of binding between anti-QM107 in post-injection serum samples and scrambled QM107 (Fig. 3.5B), presenting strong evidence that this antibody is highly specific for the QM107 peptide structure. This discovery confirmed firstly that an antibody against QM107 had been produced, and secondly that it can be used to detect QM107 *in vitro*.

We subsequently found that samples taken after the first injection of QM107 resulted in higher QM107 detection compared to samples acquired at later points from the same rabbit. Going forward, we used antibodies purified from the serum from the first post-QM107 injection bleeds only.

A QM107 sequence: **PAEEDTNVYTEKHSDSLF**

Scrambled sequence: **FTSLESKDHADNYEVTEP**

B

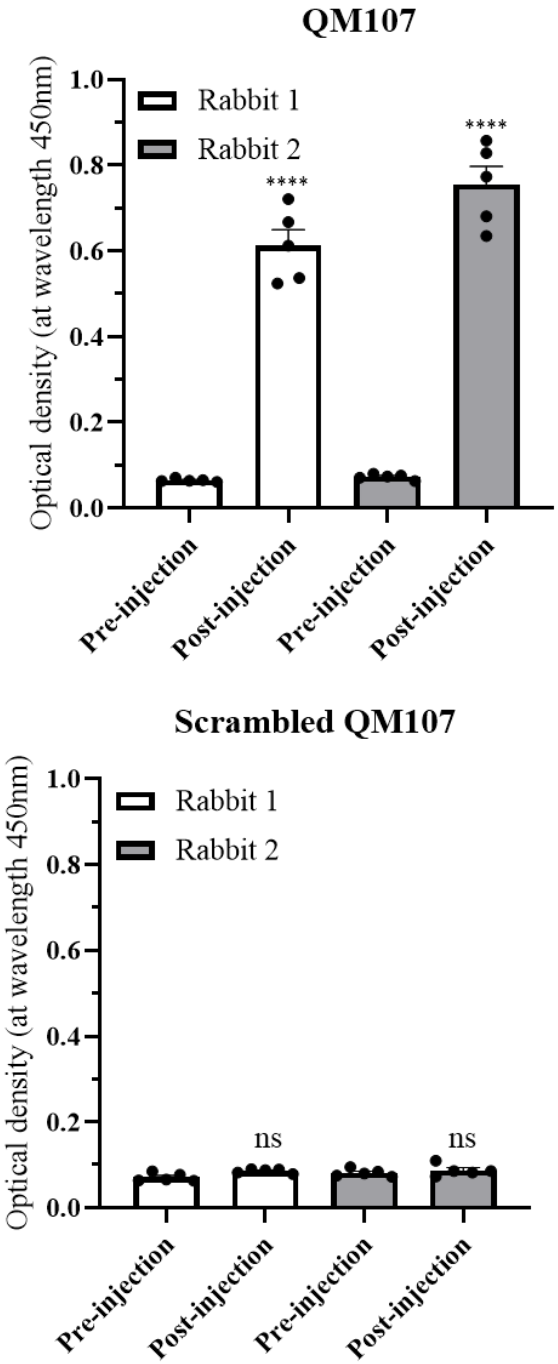

Figure 3.5. **Rabbit polyclonal anti-QM107 antibodies do not recognise a scrambled form of QM107. (A)** Amino acid sequences of QM107 and scrambled QM107. **(B)** Wells were coated with QM107 or scrambled QM107 peptides (both 10µM), followed by detection by ELISA with post-injection rabbit serum samples (n=2).

3.2.3. Antibody characterisation

3.2.3.1. Detection of recombinant SDC2

Evidence suggests that the endogenous shed human SDC2 is found in the blood [218, 347]. As QM107 is a derivative of the SDC2 ectodomain core protein, there is a risk of interference in detection assays as the QM107 antibody may detect endogenous SDC2, causing false detection of QM107 in the biological sample, which may limit the application of the antibody. To determine whether this would be the case, the QM107 antibody was tested using a western blot to determine if it was able to detect recombinant human SDC2 in human serum (Fig. 3.6). Results show a lack of detection of recombinant SDC2 by anti-QM107, which both reinforces previous results showing the specificity of this antibody for QM107 (Figs. 3.4. and 3.5.) and suggests that *in vitro* detection of QM107 in biological samples is possible, as the optical density readouts correspond with QM107 amounts without interference from endogenous shed SDC2.

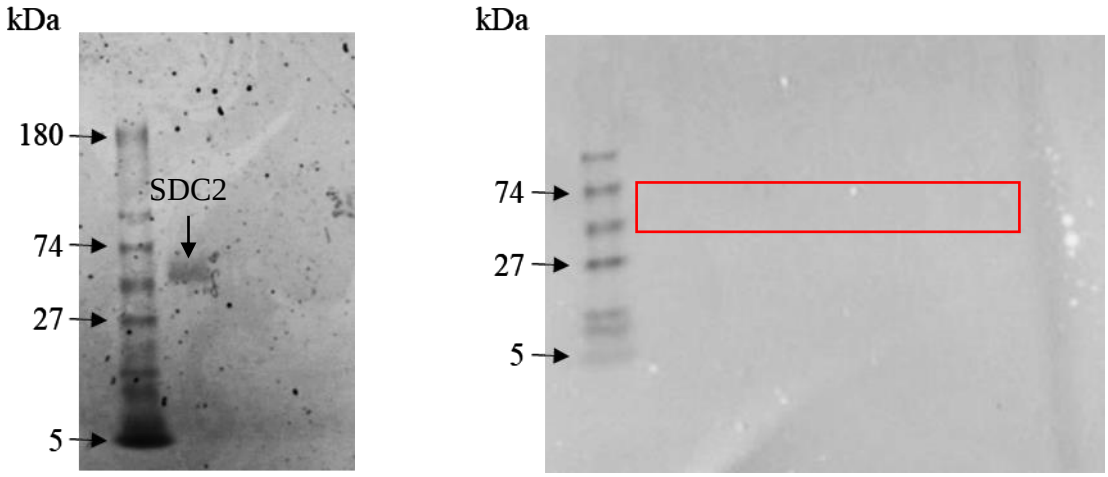

Figure 3.6. **Anti-QM107 does not detect syndecan-2. (A)** SDS-PAGE and Coomassie blue staining of 1µg SDC2 (n=1). **(B)** Western blot showing a lack of detection of recombinant human SDC2 at various concentrations (from the ladder, left to right: 1µg, 0.5µg, 0.25µg, 0.125µg) with anti-QM107 primary antibody followed by goat anti-rabbit HRP secondary antibody, followed by BCL detection (n=1). The red box indicates where we would expect to see SDC2 if detected.

Next, we wanted to assess the proteolytic sensitivity of QM107 against trypsin. We performed a degradation experiment in which QM107 was incubated with trypsin and detection was carried out at different time points, to establish QM107's degradability (Fig. 3.7.). Degradation reactions were terminated by the addition of PFA to samples and anti-QM107 was used for QM107 detection. Ultimately, optical density was measured following TMB1 detection of the secondary antibody. This data was compared with the readouts for QM107 standards of known concentrations (Fig. 3.7.B), to quantify the amount of QM107 remaining in trypsin-degraded samples. The results obtained confirm that QM107 is degraded by trypsin and this degradation increases with time: 10 minutes' incubation produced a readout equating to 2.5µg of QM107; 60 minutes' incubation resulted in no more than 1µg (Fig. 3.7C).

This assay confirmed that this methodology could be used to ascertain the stability of QM107 in biological samples *in vitro* since anti-QM107 detects full-length QM107 and not fragments produced after degradation, indicated by the fact the signal disappears after trypsin degradation. Therefore, readouts from stability assays in biological samples should correspond with remaining, un-degraded QM107, allowing us to calculate the extent of its degradation across different samples.

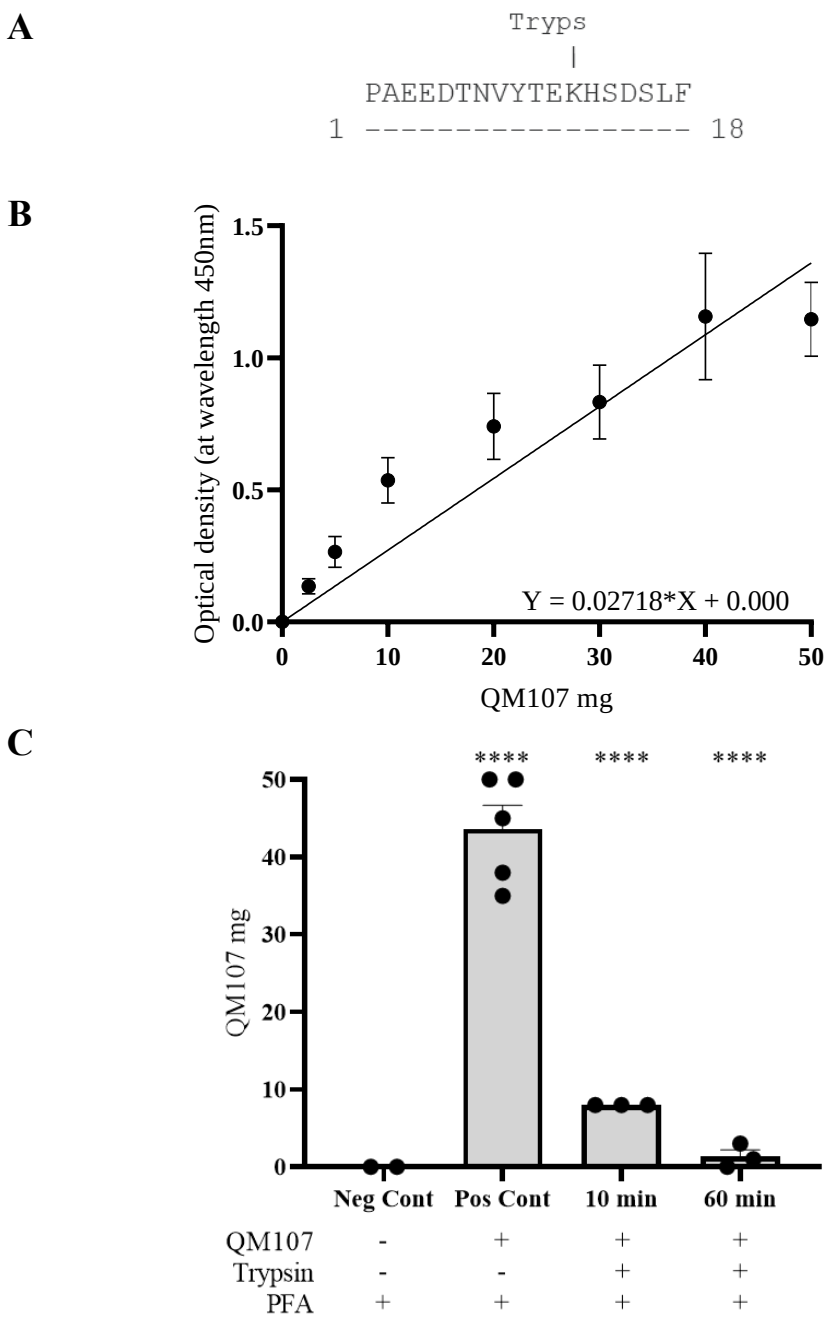

Figure 3.7. **QM107 is degraded by trypsin. (A)** Predicted trypsin degradation site identified on the QM107 peptide sequence, at the N-terminal side of the indicated amino acid. **(B)** Following a QM107 dilution series, optical density measurements were acquired and used to create a standard curve (n=1). **(C)** QM107 was incubated with trypsin for 10 minutes of 60 minutes before treatment with PFA to prevent further degradation. Optical density was measured and compared with both QM107 and PBS controls, whereby amounts of QM107 were calculated for each sample. Detection was with anti-QM107 primary antibody followed by goat anti-rabbit HRP secondary antibody, followed by TMB1 detection (n=1).

3.2.4. Detection assays

Having successfully developed an antibody against QM107, the next stage was to use it for detection of QM107 in biological samples. This is necessary in the development of QM107 as a therapeutic, as its detection in biological samples, such as blood, both *in vitro* and *in vivo* will be imperative in pharmacokinetic and toxicology studies.

3.2.4.1. Stability of QM107 in human serum

The therapeutic target of QM107 is CD148, located on cells of the vasculature, hence its stability in the blood needs to be determined. This also allows us to explore further routes of administration, for example via intravenous injection, if QM107 is in fact stable in blood. Furthermore, if QM017 enters the bloodstream via the retinal vasculature, we need to establish whether this will affect physiological angiogenesis elsewhere in the body. Thus, we developed an *in vitro* assay to establish QM107 stability in human serum. Serum was prepared from human whole blood samples, kindly donated by a number of volunteers. Following this, QM107 standards of known concentrations were made up and combined with human serum, then treated with PFA. Optical density readouts were obtained to plot a standard curve (Fig. 3.8A). The initial experiments used serum from one donor only and, using readouts from the standard curve produced, results showed QM107 was detectable at 0h, but had degraded after 24h (Fig. 3.8B).

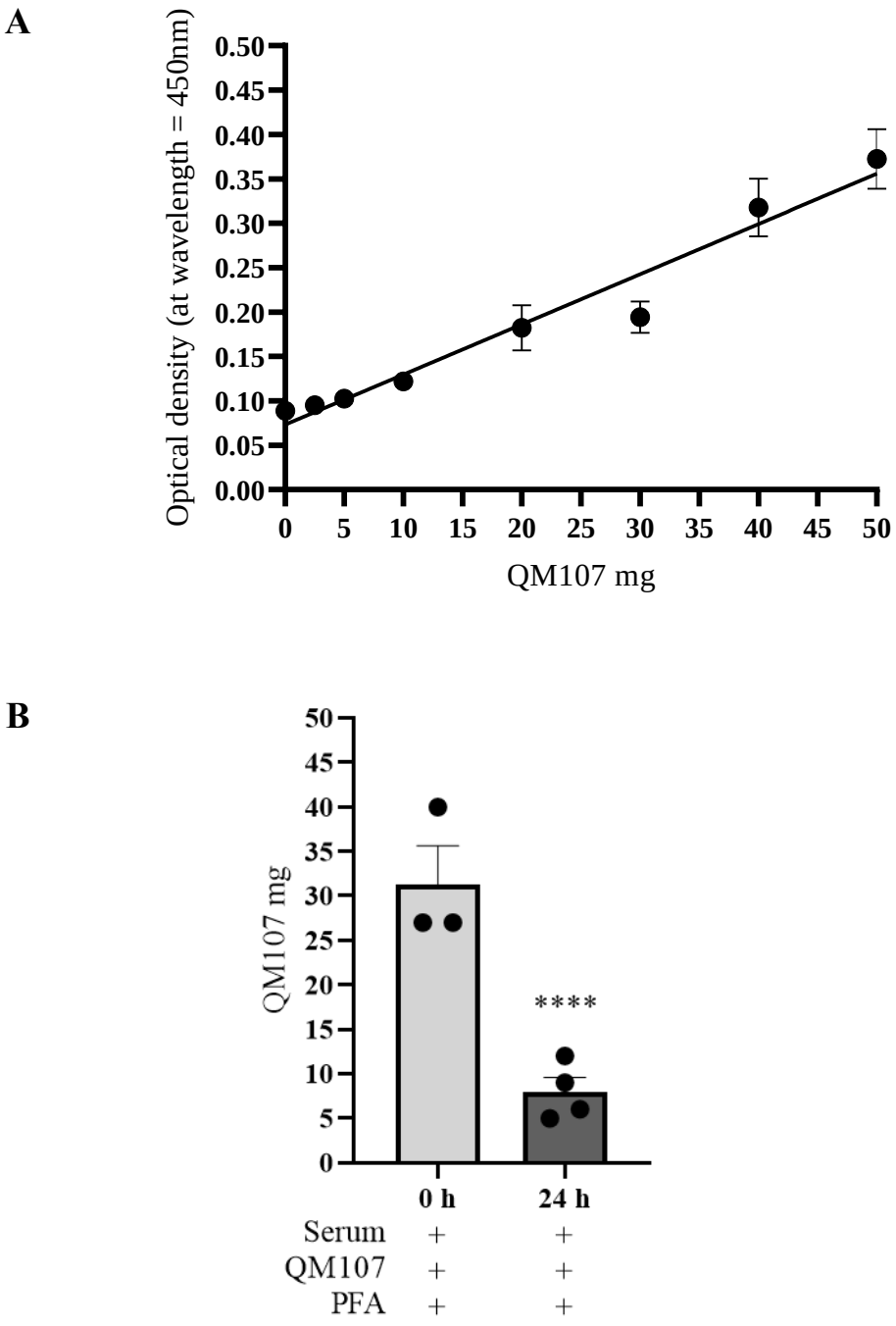

Figure 3.8. **QM107 degrades in human serum after 24h. (A)** Following a QM107 dilution series in human serum in the presence of PFA, optical density measurements were acquired and used to create a standard curve (n=1). **(B)** QM107 was incubated at 37°C with human serum and PFA added at different time points. Detection was with anti-QM107 primary antibody followed by anti-rabbit HRP secondary antibody, followed by TMB1 (n=1).

Subsequent validation experiments incorporated serum from five further volunteers. In this assay, just three QM107 concentrations were chosen (0, 25 and 50mg), incubated in serum for 10 minutes, and treated with PFA, before optical density readouts were measured (Fig. 3.9). There was variability between serum from different patients and between technical repeats in serum from the same patient. This was true at each QM107 concentration, including 0mg, where optical density readouts ranged from 0.08 – 1.45 (Fig. 3.9A). These values were much greater than those from initial experiments were where 0mg QM107 produced readouts of 0.1. Consequently, we determined that the variability across patient samples made this methodology unsuitable to determine QM107 stability in human serum.

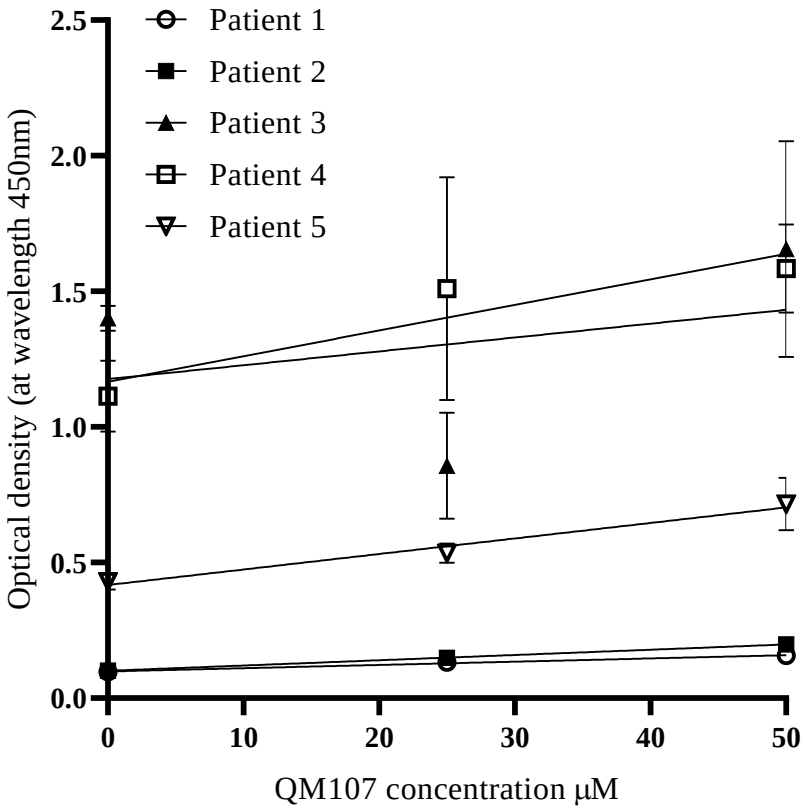

Figure 3.9. **QM107 in human sera was indeterminable.** Following a QM107 dilution series in human serum in the presence of PFA, optical density measurements were acquired for each sample (n=2). However, readouts varied across each patient sample.

3.2.4.2. Stability of QM107 in porcine vitreous humour

The proposed route of administration of QM107 is intravitreal injection, as is used already in administration of current anti-VEGF therapies. We therefore set out to establish how stable QM107 is in porcine vitreous humour (Fig. 3.10). If QM107 is stable in vitreous humour, it is more likely to reach its target: CD148 expressed on cells of the retinal vasculature at the back of the eye. Due to its high viscosity, vitreous humour was combined with 1x PBS in a 50:50 ratio. QM107 standards of known concentrations (0-50mg) were made and combined with vitreous humour, then treated with PFA. Optical density readouts were obtained to plot a standard curve (Fig. 3.10A). From this, the amount of QM107 in vitreous humour samples could be quantified, following incubation at 37°C. At both time points, high quantities of QM107 were detected (between 35 and 50mg in both samples, Fig. 3.10B), indicating that it is stable in vitreous humour. Furthermore, this methodology can be successfully utilised for detecting QM107 in biological samples. It is worth noting that these experiments were performed with higher concentrations of QM107 than would be administered to patients, due to a lack of sensitivity of the antibody. This is an important consideration to include when planning QM107 detection *in vivo* using this methodology.

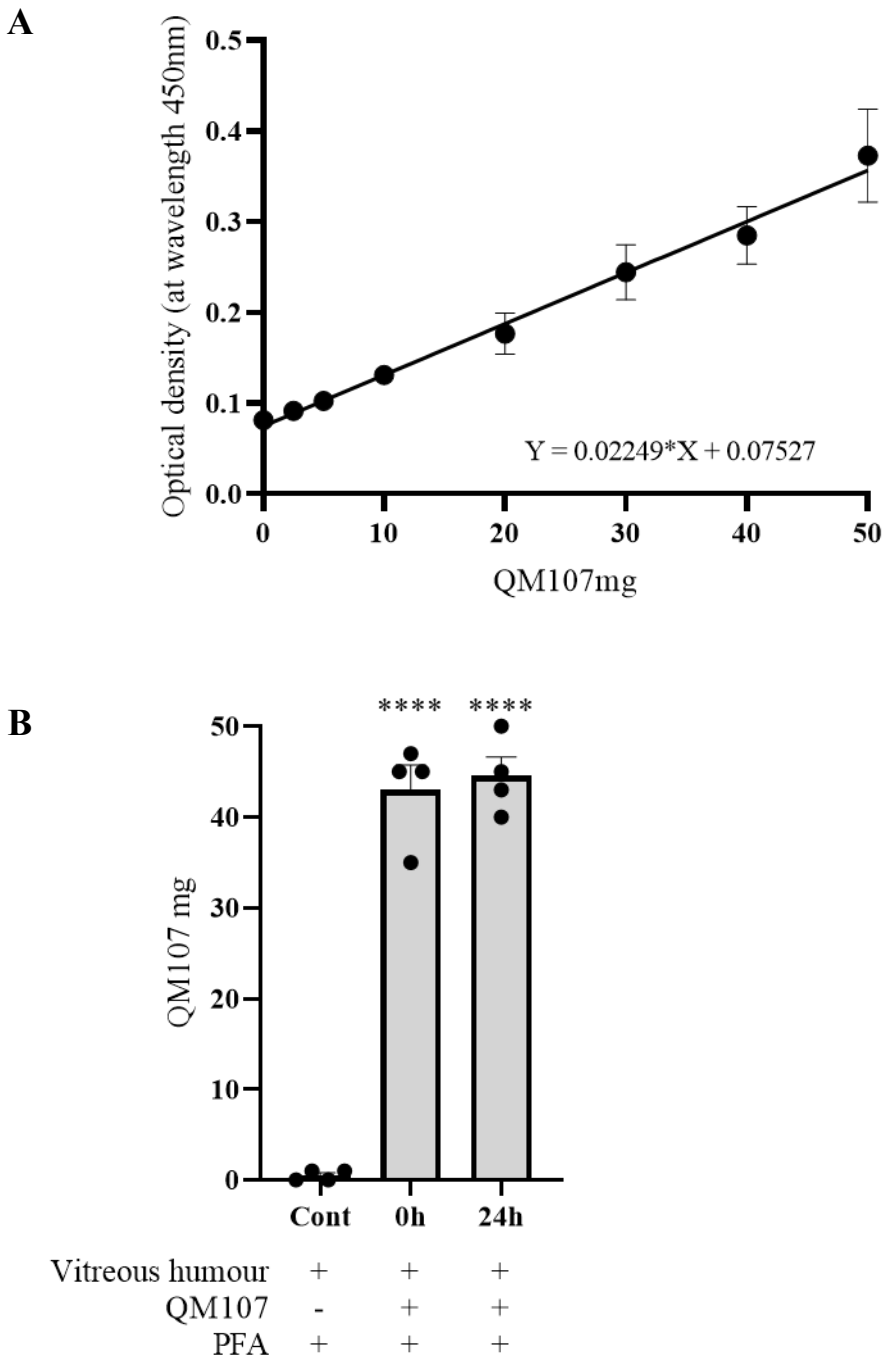

Figure 3.10. **QM107 is stable in vitreous humour. (A)** Following a QM107 dilution series in porcine vitreous humour in the presence of PFA, optical density measurements were acquired and used to create a standard curve (n=1). **(B)** QM107 was incubated at 37°C with porcine vitreous humour and PFA added at different time points. Detection was with anti-QM107 primary antibody followed by anti-rabbit HRP secondary antibody, followed by TMB1 (n=2).

3.3. Discussion

In this chapter, following successful production of an in-house antibody against QM107, we established a methodology for detecting QM107 *in vitro*, which can be used for initial QM107 stability assays. The therapeutic target of QM107 is the retinal vasculature located in the eye – hence, a very inaccessible site from which to obtain samples to quantify QM107, demonstrating the necessity of developing a methodology with which to measure QM107 in various other biological samples. Furthermore, changes in plasma drug concentration indicate changes in other tissues, crucially those at the receptor site. In essence, it is assumed that the higher the plasma drug concentration, the higher its concentration in other body tissues (and vice versa), though this is not necessarily true for all drugs [398]. The kinetic homogeneity is imperative for verifying therapeutic and toxic plasma drug concentrations. In order to determine these parameters with regard to QM107, we need to measure QM107 concentrations at different time points in various biological samples.

The principal goal was to develop a methodology for *in vitro* QM107 detection in biological samples, predominantly in vitreous humour and blood, due to the location of QM107's therapeutic target: the retinal vasculature. Current treatment of diabetic retinopathy and other neovascular eye diseases necessitates an intravitreal injection, allowing the drugs to diffuse through the vitreous humour towards the back of the eye whereby they block VEGFA activity in the damaged blood vessels supplying the retina. We show that QM107 is stable in porcine vitreous humour, indicating that application via the intravitreal route would allow QM107 to reach its therapeutic target, CD148, at the back of the eye. We also established a methodology to use the antibody for QM107 detection in human serum; however, this posed a number of confounding factors that require resolution before this methodology can be utilised.

In QM107 stability assays with human serum samples, there was much variability across patient samples. In initial detection assays (Fig. 3.8), QM107 was detectable at 0h but was shown to degrade after 24h. Subsequent validation experiments using serum isolated from blood donated by other volunteers did not support these initial findings, with inconsistent readouts both between patients and between technical repeats of the same serum sample (Fig. 3.9). Whether these variable results indicate detection of endogenous shed SDC2, despite its lack of detectability *in vitro*, or whether factors such as diet, age and sex of the donors confound the QM107 readout are yet to be determined. Consequently, we determined that patient variability confounded the results of QM107 readouts, making this detection method ineffective for detecting QM107 *in vitro*. Going forward, incorporating a larger sample size to test more serum samples will be imperative, to overcome this variability or to determine the cause for it.

From our data, it has also become clear that the sensitivity of anti-QM107 to detect QM107 in biological samples is limited. Its therapeutic dose will be much lower than that of the *in vitro* standard concentrations (with a maximum dose of 0.5µM) and, therefore, mass spectrometry will be necessary going forward in toxicology studies. Following the success of raising an antibody to QM107, future work could include refining this, perhaps developing a monoclonal anti-QM107 or using phage display to produce antibodies that enable the detection to be more specific and efficient.

To further characterise QM107, its rate of degradation was ascertained. This is imperative for therapeutic development, for numerous reasons, including calculation of half-life. Using Expasy protein cutter software, a potential trypsin enzyme degradation site was discovered in the QM107 peptide sequence (Fig. 3.7A). Therefore, we determined the rate of QM107 degradation by trypsin *in vitro*.

To date, in our hands there has been no reliable SDC2 antibody, despite their commercial availability. The reason for this is unclear, but perhaps because the SDC molecules do not produce a strong immunogenic response, when SDC antibodies are commercially made, they are of a lower concentration or potency than other marketed antibodies. As part of this project, we carried out western blot analysis to determine whether the QM107 antibody was able to detect SDC2, due to the sequence homology between QM107 and SDC2. Despite this homology, we determined that the antibody does not detect full-length recombinant human SDC2 *in vitro*. It remains unclear whether the antibody does detect endogenous SDC2, though future work with human sera could shed some light on this question. It would also be interesting to explore the possibility of producing SDC2 antibodies from a SDC2-null mouse, as these animals have never encountered SDC2 molecules previously, and therefore the immunogenic response to SDC2 injection may be much greater than that in wild-type animals.

3.3.1. Summary points

- QM107 does retain the same anti-angiogenic properties as the SDC2 core protein, demonstrated in murine aortic ring and scratch wound migration assays
- We successfully raised an antibody against QM107 and used it to characterise QM107 in *in vitro* stability assays, through detection of the peptide in biological samples
- While further work needs to be carried out to determine QM107 stability in human serum, we have shown that it is stable in porcine vitreous humour

Chapter 4

4. Determining the QM107 interaction site on CD148

4.1. Introduction

There is an abundance of work that suggests a role for SDC2 in angiogenesis. SDC2 expression is traditionally associated with cells of the vasculature, and studies in zebrafish and mice have shown that when SDC2 gene expression is knocked down or ablated, normal vascular development is delayed [346, 399]. These studies have linked SDC2 with the VEGFA/ VEGFR2 signalling axis via interactions with its heparan sulphate (HS) chains. In work from our group, it was established that SDC2 in its shed form can inhibit angiogenesis. Conditioned media from HEK293T cells transduced to overexpress an HA-tagged form of SDC2 after stimulation with TNFα was found not only to contain significant amounts of shed SDC2, but this media also substantially inhibited angiogenic sprout formation from rat aortic rings, specifically through its interaction with β1 integrin and CD148 [347]. Furthermore, in a xenograft flank tumour model, SCID SHO mice were injected with empty vector cells or cells that constitutively released shed syndecan-2 (eS2ED) and tumour sizes were quantified at 21 days. The mice injected with control cells developed vascularised tumours that were significantly larger in both diameter and weight compared with tumours derived from mice injected with the eS2ED cells. Following immunofluorescence staining for the EC marker CD31 (PECAM1), tumours generated from empty vector control cells revealed CD31-positive structures consistent with blood vessels. However, these structures were greatly reduced in tumour sections originating from eS2ED cells. Together, this suggests that constitutive release of the SDC2 ectodomain in this model is inhibitory to angiogenesis.

In a previous study, it was shown that the extracellular core protein of SDC2 could influence cell behaviour independently of SDC2 HS chains. A glutathione-S-transferase (GST) fusion protein was generated, in which the full coding sequence of the SDC2 extracellular core protein was translationally fused at the N-terminus to GST. This protein could support cell adhesion in serum free media in a variety of cell types (primarily mesenchymal). It was established that these adhesion responses to the SDC2 extracellular domain core protein (S2ED) require β1 integrins [218]. However, no direct interaction between β1 integrin and S2ED could be established, so it was hypothesised that this adhesion response requires the action of an additional cell surface receptor. Protein phosphorylation is a vital mechanism for regulating cellular processes (including cell adhesion), involving a number of protein kinases and counteracting protein phosphatases [218]. Fibroblasts seeded on S2ED formed focal adhesions and positive staining of phosphotyrosine was observed [218, 400]. Further observations confirmed increases in the phosphorylation of key focal adhesion components such as paxillin and focal adhesion kinase [401]. Three common PTP inhibitors (pervanadate, phenylarsine oxide and dephostatin) bind irreversibly to the catalytic cysteine required for dephosphorylation of phosphotyrosine residues [402, 403]. Their effect on rat embryonic fibroblasts seeded on S2ED was a reduction in cell attachment and spreading. Due to the importance of phosphatase activity in processes governing adhesion to S2ED, investigations were carried out into whether a PTPR might be the intermediary molecule interacting with S2ED, leading to β1 integrin–dependent cell adhesion and spreading. CD148 was identified as being potentially important following a small interfering RNA (siRNA) screen of the 207 phosphatase genes in the human genome. The importance of CD148 in cell adhesion responses to S2ED was confirmed in WI38 human lung fibroblasts following transfection with siRNA targeted to CD148.

These fibroblasts had significantly reduced adhesion to S2ED. Significantly, in this study an 'adhesion regulatory domain' of SDC2 was identified between P^{124} and F^{141} of murine SDC2. Proteins lacking this sequence could not support cell adhesion.

Of importance, it was later shown that the SDC2-GST fusion protein could also inhibit angiogenesis both *in vivo* (Matrigel plug assay) and *ex vivo* (aortic ring assay). An interaction between S2ED and CD148 was confirmed by a pull down assay, in which glutathione agarose beads were used to 'pull down' interacting proteins from EC lysates. Lysates probed with full length S2ED contained CD148, but lysates probed with S2ED in which the adhesion regulatory domain had been deleted did not. This was supported by previous work, in which the 18 amino acid adhesion regulatory domain between P^{124} and F^{141} was deleted. The importance of the 18 amino acids was confirmed in functional assays where the anti-angiogenic properties of S2ED are lost when this 18 amino acid motif is not present. Treatment of ECs with S2ED also revealed a change in β1 activation status, as determined by the conformer specific monoclonal antibody (9EG7).

Ultimately, the data from these studies suggest that two key angiogenic processes, cell adhesion and inhibition of angiogenic sprout formation, are driven by CD148 via its direct interaction between its extracellular N-terminus and the 18 amino acid adhesion regulatory motif of S2ED. Furthermore, the anti-migratory effects of S2ED on ECs may be mediated by CD148 signalling, an interaction that could lead to reduced active β1 integrins on the surface of ECs.

Building on this work, the overarching aim of this chapter was to confirm whether QM107 binds to CD148, and to try to ascertain where on the CD148 extracellular core protein this occurs. Previous studies indicated that this interaction site is likely to be somewhere within the first five FNIII

repeats, since S2ED binds to this protein. This would provide insight into how QM107 functions as a therapeutic, to inhibit angiogenesis.

To this end, the following aims will be addressed in this chapter:

1. To determine whether QM107 interacts with CD148SF?

2. To define the precise amino acid motif on CD148SF responsible for this interaction with CD148SF

3. To identify a specific amino acid motif in the QM107 sequence responsible for its interaction with CD148

4.2. Results

4.2.1. Developing methodology to identify QM107 interaction site on CD148

4.2.1.1. Production of CD148-derived proteins

From previous studies, it is known that shed SDC2 binds to a bacterially expressed version of a truncated splice variant of CD148 (consisting of the first five FNIII repeats of CD148's extracellular domain – protein termed CD148SF) [167]. As QM107 is a derivative of SDC2, we investigated whether QM107 could also interact with CD148SF. In order to establish this, we first had to optimise a methodology for assaying the interaction between QM107 and CD148SF.

Initially we expressed and purified CD148SF recombinant protein from bacteria. We also generated two truncated forms of CD148SF: CD148NT and CD148CT (Fig. 4.1). CD148NT comprised the first two FNIII repeats from A^{36} – L^{291} of the CD148SF sequence. CD148CT comprised the remaining three FNIII repeats from D^{192} – G^{539}. These were expressed and purified, as described in Materials and Methods (Chapter 2).

A

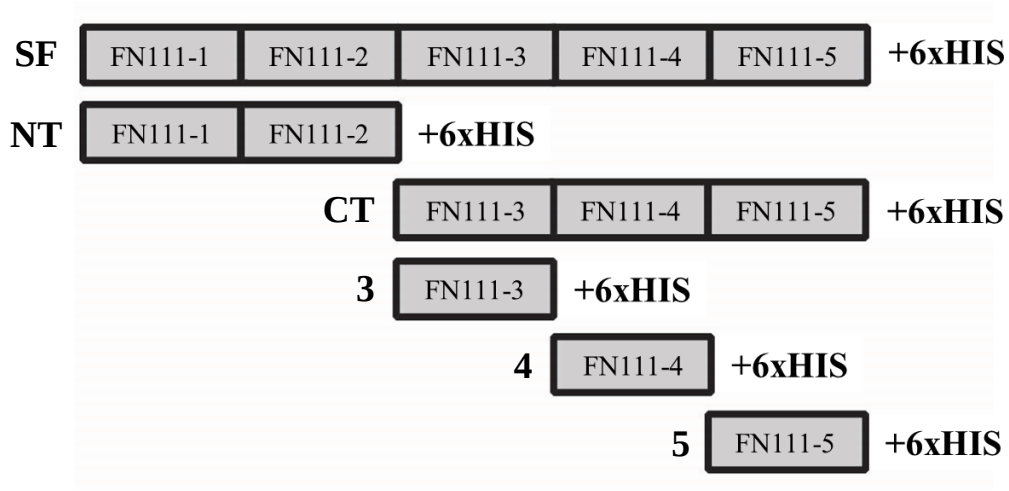

B

```
 36 AGGTPSPIPD PSVATVATGE NGITQISSTA ESFHKQNGTG TPQVETNTSE
 86 DGESSGANDS LRTPEQGSNG TDGASQKTPS STGPSPVFDI KAVSISPTNV
136 ILTWKSNDTA ASEYKYVVKH KMENEKTITV VHQPWCNITG LRPATSYVFS
186 ITPGIGNETW GDPRVIKVIT EPIPVSDLRV ALTGVRKAAL SWSNGNGTAS
236 CRVLLESIGS HEELTQDSRL QVNISGLKPG VQYNINPYLL QSNKTKGDPL
286 GTEGGLDASN TERSRAGSPT APVHDESLVG PVDPSSGQQS RDTEVLLVGL
336 EPGTRYNATV YSQAANGTEG QPQAIEFRTN AIQVFDVTAV NISATSLTLI
386 WKVSDNESSS NYTYKIHVAG ETDSSNLNVS EPRAVIPGLR SSTFYNITVC
436 PVLGDIEGTP GFLQVHTPPV PVSDFRVTVV STTEIGLAWS SHDAESFQMH
486 ITQEGAGNSR VEITTNQSII IGGLFPGTKY CFEIVPKGPN GTEGASRTVC
536 NRTG
```

C

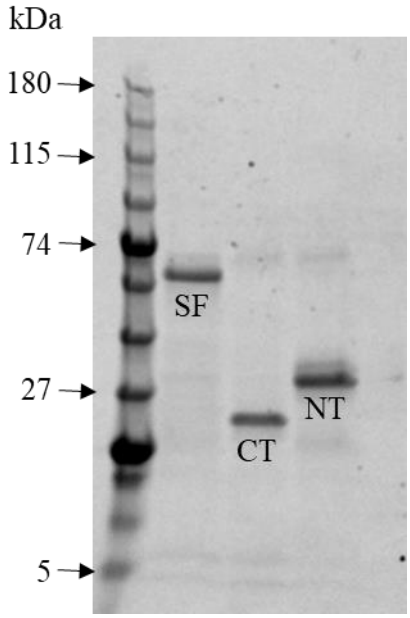

Figure 4.1. **Recombinant expression of CD148-derived proteins. (A)** SF corresponds to the first five N-terminal fibronectin type-III (FNIII) repeats of CD148. This can be divided into two domains, the N-terminus and C-terminus. These can be bacterially expressed. **(B)** CD148NT A^{36} – L^{291}, shown in black. CD148CT D^{292} – G^{539}, shown in red. **(C)** SDS-PAGE gel image, following protein purification and dialysis with 1x PBS. 10µl samples of the proteins were analysed and results confirmed the presence of CD148SF (53kDa), CD148CT (26.4kDa) and CD148NT (26.9kDa). SDS-PAGE was used to verify the correct molecular weight and purity of the proteins.

4.2.1.2. Solid phase binding assay with QM107 antibody detection method

In the first instance, we tested whether our antibody raised against QM107, as described in the previous chapter, could be utilised for this purpose. For initial experiments, we compared binding of QM107 to CD148 with binding to fibronectin as a negative control (Fig. 4.2). Fibronectin contains 16 FNIII repeats and previous work showed that S2ED does not interact with these. Using an ELISA-based methodology, we measured the amount of QM107 that bound to both proteins after a 1-hour incubation together. Whilst optical density measurements revealed enhanced binding of QM107 to CD148SF this was not the case for fibronectin, particularly at high coating concentrations. Although the trend was positive, the difference between CD148SF and fibronectin was not significant and there were concerns about the sensitivity of the QM107 antibody – in essence, whether it would be able to detect low concentrations of QM107. However, as this data did show that there might be an interaction between CD148SF and QM107, going forward we decided to explore other detection methodologies for use in solid phase binding assays.

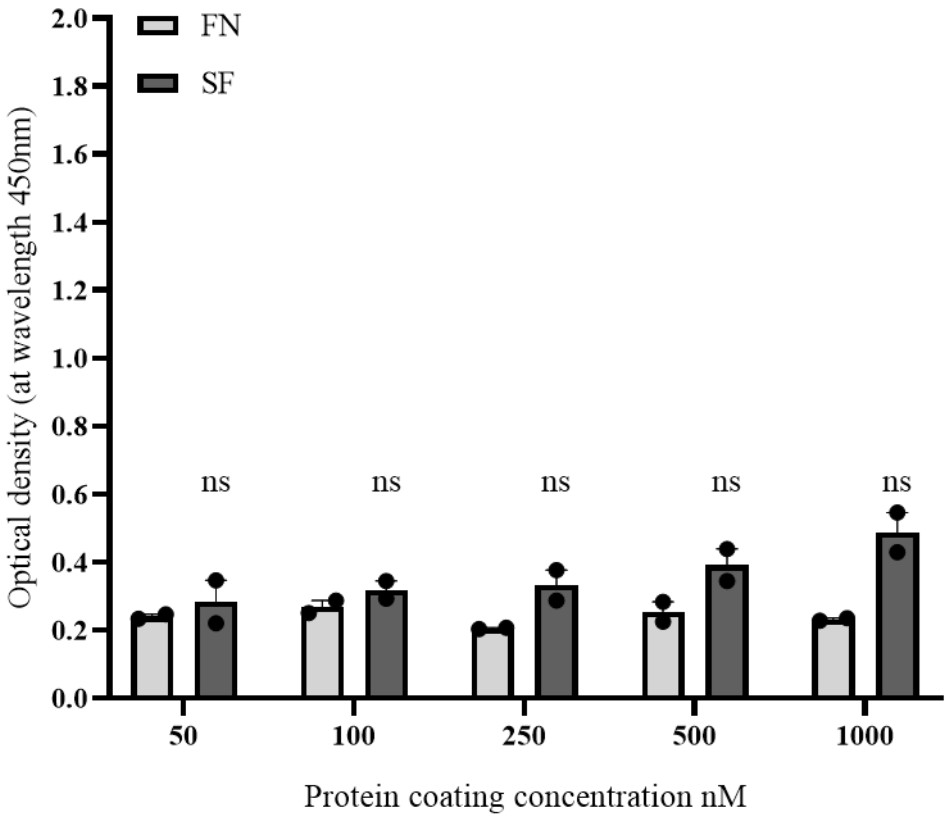

Figure 4.2. **Solid phase binding assay using anti-QM107 shows a greater interaction between QM107 and CD148SF than with fibronectin.** Following the administration of 10µM QM107 for 1 hour at room temperature in wells of a 96 well plate coated with CD148SF (SF) or fibronectin (FN), anti-QM107 was used to detect QM107. Detection with an anti-rabbit HRP-conjugated secondary antibody in conjunction with TMB1 revealed a difference in optical density readouts for QM107 between SF and FN (n=1).

4.2.1.3. Solid phase binding assays with biotinylated QM107

Since the anti-QM107 antibody was not optimal for use in our solid phase binding assays, we next investigated whether a biotinylated form of QM107 (bio-QM107) could be used in conjunction with streptavidin conjugated to HRP. N-terminal bioconjugation was used to bind the biotin molecule to the proline amino acid in position 1 on the QM107 sequence (Figure 4.3). Conjugating molecules on to terminals is unlikely to affect protein function [404, 405].

Figure 4.3: QM107 molecule after biotinylation. The biotin molecule is bound to the N-terminus of QM107.

In the first assay, we set out to comprehend whether there was an interaction between QM107 and CD148SF (Fig. 4.4). This methodology involved coating the microplate with CD148-derived recombinant proteins, also using fibronectin as a control, followed by the addition of bio-QM107. Several optimisation steps were required to establish this assay. The CD148SF protein (and others used in this study) is 6xHis-tagged and purified using a cobalt affinity resin. Contained within the elution buffer is imidazole, and we established the assay works best if this is removed via dialysis.

Initial assays demonstrated an interaction between bio-QM107 and CD148SF but not with the fibronectin control. Higher optical densities were recorded when bio-QM107 was incubated with CD148SF-coated wells. Additionally, a dose-response can be observed: optical density output readings decrease in accordance with declining CD148SF protein coating concentration.

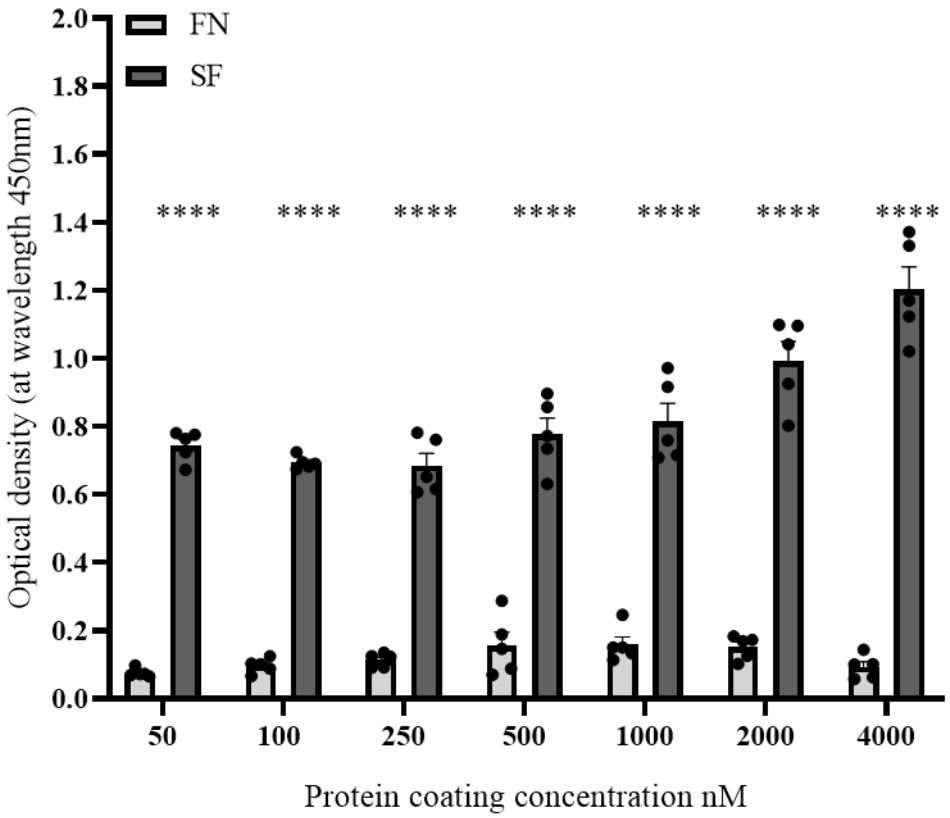

Figure 4.4. **Use of biotinylated QM107 provides a more robust methodology for establishing that QM107 interacts with CD148SF.** Solid phase binding assays in which plates were coated with CD148SF and fibronectin, prior to the addition of 10μM bio-QM107, showed interaction between QM107 and CD148SF (n=3).

4.2.2. Mapping which region of CD148 interacts with bio-QM107

Having established an interaction between CD148SF and bio-QM107, we next sought to identify which part of CD148SF was responsible for this interaction. We assayed the truncated forms of CD148SF (CD148CT and CD148NT, Fig. 4.1). This time, the microplate was coated with CD148-derived recombinant proteins, also using fibronectin as a control, followed by the addition of bio-QM107. As with the CD148SF protein, the CD148CT and CD148NT proteins are 6xHis-tagged and purified using a cobalt affinity resin, followed by dialysis with PBS to remove residual imidazole.

Upon testing these proteins in our binding assay, it was evident that there was an interaction between bio-QM107 and both CD148SF and CD148CT, but not with CD148NT or the fibronectin negative control (Fig. 4.5). This data suggested that the interaction site for QM107 resided somewhere in FNIII repeats 3-5.

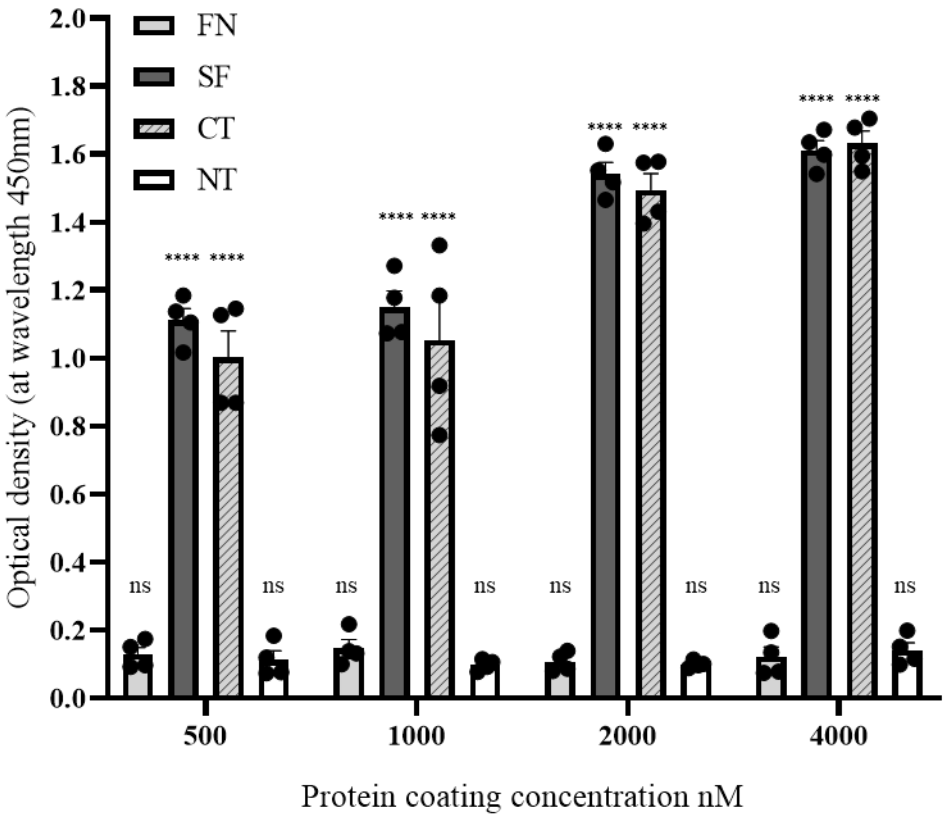

Figure 4.5. **QM107 interacts with CD148CT.** Solid phase binding assays in which plates were coated with CD148-dervied recombinant proteins CD148SF, CT and NT and fibronectin, prior to the addition of 10µM bio-QM107, showed interaction between QM107 and CD148CT, as well as SF. Bio-QM107 did not interact with CD148NT (n=3).

To further refine the interaction site within the CD148CT sequence, we set out to express each individual FNIII repeat that makes up CD148CT as a distinct peptide (Fig. 4.6) to be tested in solid phase binding assays (Fig. 4.7). Using the same methodology as used previously to recombinantly express CD148-derived proteins, we successfully expressed FNIII repeats 3, 4 and 5 as distinct proteins, as shown in Fig. 4.6.

A

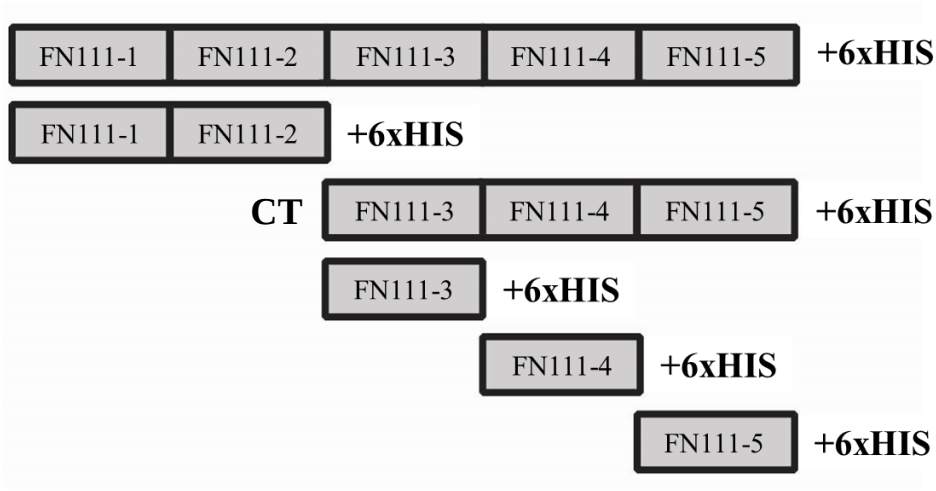

B

```
 36 AGGTPSPIPD PSVATVATGE NGITQISSTA ESFHKQNGTG TPQVETNTSE
 86 DGESSGANDS LRTPEQGSNG TDGASQKTPS STGPSPVFDI KAVSISPTNV
136 ILTWKSNDTA ASEYKYVVKH KMENEKTITV VHQPWCNITG LRPATSYVFS
186 ITPGIGNETW GDPRVIKVIT EPIPVSDLRV ALTGVRKAAL SWSNGNGTAS
236 CRVLLESIGS HEELTQDSRL QVNISGLKPG VQYNINPYLL QSNKTKGDPL
286 GTEGGLDASN TERSRAGSPT APVHDESLVG PVDPSSGQQS RDTEVLLVGL
336 EPGTRYNATV YSQAANGTEG QPQAIEFRTN AIQVFDVTAV NISATSLTLI
386 WKVSDNESSS NYTYKIHVAG ETDSSNLNVS EPRAVIPGLR SSTFYNITVC
436 PVLGDIEGTP GFLQVHTPPV PVSDFRVTVV STTEIGLAWS SHDAESFQMH
486 ITQEGAGNSR VEITTNQSII IGGLFPGTKY CFEIVPKGPN GTEGASRTVC
536 NRTG
```

FNIII-1 $A^{36} – E^{206}$
FNIII-2 $P^{207} – L^{291}$
FNIII-3 $D^{292} – T^{364}$
FNIII-4 $N^{365} – V^{455}$
FNIII-5 $P^{456} – G^{539}$

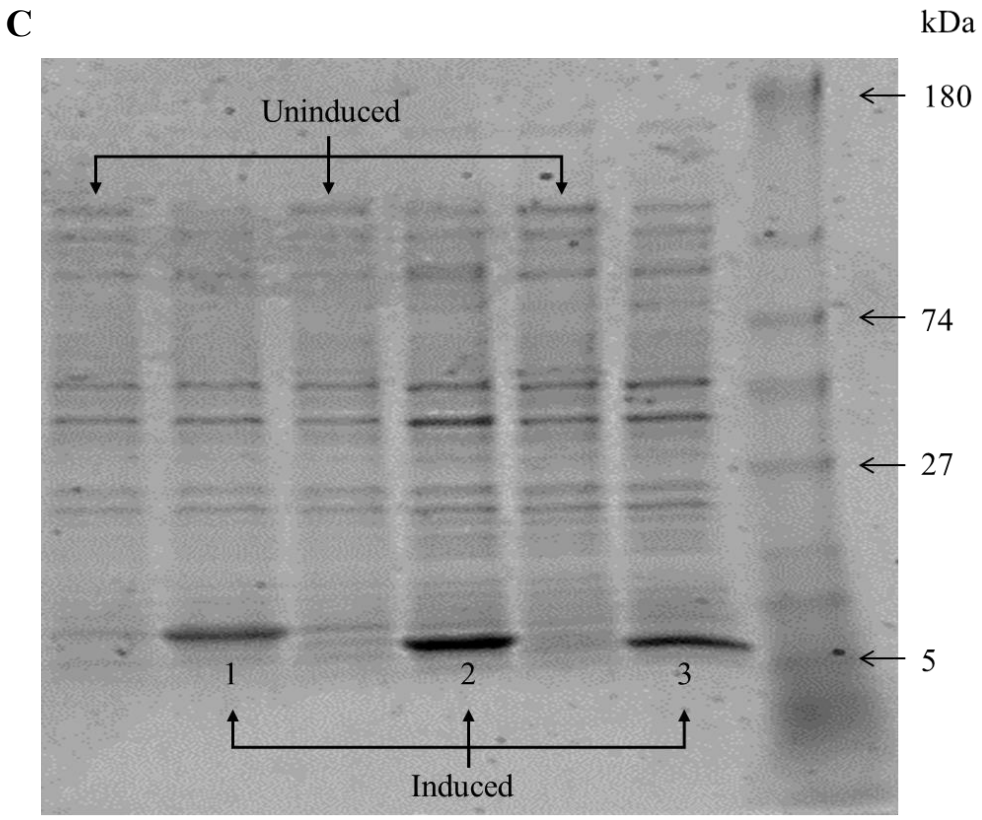

Figure 4.6. **Recombinant expression and purification of CD148CT-derived FNIII repeats. (A)** NT consists of FNIII repeats 1 and 2, CT consists of FNIII repeats 3-5, which can also be bacterially expressed. **(B)** Full-length CD148SF sequence shown, with individual FNIII repeats indicated in different colours. **(C)** SDS-PAGE gel image, following IPTG-induction of BL21 cultures, confirming the presence of FNIII repeats 3 (9.9kDa), 4 (9.5kDa) and 5 (9.0kDa). Uninduced BL21 culture samples were run alongside induced samples for each protein (indicated in the figure), to confirm that the proteins were only produced by bacterial cultures following IPTG-induction. SDS-PAGE was used to verify the correct molecular weight of the proteins.

Interaction between bio-QM107 and all three FNIII repeats was determined, though this interaction was deemed to be strongest with repeats 3 and 5, perhaps indicating multiple QM107 interaction sites across CD148CT (Fig. 4.7A).

A

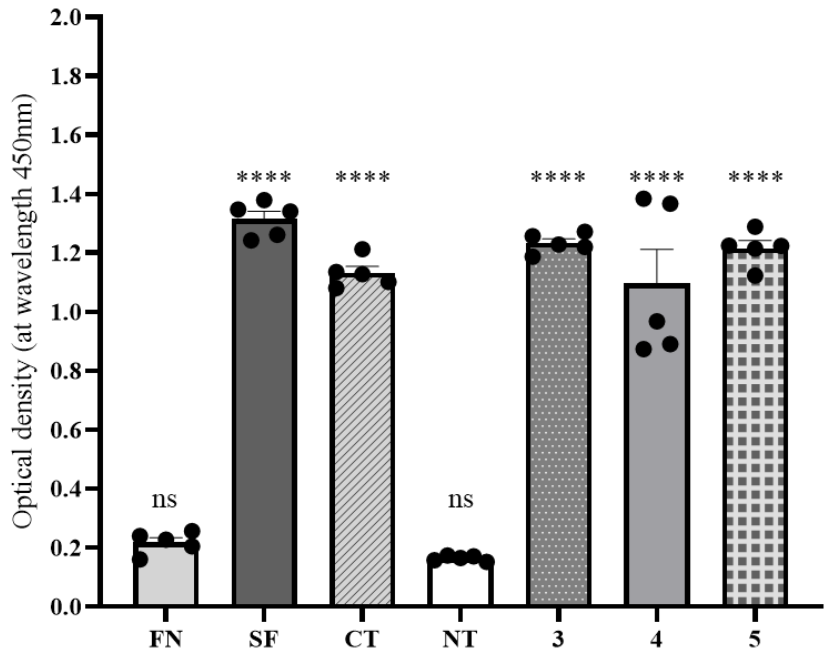

B

```
 36 AGGTPSPIPD PSVATVATGE NGITQISSTA ESFHKQNGTG TPQVETNTSE
 86 DGESSGANDS LRTPEQGSNG TDGASQKTPS STGPSPVFDI KAVSISPTNV
136 ILTWKSNDTA ASEYKYVVKH KMENEKTITV VHQPWCNITG LRPATSYVFS
186 ITPGIGNETW GDPRVIKVIT EPIPVSDLRV ALTGVRKAAL SWSNGNGTAS
236 CRVLLESIGS HEELTQDSRL QVNISGLKPG VQYNINPYLL QSNKTKGDPL
286 GTEGGLDASN TERSRAGSPT APVHDESLVG PVDPSSGQQS RDTEVLLVGL
336 EPGTRYNATV YSQAANGTEG QPQAIEFRTN AIQVFDVTAV NISATSLTLI
386 WKVSDNESSS NYTYKIHVAG ETDSSNLNVS EPRAVIPGLR SSTFYNITVC
436 PVLGDIEGTP GFLQVHTPPV PVSDFRVTVV STTEIGLAWS SHDAESFQMH
486 ITQEGAGNSR VEITTNQSII IGGLFPGTKY CFEIVPKGPN GTEGASRTVC
536 NRTG
```

Figure 4.7. **QM107 interacts with multiple FNIII repeats on CD148's extracellular domain. (A)** Solid phase binding assays, in which plates were coated with 1000nM CD148-derived recombinant proteins SF, CT, NT; individual FNIII repeats 3, 4 and 5; and fibronectin, prior to the addition of 10µM bio-QM107, showed interaction between QM107 and individual FNIII repeats comprising CD148CT (n=3). **(B)** SF ($A^{36} - G^{539}$) full-length amino acid sequence, with yellow highlighted areas indicating conserved regions across CT that were identified.

4.2.2.1. Deleted SF mutants

Following the detection of bio-QM107 with FNIII repeats 3, 4 and 5 (Fig. 4.7A), which comprise the C-terminal end of CD148SF (CD148CT), we identified conserved regions across the amino acid sequences of these FNIII repeats (according to the UniProt database which can be found here: https://www.uniprot.org/uniprotkb/Q12913/entry). FNIII repeats 3 and 5 share an identical amino acid motif and a similar, but non-identical, motif was recognised in FNIII repeat 4 (shown in Fig. 4.7B). We explored this as a potential interaction site for QM107 as solid phase binding assays showed strongest interactions between bio-QM107 and FNIII repeats 3 and 5; these repeats share identical amino acid motifs, whereas the motif identified in repeat 4 is not identical and there appears to be a weaker interaction between this FNIII repeat and bio-QM107. This disparity in motifs across FNIII repeats 3 and 5 compared with 4 may explain the difference seen in bio-QM107 interaction.

To begin with, we successfully produced a plasmid using only FNIII5, with the GTEG motif deleted from the full-length amino acid sequence (Fig. 4.8).

A

```
456 PVSDFRVTVV STTEIGLAWS SHDAESFQMH ITQEGAGNSR VEITTNQSII
506 IGGLFPGTKY CFEIVPKGPN GTEGASRTVC NRTG

456 PVSDFRVTVV STTEIGLAWS SHDAESFQMH ITQEGAGNSR VEITTNQSII
506 IGGLFPGTKY CFEIVPKGPN ASRTVCNRTG
```

B

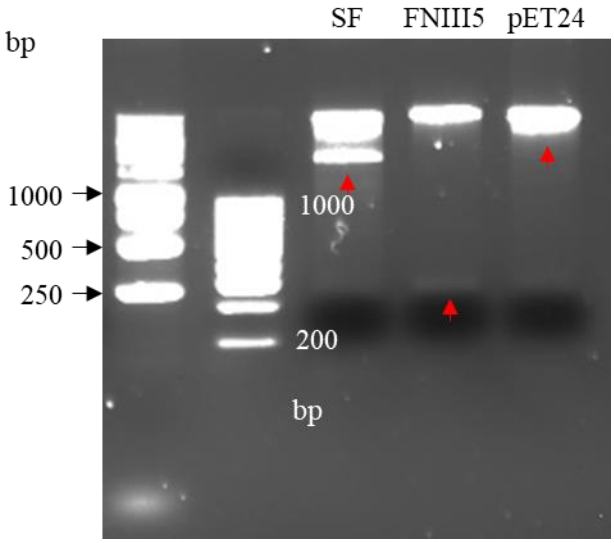

Figure 4.8. **Mutated FNIII5 plasmid made. (A)** FNIII5 ($P^{456} - G^{539}$) full-length amino acid sequence, with yellow highlighted areas indicating conserved region that was deleted, followed by FNIII5 deletion new sequence, with deleted motif removed. **(B)** The coding sequence corresponding to FNIII5 deletion (FNIII5, indicated) amplified by PCR and later ligated into the pET24 vector (indicated). Plasmid was digested with BamH1 and HindIII.

Unfortunately, it subsequently became apparent that the new FNIII5 deletion protein was unable to withstand purification, possibly due to its small size causing it to become insoluble and therefore non-retainable during the purification process. Therefore, we produced a new plasmid, wherein the GTEG and EGPTG motifs were deleted from the full-length CD148SF sequence in the FNIII3, 4 and 5 regions (as shown in Fig. 4.9A and 4.9B). This plasmid was used to produce mutated recombinant protein with these motifs removed (Fig. 4.9C), which we called SF deletion 1 (SFd1), via the *E. Coli* BL21 cell expression system. We used SFd1 in solid phase binding assays with bio-QM107 (Fig. 4.9D); if the motif we have identified is indeed the interaction site motif, its removal from the sequence should cause a reduction or elimination of interaction with bio-QM107. However, we found that the absence of the previously identified motifs did not prevent interaction with bio-QM107 – indeed, it seemed to intensify the interaction (Fig. 4.9D). Our conclusion from this was that we had misidentified the amino acid motif containing the sequence responsible for the interaction.

A

```
 36 AGGTPSPIPD PSVATVATGE NGITQISSTA ESFHKQNGTG TPQVETNTSE
 86 DGESSGANDS LRTPEQGSNG TDGASQKTPS STGPSPVFDI KAVSISPTNV
136 ILTWKSNDTA ASEYKYVVKH KMENEKTITV VHQPWCNITG LRPATSYVFS
186 ITPGIGNETW GDPRVIKVIT EPIPVSDLRV ALTGVRKAAL SWSNGNGTAS
236 CRVLLESIGS HEELTQDSRL QVNISGLKPG VQYNINPYLL QSNKTKGDPL
286 GTEGGLDASN TERSRAGSPT APVHDESLVG PVDPSSGQQS RDTEVLLVGL
336 EPGTRYNATV YSQAANGTEG QPQAIEFRTN AIQVFDVTAV NISATSLTLI
386 WKVSDNESSS NYTYKIHVAG ETDSSNLNVS EPRAVIPGLR SSTFYNITVC
436 PVLGDIEGTP GFLQVHTPPV PVSDFRVTVV STTEIGLAWS SHDAESFQMH
486 ITQEGAGNSR VEITTNQSII IGGLFPGTKY CFEIVPKGPN GTEGASRTVC
536 NRTG
```

↓

```
 36 AGGTPSPIPD PSVATVATGE NGITQISSTA ESFHKQNGTG TPQVETNTSE
 86 DGESSGANDS LRTPEQGSNG TDGASQKTPS STGPSPVFDI KAVSISPTNV
136 ILTWKSNDTA ASEYKYVVKH KMENEKTITV VHQPWCNITG LRPATSYVFS
186 ITPGIGNETW GDPRVIKVIT EPIPVSDLRV ALTGVRKAAL SWSNGNGTAS
236 CRVLLESIGS HEELTQDSRL QVNISGLKPG VQYNINPYLL QSNKTKGDPL
286 GTEGGLDASN TERSRAGSPT APVHDESLVG PVDPSSGQQS RDTEVLLVGL
336 EPGTRYNATV YSQAANQPQA IEFRTNAIQV FDVTAVNISA TSLTLIWKVS
386 DNESSSNYTY KIHVAGETDS SNLNVSEPRA VIPGLRSSTF YNITVCPVLG
436 DIEFLQVHTP PVPVSDFRVT VVSTTEIGLA WSSHDAESFQ MHITQEGAGN
486 SRVEITTNQS IIIGGLFPGT KYCFEIVPKG PNASRTVCNR TG
```

B

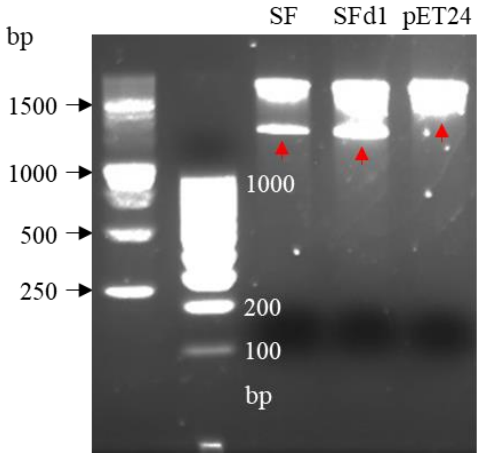

C

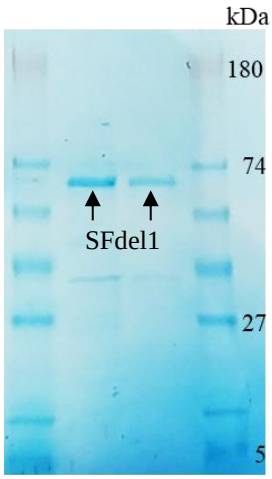

D

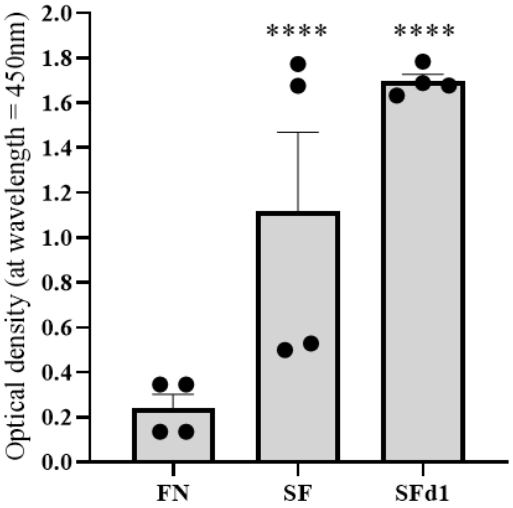

Figure 4.9. **Mutated CD148SF proteins interact with QM107 (1). (A)** CD148SF (A^{36} – G^{539}) full-length amino acid sequence, with yellow highlighted areas indicating conserved regions which were deleted, followed by CD148SFd1 new sequence, with deleted motifs removed. **(B)** The coding sequence corresponding to SFdel1 amplified by PCR and later ligated into the pET24 vector (indicated). Plasmids were digested with BamH1 and HindIII. All plasmids were transformed into BL21 cells and proteins expressed and purified as shown in (C). **(C)** SDS-PAGE gel image, following protein purification and dialysis with 1x PBS. 10µl samples of the proteins were analysed and results confirmed the presence of SFdel1 protein. **(D)** Solid phase binding assays in which plates were coated with 1000nM SFd1, prior to the addition of 10µM bio-QM107 (n=2). Interaction was observed between bio-QM107 and SFd1, as well as SF. Bio-QM107 did not interact with FN.

Therefore, we identified and deleted a larger conserved amino acid region across the DNA regions corresponding with FNIII repeats 3, 4 and 5 (Fig. 4.10A and 4.10B). This new plasmid was used to produce a second mutated recombinant protein SF deletion 2 (SFd2), again using the *E. Coli* BL21 cell expression system (Fig. 4.10C). We used this mutated protein in further solid phase binding assays and observed interaction between SFd2 and bio-QM107, despite the deletion of this sequence motif (Fig. 4.10D). This result suggested that this conserved region identified across all FNIII repeats that comprise CD148CT was also not the sequence region containing the interaction site. Alternatively, it is possible that by truncating the original sequence, the mutant proteins produced differ from CD148SF such that the results we produced do not reflect the binding and interaction ability of CD148SF, regardless of which sequences are deleted.

A

```
 36 AGGTPSPIPD PSVATVATGE NGITQISSTA ESFHKQNGTG TPQVETNTSE
 86 DGESSGANDS LRTPEQGSNG TDGASQKTPS STGPSPVFDI KAVSISPTNV
136 ILTWKSNDTA ASEYKYVVKH KMENEKTITV VHQPWCNITG LRPATSYVFS
186 ITPGIGNETW GDPRVIKVIT EPIPVSDLRV ALTGVRKAAL SWSNGNGTAS
236 CRVLLESIGS HEELTQDSRL QVNISGLKPG VQYNINPYLL QSNKTKGDPL
286 GTEGGLDASN TERSRAGSPT APVHDESLVG PVDPSSGQQS RDTEVLLVGL
336 EPGTRYNATV YSQAANGTEG QPQAIEFRTN AIQVFDVTAV NISATSLTLI
386 WKVSDNESSS NYTYKIHVAG ETDSSNLNVS EPRAVIPGLR SSTFYNITVC
436 PVLGDIEGTP GFLQVHTPPV PVSDFRVTVV STTEIGLAWS SHDAESFQMH
486 ITQEGAGNSR VEITTNQSII IGGLFPGTKY CFEIVPKGPN GTEGASRTVC
536 NRTG
```

↓

```
 36 AGGTPSPIPD PSVATVATGE NGITQISSTA ESFHKQNGTG TPQVETNTSE
 51 DGESSGANDS LRTPEQGSNG TDGASQKTPS STGPSPVFDI KAVSISPTNV
101 ILTWKSNDTA ASEYKYVVKH KMENEKTITV VHQPWCNITG LRPATSYVFS
151 ITPGIGNETW GDPRVIKVIT EPIPVSDLRV ALTGVRKAAL SWSNGNGTAS
201 CRVLLESIGS HEELTQDSRL QVNISGLKPG VQYNINPYLL QSNKTKGDPL
251 GTEGGLDASN TERSRAGSPT APVHDESLVG PVDPSSGQQS RDTEVLLVQP
301 QAIEFRTNAI QVFDVTAVNI SATSLTLIWK VSDNESSSNY TYKIHVAGET
351 DSSNLNVSEP RAVIPFLQVH TPPVPVSDFR VTVVSTTEIG LAWSSHDAES
401 FQMHITQEGA GNSRVEITTN QSIIIGASRT VCNRTG
```

B

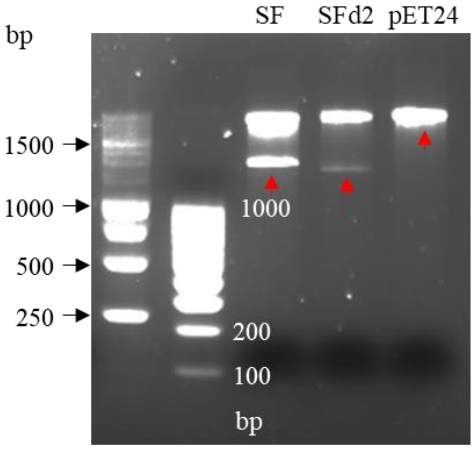

C

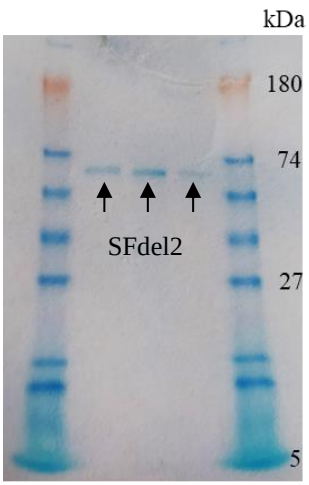

D

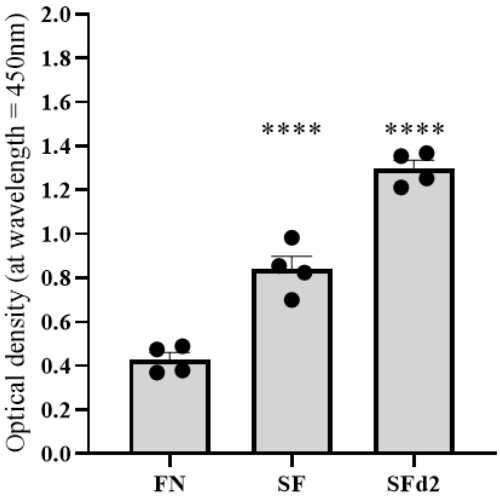

Figure 4.10. **Mutated CD148SF proteins interact with QM107 (2). (A)** CD148SF (A^{36} – G^{539}) full-length amino acid sequence, with yellow highlighted areas indicating conserved regions which were deleted, followed by CD148SFd2 new sequence, with deleted motifs removed. **(B)** The coding sequence corresponding to SFdel2 amplified by PCR and later ligated into the pET24 vector (indicated). Plasmids were digested with BamH1 and HindIII. All plasmids were transformed into BL21 cells and proteins expressed and purified as shown in (C). **(C)** SDS-PAGE gel image, following protein purification and dialysis with 1x PBS. 10µl samples of the proteins were analysed and results confirmed the presence of SFdel2 protein. **(D)** Solid phase binding assays in which plates were coated with 1000nM of a second mutated CD148SF recombinant protein, SFd2, prior to the addition of 10µM bio-QM107 (n=2). Interaction was observed between bio-QM107 and SFd1, as well as SF. Bio-QM107 did not interact with FN.

4.2.2.2. Deleted QM107 mutant

To characterise QM107 further, as well as identifying its interaction site on CD148, we explored the adhesion site on the QM107 molecule. On shed SDC2, the amino acid sequence motif for this site comprises four residues identified in the C-terminal portion of the molecule: DNLF [218]. Based on this, we designed a new biotinylated peptide, wherein this same motif (DNLF) was substituted with four alanine (A) residues (bio-QMd). When used in solid phase binding assays with CD148SF, we observe interaction between these proteins to the same extent as compared to bio-QM107. Furthermore, interaction with fibronectin is not apparent with bio-QMd or bio-QM107. The conclusion drawn here is that the DNLF motif on QM107 is not the adhesion site for its interaction with CD148.

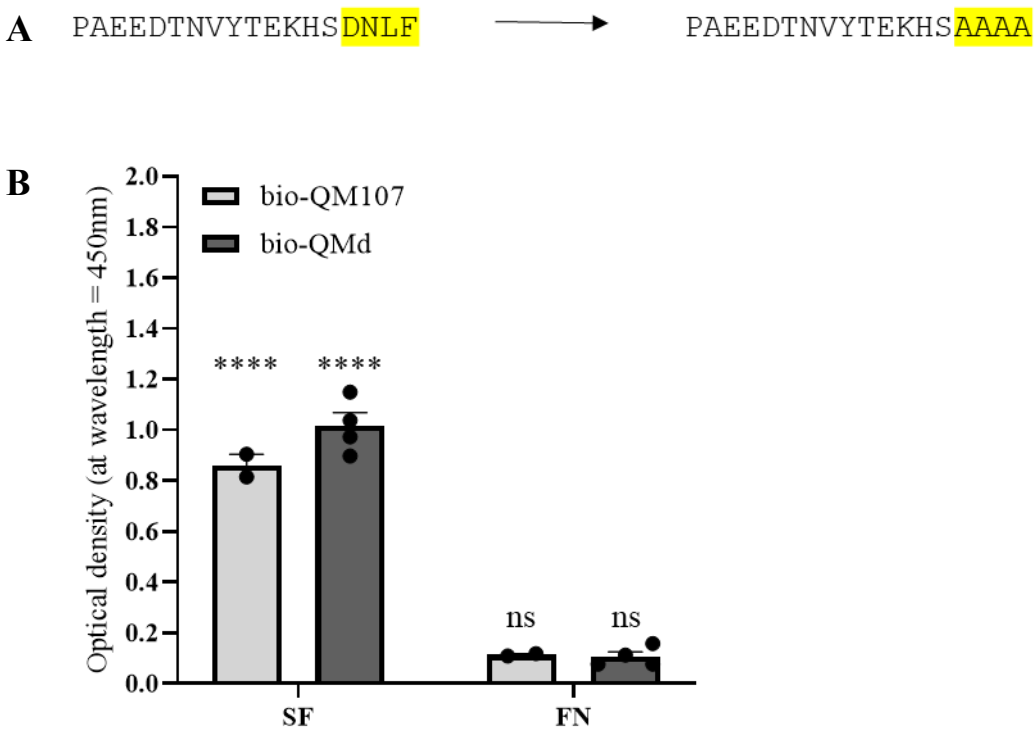

Figure 4.11. **Mutated QM107 peptide without DNLF motif interacts with CD148SF to the same extent as QM107. (A)** QM107 amino acid sequence. Yellow highlighted regions indicate substitutions with alanine residues. **(B)** Solid phase binding assays, in which plates were coated with 1000nM CD148SF and fibronectin, prior to the addition of 10µM bio-QM107 and bio-QMd (wherein DNLF residues have been substituted with AAAA), showed interaction between both biotinylated peptides and CD148SF (n=2).

4.3. Discussion

We have shown for the first time that QM107 interacts directly with CD148SF and have refined the precise interaction site to the C-terminal end of CD148SF. Our results show that there is interaction of QM107 with all FNIII repeats 3, 4 and 5 (Fig. 4.7), thus at present it remains unclear whether QM107 has multiple interaction sites on the CD148 extracellular domain or whether it requires the whole CD148CT portion to interact. The methodology developed to enable this discovery can be utilised in ongoing studies to decipher the interaction site on the CD148SF sequence. As we have shown, mutated recombinant CD148SF proteins, with specific amino acid residues deleted from the polypeptide sequence, can be successfully expressed and used in solid phase binding assays. In our assays, it is possible that we misidentified the interaction site in the amino acid sequence. However, it is important to acknowledge that this is a very artificial system and that altering the amino acid sequence, for example by deleting various motifs throughout the full-length sequence, we do not fully understand what this causes at a molecular level. The conformation of the mutated proteins may prevent the binding and interaction ability of CD148SF, whether or not the deleted sequence was in fact the interaction site. Going forward, additional sequence alignments can be carried out to identify alternative motifs that may be responsible for the interaction with QM107. Ultimately, structural experiments will need to be carried out, to determine the impact of deleting certain amino acid residues from the sequence and help to predict the interaction site. To establish QM107's mode of action to downregulate angiogenesis through its activation of CD148, it is crucial that the position of the interaction site is known. This will aid investigations into potential adverse effects, as well as determining the therapeutic dose required, as we pursue the use of QM107 as a treatment option for pathological neovascularisation. Identification of the ligand interaction site on CD148

will also be important for identifying other potential therapeutics, by screening small molecule libraries.

Furthermore, we explored the possibility that the amino acid motif on the QM107 molecule responsible for its binding with CD148 was the last 4 residues on the QM107 C-terminal: DNLF. When this was substituted with 4 amine residues, no change in binding was observed. However, as with the CD148 amino acid sequence, structural studies will also be necessary to establish the interaction site on the QM107 molecule.

4.3.1. Summary points

- We have confirmed that QM107 interacts with CD148SF *in vitro*
- We have identified that this interaction site is within the C-terminus of the CD148SF protein
- Further work needs to be carried out to determine how QM107 interacts with CD148SF

Chapter 5

5. Anti-angiogenic properties of the CD148 short form protein

5.1. Introduction

CD148 is a PTPR expressed on many cell types, including those of the vasculature. It has been functionally implicated in a number of physiological and pathological processes, including regulation of cell growth, differentiation, transformation and proliferation [368, 376, 380, 406-408]. The full-length molecule comprises an extracellular domain of nine fibronectin type-III repeats, which facilitates binding of ligands such as shed SDC2 and thrombospondin-1 [218, 409], while its cytosolic domain consists of a single catalytic domain [410] responsible for its phosphatase activity. Upon ligand binding, CD148 exerts its effects through its intracellular phosphatase domain. Work from our group and others has shown that when shed SDC2 interacts with the CD148 extracellular domain, the p85 subunit of PI3 kinase is dephosphorylated and this is associated with an inhibition of angiogenesis and fibrosis [218, 347, 411].

Alternative splicing of messenger RNA (mRNA) is a crucial post-translational regulatory mechanism, by which many soluble receptors are produced in eukaryotic cells. This alternative splicing of genes produces multiple versions of the same protein, leading to the translation of numerous proteins with different functions from one gene [380, 412, 413]. Alternatively spliced isoforms of many PTPRs have been identified and shown to have diverse functions across the variants [380, 414, 415]. As well as the full-length PTPR, CD148, the *PTPRJ* gene also codes for an alternative splice variant (NM_001098503 – NCBI Gene database), whose mRNA encodes the first five FNIII repeats of the CD148 extracellular domain (Fig. 5.1). This isoform has since been characterised and shown to

be expressed by a number of cell types, including HUVECs [380]. This work also identified that this truncated isoform of CD148 was glycosylated and secreted into cell culture medium. It was also found to promote angiogenesis and cell migration, and was upregulated in high-grade glioma, a tumour for which increased angiogenesis has a crucial role [380, 416-420]. In contrast, our group have shown that a bacterially expressed form of this truncated isoform (CD148SF) potently inhibited angiogenic sprout formation in the rat aortic rings model. An effect that was further enhanced when rings were treated with both the SDC2 extracellular core protein and CD148SF. These findings indicate a role for the truncated form of CD148 in regulating angiogenesis, either independently of or dependent on full-length CD148.

Based on our own group's work and others, there appear to be conflicting findings as to the role of the truncated form of CD148 in angiogenesis. To understand this further, the overall objective of this chapter is to test whether truncated CD148 does indeed possess anti-angiogenic properties. To this end, the following aims will be addressed:

1. To quantify the anti-angiogenic properties of CD148SF using both *in vitro* and *ex vivo* models of angiogenesis

2. To determine where the inhibitory domain resides in the CD148SF sequence, through these angiogenesis models

3. To establish a novel cell-based assay to measure angiogenesis *in vitro* and use this to test the inhibitory effects of CD148-derived proteins on angiogenesis

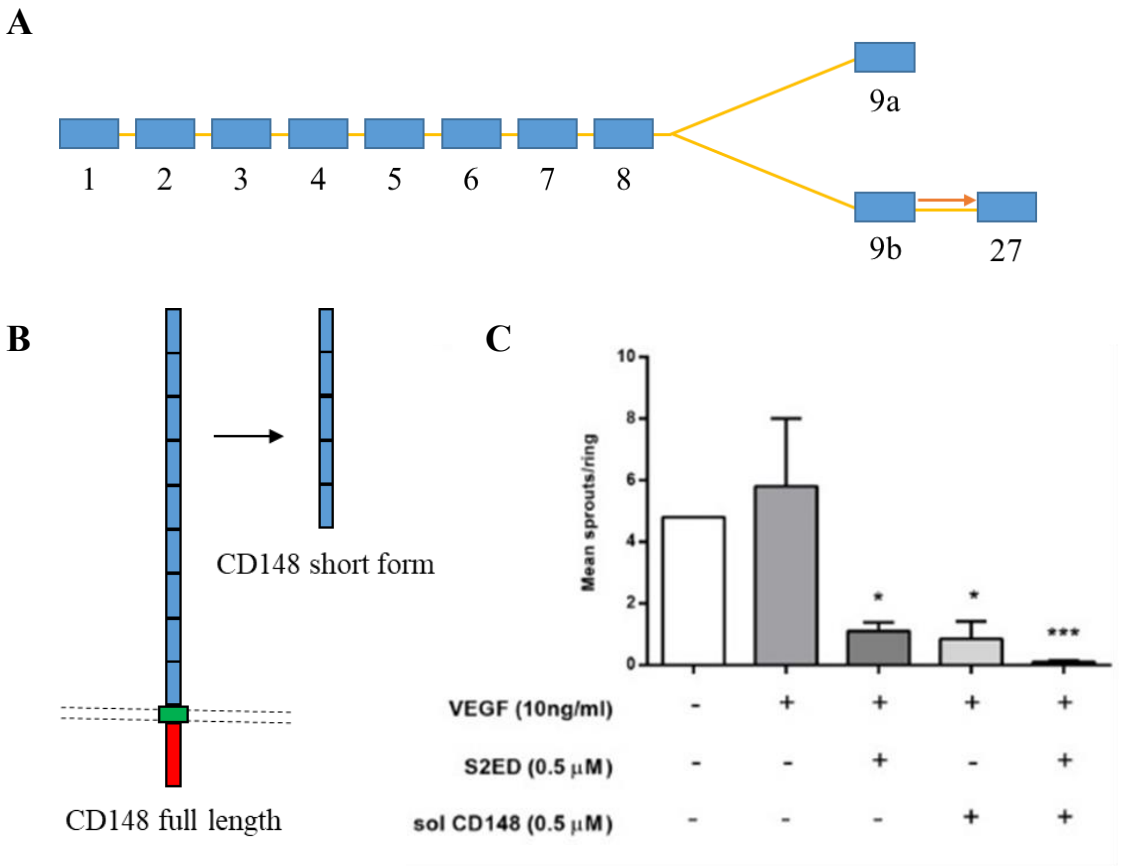

Figure 5.1. **CD148SF has distinct anti-angiogenic properties. (A)** Depicted are the two mRNA variants of CD148 produced by alternative exons (9a/ b). 9a encodes the spliced variant (3193bp), 9b encodes full-length CD148 (7854bp). Redrawn from: Bilotta, A., et al., *A novel splice variant of the protein tyrosine phosphatase PTPRJ that encodes for a soluble protein involved in angiogenesis. Oncotarget, 2017.* ***8****(6): p. 10091-10102*. **(B)** CD148 has two splice variants: the full-length molecule and the short form (SF), comprising the first five N-terminus fibronectin type-III repeats on the CD148 extracellular domain. **(C)** Rat aortic ring assays were carried out using purified recombinant human CD148SF (sol CD148), which proved to be as anti-angiogenic as the human SDC2 ectodomain (S2ED). Furthermore, when used in conjunction with S2ED, it appeared that angiogenesis was inhibited to a greater extent than with S2ED or sol CD148 (CD148SF) alone. Taken from: *De Rossi, G., et al., Shed syndecan-2 inhibits angiogenesis.*

5.2. Results

5.2.1. Scratch wound migration assay

A key feature of angiogenesis is EC migration. A simple *in vitro* assay to measure cell migration is a scratch wound migration assay, wherein a 6 well plate is seeded with ECs which are left to grow into a confluent monolayer. A pipette tip can be used to produce a scratch in the centre of the well, creating a cell-free area that induces cell migration into the scratch area to close the gap [421]. To establish where on the CD148SF protein is responsible for its anti-angiogenic effects (Fig. 5.1), purified recombinant proteins CD148SF, CD148CT and CD148NT (as described in Chapter 4) were used in angiogenesis assays.

In this case, micrographs acquired at 0 and 16 hours were compared (Fig. 5.2A) and it is clear that there was significant reduction in wound closure for cells treated with CD148SF compared with PBS, CD148CT or CD148NT, suggesting that CD148SF inhibits EC migration. Quantification of the percentage change in wound area reinforces this, with a significant reduction in wound closure in the presence of CD148SF (Fig 5.2B). It also suggests a slight reduction in wound closure time in the presence of CD148CT and -NT versus PBS, however this difference is non-significant, which suggests that in this assay the full-length CD148SF recombinant protein is required to reduce EC migration in this particular cell type.

A

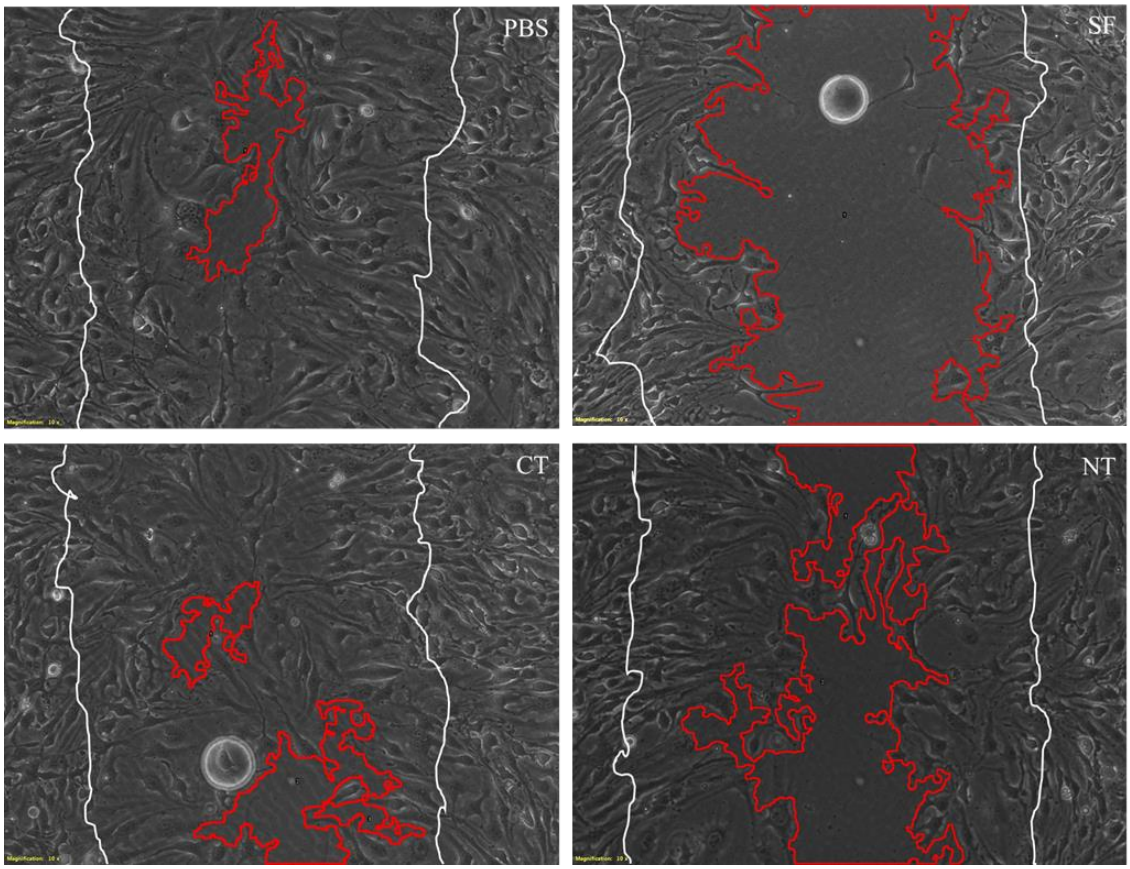
PBS
SF
CT
NT

B

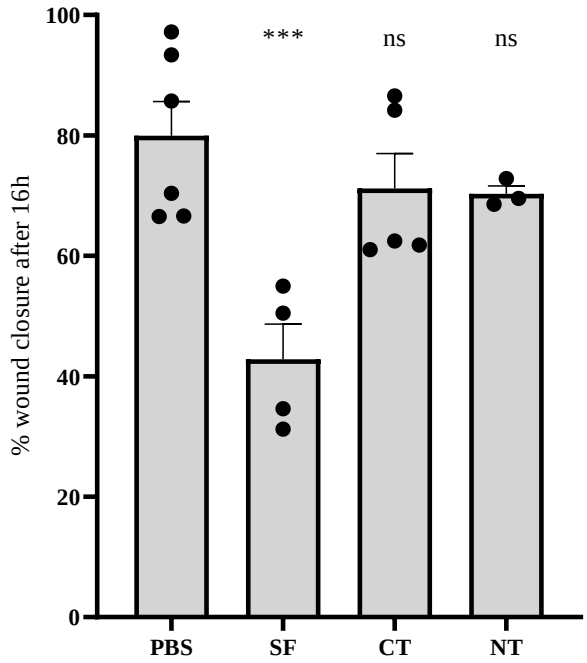
% wound closure after 16h
100
80
60
40
20
0
***
ns
ns
PBS
SF
CT
NT

Figure 5.2. **Effect of CD148-derived proteins on EC migration. (A)** Confluent monolayers of sENDs were scratched with a pipette tip before 0.5µM of the indicated proteins were added. Micrographs were taken immediately after the administration of the treatment (0h) and after 16 hours (16h). The initial scratch is highlighted in white and the closed area in red, to better visualise cell migration at the final time point. Pictures are representative of 2 experiments where at least 1 spot per condition was analysed. **(B)** CD148 inhibits sEND migration. Cell migration after 16h was quantified and wound closure was expressed as a percentage. Results are mean±SEM (n=2 experiments/ condition *** $p<0.0009$, one-way ANOVA comparing to PBS controls using Dunnett's multiple comparisons test).

5.2.2. Developing endothelial cell spheroid assay

5.2.2.1. Developing methodology

In order to initiate angiogenesis, cells secrete VEGFA to induce new blood vessel formation. As described in Chapter 1 (Fig. 1.3), in response to VEGFA production, ECs undergo morphological changes to develop into a new blood vessel. *In vitro* angiogenesis assays allow researchers to examine the direct impact of certain compounds on angiogenesis processes. Scratch wound migration assays, while informative, have drawbacks, as this is a 2D culture system. In the spheroid-based sprouting assay (first developed by Drs Thomas Korff and Hellmut Augustin [422]), sprout formation can be measured in a 3D environment. This allows direct signalling between ECs, thus reflecting more closely the sprout formation seen *in vivo* when ECs are exposed to VEGFA [423]. There are examples of published data using this methodology [424, 425]. However, in this case, to enable us develop an angiogenesis assay, we intended to use an immortalised skin endothelial cell line (sENDs); therefore the protocol from the 2018 study by Tetzlaff and

Fischer, which utilised ECs, also informed the protocol developed in this chapter [425].

For the methodology we developed in this chapter, sENDs were suspended in cell medium mixed with methylcellulose stock. This solution was transferred onto a petri dish in 25µl droplets and then inverted, causing the drops to hang from the surface of the plate. The plate was incubated for 24 hours, before formed spheroids were removed from the plate and embedded in collagen I (Fig. 5.3).

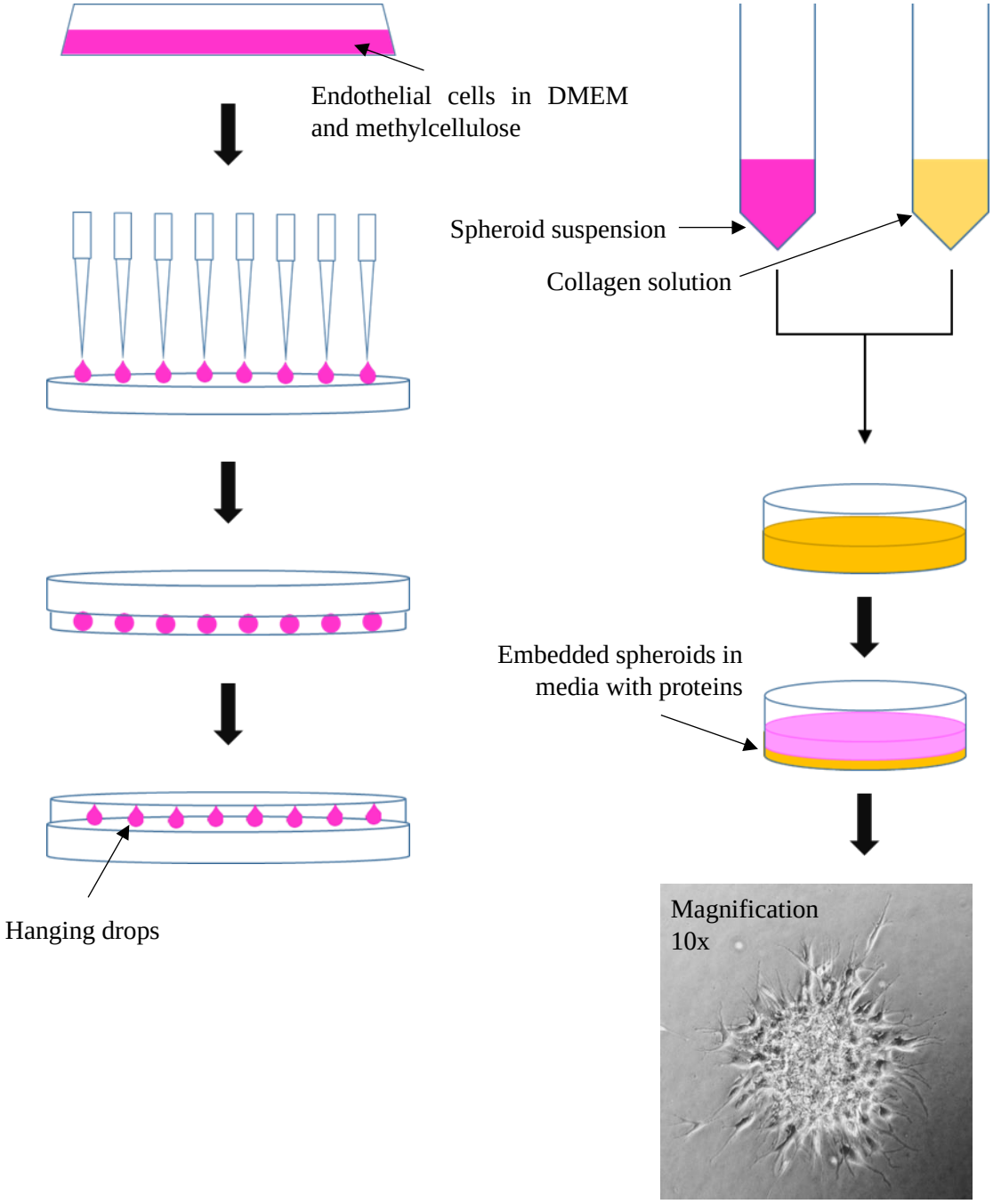

Figure 5.3. **Overall schematic showing hanging drops method used to produce EC spheroids. (A)** EC spheroid production utilised the hanging drops technique, whereby ECs were suspended in solution in an inverted petri dish for 24 hours. This produced cell spheroids within the droplets. **(B)** Spheroids were then embedded in collagen with proteins of interest and micrographs were acquired after 4 hours for analysis.

5.2.2.2. Use of spheroids in angiogenesis assay

For this angiogenesis assay, spheroids were embedded using the methodology previously described for aortic ring assays; however, micrographs were acquired after 4 hours' incubation in cell media (Fig. 5.4A, arrows indicate angiogenic sprouts). In the Tetzlaff and Fischer study from 2018, spheroids were subjected to growth stimulation by VEGFA and FGF2 [425]. However, in our initial assays, sprouting and cell migration were observed in control wells, in which spheroids were treated with cell medium (DMEM with 10% FBS) alone (although it is important to note that this was also included in the collagen I). Therefore, going forward we used DMEM only as a control and test proteins were diluted in DMEM, all without VEGFA. Regarding test proteins, purified recombinant CD148SF, -CT and -NT proteins were used to explore any inhibitory effects from these sequences, along with PBS and QM107 controls. The proteins were again incorporated into the collagen I matrix and in the medium administered throughout the course of the assay.

In the publications using the 3D spheroid assay [424, 425], angiogenic potential was determined based on both the number and length of sprouts formed [422, 425]. However, in our assay we omitted the length of sprout formation parameter, as the clarity of micrographs was compromised, and sprout length was indeterminable (Fig. 5.4A). We observed an increase in spheroid size after 4 hours, likely due to the aggregation of cells. This prompted us to additionally measure the change in area of each spheroid from 0 hours to 4 hours after the application of CD148SF-derived proteins, using ImageJ software (Fig. 5.4B). Results showed no significant change across every test condition, compared to PBS: under all conditions, the spheroid area was increased at least 4-fold, suggesting EC migration is taking place. However, the other parameter measured was number of sprouts formed and results from this showed CD148SF and CD148CT proteins both

inhibited sprout formation, almost to the same extent as QM107 (Fig. 5.4C). The N-terminus protein did not show angiogenic inhibition in this assay, compared to PBS control, as shown in the Fig. 5.4C. Where CD148SF and CD148CT proteins inhibited sprout formation, results from spheroids treated with NT showed no significant reduction in angiogenic sprout formation. Together, these findings suggest that the inhibitory effect of CD148SF is located in its C-terminus. However, due to the disparity between this assay and the aortic ring assay, it is worth noting that the cells used here were immortalised. A primary EC line should be tested to determine if this has an effect on the cell behaviour with regard to, for example, cell migration or the response to CD148NT.

A

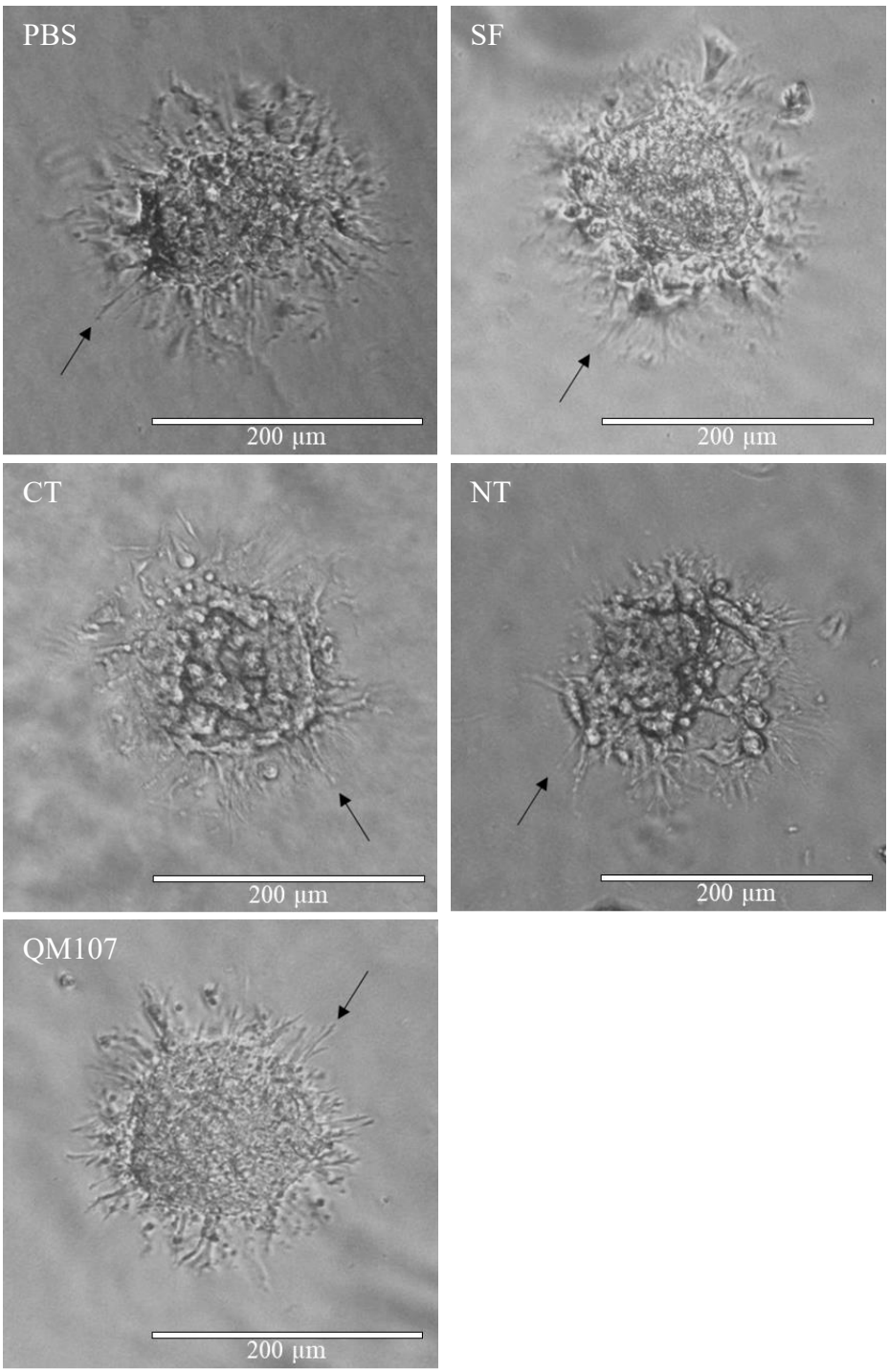

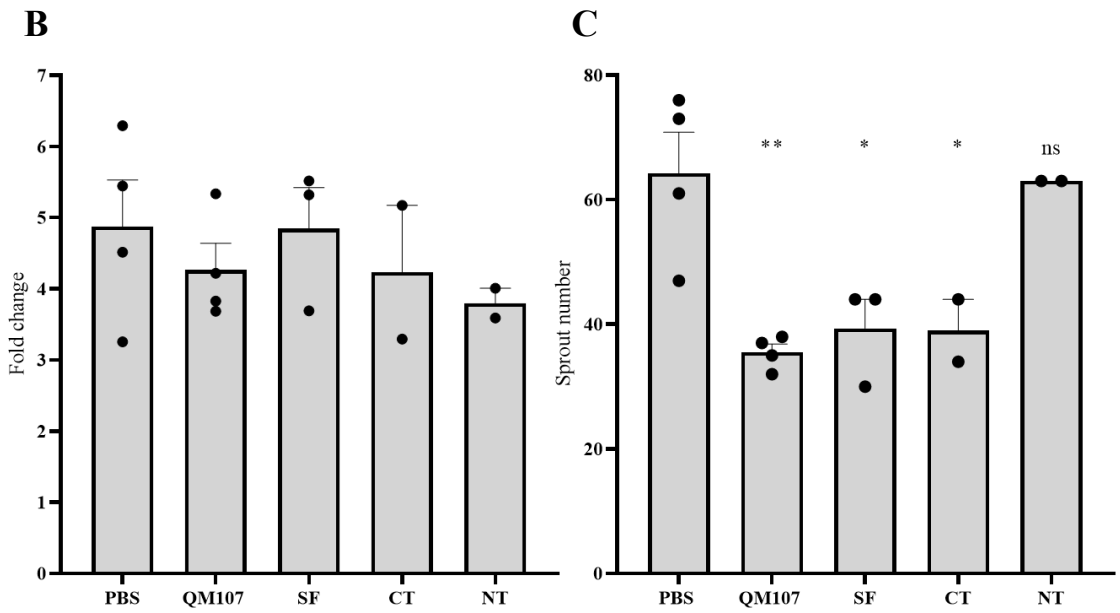

Figure 5.4. **Effect of CD148-derived proteins on sprout formation in EC spheroids. (A)** 0.5µM of each protein was incorporated into the collagen I matrix before seeding with cell spheroids (as described in Materials and Methods). Micrographs were taken on an Olympus IX81 inverted microscope with a 10x objective immediately after administration of media (0h) and after 4 hours (4h). Arrows indicate examples of angiogenic sprouts and scale bar represents 200µm. **(B-C)** Analysis included both change in area (expressed as fold change) and sprout number for each condition. (B) Total spheroid area was measured at 0h and 4h and fold change in area was calculated, with results expressed as mean±SEM for 2-4 spheroids from two experiemtns (n=2). No statistically significant change was observed compared to PBS control. (C) CD148SF and CT inhibit angiogenic sprout formation, along with QM107 control. Sprouts from 2-4 spheroids from two experiments were counted (n=2) and results are mean±SEM (** $p<0.0027$, * $p<0.22$, one-way ANOVA comparing to PBS controls using Dunnett's multiple comparisons test).

5.2.3. Angiogenic sprout formation

The aortic ring assay is a widely used *ex vivo* angiogenesis model and has the advantage of involving a number of cell types (including ECs, smooth muscle cells and pericytes) due to utilising a tissue explant. Here, aortas were dissected from six rats and cut into rings. These were embedded in a thin layer of collagen I and fed every 3 days with medium supplemented with serum and VEGFA as a pro-angiogenic factor. After 1 week, angiogenic sprouts developed and the number of sprouts formed was considered directly proportional to the extent of angiogenic response.

To identify the inhibitory domain within the full-length CD148SF sequence, purified recombinant CD148SF, -CT and -NT were used, along with PBS and QM107. These were incorporated into the collagen I matrix and in the medium administered throughout the course of the assay. Micrographs acquired after 7 days are shown in Fig. 5.5A, with examples of sprouts shown under each condition. Results showed that purified recombinant CD148SF inhibited sprout formation, demonstrating its anti-angiogenic effect. Both the C- and N-terminal proteins also showed inhibition of sprout formation compared to PBS, almost to the same extent as QM107 (Fig. 5.5B). These findings suggest that there are inhibitory sequences present in both terminals of CD148SF, as they can inhibit angiogenic sprout formation in their own right, outside of the full-length sequence, though the inhibition is less than for the full-length protein.

A

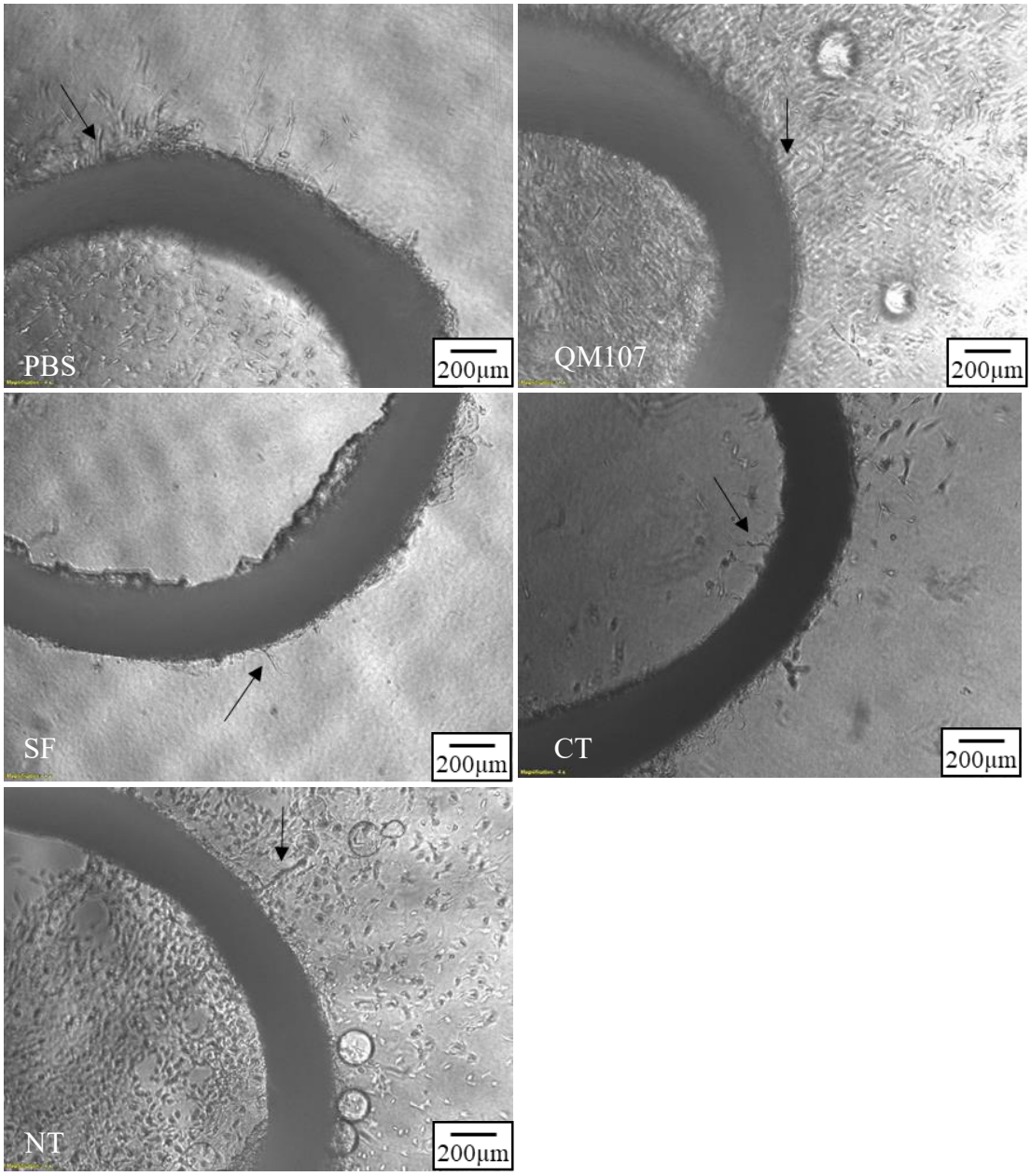
PBS
200µm
QM107
200µm
SF
200µm
CT
200µm
NT
200µm

B

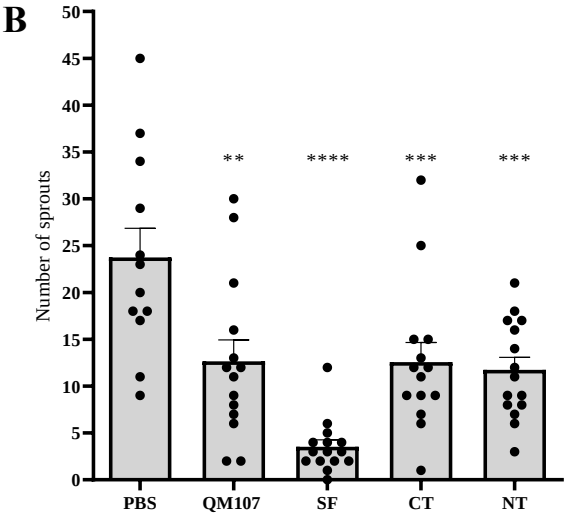
Number of sprouts
50
45
40
35
30
25
20
15
10
5
0
**
****
***
***
PBS
QM107
SF
CT
NT

Figure 5.5. **Effect of CD148-derived proteins on angiogenic sprout formation. (A)** 0.5μM of each protein was incorporated into the collagen I matrix before seeding with rat aortic rings from 6 rats (as described in Materials and Methods). Micrographs of each ring were captured on an Olympus IX81 inverted microscope with a 4x objective after 7 days. Arrows indicate examples of angiogenic sprouts. **(B)** CD148SF, -CT and -NT inhibit angiogenic sprout formation, along with QM107 control. Sprouts from 12-15 rings from 6 rats (n=6) were counted and results are mean±SEM (**** $p<0.0001$, *** $p<0.001$, ** $p<0.001$, one-way ANOVA comparing to PBS controls using Dunnett's multiple comparisons test).

5.3. Discussion

Taken together, the data outlined in this chapter provide strong evidence that the recombinantly expressed version of the shorter isoform of CD148 (CD148SF) has anti-angiogenic effects in a variety of angiogenesis assays: in all of the models utilised here, it has displayed inhibitory effects. In two of the models, the CD148CT protein also demonstrated inhibitory activity (Figs. 5.4 and 5.5), while CD148NT only proved inhibitory in one case (Fig. 5.5).

The most robust angiogenesis assay utilised in this chapter is the aortic ring assay, as a tissue explant provides a model with multiple primary cell types in a 3D environment, making it a better recapitulation of the *in vivo* process. While the EC spheroids are cultured in 3D, this assay comprises only one immortalised cell type, which is less representative of the *in vivo* scenario. However, carrying this assay out with a primary cell line, such as HUVECs, would provide some resolution for this. As an initial angiogenesis assay, the scratch wound migration assay provides a good model for measuring cell migration as it does present some idea of the anti-angiogenic abilities of our proteins, although it is in 2D culture and represents only one aspect of angiogenesis. In this case, an immortalised cell line was used, so in the future HUVECs should be tested additionally.

Further angiogenesis assays that should be utilised to further validate this work include oxygen-induced retinopathy (OIR) and laser-induced choroidal neovascularisation (CNV) animal models. The OIR model closely resembles pathological ROP, as neovascularisation is induced by hyperoxia [426]. Mouse pups are exposed to hyperoxic conditions during their retinal vasculature development stage, causing capillary depletion. This is followed by exposure of the pups to normoxic conditions, where the oxygen level is normal, causing retinal ischaemia, which initiates neovascularisation that can lead to proliferative vascular disease in the retinal vasculature [427]. This

is OIR. Anti-angiogenic compounds can promote revascularisation of the ischaemic areas of the retina, with healthy blood vessels [427]. Laser-induced CNV mouse models are also used to test anti-angiogenic compounds. In this model, a laser is used to break the Bruch's membrane to produce lesions on the choroid, prompting the initiation of CNV as a physiological repair mechanism [426]. Animals treated with compounds that inhibit angiogenesis (such as anti-VEGF drugs) develop smaller areas of CNV compared with animals that do not receive this treatment [426], making it a suitable model for further testing of the inhibitory effects of CD148SF.

The outstanding question going forward is by what mechanism does CD148SF inhibit angiogenesis? We propose a number of potential mechanisms to answer this. The first potential mode of action we offer (mechanism 1, Fig. 5.6) is that CD148SF interacts with the extracellular domain of cell surface full length CD148, activating it in the same manner as shed SDC2 (Fig. 5.6 and see Chapter 1, Fig. 1.10). Upon stimulation, CD148 dephosphorylates PI3 kinase, inactivating β1 integrin and preventing cell migration. This mode of action is perhaps less likely than the other proposed mechanisms, due to the synergistic effect on inhibition of sprout formation demonstrated in the 2014 paper (see Fig. 5.1), which does suggest that CD148SF acts via a different route to shed SDC2.

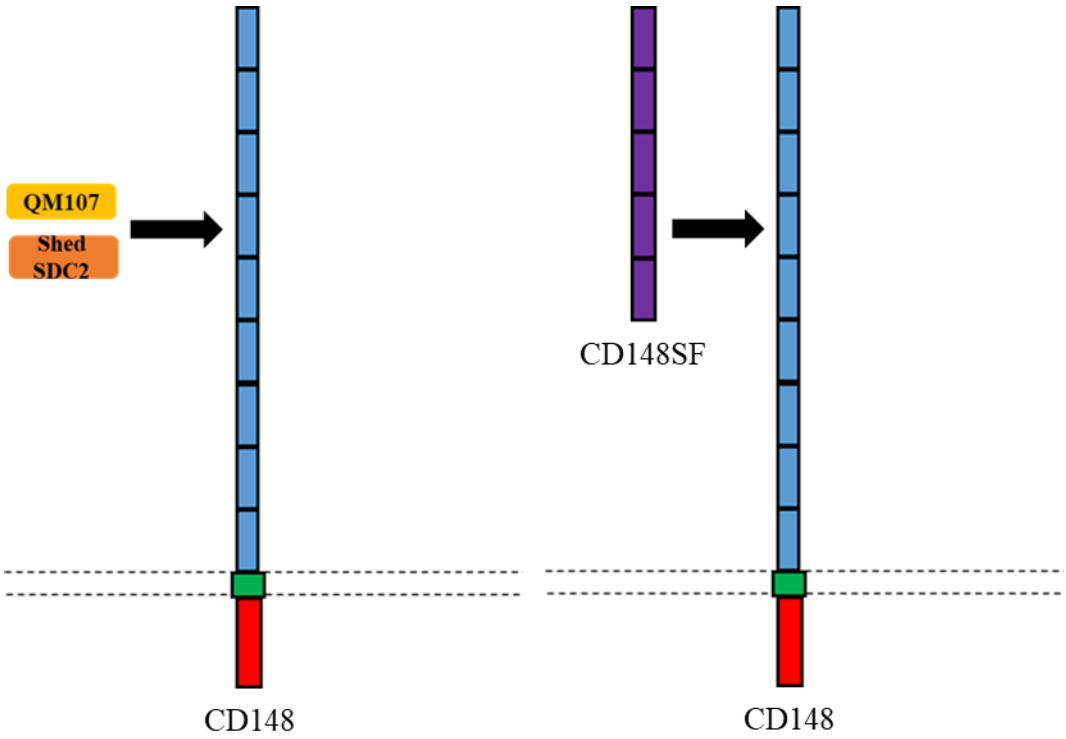

Figure 5.6. **Mechanism 1 to explain inhibitory effect of CD148SF on angiogenesis.** CD148SF interacts with the extracellular domain on full-length CD148 molecule, in the same way as shed SDC2 and QM107.

An alternative suggestion (mechanism 2, Fig. 5.7) is an interaction between CD148SF and cell surface SDC2. This would inhibit an interaction between SDC2 and VEGFR2, disrupting VEGFR2 activation by VEGFA and preventing pro-angiogenic downstream signalling [428]. This theory is supported by several studies showing SDC2 involvement in VEGFA binding with VEGFR2 *in vivo* [334, 428].

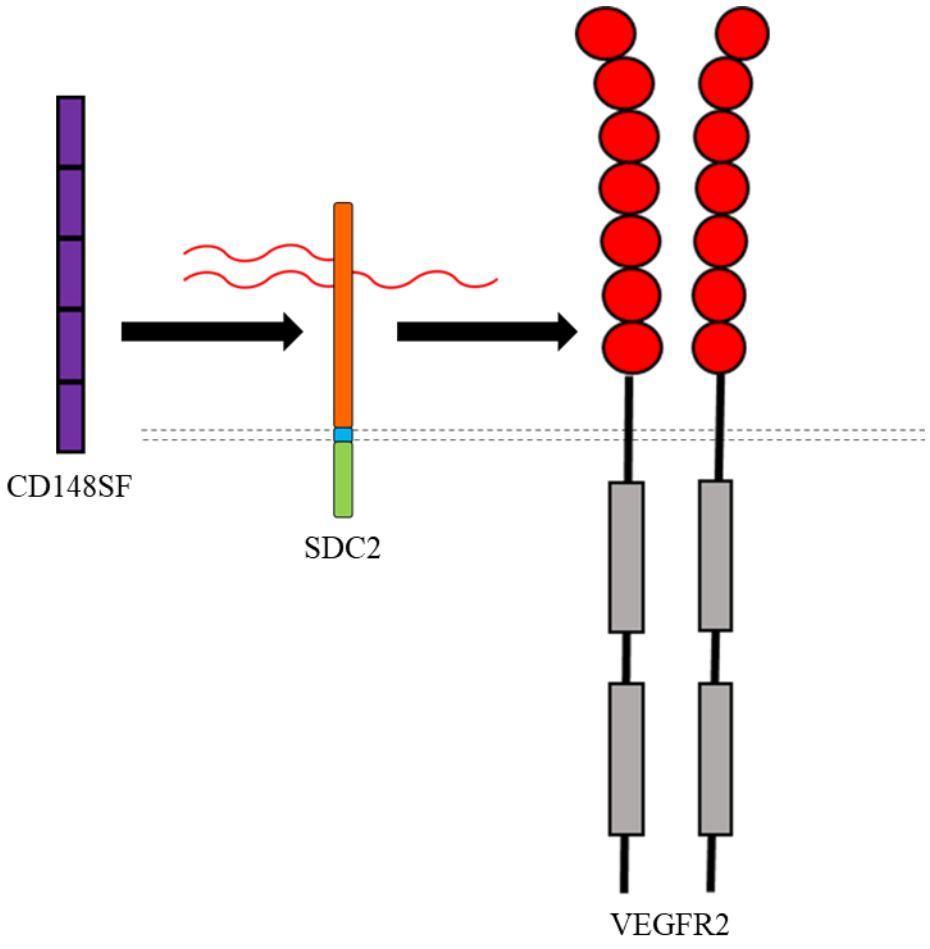

Figure 5.7. **Mechanism 2 to explain inhibitory effect of CD148SF on angiogenesis.** CD148SF activates SDC2, which leads to its interaction with VEGFR2, inhibiting receptor stimulation and preventing downstream pro-angiogenic signalling.

Our third and final suggestion (mechanism 3, Fig. 5.8) is that CD148SF interacts directly with VEGFR2, interfering with its stimulation by binding with VEGFA. CD148 is expressed by ECs and its role in angiogenesis has been identified, where it acts as a mediator for the dephosphorylation of VEGFR2, ultimately inhibiting VEGFA-induced mitogenic signals (vital for angiogenesis) [368, 378, 380, 429]. With current antibody therapies targeting the VEGFA/ VEGFR2 pro-angiogenic system, this mode of action would be particularly interesting to explore, with the potential to pursue CD148SF as an alternative therapeutic protein. Two key advantages here would be that it is produced endogenously, and the mode of action if used as a therapeutic would harness an established endogenous process, as with QM107. Therefore, the risk of adverse side effects may be reduced compared with artificially produced therapeutics.

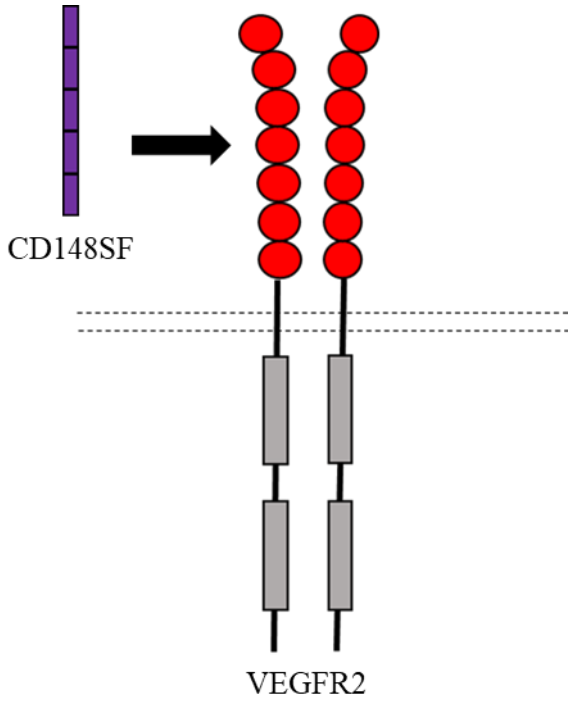

Figure 5.8. **Mechanism 3 to explain inhibitory effect of CD148SF on angiogenesis.** CD148SF interacts directly with VEGFR2, similarly to SDC2, preventing its activation and downstream pro-angiogenic effects.

Furthermore, we propose *in vitro* assays to test these theories. Throughout this project, various detection methods have been utilised and any of these could be applied to CD148SF detection (fluorescent or biotin labelling, for example). Moreover, our group has established a CD148 KD cell line using a lentivirus in ECs, both immortalised and primary cell lines. Using this methodology, mechanism 1 could be verified by applying fluorescently labelled CD148SF recombinant proteins to CD148 KD cells in culture and comparing the amount of fluorescent CD148SF bound to CD148 KD cells to that of control cells (wherein CD148 has not been knocked down). This model could also be used to test mechanism 2, but using SDC2 KD cell lines or primary cells from SDC2 KO animal models. Similarly, fluorescent labelling of CD148SF would allow comparison between the amount of this protein retained in cells lacking SDC2 and cells expressing SDC2 protein. There is a plethora of evidence to suggest that endogenous SDC2 interacts with VEGFR2 via its HS chains, to facilitate binding its binding with VEGFA-165 (the most abundant VEGFA isoform) [334, 428]. For mechanism 3, an assay could be designed utilising an already-established methodology, wherein blocking monoclonal antibodies specific to VEGFR2 has been used to confirm this receptor's involvement in VEGFA/ TNF-α-induced tube formation in *in vitro* assays [430]. If these blocking monoclonal antibodies were applied to cultured primary ECs to be used in angiogenic assays (such as the scratch wound migration assay) with CD148SF recombinant proteins, VEGFR2 activation would be prevented and its involvement in angiogenesis inhibition by CD148SF could be established.

The work in this chapter also confirms our group's original observation that CD148SF is inhibitory to angiogenesis. These findings would appear at odds with the 2017 study from Bilotta [380]; however, there are a number of substantial differences between the approach we have used and those used in this study. We have been applying a recombinantly

expressed version of CD148SF to ECs, whereas the effects on angiogenesis of overexpressing the alternatively spliced version of CD148 are described in the Bilotta study [380]. Additionally, the study did not measure the level of alternatively spliced CD148 mRNA in the cell lines described, or fully characterise the antibodies used to identify this truncated form of CD148 protein. CD148 is likely highly N-glycosylated and it would be useful for us to express the truncated sequence in a eukaryotic system to understand the effects of this on angiogenesis.

5.3.1. Summary points

- CD148SF was shown to inhibit angiogenesis in three distinct angiogenesis models
- CD148CT appears to inhibit angiogenesis, suggesting the C-terminus of the CD148SF protein is responsible for its anti-angiogenic activity
- We successfully developed and optimised a novel cell-based assay which was used to test the inhibitory effect of various recombinant proteins on angiogenesis *in vitro*. This methodology has advantages over existing models, such as the aortic ring assay, including its lesser cost and shorter duration from start to finish (3 days, rather than 7 days)

Chapter 6

6. General Discussion

6.1. QM107

6.1.1. Peptide therapies

A commonly used biopharmaceutical in disease treatment is antibody therapy. The major advantages of antibodies include target specificity [363] and slow clearance (which also gives them a longer half-life than most small molecules [431]), less variation in plasma concentration [432] and a lower rate of attrition than peptide therapies [433]. However, therapeutic antibodies do have some drawbacks. One is an inability to penetrate plasma cell membranes because of their large size [434], so their endogenous targets are limited to extracellular only. Furthermore, as they are such complex proteins, their production is costly [363] and complicated: on average, it takes 12 months to create a new antibody and 3-4 months to manufacture an existing one [435].

Peptides are short linear chains of less than 50 amino acids, stabilised by disulphide bonds [436, 437]. The peptide sequence can be modulated with relative ease due to their simple synthesis, using chemical or molecular biological techniques [438], and they are designed to have high binding specificity to modulate protein interactions [437], making them attractive for therapeutic use. In a disease setting, if an interaction between two proteins is known, a peptide can be designed that inhibits this interaction [439]. Alternatively, if a particular target protein can stimulate an endogenous pathway that is beneficial for preventing a pathological process, such as angiogenesis in a disease setting, and the binding site of this target protein is known, then a peptide could be designed that stimulates this. This is the

approach we are using in development of therapeutic QM107. Based on our group's previous research into SDC2, we knew that CD148 was the target protein and we gathered evidence to suggest that the endogenous pathway following CD148 stimulation would be therapeutically beneficial – in this case, by inhibiting pathological angiogenesis.

The first commercially available therapeutic peptide was insulin for the treatment of Type 1 diabetes in humans [440]. Since the commercialisation of insulin, numerous other peptide therapies have been manufactured and are used in treatment in a range of therapeutic areas, including respiratory, pain, oncology and metabolic (there are many peptides used in Type 2 diabetes treatment) [441-443]. There are many advantages to using peptides therapeutically: they can be synthesised easily and rapidly [437, 444] (this was the case for QM107, as shown in Fig. 3.2) and their small size allows them to penetrate cell membranes so they can reach intracellular targets, also minimising drug-drug interactions [437]. They can be easily modified [444], increasing their biological and chemical diversity (and so increasing their range of targets) and providing them with high specificity and high target affinity [437]. Importantly, peptide therapies do not accumulate in specific organs and, although this is a result of their rapid clearance, this minimises toxic adverse effects [445]. This is a major advantage, as not only do clinical therapeutics need to be efficacious, but also safe for use in humans.

The fundamental disadvantage of peptide therapies is their poor *in vivo* stability, as they have little or no resistance to cleavage by serum proteases [446]. As a result, they have a short half-life due to their rapid clearance from the body [437, 444], low oral bioavailability and can present production and manufacturing challenges [445]. Most peptide therapeutics are administered via injection, either subcutaneously or intramuscularly, due to their poor bioavailability when administered orally. However,

modifications can be made during their production to increase their stability, which perhaps needs to be explored for QM107 as preliminary data regarding QM107 stability seems to support this.

The chemical structure of peptides determines their biological activity, therefore identification of essential peptide residues, and subsequently substituting non-essential residues with alternative amino acid groups, can improve the stability of the peptide, while conserving the active parts of the peptide sequence [440]. Chemical modifications that are routinely used to improve peptide stability at a DNA level include the addition of turns, helices and extended modifications in the peptide secondary sequence [447, 448], to construct a stable secondary structure [449]. Backbone modifications are used to improve proteolytic stability of peptides [440]. After proteolytic sites have been identified, there are several non-natural amino acids that can be incorporated into the peptide backbone, improving the proteolytic resistance. Examples include substitution L-amino acids (naturally produced during protein synthesis) with D-amino acids (mirror image of the L-form) [450, 451]; insertion of methyl-amino acids [450-452]; and incorporation of β-amino acids [453] and peptoids (a type of biomimetic that replicates the behaviour of a biological molecule) [454-456]. All of these examples extend the plasma half-life of peptides.

6.1.2. QM107

We have shown QM107 to be anti-angiogenic in a number of *in vitro* assays, including HUVEC cell migration and tube formation; in *ex vivo* settings (aortic ring and CNV assays); and *in vivo*, for example in OIR and tumour flank mouse models. Despite the evidence for its inhibitory effects on angiogenesis, we also have some substantial preliminary data suggesting that a recombinantly expressed protein based on a CD148 splice variant, CD148 short form, has inhibitory effects also, and when compared with the

CD148SF protein, QM107 appears to be less efficacious (Chapter 5). Therefore, together our data suggest that the inhibitory effect of QM107 is perhaps less impactful than first thought; it may not be efficacious enough alone to replace or enhance current treatments for neovascular eye diseases. This highlights the need for further investigation into improving its efficacy.

With regard to QM107 clearance rate, it is estimated that the residence time for QM107 in the eye is 20 seconds and we propose a maximum therapeutic dose of 20µg, which is significantly lower than that of anti-VEGF therapies (150µg). This suggests that QM107 would undergo rapid clearance. In spite of peptide backbone modifications that could be made to slow the clearance rate, this rapid clearance may be advantageous to prevent QM107 producing off-target effects. As demonstrated in the trypsin degradation experiment (Fig. 3.7), QM107 degrades rapidly at 37°C in the presence of trypsin. If endogenous proteolytic enzymes also rapidly degrade QM107, then this should limit its interaction site to CD148 in the ocular vasculature (before QM107 is degraded), rather than with CD148 expressed on other tissues. Significantly, we have shown QM107 to be highly stable in vitreous humour, suggesting that following its intravitreal administration, its structure will be maintained and allow it to reach the ocular vasculature, wherein lies its therapeutic target. Furthermore, since full length CD148 is a cell surface receptor, a residence time of 20 seconds should be sufficient for QM107 to reach CD148 and allow their interaction before it is cleared from the eye. This is another potential benefit of QM107: its dosage can be lower than that of anti-VEGF therapies, as its target receptor is expressed on the cell surface. This means its quicker clearance rate should not negatively affect its therapeutic outcome. Anti-VEGFs, on the other hand, target secreted VEGFA and therefore require a slower clearance rate and, as such, a higher dosage. This increases the cost of each injection and has the potential to produce off-target effects.

While anti-VEGF therapies do have benefits (such as their well-established mechanism of action; their slow clearance, which allows their therapeutic effects to be long lasting; and the fact they are already in clinical use), they are not effective in all patients and their production and administration make them an expensive therapeutic option. Other pro-angiogenic pathways are not inhibited by these therapeutics and compensatory mechanisms can cause other signalling pathways to be upregulated following interference with the VEGFA/ VEGFR pathway.

Despite some limiting factors of peptide therapies, a major advantage of QM107 as a therapeutic is its endogenous target. We propose that QM107 interacts with the CD148 extracellular domain, specifically within the FNIII repeats 3-5 region (CD148CT), to inhibit angiogenesis. This is based both on previous work establishing that shed SDC2 interacts with CD148 [347] and on work described in Chapter 4 and Chapter 5 of this thesis, suggesting that QM107 interacts with CD148SF.

During angiogenesis, VEGFA binds to its receptor, upregulating pro-angiogenic signalling molecules such as FAK, Src and Erk, leading to increased angiogenesis (Fig. 6.1). Current anti-angiogenesis therapies are predominantly antibody therapies that target VEGFA, either by binding directly with this molecule or to its receptor. They prevent binding between VEGFA and VEGFR2, blocking this endogenous angiogenesis “on switch”.

A key difference in using QM107 would be that its interaction with CD148 harnesses an endogenous “off switch” for angiogenesis. Upon ligand binding, CD148 is activated and its intracellular phosphatase domain dephosphorylates PI3 kinase, downregulating signalling molecules that regulate vascular permeability and EC migration (key components of angiogenesis), such as eNOS, GSK3 and WNK1. Ultimately, this leads to a reduction in angiogenesis via stimulation of an endogenous pathway.

Stimulation of CD148 promotes inhibition of angiogenesis, making it an angiogenesis “off switch” (Fig. 6.1). The novelty of this approach, differing from the current approach to treating pathological angiogenesis, which is to block a pro-angiogenic pathway, makes it distinctive. Moreover, because CD148 is a transmembrane cell receptor, perhaps this makes a more attractive therapeutic target than a secreted molecule (such as VEGFA), as an administered drug is more likely to reach and activate the target.

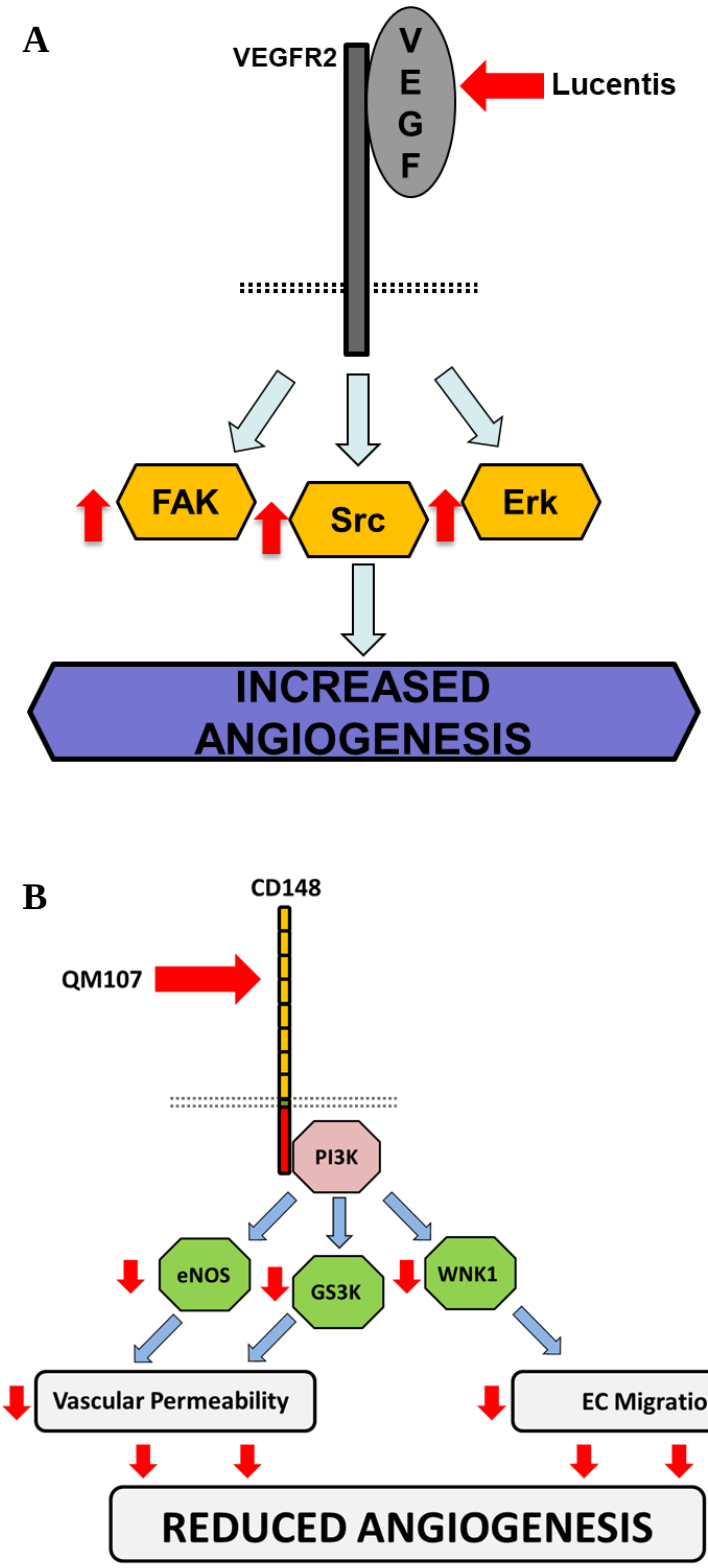

Figure 6.1. **Schematic showing the mode of action of anti-VEGF drugs and potential mode of action of QM107. (A)** Lucentis blocks activation of VEGFR2 by its ligand VEGFA (an angiogenesis "on switch"). **(B)** QM107 stimulates CD148 dephosphorylation activity, "switching off" angiogenesis.

6.1.2.1. Syndecan-3 and QM111

SDC3 is expressed in neural tissue and in the developing musculoskeletal system. More recently, it has also been found on the endothelium of different vascular beds, including the joints, dermis and cremaster muscle [337, 457].

There is evidence for SDC3's role in angiogenesis: it is expressed on ECs from a variety of tissues, including ECs in early retinal development in rats [458] and on cultured HUVECs [459], human coronary artery ECs and human coronary artery smooth muscle cells [460]. Furthermore, shed SDC3 has been identified in conditioned media in a number of assays, although the precise mechanism has not yet been confirmed [461]. Sequences within its extracellular core protein exert anti-angiogenic effects by blocking EC migration [351]. A fusion protein consisting of GST fused to the SDC3 ectodomain N-terminus was shown to inhibit angiogenic sprout formation on aortic explants, EC micro-capillary formation and EC migration [351]. Due to the prokaryotic expression system used to produce this protein, it lacked any GAG substitutions and so this effect on EC migration is an intrinsic property of the core protein [351].

Our group is developing a second small peptide (developmental name: QM111), derived from SDC3. In the same way as with QM107, we are exploring its use as a therapeutic peptide in treating pathological angiogenesis. Fusion proteins comprising QM107 and QM111 could be a potential improvement to the current QM107 peptide model. If both peptides inhibit angiogenesis through different mechanisms, utilising the two could produce a synergistic effect, enhancing the anti-angiogenic effects of each other. Currently, this work is in its very preliminary phase; however, it could be a viable option in the future.

6.1.3. Future work for QM107 therapeutic development

In terms of improving QM107 stability, modifications will need to be explored (as described in 6.1), such as L-amino acid substitutions with D-amino acids, to help reduce proteolytic degradation without altering its anti-angiogenic activity.

To advance QM107 as a therapeutic peptide, the MHRA (Medicines & Healthcare products Regulatory Agency) will require further *in vitro* testing with cells from pharmacologically relevant species. Scratch wound assays and spheroid sprouting assays will be carried out with retinal ECs and RPEs from New Zealand white rabbits and simians (nonhuman primates). The use of cells from ocular vasculature will also provide more relevant data as the intended use of QM107 is for treatment of neovascular eye diseases.

Furthermore, *in vivo* assays in larger mammal studies will need to be carried out. Although QM107 has undergone rigorous *in vivo* testing, and data generated from this has shown its inhibitory effect on angiogenesis, this work was completed using rodents – these animals lack a macula and so limits their relevance to neovascular eye diseases. Additional *in vivo* testing will be carried out in pharmacologically relevant species also, as described above, to establish PK of QM107 (such as determining its bioavailability after administration and its metabolism, including calculating half-life). QM107 activity can also be explored in tumour angiogenesis assays, such as in the tumour flank mouse model, potentially diversifying its therapeutic use beyond neovascular eye diseases exclusively.

6.2. CD148SF therapeutic

Alongside characterisation of QM107, we tested CD148SF as a potential inhibitor of angiogenesis. Full length CD148SF proved anti-angiogenic in *in vitro* assays (EC scratch wound and EC spheroid sprouting assays) and the *ex vivo* aortic ring assay. Furthermore, when both termini were tested independently, angiogenic sprout formation was inhibited in the aortic ring assay and the C-terminus of CD148SF was found to inhibit angiogenic sprout formation in EC spheroid sprouting also.

Together, these data present preliminary evidence for another potential route for treating pathological angiogenesis. Benefits of using CD148SF as a therapeutic include its production, as it is not a biologic and so could be manufactured more easily than current anti-VEGF therapies. It is endogenously expressed, making it another example of harnessing an endogenous molecule and its pathway, rather than using a synthetic molecule to block an endogenous pathway. Importantly, CD148SF has the potential to be further miniaturised, as demonstrated by the anti-angiogenic effects of CD148CT shown in Chapter 5. This would produce a therapeutic molecule that is smaller than current anti-VEGF antibodies (ranibizumab is 48 kDa, while recombinant CD148CT is currently 26.4 kDa).

Future work, going forward, is to measure CD148SF and its derivatives in more angiogenesis assays, to determine how strong its inhibitory effects are and to refine where on CD148SF is responsible for these inhibitory effects. Ultimately, it will need to be compared directly with current therapies, to determine whether it is more inhibitory and to further characterise it, for example to establish its mode of action.

6.2.1. Would an antibody against CD148 be better than QM107?

There is a growing market for biotherapeutic agents (such as monoclonal antibodies), which target the extracellular domain of cell receptors [363,

462]. For PTPRs, antibodies can be developed that target less well conserved regions of the extracellular domains with high specificity and target affinity, which would help to avoid off-target toxic effects [363]. Monoclonal antibodies can act in a number of ways to promote their therapeutic effect, such as by binding a ligand to prevent it binding with its receptor. Alternatively, they can interfere with activation of an endogenous receptor target in a number of ways: stabilising the receptor in its inactive conformation; blocking ligand binding by directly competing for the binding site; promoting internalisation of a cell-surface receptor [363].

A monoclonal antibody targeting the CD148 extracellular domain has been developed and its effect on EC growth has been investigated [409]. The antibody inhibited serum-stimulated EC growth and blocked vessel formation in an *in vivo* mouse corneal angiogenesis assay [363, 409]. The mechanism of action has not yet been determined, although one potential mechanism could be stimulation of CD148 catalytic activity, leading to dephosphorylation of substrate proteins, and inhibition of EC growth as a result (as with thrombospondin-1). Another may be that antibody binding stimulates cell adhesion and focal adhesion formation, potentially leading to down-regulation of cell proliferation and growth (as is the case for shed SDC2 stimulation of CD148) [363]. It has been shown that CD148 suppresses signals from other growth factor receptors (including PDGF and VEGFR) [463]. Although there were negligible antibody-induced changes in CD148 cell surface expression recorded in the 2011 study, there may have been changes in the cell surface expression and activity of growth factor receptors that interact with CD148, which led to the biological effect.

Other studies have explored CD148-directed antibodies in therapeutically relevant contexts. One study found that CD148's negative regulation of T-cell receptor activation was neutralised following antibody administration. This resulted in increased T-cell proliferation and an increase

in T-cell surface antigen expression [464]. Another found that there was an upregulation of CD148 mRNA in macrophages and T-cells from arthritic joints (both from mice and humans) and proposed CD148 as a therapeutic target [465]. When macrophages were treated with an anti-CD148 monoclonal antibody it caused inhibition of macrophage activation, which could lessen the damage these cells cause to joints in individuals with arthritis [466]. Together, these studies provide preliminary data to indicate that targeting CD148 extracellular domain with monoclonal antibodies may be therapeutically beneficial in several diseases. This poses a significant question: would a monoclonal antibody be superior to a therapeutic peptide for targeting CD148?

As we have explored already, antibody therapies have several advantages. However, their drawbacks must also be considered: although anti-CD148 may have longer-lasting effects due to the slower clearance of antibodies, their production times are far greater than for small peptide therapies. Their method of administration is limited to injection, which requires specialist administration, further increasing their overall cost. Furthermore, we do not yet know whether these antibodies interfere with the endogenous shed SDC2/ CD148 pathway and, if they do, whether this will cause issues such as increased SDC2 shedding under basal conditions.

6.3. Overall project evaluation

6.3.1. QM107 stability

Additional work I would carry out given unlimited time and resources includes exploration into raising an antibody to QM107 in a SDC2 null animal. In these models, the animals do not produce the SDC2 molecule from which QM107 is derived and it would be interesting to observe whether an antibody can be produced. In the production of anti-QM107 for this project (Fig. 3.4), QM107 was conjugated to Freud's Adjuvant in order to elicit an immune response because SDC molecules are not highly immunogenic. In the case of a SDC2 null animal, I propose that QM107 would be immunogenic as it would be foreign to the animal, which was not the case in the animals used to produce anti-QM107. However due to the conservation of SDC molecules across both family members and species, it is possible that it would not induce an immune response, despite the lack of recognition.

In addition, it would be pertinent to explore phage display as an option to produce anti-QM107. Phage display exploits bacteriophage technology to produce antibodies using live bacterial (usually *E. Coli*) cells in culture, instead of live animals [467]. Phage display allows production of large amounts of high-affinity, identical antibodies, due to the physical link between phage phenotype and genotype, ensuring that identical antibodies are attained from the same bacterial clone using this methodology [467, 468]. This could be completed in-house relatively cheaply, while also reducing the number of animals required for the project. Additionally, it would remove the need for additional requirements like using Freud's adjuvant as it does not rely on provoking an immune response.

6.3.2. Determining the QM107 interaction site on CD148

While the recombinant expression system is a simple one and allows rapid production of CD148-derived proteins, bacteria are not able to produce an exact replica of the mammalian protein. As stated in the case of SDC molecules, their heparan sulphate chains are not expressed through bacterial expression systems. It would be interesting, therefore, to include a binding assay with mammalian-expressed CD148 in addition to those completed with recombinant CD148 proteins, to determine whether any structural differences (and sequence disparities) in mammalian CD148 affect its interaction with QM107. This could potentially aid our investigation into determining the interaction site between the two molecules, as the amino acid sequences for both bacterially- and mammalian-expressed can be compared and if there are conserved regions, this may be indicative of the interaction site.

Furthermore, a cell-based binding assay with QM107, perhaps fluorescently labelled, would produce data to potentially support our *in vitro* findings. CD148 is expressed on cells of the vasculature, so HUVECs could be cultured and combined with fluorescently labelled QM107. Readouts would indicate whether there was any interaction between QM107 and CD148 expressed at the cell surface.

6.3.3. Anti-angiogenic properties of the CD148 short form protein

Proposed improvements for the pursuit of CD148SF as an anti-angiogenic therapy include further miniaturisation of CD148SF. The QM107 peptide is approximately 2082 Da, while the CD148SF protein is currently 53, 000 Da – this is approximately 25 times as big as QM107. If CD148CT can inhibit angiogenesis to the same extent as CD148SF, this would be beneficial as the CT protein is almost half the size of SF (26, 400 Da).

6.4. Concluding remarks

Overall, this PhD project has produced a body of work that encompasses preliminary data regarding the characterisation of QM107, a novel therapeutic peptide. We have successfully produced an antibody against QM107, which we have used to characterise QM107 regarding its proteolytic degradation and its stability in multiple different biological materials (human serum and porcine vitreous humour). Furthermore, we have established a robust methodology for quantifying *in vitro* interaction between CD148SF and QM107, refining the interaction site to three FNIII repeats. This has enabled us to begin to identify the specific amino acid sequence responsible for the QM107 interaction site on CD148.

Finally, we have produced data to confirm the anti-angiogenic ability of CD148SF, as well as producing a completely novel angiogenesis assay to test this. We have also made progress in refining the portion of CD148SF that is responsible for its inhibitory activity.

This will aid the progress of QM107 as a therapeutic peptide, having identified which areas within its development require further work, and the preliminary data supporting the anti-angiogenic activity of CD148SF provides a starting point for its development as another alternative treatment to current anti-VEGF therapies.

References

1. Trust, M.E.H.N.F. Anatomy of the Eye. 2017 [cited 2020; Available from: https://www.moorfields.nhs.uk/content/anatomy-eye.

2. Willoughby, C.E., et al., Anatomy and physiology of the human eye: effects of mucopolysaccharidoses disease on structure and function – a review. Clinical & Experimental Ophthalmology, 2010. 38: p. 2-11.

3. Optometrists, T.C.o. How your eye works (parts of the eye). 2021 [cited 2021; Available from: https://lookafteryoureyes.org/eye-care/how-your-eye-works/.

4. JW., K., The Ocular Circulation. 2010, San Rafael (CA): Morgan & Claypool Life Sciences. Chapter 2.

5. Institute, N.E. Corneal Conditions. 2019 [cited 2021; Available from: https://www.nei.nih.gov/learn-about-eye-health/eye-conditions-and-diseases/corneal-conditions#:~:text=The%20cornea%20is%20the%20clear,so%20you%20can%20see%20clearly.

6. Prevention, C.f.D.C.a. Common Eye Disorders and Diseases - Vision Health Initiative. 2020; Available from: https://www.cdc.gov/visionhealth/basics/ced/index.html.

7. NIH. Refractive Errors. 2022 [cited 2022; Available from: https://www.nei.nih.gov/learn-about-eye-health/eye-conditions-and-diseases/refractive-errors#:~:text=Refractive%20errors%20are%20a%20type,common%20type%20of%20vision%20problem.

8. Clinic, M. Cataracts. 2022 [cited 2022; Available from: https://www.mayoclinic.org/diseases-conditions/cataracts/symptoms-causes/syc-20353790.

9. Trust, M.E.H.N.F. Having Cataract surgery. 2017 [cited 2020; Available from: https://www.moorfields.nhs.uk/content/having-cataract-surgery.

10. Trust, M.E.H.N.F. Glaucoma. 2013 [cited 2020; Available from: https://www.moorfields.nhs.uk/news/glaucoma.

11. NHS. Glaucoma. 2021 [cited 2022; Available from: https://www.nhs.uk/conditions/glaucoma/#:~:text=Glaucoma%20is%20a%20common%20eye,not%20diagnosed%20and%20treated%20early.

12. Sun, Y. and L. Smith, Retinal Vasculature in Development and Diseases Annual Review of Vision Science, 2018. 4: p. 101-122.

13. Risau, W., Mechanisms of angiogenesis. . Nature, 1997. 386(6626): p. 671-4.

14. Maahs , D.M., et al., Chapter 1: Epidemiology of Type 1 Diabetes. Endocrinol Metab Clin North Am, 2010. 39(3): 481–497.

15. Organisation, W.H. Diabetes. 2020 [cited 2020 12 June]; Available from: https://www.who.int/news-room/fact-sheets/detail/diabetes.

16. Saeedi, P., et al., Global and regional diabetes prevalence estimates for 2019 and projections for 2030 and 2045: Results from the International Diabetes Federation Diabetes Atlas, 9 th edition. Diabetes Research and Clinical Practice, 2019. 157.

17. Kaser S and K.-S.L. Winhofer-Stöckl Y, et al., Other specific forms of diabetes and exocrine pancreatic insufficiency (Update 2019). Wien Klin Wochenschr . , 2019. 131: p. 16-26.

18. Kahn, R., Report of the Expert Committee on the Diagnosis and Classification of Diabetes Mellitus. 1997, American Diabetes Association.

19. M, B., et al., Assessment of human pancreatic islet architecture and composition by laser scanning confocal microscopy. J Histochem Cytochem., 2005. 53.

20. Sapra, A. and P. Bhandari, Diabetes Mellitus. Updated 27 Feb 2020, StatPearls Publishing: Treasure Island (FL).

21. Moin, A.S.M. and A.E. Butler, Alterations in Beta Cell Identity in Type 1 and Type 2 Diabetes. Curr Diab Rep . 2019. 19(9).

22. Suckale, J. and M. Solimena, Pancreas islets in metabolic signaling - focus on the beta-cell. Frontiers in Bioscience 13, 2008. 13.

23. Khan, A. and P. Pessin, Insulin regulation of glucose uptake: a complex interplay of intracellular signalling pathways. <i data-test="journal-title" style="box-sizing: inherit;">Diabetologia, 2002.

24. Powley, T.L., Vagal circuitry mediating cephalic-phase responses to food. Appetite, 2000. 34(2): p. 184-188.

25. Ahren, B. and J.J. Holst, The Cephalic Insulin Response to Meal Ingestion in Humans Is Dependent on Both Cholinergic and Noncholinergic Mechanisms and Is Important for Postprandial Glycemia. Diabetes, 2001. 50(5): p. 1030 - 1038.

26. Gromada, J., et al., Adrenaline Stimulates Glucagon Secretion in Pancreatic A-Cells by Increasing the Ca2+ Current and the Number of Granules Close to the L-Type Ca2+ Channels. Journal of General Physiology, 1997(110 (3)).

27. Utiger, R.D., Insulin, i. Encyclopædia Britannica, Editor. 2020, Encyclopædia Britannica.

28. Bach, J.-F., The Effect of Infections on Susceptibility to Autoimmune and Allergic Diseases. N Engl J Med, 2002. 347:911-920.

29. Cerna, M., Epigenetic Regulation in Etiology of Type 1 Diabetes Mellitus. Int J Mol Sci . 2020. 21(1): 36.

30. Marfa Blanter , 2 Helena Sork , 1 Soile Tuomela , 1 and Malin Flodström-Tullberg, Genetic and Environmental Interaction in Type 1 Diabetes: a Relationship Between Genetic Risk Alleles and Molecular Traits of Enterovirus Infection? Curr Diab Rep . 2019. 19(9).

31. TC, T., et al., Superoxide production by macrophages and T cells is critical for the induction of autoreactivity and type 1 diabetes. Diabetes, 2011. 60(8): p. 2144-51.

32. LE, P., et al., Loss of NOX-Derived Superoxide Exacerbates Diabetogenic CD4 T-Cell Effector Responses in Type 1 Diabetes. Diabetes, 2015. 64(12): p. 4171-83.

33. Kaestner , K.H., et al., NIH Initiative to Improve Understanding of the Pancreas, Islet, and Autoimmunity in Type 1 Diabetes: The Human Pancreas Analysis Program (HPAP). American Diabetes Association, 2019. 68(7): p. 1394 - 1402.

34. Paun , A., C. Yau, and J.S. Danska, The Influence of the Microbiome on Type 1 Diabetes. J Immunol, 15 January 2017. 198 (2) 590-595.

35. Boerner, B.P. and N.E. Sarvetnick Type 1 diabetes: role of intestinal microbiome in humans and mice. New York Academy of Sciences, 2011. 1243(1).

36. ., G.P.-W.E., The gut microbiota in type 1 diabetes : friend or foe? Current opinion in endocrinology, diabetes, and obesity., 2019.

37. Pabst , O., et al., Adaptation of Solitary Intestinal Lymphoid Tissue in Response to Microbiota and Chemokine Receptor CCR7 Signaling. J Immunol, 2006. 177(10): p. 6824-6832.

38. UK, D. Do you know the 4 Ts of Type 1 diabetes? 2012 [cited 2020 20 April 2020].

39. Hamdy, O. and R. Khardori, Diabetic Ketoacidosis (DKA). MedScape, 2019.

40. Jefferies CA, et al., Preventing Diabetic Ketoacidosis. . Pediatr Clin North Am . 2015. 62(4): p. 857-871.

41. Maletkovic J and D. A., Diabetic ketoacidosis and hyperglycemic hyperosmolar state. . Endocrinol Metab Clin North Am . 2013. 42(4): p. 677-695. .

42. Gonzalez, A.G. and S. Adi, Type 1 Diabetes Mellitus: An Overview. Nutritional and Therapeutic Interventions for Diabetes and Metabolic Syndrome, 2012.

43. Care, A.D. FreeStyle Libre. 2020 [cited 2020 23 April 2020]; Available from: https://www.freestylelibre.co.uk/libre/.

44. (JDRF), J.D.R.F.L. Insulin pump therapy. 2018 [cited 2020 23 April 2020]; Available from: https://jdrf.org.uk/information-support/treatments-technologies/insulin-pump-therapy/.

45. Golden SH and S. T, Methods for insulin delivery and glucose monitoring in diabetes: summary of a comparative effectiveness review. . J Manag Care Pharm . 2012. 18: p. S1-S17.

46. Bird , S.R. and J.A. Hawley Update on the effects of physical activity on insulin sensitivity in humans. BMJ Open Sport Exerc Med . 2016. 2(1).

47. RJ., H., Type-2 diabetes mellitus and cardiovascular disease. . Future Cardiol . 2018. 14(6): p. 491-509.

48. Diabetes.co.uk. Type 2 Diabetes. 2019 15 January 2019 [cited 2020 1 July]; Available from: https://www.diabetes.co.uk/type2-diabetes.html.

49. Fletcher B, Gulanick M, and L. C., Risk factors for type 2 diabetes mellitus. . J Cardiovasc Nurs . 2016. 16(2): p. 17-23.

50. Vijan, S., Type 2 diabetes. Annals of Internal Medicine, 2019.

51. Wu, Y., et al., Risk Factors Contributing to Type 2 Diabetes and Recent Advances in the Treatment and Prevention. Int J Med Sci . 2014. 11(11): p. 1185–1200

52. Stratton, I.M., et al., Association of glycaemia with macrovascular and microvascular complications of type 2 diabetes (UKPDS 35): prospective observational study. BMJ, 2000. 321.

53. Zheng, Y., S.H. Ley, and F.B. Hu, Global aetiology and epidemiology of type 2 diabetes mellitus and its complications. Nature Reviews Endocrinology, 2017. 14: p. 88-98.

54. Lim, A.K.H., Diabetic nephropathy – complications and treatment. Int J Nephrol Renovasc Dis, 2014. 7: p. 361–381.

55. Volmer-Thole M and L. R., Neuropathy and Diabetic Foot Syndrome. . Int J Mol Sci . , 2016. 17(6).

56. Kim, Y.-W. and T.V. Byzova, Oxidative stress in angiogenesis and vascular disease. Blood, 2014. 123(5): p. 625-631.

57. Dodson, M., V. Darley-Usmar, and J. Zhang, Cellular metabolic and autophagic pathways: traffic control by redox signaling. Free radical biology & medicine, 2013. 63: p. 207-221.

58. Singh, S.B., et al., The Fatty Acid Synthase Inhibitor Platensimycin Improves Insulin Resistance without Inducing Liver Steatosis in Mice and Monkeys. PloS one, 2016. 11(10): p. e0164133-e0164133.

59. Wei, X., et al., Fatty acid synthesis configures the plasma membrane for inflammation in diabetes. Nature, 2016. 539: p. 294.

60. Kolb, H. and S. Martin, Environmental/lifestyle factors in the pathogenesis and prevention of type 2 diabetes. BMC Medicine, 2017. 15(131).

61. Collaboration, E.R.F., Sarwar N, and e.a. Gao P, Diabetes mellitus, fasting blood glucose concentration, and risk of vascular disease: a collaborative meta-analysis of 102 prospective studies Lancet. 376(9754).

62. Neely, K.A. and T. Gardner, Ocular neovascularization: clarifying complex interactions. The American journal of pathology, 1998. 153(3): p. 665-670.

63. Arevalo, J.F., et al., Intravitreal Bevacizumab (Avastin) for Diabetic Retinopathy: The 2010 GLADAOF Lecture. Journal of ophthalmology, 2011. 2011: p. 584238-584238.

64. Lee, R., T.Y. Wong, and C. Sabanayagam, Epidemiology of diabetic retinopathy, diabetic macular edema and related vision loss. Eye and vision (London, England), 2015. 2: p. 17-17.

65. Wolfram, C., et al., The Prevalence of Visual Impairment in the Adult Population. Dtsch Arztebl International, 2019. 116(17): p. 289-295.

66. Schreur, V., et al., Risk factors for development and progression of diabetic retinopathy in Dutch patients with type 1 diabetes mellitus. Acta ophthalmologica, 2018. 96(5): p. 459-464.

67. The Effect of Intensive Treatment of Diabetes on the Development and Progression of Long-Term Complications in Insulin-Dependent Diabetes Mellitus. New England Journal of Medicine, 1993. 329(14): p. 977-986.

68. Intensive blood-glucose control with sulphonylureas or insulin compared with conventional treatment and risk of complications in patients with type 2 diabetes (UKPDS 33). The Lancet, 1998. 352(9131): p. 837-853.

69. Schwartz, S.G. and H.W. Flynn, Pars plana vitrectomy for primary rhegmatogenous retinal detachment. Clinical ophthalmology (Auckland, N.Z.), 2008. 2(1): p. 57-63.

70. Stewart, M.W., Corticosteroid Use for Diabetic Macular Edema: Old Fad or New Trend? Current Diabetes Reports, 2012. 12(4): p. 364-375.

71. Grover D, Li TJ, and C. CC, Intravitreal steroids for macular edema in diabetes. . Cochrane Database Syst Rev . 2008. 1.

72. Gheorghe A, Mahdi L, and M. O, AGE-RELATED MACULAR DEGENERATION. . Rom J Ophthalmol . , 2015. 59(2): p. 74-77.

73. Al-Zamil WM and Y. SA, Recent developments in age-related macular degeneration: a review. . Clin Interv Aging . 2017. 12: p. 1313-1330.

74. Smith, W., et al., Risk factors for age-related macular degeneration: Pooled findings from three continents. . Ophthalmology. , 2001. 108(4): p. 697-704.

75. Mullins, R., et al., Drusen associated with aging and age-related macular degeneration contain proteins common to extracellular deposits associated with atherosclerosis, elastosis, amyloidosis, and dense deposit disease. Federation of American Societies for Experimental Biology, 2000. 14(7): p. 835-846.

76. Al-Zamil, W. M, and S.A. Yassin, Recent developments in age-related macular degeneration: a review. Clinical interventions in aging, 2017. 12: p. 1313-1330.

77. CATT Research Group, et al., Ranibizumab and bevacizumab for neovascular age-related macular degeneration. N Engl J Med. , 2011. 19 (20): p. 1897-908.

78. Klein R, et al., Fifteen-year cumulative incidence of age-related macular degeneration: the Beaver Dam Eye Study. . Ophthalmology . 2007. 114(2): p. 253-262.

79. Bressler, N., et al., Clinicopathologic correlation of drusen and retinal pigment epithelial abnormalities in age-related macular degeneration. . Retina., 1994. 14(2): p. 130-142.

80. Zhang, X. and S. Sivaprasad, Drusen and pachydrusen: the definition, pathogenesis, and clinical significance. Eye, 2021. 35(1): p. 121-133.

81. Ruggeri, Z.M. and S.P. Jackson, Chapter 20 - Platelet Thrombus Formation in Flowing Blood, in Platelets (Third Edition), A.D. Michelson, Editor. 2013, Academic Press. p. 399-423.

82. Liu, C.C., et al., Apolipoprotein E and Alzheimer disease: risk, mechanisms and therapy. Nat Rev Neurol, 2013. 9(2): p. 106-18.

83. Sivaprasad, S. and N.V. Chong, The complement system and age-related macular degeneration. Eye, 2006. 20(8): p. 867-872.

84. Biesemeier, A., et al., Choriocapillaris breakdown precedes retinal degeneration in age-related macular degeneration. . Neurobiology of Aging, 2014. 35(11): p. 2562-2573.

85. Society, M. Charles Bonnet syndrome. 2022 [cited 2022; Available from: https://www.macularsociety.org/macular-disease/macular-conditions/charles-bonnet-syndrome/.

86. Haddad S, et al., The genetics of age-related macular degeneration: a review of progress to date. . Surv Ophthalmol, 2006. 51(4): p. 316-363.

87. Gheorghe, A., L. Mahdi, and O. Musat, AGE-RELATED MACULAR DEGENERATION. . Romanian journal of ophthalmology, 2015. 59(2): p. 74–77.

88. Chakravarthy, U., et al., Clinical risk factors for age-related macular degeneration: a systematic review and meta-analysis. . BMC Ophthalmology, 2010.

89. McCarty, C., et al., Risk factors for age-related maculopathy: the Visual Impairment Project. . Archives of Ophthalmology., 2001. 119(10): p. 1455-1462.

90. Klein, R., B. Klein, and K. Linton, Prevalence of age-related maculopathy. The Beaver Dam Eye Study. . Ophthalmology., 1992. 99(6): p. 933-943.

91. Cougnard-Grégoire, A., et al., Long-term blood pressure and age-related macular degeneration: the ALIENOR study. . Investigative ophthalmology and visual science, 2013 54(3): p. 1905-1912.

92. Blasiak J, et al., Expression of VEGFA-regulating miRNAs and mortality in wet AMD. J Cell Mol Med., 2019. 23(12): p. 8464-8471.

93. Lim, L., et al., Age-related macular degeneration. . Lancet, 2012. 379(9827): p. 1728-1738.

94. Hellström, A., L.E. Smith, and O. Dammann, Retinopathy of Prematurity. The Lancet, 2013. 382(9902): p. 1445-1457.

95. Mach, W.J., et al., Consequences of hyperoxia and the toxicity of oxygen in the lung. Nurs Res Pract, 2011. 2011: p. 260482.

96. Institute, N.E. Retinopathy of Prematurity. 2019 [cited 2021 16th February]; Available from: https://www.nei.nih.gov/learn-about-eye-health/eye-conditions-and-diseases/retinopathy-prematurity.

97. Blencowe H, L.J., Vazquez T, Fielder A, Gilbert C., Preterm-associated visual impairment and estimates of retinopathy of prematurity at regional and global levels for 2010. 2013. 74: p. 35-49.

98. Adams, G.G.W., et al., Treatment trends for retinopathy of prematurity in the UK: active surveillance study of infants at risk. BMJ Open, 2017. 7(3).

99. Blencowe H, L.J., Vazquez T, Fielder A, Gilbert C., Preterm-associated visual impairment and estimates of retinopathy of prematurity at regional and global levels for 2010. Pediatric Research, 2013. 74: p. 35-49.

100. Moore, T., et al., Neurological and developmental outcome in extremely preterm children born in England in 1995 and 2006: the EPICure studies. BMJ, 2012. 345.

101. Gilbert , C.F., Alistair Gordillo , Luz Quinn , Graham Semiglia , Renato Visintin , Patricia Zin, Andrea, Characteristics of Infants With Severe Retinopathy of Prematurity in Countries With Low, Moderate, and High Levels of Development: Implications for Screening Programs. Pediatrics 2005. 115: p. 518-525.

102. Bashinsky, A.L., Retinopathy of Prematurity. North Carolina Medical Journal 2017. 78(2): p. 124-128.

103. Aspelund, A., et al., Lymphatic System in Cardiovascular Medicine. 2016. 118(3): p. 515-530.

104. Pugsley, M.K. and R. Tabrizchi, The vascular system: An overview of structure and function. Journal of Pharmacological and Toxicological Methods, 2000. 44(2): p. 333-340.

105. U. S. National Institutes of Health, N.C.I. SEER Training Modules, Classification & Structure of Blood Vessels. [cited 2021 29th September]; Available from: https://training.seer.cancer.gov/anatomy/cardiovascular/blood/classification.html.

106. Alberts B, J.A., Lewis J, et al. , Molecular Biology of the Cell. Blood Vessels and Endothelial Cells. 4th edition. ed. 2002: New York: Garland Science;.

107. Knuttinen, M.G., et al., Review of pharmacology and physiology in thrombolysis interventions. Seminars in interventional radiology, 2010. 27(4): p. 374-383.

108. Pucovský, V., Interstitial cells of blood vessels. ScientificWorldJournal, 2010. 10: p. 1152-68.

109. Palade, G., M. Simionescu, and N.J.B. Simionescu, Differentiated micro domains on the luminal surface of the capillary endothelium. 1981. 18(3-6): p. 563-568.

110. Marelli-Berg, F.M., et al., An immunologist's guide to CD31 function in T-cells. J Cell Sci, 2013. 126(Pt 11): p. 2343-52.

111. Rakocevic, J., et al., Endothelial cell markers from clinician's perspective. Exp Mol Pathol, 2017. 102(2): p. 303-313.

112. Jose M Lopez-Novoa , C.B. ENG (endoglin). 2012 [cited 2023.

113. Hirschi, K.K. and P.A. D'Amore, Pericytes in the microvasculature. Cardiovascular Research, 1996. 32(4): p. 687-698.

114. Schor, A.M., et al., Pericyte differentiation. 1995(313): p. 81-91.

115. Crisan, M., et al., A perivascular origin for mesenchymal stem cells in multiple human organs. Cell Stem Cell, 2008. 3(3): p. 301-13.

116. Farrington-Rock, C., et al., Chondrogenic and adipogenic potential of microvascular pericytes. Circulation, 2004. 110(15): p. 2226-32.

117. Baek, S.-H., et al., Single Cell Transcriptomic Analysis Reveals Organ Specific Pericyte Markers and Identities. 2022. 9.

118. Schiffer, D., et al., The Significance of Chondroitin Sulfate Proteoglycan 4 (CSPG4) in Human Gliomas. Int J Mol Sci, 2018. 19(9).

119. Winkler, E.A., R.D. Bell, and B.V. Zlokovic, Pericyte-specific expression of PDGF beta receptor in mouse models with normal and deficient PDGF beta receptor signaling. Mol Neurodegener, 2010. 5: p. 32.

120. Sims, D.E., The pericyte—A review. Tissue and Cell, 1986. 18(2): p. 153-174.

121. Bergers, G. and S. Song, The role of pericytes in blood-vessel formation and maintenance. Neuro Oncol, 2005. 7(4): p. 452-64.

122. Ramsauer, M., D. Krause, and R. Dermietzel, Angiogenesis of the blood-brain barrier in vitro and the function of cerebral pericytes. 2002. 16(10): p. 1274-1276.

123. Franco, M., et al., Pericytes promote endothelial cell survival through induction of autocrine VEGF-A signaling and Bcl-w expression. Blood, 2011. 118(10): p. 2906-17.

124. Ciulla, T.A., A.G. Amador, and B. Zinman, Diabetic Retinopathy and Diabetic Macular Edema: Pathophysiology, screening, and novel therapies. Diabetes Care, 2003. 26(9): p. 2653-2664.

125. Berridge, B.R., J.F. Van Vleet, and E. Herman, Chapter 46 - Cardiac, Vascular, and Skeletal Muscle Systems, in Haschek and Rousseaux's Handbook of Toxicologic Pathology (Third Edition), W.M. Haschek, C.G. Rousseaux, and M.A. Wallig, Editors. 2013, Academic Press: Boston. p. 1567-1665.

126. Basatemur, G.L., et al., Vascular smooth muscle cells in atherosclerosis. Nature Reviews Cardiology, 2019. 16(12): p. 727-744.

127. Hafen BB, B.B., Physiology, Smooth Muscle.: Treasure Island (FL): StatPearls Publishing.

128. Smyth, L.C.D., et al., Markers for human brain pericytes and smooth muscle cells. J Chem Neuroanat, 2018. 92: p. 48-60.

129. Carmeliet, P., Mechanisms of angiogenesis and arteriogenesis. Nature Medicine, 2000. 6(4): p. 389-395.

130. Dvorak, H.F., Vascular Permeability Factor/Vascular Endothelial Growth Factor: A Critical Cytokine in Tumor Angiogenesis and a Potential Target for Diagnosis and Therapy. Journal of Clinical Oncology, 2002. 20(21): p. 4368-4380.

131. Ferrara, N. and T. Davis-Smyth, The Biology of Vascular Endothelial Growth Factor. Endocrine Reviews, 1997. 18(1): p. 4-25.

132. Cao, Y., Positive and Negative Modulation of Angiogenesis by VEGFR1 Ligands. 2009. 2(59): p. re1-re1.

133. Bresnick, G.H. and F.L. Myers, Vitrectomy Surgery for Diabetic Retinopathy. Annual Review of Medicine, 1979. 30(1): p. 331-338.

134. Shibuya, M., Vascular endothelial growth factor and its receptor system: physiological functions in angiogenesis and pathological roles in various diseases. Journal of biochemistry, 2013. 153(1): p. 13-19.

135. Shibuya, M., VEGF-VEGFR Signals in Health and Disease. Biomolecules & therapeutics, 2014. 22(1): p. 1-9.

136. Peach, C.J., et al., Molecular Pharmacology of VEGF-A Isoforms: Binding and Signalling at VEGFR2. International journal of molecular sciences, 2018. 19(4): p. 1264.

137. Li, X., et al., VEGF-B: a survival, or an angiogenic factor? Cell adhesion & migration, 2009. 3(4): p. 322-327.

138. Shaik, F., et al., Structural Basis for Vascular Endothelial Growth Factor Receptor Activation and Implications for Disease Therapy. Biomolecules, 2020. 10(12): p. 1673.

139. Autiero, M., et al., Placental growth factor and its receptor, vascular endothelial growth factor receptor-1: novel targets for stimulation of ischemic tissue revascularization and inhibition of angiogenic and inflammatory disorders. J Thromb Haemost, 2003. 1(7): p. 1356-70.

140. Otrock, Z.K., J.A. Makarem, and A.I. Shamseddine, Vascular endothelial growth factor family of ligands and receptors: review. Blood Cells Mol Dis, 2007. 38(3): p. 258-68.

141. Carmeliet, P., et al., Synergism between vascular endothelial growth factor and placental growth factor contributes to angiogenesis and plasma extravasation in pathological conditions. Nat Med, 2001. 7(5): p. 575-83.

142. Odorisio, T., et al., Mice overexpressing placenta growth factor exhibit increased vascularization and vessel permeability. J Cell Sci, 2002. 115(Pt 12): p. 2559-67.

143. Carmeliet, P., et al., Abnormal blood vessel development and lethality in embryos lacking a single VEGF allele. Nature, 1996. 380(6573): p. 435-9.

144. Olsson, A.K., et al., VEGF receptor signalling - in control of vascular function. Nat Rev Mol Cell Biol, 2006. 7(5): p. 359-71.

145. Hoeben, A., et al., Vascular Endothelial Growth Factor and Angiogenesis. Pharmacological Reviews, 2004. 56(4): p. 549-580.

146. Kärpänen, T., et al., Functional interaction of VEGF-C and VEGF-D with neuropilin receptors. Faseb j, 2006. 20(9): p. 1462-72.

147. Takahashi, H. and M. Shibuya, The vascular endothelial growth factor (VEGF)/VEGF receptor system and its role under physiological and pathological conditions. Clin Sci (Lond), 2005. 109(3): p. 227-41.

148. Sawano, A., et al., Flt-1 but not KDR/Flk-1 tyrosine kinase is a receptor for placenta growth factor, which is related to vascular endothelial growth factor. Cell Growth Differ, 1996. 7(2): p. 213-21.

149. Baldwin, M.E., et al., Generation of mice carrying floxed VEGFR-1 and VEGFR-2 alleles to study the effects of postnatal gene ablation on angiogenesis and hematopoiesis. Cancer Research, 2004. 64(7 Supplement): p. 596.

150. Ramakrishnan, S., V. Anand, and S. Roy, Vascular endothelial growth factor signaling in hypoxia and inflammation. Journal of neuroimmune pharmacology : the official journal of the Society on NeuroImmune Pharmacology, 2014. 9(2): p. 142-160.

151. Olenyuk, B.Z., et al., Inhibition of vascular endothelial growth factor with a sequence-specific hypoxia response element antagonist. Proceedings of the National Academy of Sciences of the United States of America, 2004. 101(48): p. 16768-16773.

152. Ferrara, N., H.P. Gerber, and J. LeCouter, The biology of VEGF and its receptors. Nat Med, 2003. 9(6): p. 669-76.

153. López-García, M., et al., Quantifying the phosphorylation timescales of receptor-ligand complexes: a Markovian matrix-analytic approach. Open biology, 2018. 8(9): p. 180126.

154. Neagoe, P.E., C. Lemieux, and M.G. Sirois, Vascular endothelial growth factor (VEGF)-A165-induced prostacyclin synthesis requires the activation of VEGF receptor-1 and -2 heterodimer. J Biol Chem, 2005. 280(11): p. 9904-12.

155. Cudmore, M.J., et al., The role of heterodimerization between VEGFR-1 and VEGFR-2 in the regulation of endothelial cell homeostasis. Nat Commun, 2012. 3: p. 972.

156. Mac Gabhann, F. and A.S. Popel, Dimerization of VEGF receptors and implications for signal transduction: a computational study. Biophysical chemistry, 2007. 128(2-3): p. 125-139.

157. Koch, S. and L. Claesson-Welsh, Signal transduction by vascular endothelial growth factor receptors. Cold Spring Harbor perspectives in medicine, 2012. 2(7): p. a006502-a006502.

158. Abhinand, C.S., et al., VEGF-A/VEGFR2 signaling network in endothelial cells relevant to angiogenesis. Journal of cell communication and signaling, 2016. 10(4): p. 347-354.

159. Ebos, J.M., et al., A naturally occurring soluble form of vascular endothelial growth factor receptor 2 detected in mouse and human plasma. Mol Cancer Res, 2004. 2(6): p. 315-26.

160. Cross, M.J., et al., VEGF-receptor signal transduction. Trends in Biochemical Sciences, 2003. 28(9): p. 488-494.

161. Harris, H., et al., Soluble vascular endothelial growth factor receptors 2 (sVEGFR-2) and 3 (sVEGFR-3) and breast cancer risk in the Swedish Mammography Cohort. International journal of molecular epidemiology and genetics, 2016. 7(1): p. 81-86.

162. Singh, N., et al., Soluble vascular endothelial growth factor receptor 3 is essential for corneal alymphaticity. Blood, 2013. 121(20): p. 4242-4249.

163. Nilsson, I., et al., VEGF receptor 2/-3 heterodimers detected in situ by proximity ligation on angiogenic sprouts. The EMBO journal, 2010. 29(8): p. 1377-1388.

164. Adair TH, M.J., Angiogenesis. San Rafael (CA): Morgan & Claypool Life Sciences; 2010. Chapter 1, Overview of Angiogenesis. 2010.

165. Gerhardt, H., et al., VEGF guides angiogenic sprouting utilizing endothelial tip cell filopodia. J Cell Biol, 2003. 161(6): p. 1163-77.

166. Siekmann, A.F. and N.D. Lawson, Notch signalling limits angiogenic cell behaviour in developing zebrafish arteries. Nature, 2007. 445(7129): p. 781-784.

167. Gerhardt, H., et al., Neuropilin-1 is required for endothelial tip cell guidance in the developing central nervous system. 2004. 231(3): p. 503-509.

168. Tammela, T., et al., Blocking VEGFR-3 suppresses angiogenic sprouting and vascular network formation. Nature, 2008. 454(7204): p. 656-660.

169. Smet, F.D., et al., Mechanisms of Vessel Branching. 2009. 29(5): p. 639-649.

170. Suchting, S., et al., The Notch ligand Delta-like 4 negatively regulates endothelial tip cell formation and vessel branching. Proc Natl Acad Sci U S A, 2007. 104(9): p. 3225-30.

171. Dejana, E., E. Tournier-Lasserve, and B.M. Weinstein, The control of vascular integrity by endothelial cell junctions: molecular basis and pathological implications. Dev Cell, 2009. 16(2): p. 209-21.

172. Iruela-Arispe, M.L. and G.E. Davis, Cellular and molecular mechanisms of vascular lumen formation. Dev Cell, 2009. 16(2): p. 222-31.

173. Phng, L.K. and H. Gerhardt, Angiogenesis: a team effort coordinated by notch. Dev Cell, 2009. 16(2): p. 196-208.

174. Blanco, R. and H. Gerhardt, VEGF and Notch in tip and stalk cell selection. Cold Spring Harb Perspect Med, 2013. 3(1): p. a006569.

175. Kopan, R., Notch signaling. Cold Spring Harb Perspect Biol, 2012. 4(10).

176. Lawson, N.D., A.M. Vogel, and B.M. Weinstein, sonic hedgehog and vascular endothelial growth factor Act Upstream of the Notch Pathway during Arterial Endothelial Differentiation. Developmental Cell, 2002. 3(1): p. 127-136.

177. Villa, N., et al., Vascular expression of Notch pathway receptors and ligands is restricted to arterial vessels. Mechanisms of Development, 2001. 108(1): p. 161-164.

178. Claxton, S. and M. Fruttiger, Periodic Delta-like 4 expression in developing retinal arteries. Gene Expression Patterns, 2004. 5(1): p. 123-127.

179. Benedito, R. and A. Duarte, Expression of Dll4 during mouse embryogenesis suggests multiple developmental roles. Gene Expression Patterns, 2005. 5(6): p. 750-755.

180. Carmeliet, P., F. De Smet, and S.e.a. Loges, Branching morphogenesis and antiangiogenesis candidates: tip cells lead the way. . Nat Rev Clin Oncol 2009. 6: p. 315-326.

181. Horowitz, A. and M. Simons, Branching morphogenesis. Circ Res, 2008. 103(8): p. 784-95.

182. Ferrara, N., et al., Heterozygous embryonic lethality induced by targeted inactivation of the VEGF gene. Nature, 1996. 380(6573): p. 439-42.

183. Jain, R.K., Normalization of tumor vasculature: an emerging concept in antiangiogenic therapy. Science, 2005. 307(5706): p. 58-62.

184. Burri, P.H., R. Hlushchuk, and V. Djonov, Intussusceptive angiogenesis: Its emergence, its characteristics, and its significance. Developmental Dynamics, 2004. 231(3): p. 474-488.

185. Ackermann, M., et al., Pulmonary Vascular Endothelialitis, Thrombosis, and Angiogenesis in Covid-19. The New England journal of medicine, 2020. 383(2): p. 120-128.

186. Kurz, H., P.H. Burri, and V.G. Djonov, Angiogenesis and vascular remodeling by intussusception: from form to function. News Physiol Sci, 2003. 18: p. 65-70.

187. Djonov, V.G., H. Kurz, and P.H. Burri, Optimality in the developing vascular system: branching remodeling by means of intussusception as an efficient adaptation mechanism. Dev Dyn, 2002. 224(4): p. 391-402.

188. Djonov, V., O. Baum, and P.H. Burri, Vascular remodeling by intussusceptive angiogenesis. Cell Tissue Res, 2003. 314(1): p. 107-17.

189. Patan, S., et al., Intussusceptive microvascular growth: a common alternative to capillary sprouting. Arch Histol Cytol, 1992. 55 Suppl: p. 65-75.

190. Boesiger, J., et al., Mast cells can secrete vascular permeability factor/ vascular endothelial cell growth factor and exhibit enhanced release after immunoglobulin E-dependent upregulation of fc epsilon receptor I expression. The Journal of experimental medicine, 1998. 188(6): p. 1135-1145.

191. Galli, S.J., The Paul Kallos Memorial Lecture. The mast cell: a versatile effector cell for a challenging world. Int Arch Allergy Immunol, 1997. 113(1-3): p. 14-22.

192. Nagy, J.A., et al., Vascular permeability, vascular hyperpermeability and angiogenesis. Angiogenesis, 2008. 11(2): p. 109-119.

193. Bates, D.O. and S.J. Harper, Regulation of vascular permeability by vascular endothelial growth factors. Vascular Pharmacology, 2002. 39(4): p. 225-237.

194. Dvorak, H.F., et al., Vascular permeability factor/vascular endothelial growth factor, microvascular hyperpermeability, and angiogenesis. The American journal of pathology, 1995. 146(5): p. 1029-1039.

195. Dvorak, H.F., et al., Tumor shedding and coagulation. Science, 1981. 212(4497): p. 923-4.

196. VanDeWater, L., et al., Tumor cell generation of thrombin via functional prothrombinase assembly. Cancer Res, 1985. 45(11 Pt 1): p. 5521-5.

197. Schoefl, G.I., Studies on inflammation. Virchows Archiv für pathologische Anatomie und Physiologie und für klinische Medizin, 1963. 337(2): p. 97-141.

198. Patel-Hett, S. and P.A. D'Amore, Signal transduction in vasculogenesis and developmental angiogenesis. The International journal of developmental biology, 2011. 55(4-5): p. 353-363.

199. Mitchell, T., Understanding endothelial protein trafficking in angiogenesis using a novel biochemical and bioinformatics approach., in Microvascular Research. 2021, Queen Mary University of London.

200. Shahrabi-Farahani, S., et al., Neuropilin 1 expression correlates with differentiation status of epidermal cells and cutaneous squamous cell carcinomas. Lab Invest, 2014. 94(7): p. 752-65.

201. Roy, S., et al., Multifaceted Role of Neuropilins in the Immune System: Potential Targets for Immunotherapy. Front Immunol, 2017. 8: p. 1228.

202. Plein, A., A. Fantin, and C. Ruhrberg, Neuropilin regulation of angiogenesis, arteriogenesis, and vascular permeability. Microcirculation, 2014. 21(4): p. 315-23.

203. Kawasaki, T., et al., A requirement for neuropilin-1 in embryonic vessel formation. Development, 1999. 126(21): p. 4895-902.

204. Chen, H., et al., Neuropilin-2 regulates the development of selective cranial and sensory nerves and hippocampal mossy fiber projections. Neuron, 2000. 25(1): p. 43-56.

205. Giger, R.J., et al., Neuropilin-2 is required in vivo for selective axon guidance responses to secreted semaphorins. Neuron, 2000. 25(1): p. 29-41.

206. Takashima, S., et al., Targeting of both mouse neuropilin-1 and neuropilin-2 genes severely impairs developmental yolk sac and embryonic angiogenesis. Proceedings of the National Academy of Sciences of the United States of America, 2002. 99(6): p. 3657-3662.

207. Favier, B., et al., Neuropilin-2 interacts with VEGFR-2 and VEGFR-3 and promotes human endothelial cell survival and migration. Blood, 2006. 108(4): p. 1243-50.

208. Herzog, Y., et al., Differential expression of neuropilin-1 and neuropilin-2 in arteries and veins. Mech Dev, 2001. 109(1): p. 115-9.

209. Xu, Y., et al., Neuropilin-2 mediates VEGF-C–induced lymphatic sprouting together with VEGFR3. Journal of Cell Biology, 2010. 188(1): p. 115-130.

210. Whitaker, G.B., B.J. Limberg, and J.S. Rosenbaum, Vascular endothelial growth factor receptor-2 and neuropilin-1 form a receptor complex that is responsible for the differential signaling potency of VEGF(165) and VEGF(121). J Biol Chem, 2001. 276(27): p. 25520-31.

211. Koch, S., et al., NRP1 presented in trans to the endothelium arrests VEGFR2 endocytosis, preventing angiogenic signaling and tumor initiation. Dev Cell, 2014. 28(6): p. 633-46.

212. Hynes, R., Integrins: bidirectional, allosteric signaling machines. Cell., 2002. 110(6): p. 673-87.

213. Mezu-Ndubuisi, O.J. and A. Maheshwari, The role of integrins in inflammation and angiogenesis. Nature: Pediatric Research 2020.

214. Alberts, B., et al., Molecular Biology of the Cell. Integrins. 4th edition ed. 2002: New York: Garland Science.

215. Arnaout, M.A., B. Mahalingam, and J.-P. Xiong, Integrin structure, allostery, and bidirectional signaling. Annual review of cell and developmental biology, 2005. 21: p. 381-410.

216. Takada, Y., X. Ye, and S. Simon, The integrins. Genome biology, 2007. 8.

217. Avraamides, C., B. Garmy-Susini, and J. Varner, Integrins in angiogenesis and lymphangiogenesis. . Nature Reviews Cancer. , 2008 8(8): p. 604-17. .

218. Whiteford JR, et al., Syndecan-2 is a novel ligand for the protein tyrosine phosphatase receptor CD148. . Mol Biol Cell . , 2011. 22: p. 3609-3624.

219. Streuli, C. and N. Akhtar, Signal co-operation between integrins and other receptor systems. . The Biochemical Journal 2009. 418(3): p. 491-506.

220. Tanjore, H., et al., β1 integrin expression on endothelial cells is required for angiogenesis but not for vasculogenesis. Developmental Dynamics, 2008. 237: p. 75-82.

221. Taverna, D. and R. Hynes, Reduced blood vessel formation and tumor growth in alpha5-integrin-negative teratocarcinomas and embryoid bodies. . Cancer research, 2001. 61(13): p. 5255-61.

222. Yang, J., H. Rayburn, and R. Hynes, Embryonic mesodermal defects in alpha 5 integrin-deficient mice. . Developmental, 1993. 119(4): p. 1093-105.

223. Kaneko, Y., K. Kitazato, and Y. Basaki, Integrin-linked kinase regulates vascular morphogenesis induced by vascular endothelial growth factor. . Journal of Cell Science., 2004. 117: p. 407-15.

224. McDonald PC, O.A., Mills J, Dobreva I, Maidan M, Gray V, Wederell ED, Bally MB, Foster LJ, Dedhar S., Rictor and integrin-linked kinase interact and regulate Akt phosphorylation and cancer cell survival. . Cancer research, 2008. 68(6): p. 1618-24.

225. Hodivala-Dilke, K.M., et al., Beta3-integrin-deficient mice are a model for Glanzmann thrombasthenia showing placental defects and reduced survival. The journal of clinical investigation, 1999. 103(2): p. 229-38.

226. Cheresh, D., Human endothelial cells synthesize and express an Arg-Gly-Asp-directed adhesion receptor involved in attachment to fibrinogen and von Willebrand factor. Proceedings of the National Academy of Sciences of the United States of America, 1987. 84(18): p. 6471-5.

227. Brooks, P., R. Clark, and D. Cheresh, Requirement of vascular integrin alpha v beta 3 for angiogenesis. Science., 1994. 264(5158): p. 569-71.

228. Brooks, P.C., et al., Integrin alpha v beta 3 antagonists promote tumor regression by inducing apoptosis of angiogenic blood vessels. Cell., 1994. 79(7): p. 1157-64.

229. Carmeliet, P., Angiogenesis in life, disease and medicine. Nature., 2005. 438: p. 932-6.

230. Friedlander, M., et al., Definition of two angiogenic pathways by distinct alpha v integrins. Science., 1995. 270(5241): p. 1500-2.

231. Eliceiri, B., et al., Src-mediated coupling of focal adhesion kinase to integrin alpha(v)beta5 in vascular endothelial growth factor signaling. The Journal of Cell Biology, 2002. 157(1): p. 149-60.

232. Suri, C., et al., Requisite Role of Angiopoietin-1, a Ligand for the TIE2 Receptor, during Embryonic Angiogenesis. Cell, 1996. 87(7): p. 1171-1180.

233. Huang, J., et al., Angiopoietin-1/Tie-2 activation contributes to vascular survival and tumor growth during VEGF blockade. Int J Oncol, 2009. 34(1): p. 79-87.

234. Khan, K.A., et al., Ang2 inhibitors and Tie2 activators: potential therapeutics in perioperative treatment of early stage cancer. 2021. 13(7): p. e08253.

235. Davis, S., et al., Angiopoietins have distinct modular domains essential for receptor binding, dimerization and superclustering. Nat Struct Biol, 2003. 10(1): p. 38-44.

236. Sato, T.N., et al., Distinct roles of the receptor tyrosine kinases Tie-1 and Tie-2 in blood vessel formation. Nature, 1995. 376(6535): p. 70-74.

237. Wong, A.L., et al., Tie2 Expression and Phosphorylation in Angiogenic and Quiescent Adult Tissues. 1997. 81(4): p. 567-574.

238. Kim, M., et al., Opposing actions of angiopoietin-2 on Tie2 signaling and FOXO1 activation. J Clin Invest, 2016. 126(9): p. 3511-25.

239. Akwii, R.G., et al., Role of Angiopoietin-2 in Vascular Physiology and Pathophysiology. Cells, 2019. 8(5).

240. Korhonen, E.A., et al., Tie1 controls angiopoietin function in vascular remodeling and inflammation. J Clin Invest, 2016. 126(9): p. 3495-510.

241. Grothey, A., et al., Regorafenib monotherapy for previously treated metastatic colorectal cancer (CORRECT): an international, multicentre, randomised, placebo-controlled, phase 3 trial. Lancet, 2013. 381(9863): p. 303-12.

242. Smith, B.D., et al., Ripretinib (DCC-2618) Is a Switch Control Kinase Inhibitor of a Broad Spectrum of Oncogenic and Drug-Resistant KIT and PDGFRA Variants. Cancer Cell, 2019. 35(5): p. 738-751.e9.

243. Dhillon, S., Ripretinib: First Approval. Drugs, 2020. 80(11): p. 1133-1138.

244. Adler, A.P., et al., Abstract 4492: Blockade of angiopoietin-2 or Tie2 is equally effective at inhibiting tumor growth and reducing tumor vessel density in most human tumor xenograft models. Cancer Research, 2014. 74(19_Supplement): p. 4492-4492.

245. Wang, X., et al., The role of angiopoietins as potential therapeutic targets in renal cell carcinoma. Transl Oncol, 2014. 7(2): p. 188-95.

246. Cross, M.J. and L. Claesson-Welsh, FGF and VEGF function in angiogenesis: signalling pathways, biological responses and therapeutic inhibition. Trends in Pharmacological Sciences, 2001. 22(4): p. 201-207.

247. Burgess, W.H. and T. Maciag, THE HEPARIN-BINDING (FIBROBLAST) GROWTH FACTOR FAMILY OF PROTEINS. 1989. 58(1): p. 575-602.

248. Senturk, B., et al., Inhibition of VEGF mediated corneal neovascularization by anti-angiogenic peptide nanofibers. Biomaterials, 2016. 107: p. 124-132.

249. Jin, L., et al., Dual Therapeutic Action of a Neutralizing Anti-FGF2 Aptamer in Bone Disease and Bone Cancer Pain. Molecular Therapy, 2016. 24(11): p. 1974-1986.

250. Francavilla, C., et al., Functional Proteomics Defines the Molecular Switch Underlying FGF Receptor Trafficking and Cellular Outputs. Molecular Cell, 2013. 51(6): p. 707-722.

251. Vlodavsky, I., et al., Extracellular sequestration and release of fibroblast growth factor: a regulatory mechanism? Trends in Biochemical Sciences, 1991. 16: p. 268-271.

252. Ornitz, D.M., FGFs, heparan sulfate and FGFRs: complex interactions essential for development. 2000. 22(2): p. 108-112.

253. Rapraeger, A.C., A. Krufka, and B.B. Olwin, Requirement of heparan sulfate for bFGF-mediated fibroblast growth and myoblast differentiation. Science, 1991. 252(5013): p. 1705-8.

254. Yayon, A., et al., Cell surface, heparin-like molecules are required for binding of basic fibroblast growth factor to its high affinity receptor. Cell, 1991. 64(4): p. 841-8.

255. Klagsbrun, M., The affinity of fibroblast growth factors (FGFs) for heparin; FGF-heparan sulfate interactions in cells and extracellular matrix. Current Opinion in Cell Biology, 1990. 2(5): p. 857-863.

256. Zhou, Z., et al., Impaired endochondral ossification and angiogenesis in mice deficient in membrane-type matrix metalloproteinase I. 2000. 97(8): p. 4052-4057.

257. Akl, M.R., et al., Molecular and clinical significance of fibroblast growth factor 2 (FGF2 /bFGF) in malignancies of solid and hematological cancers for personalized therapies. 2016. 7(28).

258. Roberts, P.J. and C.J. Der, Targeting the Raf-MEK-ERK mitogen-activated protein kinase cascade for the treatment of cancer. Oncogene, 2007. 26(22): p. 3291-3310.

259. Talks, K.L. and A.L. Harris, Current Status Of Antiangiogenic Factors. 2000. 109(3): p. 477-489.

260. Chung, A.S. and N. Ferrara, Developmental and Pathological Angiogenesis. Annual Review of Cell and Developmental Biology, 2011. 27(1): p. 563-584.

261. Ved, N., et al., Vascular endothelial growth factor-A(165)b ameliorates outer-retinal barrier and vascular dysfunction in the diabetic retina. Clinical science (London, England : 1979), 2017. 131(12): p. 1225-1243.

262. Institute, N.C. Angiogenesis Inhibitors. 2018 [cited 2021; Available from: https://www.cancer.gov/about-cancer/treatment/types/immunotherapy/angiogenesis-inhibitors-fact-sheet#:~:text=wet%20macular%20degeneration.-,Why%20is%20angiogenesis%20important%20in%20cancer%3F,chemical%20signals%20that%20stimulate%20angiogenesis.

263. Avraamides, C., B. Garmy-Susini, and J. Varner, Integrins in angiogenesis and lymphangiogenesis. . Nature Reviews Cancer, 2008. 8(8): p. 604-617.

264. Kamba, T. and D. McDonald, Mechanisms of adverse effects of anti-VEGF therapy for cancer. Nature: British Journal of Cancer, 2007. 96: p. 1788–1795.

265. UK, C.R. Bevacizumab (Avastin). 2019 [cited 2021; Available from: https://www.cancerresearchuk.org/about-cancer/cancer-in-general/treatment/cancer-drugs/drugs/bevacizumab.

266. Institute, N.C. When Combined with Chemotherapy, Bevacizumab Is Associated with Increased Risk of Death. 2011 [cited 2021; Available from: https://www.cancer.gov/types/colorectal/research/bevacizumab-severe-side-effects.

267. Jayson, G., et al., Antiangiogenic therapy in oncology: current status and future directions. Lancet, 2016. 388(10043): p. 518-29.

268. Seebacher, N.A., et al. Clinical development of targeted and immune based anti-cancer therapies. Journal of Experimental & Clinical Cancer Research 2019 [cited 28 156]; Available from: https://jeccr.biomedcentral.com/articles/10.1186/s13046-019-1094-2.

269. Elshabrawy, H., et al., The pathogenic role of angiogenesis in rheumatoid arthritis. Angiogenesis . , 2015. 18(4): p. 433-448.

270. Pap, T., et al., Are fibroblasts involved in joint destruction? . Annals of the rheumatic diseases, 2005. 64: p. 52-4.

271. Szekanecz, Z. and A. Koch, Vascular involvement in rheumatic diseases: 'vascular rheumatology'. . Arthritis Research and Therapy., 2008. 10(5): p. 224.

272. Veale, D. and U. Fearon, Inhibition of angiogenic pathways in rheumatoid arthritis: potential for therapeutic targeting. . Best Practical Research Clinical Rheumatology. , 2006. 20(5): p. 941-7.

273. Lu, J., et al., Vascular endothelial growth factor expression and regulation of murine collagen-induced arthritis. Journal of immunology, 2000. 164(11): p. 5922-7.

274. Wang, Y., et al., TNF- α -induced LRG1 promotes angiogenesis and mesenchymal stem cell migration in the subchondral bone during osteoarthritis. . Cell Death and Disease, 2017. 8

275. Yang, H., et al., Antrodia salmonea inhibits TNF-alpha-induced angiogenesis and atherogenesis in human endothelial cells through the

down-regulation of NF-kappaB and up-regulation of Nrf2 signaling pathways. . Journal of Ethnopharmacology 2014. 151: p. 394–406.

276. This joint statement of the American Thoracic Society (ATS), a.t.E.R.S.E.w.a.b.t.A.B.o.D., June 2001 and by the ERS Executive Committee, June 2001., American Thoracic Society/European Respiratory Society international multidisciplinary consensus classification of the idiopathic interstitial pneumonias. American Journal of Respiratory Critical Care Medicine, 2002. 165(2): p. 277–304.

277. American thoracic society (ATS), a.t.E.R.S.E., Idiopathic pulmonary fibrosis: diagnosis and treatment. American Journal Respiratory Critical Care Medicine 2000. 161(2): p. 646 –664.

278. Behr, J. and J. Ryu, Pulmonary hypertension in interstitial lung disease. . European Respiratory Journal, 2008. 31: p. 1357 –1367.

279. Farkas, L., et al., Pulmonary Hypertension and Idiopathic Pulmonary Fibrosis

A Tale of Angiogenesis, Apoptosis, and Growth Factors. American Journal of Respiratory Cell and Molecular Biology, 2010. 45(1).

280. Varone, F., et al., Nintedanib for the treatment of idiopathic pulmonary fibrosis, Expert Opinion on Pharmacotherapy. 2018. 19(2): p. 167-175.

281. Hall, S., A. Hislop, and S. Haworth, Origin, differentiation, and maturation of human pulmonary veins. . American Journal of Respiratory Cell Molecular Biology, 2002. 26 p. 333 –340.

282. Hislop, A. and L. Reid, Intra-pulmonary arterial development during fetal life-branching pattern and structure. . Journal of Anatomy . 1972. 113: p. 35 –48.

283. deMello, D., et al., Early fetal development of lung vasculature. . American Journal Respiratory Cell Molecular Biology, 1997. 16(5): p. 568 –581.

284. Farkas, L., et al., VEGF ameliorates pulmonary hypertension through inhibition of endothelial apoptosis in experimental lung fibrosis in rats. . Journal of Clinical Investigation, 2009 . 119: p. 1298 –1311.

285. Krishna, R., K. Chapman, and S. Ullah, Idiopathic Pulmonary Fibrosis. 2020: StatPearls Publishing.

286. Somogyi V, C.N., Torrisi SE, Kahn N, Müller V, Kreuter M., The therapy of idiopathic pulmonary fibrosis: what is next? European Respiratory Review, 2019. 28(153).

287. Weiner, G., When Anti-VEGF Fails in AMD Patients: 3 Treatment Approaches, in EyeNet. 2012.

288. Chakravarthy, U., B.G. Armendariz, and S. Fauser, 15 years of anti-VEGF treatment for nAMD: success or failure or something in between? Eye, 2022. 36(12): p. 2232-2233.

289. Nguyen, R.P.G.a.D., When Anti-VEGF Treatment Fails. Review of Ophthamology, 2008.

290. Fogli, S., et al., Clinical pharmacology of intravitreal anti-VEGF drugs. Eye (London, England), 2018. 32(6): p. 1010-1020.

291. Chinot, O.L., Cilengitide in glioblastoma: when did it fail? The Lancet Oncology, 2014. 15(10): p. 1044-1045.

292. Marco Tucci, S.S., Franco Silvestris, Does cilengitide deserve another chance? The Lancet Oncology, 2014. 15(13): p. E584-E585.

293. Scaringi, C., et al., Integrin Inhibitor Cilengitide for the Treatment of Glioblastoma: A Brief Overview of Current Clinical Results. Anticancer Research, 2012. 32(10): p. 4213.

294. Maurer, G.D., et al., Cilengitide modulates attachment and viability of human glioma cells, but not sensitivity to irradiation or temozolomide in vitro. Neuro Oncol, 2009. 11(6): p. 747-56.

295. Mikkelsen, T., et al., Radiation sensitization of glioblastoma by cilengitide has unanticipated schedule-dependency. Int J Cancer, 2009. 124(11): p. 2719-27.

296. Reynolds, A.R., et al., Stimulation of tumor growth and angiogenesis by low concentrations of RGD-mimetic integrin inhibitors. Nat Med, 2009. 15(4): p. 392-400.

297. Eisele, G., et al., Cilengitide treatment of newly diagnosed glioblastoma patients does not alter patterns of progression. J Neurooncol, 2014. 117(1): p. 141-5.

298. Kolte, D., J.A. McClung, and W.S. Aronow, Chapter 6 - Vasculogenesis and Angiogenesis, in Translational Research in Coronary

Artery Disease, W.S. Aronow and J.A. McClung, Editors. 2016, Academic Press: Boston. p. 49-65.

299. Patan, S., Vasculogenesis and angiogenesis. Cancer Treat Res, 2004. 117: p. 3-32.

300. SF., G., Developmental Biology. 6th edition. Endoderm. 2000.: Sunderland (MA): Sinauer Associates.

301. Nishijima, Y., et al., Chapter 19 - Vascular Remodeling After Cerebral Ischemia, in Primer on Cerebrovascular Diseases (Second Edition), L.R. Caplan, et al., Editors. 2017, Academic Press: San Diego. p. 96-101.

302. Laschke, M.W., C. Giebels, and M.D. Menger, Vasculogenesis: a new piece of the endometriosis puzzle. Hum Reprod Update, 2011. 17(5): p. 628-36.

303. Shalaby, F., et al., A requirement for Flk1 in primitive and definitive hematopoiesis and vasculogenesis. Cell, 1997. 89(6): p. 981-90.

304. Shalaby, F., et al., Failure of blood-island formation and vasculogenesis in Flk-1-deficient mice. Nature, 1995. 376(6535): p. 62-6.

305. Fong, G.H., et al., Role of the Flt-1 receptor tyrosine kinase in regulating the assembly of vascular endothelium. Nature, 1995. 376(6535): p. 66-70.

306. Tammela, T. and K. Alitalo, Lymphangiogenesis: Molecular Mechanisms and Future Promise. Cell, 2010. 140(4): p. 460-476.

307. Alitalo, K., T. Tammela, and T.V. Petrova, Lymphangiogenesis in development and human disease. Nature, 2005. 438(7070): p. 946-53.

308. Oliver, G., Lymphatic vasculature development. Nat Rev Immunol, 2004. 4(1): p. 35-45.

309. Stacker, S.A., et al., Lymphangiogenesis and lymphatic vessel remodelling in cancer. Nature Reviews Cancer, 2014. 14(3): p. 159-172.

310. Achen, M.G., et al., Vascular endothelial growth factor D (VEGF-D) is a ligand for the tyrosine kinases VEGF receptor 2 (Flk1) and VEGF receptor 3 (Flt4). Proceedings of the National Academy of Sciences of the United States of America, 1998. 95(2): p. 548-553.

311. Joukov, V., et al., A novel vascular endothelial growth factor, VEGF-C, is a ligand for the Flt4 (VEGFR-3) and KDR (VEGFR-2) receptor tyrosine kinases. Embo j, 1996. 15(2): p. 290-98.

312. Yuan, L., et al., Abnormal lymphatic vessel development in neuropilin 2 mutant mice. Development, 2002. 129(20): p. 4797-806.

313. Karpanen, T. and K. Alitalo, Molecular biology and pathology of lymphangiogenesis. Annu Rev Pathol, 2008. 3: p. 367-97.

314. Tammela, T., et al., The biology of vascular endothelial growth factors. Cardiovasc Res, 2005. 65(3): p. 550-63.

315. Tammela, T., et al., VEGFR-3 controls tip to stalk conversion at vessel fusion sites by reinforcing Notch signalling. Nature Cell Biology, 2011. 13(10): p. 1202-1213.

316. Yoshiko Kawai, K.H., Maki Kaidoh, Takashi Minami, Tatsuhiko Kodama, and Toshio Ohhashi, Heterogeneity in Immunohistochemical, Genomic, and Biological Properties of Human Lymphatic Endothelial Cells Between Initial and Collecting Lymph Vessels. Lymphatic Research and Biology, 2008. 6(1): p. 15-27.

317. Herbert, S.P. and D.Y.R. Stainier, Molecular control of endothelial cell behaviour during blood vessel morphogenesis. Nature Reviews Molecular Cell Biology, 2011. 12(9): p. 551-564.

318. Dietrich, C.P., H.B. Nader, and A.H. Straus, Structural differences of heparan sulfates according to the tissue and species of origin. Biochemical and Biophysical Research Communications, 1983. 111(3): p. 865-871.

319. Couchman, J.R., Syndecans: proteoglycan regulators of cell-surface microdomains? Nature Reviews Molecular Cell Biology, 2003. 4(12): p. 926-938.

320. De Rossi, G., A Study On The Roles And Effects Of Syndecans On Endothelial Cell Biology During Angiogenesis, in Centre for Microvascular Research. 2015, Queen May University of London.

321. Dews, I.C. and K.R. Mackenzie, Transmembrane domains of the syndecan family of growth factor coreceptors display a hierarchy of homotypic and heterotypic interactions. Proc Natl Acad Sci U S A, 2007. 104(52): p. 20782-7.

322. Alexopoulou, A.N., H.A. Multhaupt, and J.R. Couchman, Syndecans in wound healing, inflammation and vascular biology. Int J Biochem Cell Biol, 2007. 39(3): p. 505-28.

323. Tkachenko, E., J.M. Rhodes, and M. Simons, Syndecans: new kids on the signaling block. Circ Res, 2005. 96(5): p. 488-500.

324. Choi, S., et al., Transmembrane domain-induced oligomerization is crucial for the functions of syndecan-2 and syndecan-4. J Biol Chem, 2005. 280(52): p. 42573-9.

325. Barrett, P.J., et al., The amyloid precursor protein has a flexible transmembrane domain and binds cholesterol. Science, 2012. 336(6085): p. 1168-71.

326. Gopal, S., et al., Syndecan receptors: pericellular regulators in development and inflammatory disease. Open biology, 2021. 11(2): p. 200377-200377.

327. Aradska, J., et al., Gel-free mass spectrometry analysis of Drosophila melanogaster heads. 2015. 15(19): p. 3356-3360.

328. Ethell, I.M., et al., Synbindin, A novel syndecan-2-binding protein in neuronal dendritic spines. J Cell Biol, 2000. 151(1): p. 53-68.

329. Gao, Y., et al., Synectin, syndecan-4 cytoplasmic domain binding PDZ protein, inhibits cell migration. J Cell Physiol, 2000. 184(3): p. 373-9.

330. Grootjans, J.J., et al., Syntenin, a PDZ protein that binds syndecan cytoplasmic domains. Proc Natl Acad Sci U S A, 1997. 94(25): p. 13683-8.

331. Beauvais, D.M. and A.C. Rapraeger, Syndecans in tumor cell adhesion and signaling. Reprod Biol Endocrinol, 2004. 2: p. 3.

332. Chakravarti, R. and J.C. Adams, Comparative genomics of the syndecans defines an ancestral genomic context associated with matrilins in vertebrates. BMC Genomics, 2006. 7(1): p. 83.

333. Afratis, N.A., et al., Syndecans – key regulators of cell signaling and biological functions. 2017. 284(1): p. 27-41.

334. Corti, F., et al., N-terminal syndecan-2 domain selectively enhances 6-O heparan sulfate chains sulfation and promotes VEGFA165-dependent neovascularization. Nature Communications, 2019. 10(1): p. 1562.

335. Marilyn L. Fitzgerald , Z.W., Pyong Woo Park , Gillian Murphy and Merton Bernfield, Shedding of Syndecan-1 and -4 Ectodomains Is

Regulated by Multiple Signaling Pathways and Mediated by a Timp-3–Sensitive Metalloproteinase. J Cell Biol . 2000: p. 148(4): 811–824.

336. Regulated Shedding of Syndecan-1 and -4 Ectodomains by Thrombin and Growth Factor Receptor Activation. The Journal of Biological Chemistry, 1997.

337. Samantha Arokiasamy , M.J.M.B., Giulia De Rossi , and James R. Whiteford, Syndecan-3 in Inflammation and Angiogenesis. Front Immunol . 2020.

338. Tina Manon-Jensen , Y.I.a.J.R.C., Proteoglycans in health and disease: the multiple roles of

syndecan shedding. FEBS Journal, 2010(277): p. 3878-3822.

339. Park PW , F.T., Nishi E , Duncan SJ , Klagsbrun M & Chen Y, Activation of syndecan-1 ectodomain shedding by Staphylococcus aureus alpha-toxin and beta-toxin . . J Biol Chem, 2004. 279: p. 251 – 258 .

340. Beauvais, D.M. and A.C. Rapraeger, Syndecan-1-mediated cell spreading requires signaling by alphavbeta3 integrins in human breast carcinoma cells. Exp Cell Res, 2003. 286(2): p. 219-32.

341. McQuade, K.J., et al., Syndecan-1 regulates alphavbeta5 integrin activity in B82L fibroblasts. J Cell Sci, 2006. 119(Pt 12): p. 2445-56.

342. Beauvais, D.M., B.J. Burbach, and A.C. Rapraeger, The syndecan-1 ectodomain regulates alphavbeta3 integrin activity in human mammary carcinoma cells. J Cell Biol, 2004. 167(1): p. 171-81.

343. Beauvais, D.M., et al., Syndecan-1 regulates αvβ3 and αvβ5 integrin activation during angiogenesis and is blocked by synstatin, a novel peptide inhibitor. Journal of Experimental Medicine, 2009. 206(3): p. 691-705.

344. Beauvais, D.M. and A.C. Rapraeger, Syndecan-1 couples the insulin-like growth factor-1 receptor to inside-out integrin activation. Journal of Cell Science, 2010. 123(21): p. 3796-3807.

345. Rapraeger, A.C., Synstatin: a selective inhibitor of the syndecan-1-coupled IGF1R–αvβ3 integrin complex in tumorigenesis and angiogenesis. 2013. 280(10): p. 2207-2215.

346. Chen, E., S. Hermanson, and S.C. Ekker, Syndecan-2 is essential for angiogenic sprouting during zebrafish development. Blood, 2004. 103(5): p. 1710-1719.

347. De Rossi, G., et al., Shed syndecan-2 inhibits angiogenesis. J Cell Sci . 2014. 127: p. 4788-4799.

348. Fears, C.Y., C.L. Gladson, and A. Woods, Syndecan-2 is expressed in the microvasculature of gliomas and regulates angiogenic processes in microvascular endothelial cells. J Biol Chem, 2006. 281(21): p. 14533-6.

349. Noguer, O., et al., Syndecan-2 downregulation impairs angiogenesis in human microvascular endothelial cells. Exp Cell Res, 2009. 315(5): p. 795-808.

350. Kehoe, O., et al., Syndecan-3 is selectively pro-inflammatory in the joint and contributes to antigen-induced arthritis in mice. Arthritis Research & Therapy, 2014. 16(4): p. R148.

351. De Rossi, G. and J. Whiteford, A novel role for syndecan-3 in angiogenesis [version 1; peer review: 3 approved]. 2013. 2(270).

352. Echtermeyer, F., et al., Delayed wound repair and impaired angiogenesis in mice lacking syndecan-4. The Journal of Clinical Investigation, 2001. 107(2): p. R9-R14.

353. Nunes, S.S., et al., Syndecan-4 contributes to endothelial tubulogenesis through interactions with two motifs inside the pro-angiogenic N-terminal domain of thrombospondin-1. J Cell Physiol, 2008. 214(3): p. 828-37.

354. Corti, F., et al., The syndecan-4/protein kinase Cα pathway mediates prostaglandin E2-induced extracellular regulated kinase (ERK) activation in endothelial cells and angiogenesis in vivo. J Biol Chem, 2013. 288(18): p. 12712-21.

355. Murakami, M., et al., Protein kinase C (PKC) delta regulates PKCalpha activity in a Syndecan-4-dependent manner. J Biol Chem, 2002. 277(23): p. 20367-71.

356. Volk, R., et al., The role of syndecan cytoplasmic domain in basic fibroblast growth factor-dependent signal transduction. J Biol Chem, 1999. 274(34): p. 24417-24.

357. Tkachenko, E., et al., Syndecan-4 Clustering Induces Cell Migration in a PDZ-Dependent Manner. 2006. 98(11): p. 1398-1404.

358. Tkachenko, E., et al., Fibroblast growth factor 2 endocytosis in endothelial cells proceed via syndecan-4-dependent activation of Rac1 and a Cdc42-dependent macropinocytic pathway. J Cell Sci, 2004. 117(Pt 15): p. 3189-99.

359. Murakami, M., et al., The FGF system has a key role in regulating vascular integrity. The Journal of Clinical Investigation, 2008. 118(10): p. 3355-3366.

360. Hunter, T., A thousand and one protein kinases. Cell, 1987. 50(6): p. 823-829.

361. Andersen, J.N., et al., Structural and Evolutionary Relationships among Protein Tyrosine Phosphatase Domains. 2001. 21(21): p. 7117-7136.

362. Alonso, A., et al., Protein Tyrosine Phosphatases in the Human Genome. Cell, 2004. 117(6): p. 699-711.

363. Senis, Y.A. and A.J. Barr, Targeting Receptor-Type Protein Tyrosine Phosphatases with Biotherapeutics: Is Outside-in Better than Inside-Out? 2018. 23(3): p. 569.

364. Xu, Y. and G.J. Fisher, Receptor type protein tyrosine phosphatases (RPTPs) - roles in signal transduction and human disease. J Cell Commun Signal, 2012. 6(3): p. 125-38.

365. Johnson, K. and D. Vactor, Receptor Protein Tyrosine Phosphatases in Nervous System Development. Physiological reviews, 2003. 83: p. 1-24.

366. Ostman , A., Q. Yang , and N. Tonks, Expression of DEP-1, a receptor-like protein-tyrosine-phosphatase, is enhanced with increasing cell density. Proceedings of the National Academy of Sciences 1994. 91 ((21)): p. 9680-9684.

367. Whiteford, J.R., et al., Syndecan-2 is a novel ligand for the protein tyrosine phosphatase receptor CD148. Molecular biology of the cell, 2011. 22(19): p. 3609-3624.

368. Grazia Lampugnani, M., et al., Contact inhibition of VEGF-induced proliferation requires vascular endothelial cadherin, beta-catenin, and the phosphatase DEP-1/CD148. J Cell Biol, 2003. 161(4): p. 793-804.

369. Takahashi, T., et al., A mutant receptor tyrosine phosphatase, CD148, causes defects in vascular development. Mol Cell Biol, 2003. 23(5): p. 1817-31.

370. Iuliano, R., et al., The Eighth Fibronectin Type III Domain of Protein Tyrosine Phosphatase Receptor J Influences the Formation of Protein Complexes and Cell Localization. The Journal of Biochemistry, 2009. 145(3): p. 377-385.

371. Takahashi, T., et al., A monoclonal antibody against CD148, a receptor-like tyrosine phosphatase, inhibits endothelial-cell growth and angiogenesis. Blood, 2006. 108(4): p. 1234-42.

372. Iuliano, R., et al., The tyrosine phosphatase PTPRJ/DEP-1 genotype affects thyroid carcinogenesis. Oncogene, 2004. 23(52): p. 8432-8438.

373. Balavenkatraman, K.K., et al., DEP-1 protein tyrosine phosphatase inhibits proliferation and migration of colon carcinoma cells and is upregulated by protective nutrients. Oncogene, 2006. 25(47): p. 6319-6324.

374. Keane, M.M., et al., The protein tyrosine phosphatase DEP-1 is induced during differentiation and inhibits growth of breast cancer cells. Cancer Res, 1996. 56(18): p. 4236-43.

375. Zhang, L., et al., Thyroid Cell Transformation Inhibits the Expression of a Novel Rat Protein Tyrosine Phosphatase. Experimental Cell Research, 1997. 235(1): p. 62-70.

376. Kovalenko, M., et al., Site-selective dephosphorylation of the platelet-derived growth factor beta-receptor by the receptor-like protein-tyrosine phosphatase DEP-1. J Biol Chem, 2000. 275(21): p. 16219-26.

377. Pera, I.L., et al., The rat tyrosine phosphatase eta increases cell adhesion by activating c-Src through dephosphorylation of its inhibitory phosphotyrosine residue. Oncogene, 2005. 24(19): p. 3187-95.

378. Lampugnani, M.G., et al., Vascular endothelial cadherin controls VEGFR-2 internalization and signaling from intracellular compartments. J Cell Biol, 2006. 174(4): p. 593-604.

379. Tsuboi, N., et al., The tyrosine phosphatase CD148 interacts with the p85 regulatory subunit of phosphoinositide 3-kinase. Biochem J, 2008. 413(1): p. 193-200.

380. Bilotta, A., et al., A novel splice variant of the protein tyrosine phosphatase PTPRJ that encodes for a soluble protein involved in angiogenesis. Oncotarget, 2017. 8(6): p. 10091-10102.

381. Katso, R., et al., Cellular function of phosphoinositide 3-kinases: implications for development, homeostasis, and cancer. Annu Rev Cell Dev Biol, 2001. 17: p. 615-75.

382. Bart Vanhaesebroeck, et al., Synthesis and Function of 3-Phosphorylated Inositol Lipids. 2001. 70(1): p. 535-602.

383. Wu, H., Y. Yan, and J.M. Backer, Regulation of class IA PI3Ks. Biochemical Society Transactions, 2007. 35(2): p. 242-244.

384. Roymans, D. and H. Slegers, Phosphatidylinositol 3-kinases in tumor progression. 2001. 268(3): p. 487-498.

385. Tolias, K.F., L.C. Cantley, and C.L. Carpenter, Rho Family GTPases Bind to Phosphoinositide Kinases (∗). Journal of Biological Chemistry, 1995. 270(30): p. 17656-17659.

386. Cantley, L.C., et al., Oncogenes and signal transduction. Cell, 1991. 64(2): p. 281-302.

387. Gout, I., et al., The GTPase dynamin binds to and is activated by a subset of SH3 domains. Cell, 1993. 75(1): p. 25-36.

388. Maru, Y. and O.N. Witte, The BCR gene encodes a novel serine/threonine kinase activity within a single exon. Cell, 1991. 67(3): p. 459-468.

389. Zhou, S., et al., SH2 domains recognize specific phosphopeptide sequences. Cell, 1993. 72(5): p. 767-778.

390. Cuevas, B.D., et al., Tyrosine Phosphorylation of p85 Relieves Its Inhibitory Activity on Phosphatidylinositol 3-Kinase*. Journal of Biological Chemistry, 2001. 276(29): p. 27455-27461.

391. Galante, L.L. and J.E. Schwarzbauer, Requirements for sulfate transport and the diastrophic dysplasia sulfate transporter in fibronectin matrix assembly. The Journal of Cell Biology, 2007. 179(5): p. 999.

392. Klass, C.M., J.R. Couchman, and A. Woods, Control of extracellular matrix assembly by syndecan-2 proteoglycan. Journal of Cell Science, 2000. 113(3): p. 493.

393. Noguer, O., et al., Syndecan-2 downregulation impairs angiogenesis in human microvascular endothelial cells. Experimental Cell Research, 2009. 315(5): p. 795-808.

394. Chung CT, Niemela SL, and M. RH, One-step preparation of competent Escherichia coli: Transformation

and storage of bacterial cells in the same solution. Proc Natl Acad Sci U S A, 1989. 86(7): p. 2172-2175.

395. UK, L., Cleavage of structural proteins during the assembly of the head of bacteriophage T4. Nature, 1970. 227(5259): p. 680-685.

396. Nicosia, R.F. and A. Ottinetti, Growth of microvessels in serum-free matrix culture of rat aorta. A quantitative assay of angiogenesis in vitro. Lab Invest, 1990. 63(1): p. 115-22.

397. De Rossi, G. and J.R. Whiteford, Novel insight into the biological functions of syndecan ectodomain core proteins. Biofactors, 2013. 39(4): p. 374-82.

398. William J Spruill, W.E.W., Joseph T DiPiro, Robert A Blouin, Jane M Pruemer, Concepts in Clinical Pharmacokinetics, 6th Edition. 2014: ASHP.

399. Kim, C.W., et al., Members of the syndecan family of heparan sulfate proteoglycans are expressed in distinct cell-, tissue-, and development-specific patterns. Mol Biol Cell, 1994. 5(7): p. 797-805.

400. Sallee, J.L., E.S. Wittchen, and K. Burridge, Regulation of Cell Adhesion by Protein-tyrosine Phosphatases: II. CELL-CELL ADHESION**This minireview will be reprinted in the 2006 Minireview Compendium, which will be available in January, 2007. This work was supported in part by National Institutes of Health Grants GM29860 and HL45100. This is Paper II in the series “Regulation of Cell Adhesion by Protein-tyrosine Phosphatases.” Ref. 2 is Paper I in this series. Journal of Biological Chemistry, 2006. 281(24): p. 16189-16192.

401. Whiteford, J.R. and J.R. Couchman, A conserved NXIP motif is required for cell adhesion properties of the syndecan-4 ectodomain. J Biol Chem, 2006. 281(43): p. 32156-63.

402. Imoto, M., et al., Dephostatin, a novel protein tyrosine phosphatase inhibitor produced by Streptomyces. I. Taxonomy, isolation, and characterization. J Antibiot (Tokyo), 1993. 46(9): p. 1342-6.

403. Vepa, S., W.M. Scribner, and V. Natarajan, Activation of protein phosphorylation by oxidants in vascular endothelial cells: identification of

tyrosine phosphorylation of caveolin. Free Radic Biol Med, 1997. 22(1-2): p. 25-35.

404. Jiang, H., et al., Selective N-terminal modification of peptides and proteins: Recent progresses and applications. Chinese Chemical Letters, 2022. 33(1): p. 80-88.

405. Bio, P., Step-by-Step Methods for N-terminal Bioconjugation of Proteins. 2021.

406. Palka, H.L., M. Park, and N.K. Tonks, Hepatocyte growth factor receptor tyrosine kinase met is a substrate of the receptor protein-tyrosine phosphatase DEP-1. J Biol Chem, 2003. 278(8): p. 5728-35.

407. Berset, T.A., E.F. Hoier, and A. Hajnal, The C. elegans homolog of the mammalian tumor suppressor Dep-1/Scc1 inhibits EGFR signaling to regulate binary cell fate decisions. Genes Dev, 2005. 19(11): p. 1328-40.

408. Massa, A., et al., The expression of the phosphotyrosine phosphatase DEP-1/PTPeta dictates the responsivity of glioma cells to somatostatin inhibition of cell proliferation. J Biol Chem, 2004. 279(28): p. 29004-12.

409. Takahashi, K., et al., Thrombospondin-1 acts as a ligand for CD148 tyrosine phosphatase. Proc Natl Acad Sci U S A, 2012. 109(6): p. 1985-90.

410. Honda, H., et al., Molecular cloning, characterization, and chromosomal localization of a novel protein-tyrosine phosphatase, HPTP eta. Blood, 1994. 84(12): p. 4186-94.

411. Tsoyi, K., et al., CD148 Deficiency in Fibroblasts Promotes the Development of Pulmonary Fibrosis. Am J Respir Crit Care Med, 2021. 204(3): p. 312-325.

412. Modrek, B. and C. Lee, A genomic view of alternative splicing. Nat Genet, 2002. 30(1): p. 13-9.

413. Soller, M., Pre-messenger RNA processing and its regulation: a genomic perspective. Cell Mol Life Sci, 2006. 63(7-8): p. 796-819.

414. Sakurai, T., D.R. Friedlander, and M. Grumet, Expression of polypeptide variants of receptor-type protein tyrosine phosphatase beta: the secreted form, phosphacan, increases dramatically during embryonic development and modulates glial cell behavior in vitro. J Neurosci Res, 1996. 43(6): p. 694-706.

415. Ostman, A., C. Hellberg, and F.D. Böhmer, Protein-tyrosine phosphatases and cancer. Nat Rev Cancer, 2006. 6(4): p. 307-20.

416. Chaudhry, I.H., et al., Vascular endothelial growth factor expression correlates with tumour grade and vascularity in gliomas. Histopathology, 2001. 39(4): p. 409-15.

417. Jain, R.K., et al., Angiogenesis in brain tumours. Nat Rev Neurosci, 2007. 8(8): p. 610-22.

418. Das, S. and P.A. Marsden, Angiogenesis in glioblastoma. N Engl J Med, 2013. 369(16): p. 1561-3.

419. Dieterich, L.C., et al., Transcriptional profiling of human glioblastoma vessels indicates a key role of VEGF-A and TGFβ2 in vascular abnormalization. J Pathol, 2012. 228(3): p. 378-90.

420. Lund, E.L., et al., Differential regulation of VEGF, HIF1alpha and angiopoietin-1, -2 and -4 by hypoxia and ionizing radiation in human glioblastoma. Int J Cancer, 2004. 108(6): p. 833-8.

421. Jonkman, J.E., et al., An introduction to the wound healing assay using live-cell microscopy. Cell Adh Migr, 2014. 8(5): p. 440-51.

422. Korff, T. and H.G. Augustin, Tensional forces in fibrillar extracellular matrices control directional capillary sprouting. J Cell Sci, 1999. 112 (Pt 19): p. 3249-58.

423. Nowak-Sliwinska, P., et al., Consensus guidelines for the use and interpretation of angiogenesis assays. Angiogenesis, 2018. 21(3): p. 425-532.

424. Seeger; Peter Wiedemann, R.S.T.Y.J.K.W.E.A.N.I.I.M.O.A.K.Y.Y.A.B.A.T.Y.O.J., Three-Dimensional Spheroidal Culture Visualization of Membranogenesis of Bruch's Membrane and Basolateral Functions of the Retinal Pigment Epithelium. Retinal Cell Biology, 2013. 54(3).

425. Tetzlaff, F. and A. Fischer, Human Endothelial Cell Spheroid-based Sprouting Angiogenesis Assay in Collagen. Bio-protocol, 2018. 8(17): p. e2995.

426. Grossniklaus, H.E., S.J. Kang, and L. Berglin, Animal models of choroidal and retinal neovascularization. Prog Retin Eye Res, 2010. 29(6): p. 500-19.

427. Scott, A. and M. Fruttiger, Oxygen-induced retinopathy: a model for vascular pathology in the retina. Eye, 2010. 24(3): p. 416-421.

428. Corti, F., et al., Syndecan-2 selectively regulates VEGF-induced vascular permeability. Nature Cardiovascular Research, 2022. 1(5): p. 518-528.

429. Chabot, C., et al., New role for the protein tyrosine phosphatase DEP-1 in Akt activation and endothelial cell survival. Mol Cell Biol, 2009. 29(1): p. 241-53.

430. Koolwijk, P., et al., Involvement of VEGFR-2 (kdr/flk-1) but not VEGFR-1 (flt-1) in VEGF-A and VEGF-C-induced tube formation by human microvascular endothelial cells in fibrin matrices in vitro. Angiogenesis, 2001. 4(1): p. 53-60.

431. Leader, B., Q.J. Baca, and D.E. Golan, Protein therapeutics: a summary and pharmacological classification. Nature Reviews Drug Discovery, 2008. 7(1): p. 21-39.

432. Ryman, J.T. and B. Meibohm, Pharmacokinetics of Monoclonal Antibodies. 2017. 6(9): p. 576-588.

433. Reichert, J.M., et al., Monoclonal antibody successes in the clinic. Nature Biotechnology, 2005. 23(9): p. 1073-1078.

434. Trier, N., P. Hansen, and G. Houen, Peptides, Antibodies, Peptide Antibodies and More. Int J Mol Sci, 2019. 20(24).

435. Ltd, F.H.-L.R. Ten remarkable facts about making antibody medicines. 2022 [cited 2022; Available from: https://www.roche.com/stories/antibodies-in-manufacturing-production.

436. Hayashi, M.A., F. Ducancel, and K. Konno, Natural Peptides with Potential Applications in Drug Development, Diagnosis, and/or Biotechnology. Int J Pept, 2012. 2012: p. 757838.

437. Marqus, S., E. Pirogova, and T.J. Piva, Evaluation of the use of therapeutic peptides for cancer treatment. Journal of Biomedical Science, 2017. 24(1): p. 21.

438. Bidwell, G.L., 3rd and D. Raucher, Therapeutic peptides for cancer therapy. Part I - peptide inhibitors of signal transduction cascades. Expert Opin Drug Deliv, 2009. 6(10): p. 1033-47.

439. Draeger, L.J. and G.P. Mullen, Interaction of the bHLH-zip domain of c-Myc with H1-type peptides. Characterization of helicity in the H1 peptides by NMR. J Biol Chem, 1994. 269(3): p. 1785-93.

440. Wang, L., et al., Therapeutic peptides: current applications and future directions. Signal Transduction and Targeted Therapy, 2022. 7(1): p. 48.

441. Fisher, E., et al., Peptide-Based Therapeutics for Oncology. Pharmaceutical Medicine, 2019. 33(1): p. 9-20.

442. Iyengar, S., M.H. Ossipov, and K.W. Johnson, The role of calcitonin gene–related peptide in peripheral and central pain mechanisms including migraine. 2017. 158(4): p. 543-559.

443. Sloan, L.A., Review of glucagon-like peptide-1 receptor agonists for the treatment of type 2 diabetes mellitus in patients with chronic kidney disease and their renal effects. 2019. 11(12): p. 938-948.

444. Boohaker, R.J., et al., The use of therapeutic peptides to target and to kill cancer cells. Curr Med Chem, 2012. 19(22): p. 3794-804.

445. Ali, R., R. Rani, and S.J.A.i.p.c.J.O.G.e. Kumar, New peptide based therapeutic approaches. 2013.

446. McGregor, D.P., Discovering and improving novel peptide therapeutics. Curr Opin Pharmacol, 2008. 8(5): p. 616-9.

447. Bhat, A., L.R. Roberts, and J.J. Dwyer, Lead discovery and optimization strategies for peptide macrocycles. European Journal of Medicinal Chemistry, 2015. 94: p. 471-479.

448. Vinogradov, A.A., Y. Yin, and H. Suga, Macrocyclic Peptides as Drug Candidates: Recent Progress and Remaining Challenges. Journal of the American Chemical Society, 2019. 141(10): p. 4167-4181.

449. Di, L., Strategic Approaches to Optimizing Peptide ADME Properties. The AAPS Journal, 2015. 17(1): p. 134-143.

450. Werner, H.M., C.C. Cabalteja, and W.S. Horne, Peptide Backbone Composition and Protease Susceptibility: Impact of Modification Type, Position, and Tandem Substitution. 2016. 17(8): p. 712-718.

451. Wei, X., et al., Retro-Inverso Isomer of Angiopep-2: A Stable d-Peptide Ligand Inspires Brain-Targeted Drug Delivery. Molecular Pharmaceutics, 2014. 11(10): p. 3261-3268.

452. Chatterjee, J., F. Rechenmacher, and H. Kessler, N-Methylation of Peptides and Proteins: An Important Element for Modulating Biological Functions. 2013. 52(1): p. 254-269.

453. Cheloha, R.W., et al., Backbone Modification of a Parathyroid Hormone Receptor-1 Antagonist/Inverse Agonist. ACS Chemical Biology, 2016. 11(10): p. 2752-2762.

454. Liskamp, R.M.J., et al., Peptides and Proteins as a Continuing Exciting Source of Inspiration for Peptidomimetics. 2011. 12(11): p. 1626-1653.

455. Schneider, J.A., et al., Design of Peptoid-peptide Macrocycles to Inhibit the β-catenin TCF Interaction in Prostate Cancer. Nature Communications, 2018. 9(1): p. 4396.

456. Olsen, C.A., et al., Macrocyclic Peptoid–Peptide Hybrids as Inhibitors of Class I Histone Deacetylases. ACS Medicinal Chemistry Letters, 2012. 3(9): p. 749-753.

457. Reizes, O., et al., Transgenic Expression of Syndecan-1 Uncovers a Physiological Control of Feeding Behavior by Syndecan-3. Cell, 2001. 106(1): p. 105-116.

458. Krempel, P.G., et al., Bevacizumab Reduces Neurocan Content and Gene Expression in Newborn Rat Retina In Vitro. Investigative Ophthalmology & Visual Science, 2014. 55(8): p. 5109-5115.

459. Vuong, T.T., et al., Syndecan-4 Is a Major Syndecan in Primary Human Endothelial Cells In Vitro, Modulated by Inflammatory Stimuli and Involved in Wound Healing. 2015. 63(4): p. 280-292.

460. Tinholt, M., et al., Syndecan-3 and TFPI Colocalize on the Surface of Endothelial-, Smooth Muscle-, and Cancer Cells. PLOS ONE, 2015. 10(1): p. e0117404.

461. Asundi, V.K., et al., Matrix metalloproteinase-dependent shedding of syndecan-3, a transmembrane heparan sulfate proteoglycan, in Schwann cells. 2003. 73(5): p. 593-602.

462. Ecker, D.M., S.D. Jones, and H.L. Levine, The therapeutic monoclonal antibody market. mAbs, 2015. 7(1): p. 9-14.

463. Tarcic, G., et al., An Unbiased Screen Identifies DEP-1 Tumor Suppressor as a Phosphatase Controlling EGFR Endocytosis. Current Biology, 2009. 19(21): p. 1788-1798.

464. Tangye, S.G., et al., CD148: a receptor-type protein tyrosine phosphatase involved in the regulation of human T cell activation. J Immunol, 1998. 161(7): p. 3249-55.

465. Dave, R.K., et al., Differential expression of CD148 on leukocyte subsets in inflammatory arthritis. Arthritis Research & Therapy, 2013. 15(5): p. R108.

466. Dave, R.K., et al., CD148/DEP-1 association with areas of cytoskeletal organisation in macrophages. Experimental Cell Research, 2009. 315(10): p. 1734-1744.

467. Bazan, J., I. Całkosiński, and A. Gamian, Phage display--a powerful technique for immunotherapy: 1. Introduction and potential of therapeutic applications. Hum Vaccin Immunother, 2012. 8(12): p. 1817-28.

468. Kaplan, G. and J.M. Gershoni, A general insert label for peptide display on chimeric filamentous bacteriophages. Anal Biochem, 2012. 420(1): p. 68-72.

Appendices

Included below are the published manuscripts completed during my PhD.

frontiers in Immunology

REVIEW
published: 09 January 2020
doi: 10.3389/fimmu.2019.03031

Syndecan-3 in Inflammation and Angiogenesis

Samantha Arokiasamy[1], *Michaela J. M. Balderstone*[1], *Giulia De Rossi*[2] *and James R. Whiteford*[1]*

[1] Barts and the London School of Medicine and Dentistry, William Harvey Research Institute, Queen Mary University of London, London, United Kingdom, [2] Department of Cell Biology, UCL Institute of Ophthalmology, London, United Kingdom

Syndecans are a four member multifunctional family of cell surface molecules with diverse biological roles. Syndecan-3 (SDC3) is the largest of these, but in comparison to the other family members relatively little is known about this molecule. SDC3 null mice grow and develop normally, all be it with subtle anatomical phenotypes in the brain. Roles for this molecule in both neuronal and brain tissue have been identified, and is associated with altered satiety responses. Recent studies suggest that SDC3 expression is not restricted to neuronal tissues and has important roles in inflammatory disorders such as rheumatoid arthritis, disease associated processes such as angiogenesis and in the facilitation of infection of dendritic cells by HIV. The purpose of this review article is to explore these new biological insights into SDC3 functions in inflammatory disease.

Keywords: heparan sulfate, syndecan, HIV, rheumatoid arthritis, angiogenesis

OPEN ACCESS

Edited by:
Rogier M. Reijmers, Leiden University Medical Center, Netherlands

Reviewed by:
Mark Morgan, University of Liverpool, United Kingdom
Jessica Bertrand, University Hospital Magdeburg, Germany

***Correspondence:**
James R. Whiteford
j.whiteford@qmul.ac.uk

Specialty section:
This article was submitted to Inflammation, a section of the journal Frontiers in Immunology

Received: *10 October 2019*
Accepted: *10 December 2019*
Published: *09 January 2020*

Citation:
Arokiasamy S, Balderstone MJM, De Rossi G and Whiteford JR (2020) Syndecan-3 in Inflammation and Angiogenesis. Front. Immunol. 10:3031. doi: 10.3389/fimmu.2019.03031

INTRODUCTION

The proteoglycans are a diverse family of molecules with multiple roles in development, health and disease (1). Heparan Sulfate Proteoglycans (HSPGs) form a subset of these, and these can be secreted extracellular matrix molecules or membrane associated (1). The principal families of membrane associated HSPGs are the glypicans and syndecans. Glypicans are distinguished from syndecans by the fact they are tethered to the cell membrane via glycosylphosphatidylinositol anchors. Syndecans (SDC) are a four member family of type 1 transmembrane proteins consisting of two related sub-families based on sequence homology. SDC2 and 4 form one family and SDC1 and 3 form the other. All syndecans have a short highly conserved cytoplasmic domain, a single transmembrane domain, and a larger extracellular core protein. Syndecan ectodomains are far less conserved between family members or species. However, they do possess Ser-Gly GAG attachment motifs usually surrounded by acidic amino acid residues. Every cell type expresses at least one syndecan, and roles in cell adhesion, migration, growth factor signaling, receptor trafficking and ion channel modulation have been identified [for reviews see (1–5)]. Of the four family members, perhaps the least well-understood is Syndecan-3 (SDC3). Predominantly, reported roles for this molecule have been exclusively related to the brain and nervous system, but recent studies are revealing roles for SDC3 in other important biological processes such as inflammation and angiogenesis. This review aims to explore this work and provide novel insight into the biology of SDC3.

SYNDECAN-3 MOLECULAR ARCHITECTURE

The syndecan-3 (N-syndecan) gene was first cloned from rat Schwann cells and was the third syndecan of the four member family to be identified (6, 7). It bears significant homology to syndecan-1, although unlike syndecan-1, it has a homolog in fish (8). Of the four family members, syndecan-3 (SDC3) is the largest, consisting of 442 amino acids in humans. In mammals, the SDC3 ectodomain contains seven potential glycosaminoglycan (GAG) attachment sites. Four are situated toward the N-terminus and the remaining three reside closer to the transmembrane domain (**Figure 1A**). The type and extent of GAG substitution on syndecan-3 is likely to be cell type and tissue dependent. Experiments using heparan sulfate (HS) and chondroitin sulfate (CS) degrading enzymes would suggest that SDC3 (at least when purified from brain tissue) possesses both HS and CS chains (9).

HS chains consist of repeated disaccharide units consisting of glucuronic acid and N-acetylglucosamine and chain lengths can range from 50 to 200 disaccharides. It is synthesized via a stepwise series of enzymatic reactions involving multiple transferases; briefly N-acetyglucosamine within a chain can undergo N-sulphation followed by the epimerisation of some glucuronic acids, this is followed by the sequential addition of first 2-O, 6-O, and 3-O sulfate groups. The complexity of this process means that HS chains are heterogenous in terms of sulphation and there is considerable evidence of HS chains having domains of high, intermediate and low sulphation [for review see (10), **Figure 1B**. CS is structurally distinct to HS on the basis that it is comprised of repeating disaccharide units consisting of glucuronic acid and n-acetylgalactosamine (**Figure 1B**). CS chains can also be sulphated although the extent and heterogeneity of this is not as great as HS. The majority of reported interactions between SDC3 and biologically active molecules are with its HS chains, and far less is understood as to the role or function of SDC3 CS chains. The extracellular core protein also possesses a domain rich in threonine and proline residues, which is characteristic of mucin-like proteins, and are potential sites for *O*-linked glycosylation (6).

Syndecan shedding is a regulated process whereby some or all of the extracellular domain of the molecule is cleaved from the cell surface by the action of matrix-metalloproteases (MMPs). Shed SDC3 has been observed in conditioned media in a variety of experimental systems, although the precise cleavage sites and proteases have yet to be confirmed (11). Predictive algorithms would suggest roles for MMP2, 9, and 14 at multiple cleavage sites but these have not been validated experimentally (3). SDC3, along with the other family members, form SDS insoluble dimers and this self-association is mediated both by residues in the transmembrane domain, and a membrane proximal ERKE motif (12).

The syndecan-3 cytoplasmic domain consists of 33 aa and in common with the rest of the family possesses two conserved domains (C1 and C2) flanking a variable sequence (V region), which is unique to each family member (**Figure 1C**). Syndecans all have the capability of interaction with PDZ proteins possessing a conserved EFYA motif at the C-terminus of the C2 region. Interactions between SDC3 and PDZ proteins such as syntenin, CASK, TIAM1, synectin, and synbindin have been reported. The SY sequence (Ser^{418}, Tyr^{419} in human SDC3, **Figure 1C**) in the C1 region of SDC3 is common to all syndecans. Studies with SDC4 have shown that phosphorylation of either residue is important for its functionality. Syndecans have proven remarkably recalcitrant to structural analysis, none more so than SDC3, for which there are no structural records in the databases (2). However, structural analysis of peptides corresponding to the syndecan-4 cytoplasmic domain in which this serine residue is phosphorylated show that this alters the conformation of this molecule considerably, and expression of phospho-mimetic mutants of this residue leads to enhanced cell migration (13). In other work, the Y (Tyr^{180} in human SDC4) was identified as a substrate for Src kinase and this has implications for the trafficking of integrins. It would not be surprising if phosphorylation of these conserved residues impacted on SDC3 functionality in a similar fashion (14). Additionally, *in vitro* studies have indicated that the other 2 tyrosines could potentially be phosphorylated, however no functional role for this has been demonstrated (15). The V region of SDC3 also bears similarities to other syndecans in that there are 2 lysine residues (Lys^{425} and Lys^{433}). Studies with syndecan-4 have shown the importance of these lysines for binding phospho-inositides (PIP3) and this not only stabilizes the structure of SDC4 cytoplasmic domain but this interaction is also associated with upregulating the activity of PKCα which promotes many of the downstream cell adhesion pathways associated with SDC4 (16, 17). It is therefore also conceivable that the interactions with the SDC3 V region and phospho-inositides could be important for SDC3 functionality.

SYNDECAN-3 IN THE BRAIN AND NERVOUS TISSUE

The association with SDC3 and cells of a neuronal lineage is well-established and a number of phenotypes associated with both the brain and nervous tissue have been identified (18, 19). Although no gross abnormalities are observed in the developing mouse brain, stereological analysis of sections revealed differences in the cellular density of key areas. Specifically, SDC3 null animals have a higher density of cells in deep cortical areas and a reduced number in the superficial cortical layers. This was found to be due to defects in neural cell migration during development and in particular, an interaction between SDC3 and heparin binding growth associated molecule (HBGAM) (20). Syndecans are known to be key players in cell adhesion and migration, so identifying a migration defect in neural cells associated with SDC3 is entirely consistent.

SDC3 is found in other tissues of the brain, immunostaining of wild-type mice revealed SDC3 to be expressed in the hypothalamus, particularly in the paraventricular nucleus and the lateral hypothalamic area (21). SDC3 expression (uniquely amongst the family members) is upregulated in the hypothalamus in response to food deprivation and the situation is reversible once starved animals are refed. Unsurprisingly, food

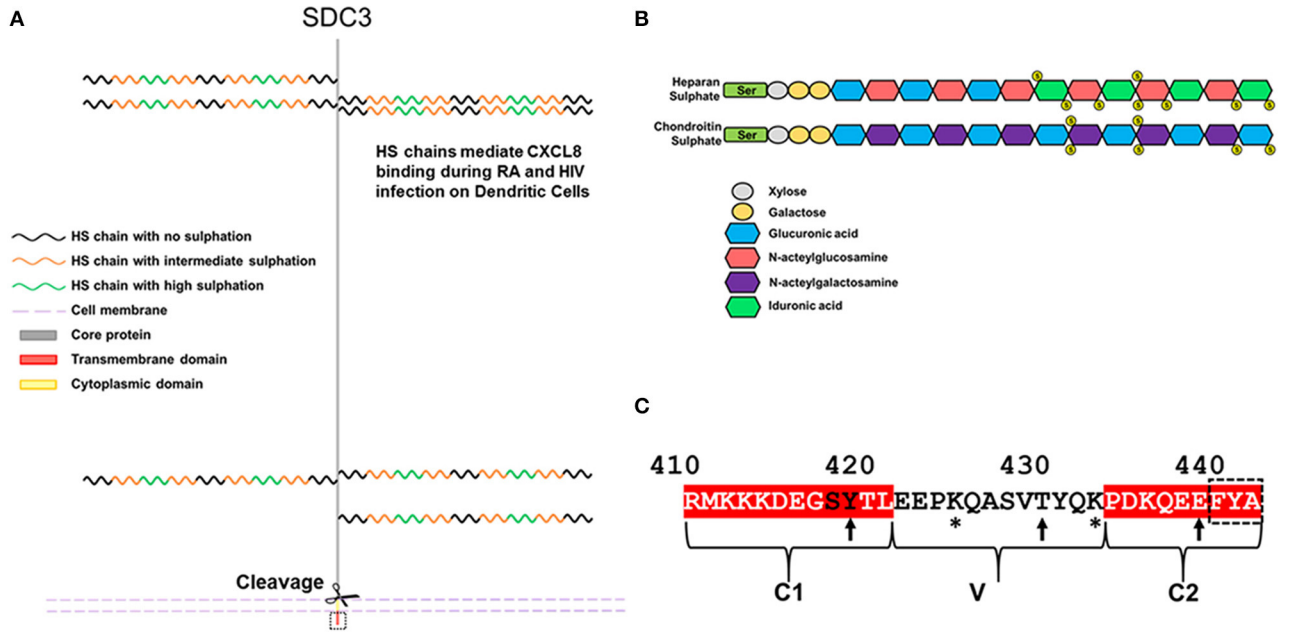

FIGURE 1 | Schematic diagram and features of SDC3. **(A)** Human SDC3 is 442aa in length and contains seven potential sites for GAG substitution. Most functions ascribed to SDC3 relate to interactions through its HS chains. HS chains are heterogenous in nature and contain regions of low, intermediate and high sulphation. **(B)** Structure of HS and CS. **(C)** The cytoplasmic domain of SDC3 is 33 amino acids in length and shares conserved C1 and C2 domains with other syndecan family members. The C-terminal PDZ binding domain is indicated by a dashed black box. Potential sites of tyrosine phosphorylation are indicated by arrows and lysine residues potentially involved in phosphoinositide binding are indicated by asterisks. The conserved SY in the C1 domain, which can be phosphorylated in other syndecan family members are denoted by black letters.

deprived animals exhibit an abnormal desire for food once the deprivation is ended. However, this response is lacking in animals null for SDC3, suggesting a role for SDC3 in feeding behaviors (21). This is further evidenced by the fact that SDC3 animals are partially resistant to obesity when given a high fat diet due to reduced food intake (22).

Several hypothalamic neuropeptides regulate feeding behaviors; for example, agouti-related protein (AgRP), melanin concentrating hormone (MCH) and neuropeptide Y stimulate increased feeding behaviors, whereas α-melanocyte stimulating hormone (αMSH) and corticotrophin releasing hormone (CRH) serve to inhibit pathways associated with increased feeding (23). It is known that many of the interactions between these peptides and their receptors at least in part have an HS involvement. There is a complex interplay between these neuropeptides and SDC3 is thought to have a role in promoting the antagonism between AgRP and αMSH for the melanocortin receptor MC-4R (24, 25). In essence, when animals are starved, SDC3 is upregulated and this promotes the binding of AgRP to MC-4R leading to a reduction in anti-satiety signals, and enhanced feeding. In animals null for SDC3, this interaction does not occur meaning αMSH is free to bind MC-4R leading to a reduction in the desire to feed in these animals. Interestingly, another consequence of starving is an upregulation of Tissue Inhibitor Metalloprotease-3 (TIMP3), this acts as an inhibitor to a variety of MMPs which also have key roles in syndecan shedding. This provides a means of regulating feeding behaviors since under conditions of starvation, SDC3 shedding is inhibited thus promoting occupation of MC-4R by AgRP and promoting feeding. On the other hand, under feeding conditions TIMP is down regulated, SDC3 shedding is up regulated and the satiety signal through the αMSH/MC-4R axis is promoted (26, 27). The hypothalamus also has key roles in modulating reward processing in addictive behaviors and SDC3 also has a role to play in these. Cocaine administration increases SDC3 expression in the lateral hypothalamic area and SDC3 knockout mice actually exhibit more addictive behaviors than wild-type counterparts. SDC3 null animals were more susceptible to cocaine addiction, a situation that could be reversed upon re-expression of SDC3. Glial cell line-derived growth factor (GDNF) acts to both increase and decrease cocaine self-administration behaviors in rodents through its interactions with a signaling complex consisting of the receptor GFR-α1 and the tyrosine kinase c-Ret (28). SDC3 is thought to disrupt this signaling complex since it can also bind GDNF and as such, is a potentially important target for treating addictions.

SYNDECAN-3 IN DISEASE

It is very evident from the studies described above that SDC3 plays a critical role in both brain development and behavior. However, other roles for SDC3 on endothelial cells (ECs) and leukocytes are emerging in inflammatory responses. The purpose of the remainder of this review is to examine the roles of SDC3

in the context of inflammatory disease (rheumatoid arthritis), angiogenesis and also HIV infection.

Syndecan-3 in Rheumatoid Arthritis

SDC3 is expressed on endothelia in both rheumatoid and non-rheumatoid synovia and is thought to have roles in binding chemokines, specifically CXCL8, during the progression of the disease (29, 30). Interestingly, mice null for SDC3 are protected in a model of antigen-induced arthritis (methylated BSA induced), in which clinical scores, leukocyte recruitment and cartilage damage were all significantly less than wild-type animals (31). This is a common feature of syndecan null animals, in that phenotypes only emerge when the animals are challenged and more often than not, deletion of syndecans leads to less severe disease progression, suggesting a role only in pathological scenarios. This study also highlighted a slight paradox; in models of both dermal and cremasteric inflammation, leukocyte rolling and adhesion was elevated in SDC3-null mice, suggesting an anti-inflammatory role for this molecule (31). This therefore suggests distinct roles for SDC3 depending on the vascular bed. SDC3 is thought to facilitate chemokine interactions via binding to its GAG chains, and it is likely that the extent and sulphation pattern of the HS chains in ECs from different tissues will vary. Administration of recombinant forms of SDC3 ectodomains, expressed in mammalian cells, have also been used in both collagen- and methylated BSA-induced murine inflammatory arthritis models with efficacious effects indicating both the therapeutic potential of targeting this molecule but also the importance of shed SDC3 in disease progression (32).

Syndecan-3 in Neovascular Diseases

Angiogenesis, the formation of new blood vessels from existing vasculature, and inflammation are intrinsically linked. SDC3-null mice exhibit no gross abnormalities suggesting that the formation of the vasculature in these animals is normal. However, in-depth studies on parameters such as vessel density, vessel diameter, vessel frequency and pericyte coverage have yet to be undertaken. SDC3 is expressed on ECs in early retinal development in rats (33), and has been found expressed on ECs from a variety of tissues. For example, along with SDC4, SDC3 is abundant on cultured human umbilical vein ECs (34), and human coronary artery endothelial cells as well as human coronary artery smooth muscle cells (35). Vascular endothelial growth factor A (VEGFA), alongside a number of other proangiogenic factors are known to bind HS (36, 37), so it would be tempting to propose a role for SDC3 in this context. Interestingly, sequences within the SDC3 extracellular core protein exert anti-angiogenic affects by blocking EC migration (38). A fusion protein consisting of GST fused to the N-terminus of the SDC3 ectodomain inhibits angiogenic sprout formation from aortic explants, and also inhibited EC micro-capillary formation and EC migration. Importantly, this protein was generated in a prokaryotic expression system so lacked any GAG substitutions, indicating that this is an intrinsic property of the core protein (38). This is also in common with other syndecan family members, whose core proteins also exhibit biological activity (39). SDC1, which is closely related to SDC3,

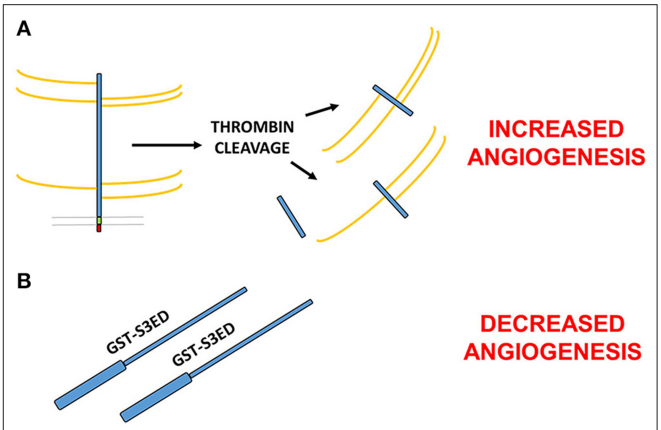

FIGURE 2 | Contrasting roles for the SDC3 ectodomain in angiogenesis. **(A)** Thrombin cleaved fragments of the SDC3 ectodomain promote pro-angiogenic processes such as EC junctional disassembly (43). **(B)** Full length bacterially expressed SDC3 extracellular core protein fused at the N-terminus to GST inhibits angiogenesis in a number of *in vitro* and *ex vivo* models (38). Since the thrombin cleavage sites of SDC3 are not known, it is possible that one or more of the cleavage products is pro-angiogenic whereas the full length sequence acts to inhibit new blood vessel formation.

has anti-angiogenic sequences within its core protein but they bear no homology to the SDC3 sequence suggesting that the anti-angiogenic properties of the latter may work via a distinct mechanism (40, 41). It remains unclear how these sequences affect the biology of the full length molecule—do they bind receptors *in cis*, as is the case for SDC1 (41) or *in trans* when shed as is the case for SDC2 (42)?

A key step in the formation of new blood vessels, and indeed inflammation, is the disassembly of EC junctions, enabling both the migration and proliferation of ECs and vascular leakage during disease. Thrombin-cleaved fragments of the SDC3 (and SDC4) ectodomain have been shown to promote this process in the human lung microvasculature, which has ramifications for conditions such as sepsis or thrombotic disease states, where thrombin is activated (43). This would suggest opposing roles for the SDC3 ectodomain in angiogenesis; on the one hand, studies would suggest that the core protein independent of GAG chains can inhibit the process (44), whereas fragments of SDC3 cleaved from mammalian cells with their GAGs intact appear to promote vascular permeability and EC migration. It is conceivable that since the thrombin cleavage sites in the SDC3 extracellular core proteins are not known, smaller fragments of the mature protein may in fact exhibit pro-angiogenic effects (**Figure 2**).

Syndecan-3 Interactions With Human Immunodeficiency Virus 1 (HIV-1)

Dendritic cells (DCs) are antigen presenting cells and play a critical role in identifying and capturing pathogens in peripheral tissues and subsequently priming T cells in the lymph nodes to initiate adaptive immune responses. Sexual transmission is the main route of HIV-1 dissemination and in the absence of surface lesions, the genital epithelia presents a barrier to viral crossing

(45, 46). HIV circumvents this by using DCs as molecular Trojan horses to cross this normally impenetrable epithelium (47). DCs induce virus-specific CD8+ T cell responses by presenting antigens bound by major histocompatibility complex molecules class-I (MHC-I) to these T cells, thus activating them. DCs infected with viruses can use viral proteins which are endogenously synthesized from viral replication as antigens for presentation on MHC-I in a process commonly called direct presentation (48). On the other hand, DCs not infected with viruses must engulf exogenous viral antigens for presentation to CD8+ T cells via a process known as cross-presentation (49). DCs have been shown to be susceptible to HIV-1 infection (50). Therefore, direct presentation usually takes place in the context of normal HIV transmission.

A number of cell surface receptors have been implicated in facilitating both the recognition, binding and transmission of the HIV-1 virus; different receptors have been shown to interact with HIV-1 on DCs, such as the C-type lectin DC-SIGN (51, 52), the mannose receptor (53), langerin (54), and CD4 (53). Most of these studies were carried out using HIV-1 glycoprotein gp120 but other experiments using HIV-1 particles suggest that other unknown receptors are also involved (55–57).

DC-SIGN, which binds with high affinity to ICAM-3 present on resting T cells, was discovered to play a key-role in the dissemination of HIV-1 by DCs (51, 58). It does not function as a receptor for HIV-1 virus entry into DCs but instead promotes efficient capture of HIV-1 viruses in the periphery and facilitate their transport to secondary lymphoid tissues to enhance infection *in trans* of cells that express CD4 and chemokine receptors (i.e., T cells) (51). More recently, de Witte et al. (59) found SDC3 to be highly expressed by DCs, namely immature monocyte-derived DCs, and was identified as a major specific HIV-1 attachment receptor. SDC3 captures HIV-1 through interaction with its HS chains and the viral envelope protein gp120; it also acts to stabilize the captured virus, enhance DC infection and like DC-SIGN, promotes HIV transmission to T cells. The authors also found that neutralization of both SDC3 and DC-SIGN leads to the complete impairment of HIV-1 binding to DCs and transmission to T cells. Neutralization of SDC3 alone led to partial inhibition of HIV-1 transmission. As current anti-viral treatments are only aimed at blocking viral replication in T-cells, this opens up a whole new avenue in terms of developing an HIV microbicide that targets DC-SIGN and SDC3 on DCs.

Interestingly, HIV-1 infected individuals known as HIV controllers (HICs) who are able to control viral replication without anti-retroviral therapy exist, but are rare. DCs from these individuals express higher levels of SDC3 and DC-SIGN and have been shown to be less susceptible to HIV-1 infection than cells from healthy donors. On the contrary, DCs from HICs show an enhanced capacity to capture HIV-1 when compared to cells from healthy donors or HIV-1 patients currently on anti-retroviral treatment with suppressed viral load (60). High levels of both SDC3 and DC-SIGN on DCs have previously been confirmed to play crucial roles in facilitating HIV-1 capture and this would, at first, seem contradictory (51, 58, 59). However, the combination of being less permissible to HIV-1 infection and having increased capacity to capture HIV-1 particles may allow DCs from HICs to preserve their function from the deleterious effect of infection—all of which might facilitate the induction of HIV-specific CD8+ T cells by cross-presentation in the context of low viremia.

CONCLUDING REMARKS

In this review, we have explored the diverse roles that the HSPG, SDC3, plays in a range of disease and developmental contexts. Although many phenotypes have been described, there is still a great deal to learn about how SDC3 is actually functioning in these scenarios. SDC1, 2 and 4 have been intrinsically linked with integrins and in particular modulating cell adhesion and migration responses. SDC1 has been shown to modulate the activity of a number of αV integrin heterodimers, as has SDC4 (14, 61). Similarly β1 integrin heterodimers have also been associated with SDC2 and 4 (14, 42, 62). The consequences of these interactions lead to cell migration and adhesion defects when they are compromised. Based on this, it seems likely that SDC3 would also interact and/or modulate integrin activity although further research is required to establish this for sure.

In many instances, it is interactions with SDC3 HS chains that appear to be driving the biological effects observed, whether it be acting to bind neuropeptides, inflammatory mediators or viral particles. However, this does raise the question as to what is driving this selectivity of the molecules toward SDC3 HS. In many cases, the other syndecans and indeed glypican family members are present in abundance but cannot perform the same functions as SDC3 despite possessing HS chains. One possibility is that sequences specific to SDC3 may influence the type and nature of GAG substitution, and it is this that differentiates SDC3 from other HSPGs. This would not be without precedent since studies have shown that sequences in the SDC2 ectodomain can influence the sulphation pattern of SDC2 HS (63). Alternatively, it could be that the expression and localization of SDC3 in cells could be more exquisitely regulated than first thought. Studies in the brain have shown that SDC3 expression can be induced both by starvation and narcotic substances and this is not the case for other family members. SDC3-null animals (like the other family members) develop normally for the most part and it is when challenged that phenotypes are observed. This is suggestive that SDC3 expression is governed by factors associated with these challenges. Molecules such as this make tempting therapeutic targets since it is to be expected that off-target effects would be negligible since the molecule is only having a role in the disease state. It is also entirely possible this selectivity of function of SDC3 HS is actually a combination of both of the above.

The studies described above point to important roles for SDC3 in inflammatory disease which require further investigation and hint that this molecule is important not just in the neuronal context but in other tissues. More detailed studies are required in both the SDC3 null mouse, and patient samples, to explore disease models where inflammation and angiogenesis are a feature. Greater mechanistic insight is required to understand how SDC3 exerts its functions. It remains a possibility that modulating SDC3 function could prove useful in the treatment

of the pathologies described above, however, the means by which this could be achieved requires elucidating.

AUTHOR CONTRIBUTIONS

JW and SA generated the text and performed the literature searches. MB prepared the figures and GD critically appraised and edited the manuscript.

FUNDING

SA, MB, GD, and JW gratefully acknowledge funding from Arthritis Research UK (Grant No. 21177), Fight for Sight (Grant No. 1558/59), Barts and The London Charity (Grant No. MGU0313), Queen Mary Innovations, William Harvey Research Foundation, The Macular Society and The Dunhill Medical Trust (Grant No. RPGF1906\173).

REFERENCES

1. Couchman JR. Transmembrane signaling proteoglycans. *Ann Rev Cell Dev Biol.* (2010) 26:89–114. doi: 10.1146/annurev-cellbio-100109-104126
2. Gondelaud F, Ricard-Blum S. Structures and interactions of syndecans. *FEBS J.* (2019) 286:2994–3007. doi: 10.1111/febs.14828
3. Bertrand J, Bollmann M. Soluble syndecans: biomarkers for diseases and therapeutic options. *Br J Pharmacol.* (2019) 176:67–81. doi: 10.1111/bph.14397
4. Mitsou I, Multhaupt HAB, Couchman JR. Proteoglycans, ion channels and cell-matrix adhesion. *Biochem J.* (2017) 474:1965–79. doi: 10.1042/BCJ20160747
5. Afratis NA. Nikitovic D, Multhaupt HA, Theocharis AD, Couchman JR, Karamanos NK. Syndecans—key regulators of cell signaling and biological functions. *FEBS J.* (2017) 284:27–41. doi: 10.1111/febs.13940
6. Carey DJ. Conner K, Asundi VK, O'Mahony DJ, Stahl RC, Showalter L, et al. cDNA cloning, genomic organization, and *in vivo* expression of rat N-syndecan. *J Biol Chem.* (1997) 272:2873–9. doi: 10.1074/jbc.272.5.2873
7. Carey DJ, Evans DM, Stahl RC, Asundi VK, Conner KJ, Garbes P, et al. Molecular cloning and characterization of N-syndecan, a novel transmembrane heparan sulfate proteoglycan. *J Cell Biol.* (1992) 117:191–201. doi: 10.1083/jcb.117.1.191
8. Chakravarti R, Adams JC. Comparative genomics of the syndecans defines an ancestral genomic context associated with matrilins in vertebrates. *BMC Genom.* (2006) 7:83. doi: 10.1186/1471-2164-7-83
9. Chernousov MA, Carey DJ. N-syndecan (syndecan 3) from neonatal rat brain binds basic fibroblast growth factor. *J Biol Chem.* (1993) 268:16810–4.
10. Li JP, Kusche-Gullberg M. Heparan Sulfate: biosynthesis, structure, and Function. *Int Rev Cell Mol Biol.* (2016) 325:215–73. doi: 10.1016/bs.ircmb.2016.02.009
11. Asundi VK, Erdman R, Stahl RC, Carey DJ. Matrix metalloproteinase-dependent shedding of syndecan-3, a transmembrane heparan sulfate proteoglycan, in Schwann cells. *J Neurosci Res.* (2003) 73:593–602. doi: 10.1002/jnr.10699
12. Asundi VK, Carey DJ. Self-association of N-syndecan (syndecan-3) core protein is mediated by a novel structural motif in the transmembrane domain and ectodomain flanking region. *J Biol Chem.* (1995) 270:26404–10. doi: 10.1074/jbc.270.44.26404
13. Koo BK, Jung YS, Shin J, Han I, Mortier E, Zimmermann P, et al. Structural basis of syndecan-4 phosphorylation as a molecular switch to regulate signaling. *J Mol Biol.* (2006) 355:651–63. doi: 10.1016/j.jmb.2005.09.087
14. Morgan MR, Hamidi H, Bass MD, Warwood S, Ballestrem C, Humphries MJ. Syndecan-4 phosphorylation is a control point for integrin recycling. *Dev Cell.* (2013) 24:472–85. doi: 10.1016/j.devcel.2013.01.027
15. Asundi VK, Carey DJ. Phosphorylation of recombinant N-syndecan (syndecan 3) core protein. *Biochem Biophys Res Commun.* (1997) 240:502–6. doi: 10.1006/bbrc.1997.7684
16. Oh ES, Woods A, Couchman JR. Syndecan-4 proteoglycan regulates the distribution and activity of protein kinase C. *J Biol Chem.* (1997) 272:8133–6. doi: 10.1074/jbc.272.13.8133
17. Oh ES, Woods A, Lim ST, Theibert AW, Couchman JR. Syndecan-4 proteoglycan cytoplasmic domain and phosphatidylinositol 4,5-bisphosphate coordinately regulate protein kinase C activity. *J Biol Chem.* (1998) 273:10624–9. doi: 10.1074/jbc.273.17.10624
18. Kim CW, Goldberger OA, Gallo RL, Bernfield M. Members of the syndecan family of heparan sulfate proteoglycans are expressed in distinct cell-, tissue-, and development-specific patterns. *Mol Biol Cell.* (1994) 5:797–805. doi: 10.1091/mbc.5.7.797
19. Kaksonen M, Pavlov I, Voikar V, Lauri SE, Hienola A, Riekki R, et al. Syndecan-3-deficient mice exhibit enhanced LTP and impaired hippocampus-dependent memory. *Mol Cell Neurosci.* (2002) 21:158–72. doi: 10.1006/mcne.2002.1167
20. Hienola A, Tumova S, Kulesskiy E, Rauvala H. N-syndecan deficiency impairs neural migration in brain. *J Cell Biol.* (2006) 174:569–80. doi: 10.1083/jcb.200602043
21. Reizes O, Lincecum J, Wang Z, Goldberger O, Huang L, Kaksonen M, et al. Transgenic expression of syndecan-1 uncovers a physiological control of feeding behavior by syndecan-3. *Cell.* (2001) 106:105–16. doi: 10.1016/S0092-8674(01)00415-9
22. Strader AD, Reizes O, Woods SC, Benoit SC, Seeley RJ. Mice lacking the syndecan-3 gene are resistant to diet-induced obesity. *J Clin Invest.* (2004) 114:1354–60. doi: 10.1172/JCI20631
23. Woods SC, Seeley RJ, Porte D Jr, Schwartz MW. Signals that regulate food intake and energy homeostasis. *Science.* (1998) 280:1378–83. doi: 10.1126/science.280.5368.1378
24. Reizes O, Clegg DJ, Strader AD, Benoit SC. A role for syndecan-3 in the melanocortin regulation of energy balance. *Peptides.* (2006) 27:274–80. doi: 10.1016/j.peptides.2005.02.030
25. Zheng Q, Zhu J, Shanabrough M, Borok E, Benoit SC, Horvath TL, et al. Enhanced anorexigenic signaling in lean obesity resistant syndecan-3 null mice. *Neuroscience.* (2010) 171:1032–40. doi: 10.1016/j.neuroscience.2010.09.060
26. Reizes O, Benoit SC, Strader AD, Clegg DJ, Akunuru S, Seeley RJ. Syndecan-3 modulates food intake by interacting with the melanocortin/AgRP pathway. *Ann N Y Acad Sci.* (2003) 994:66–73. doi: 10.1111/j.1749-6632.2003.tb03163.x
27. Reizes O, Benoit SC, Clegg DJ. The role of syndecans in the regulation of body weight and synaptic plasticity. *Int J Biochem Cell Biol.* (2008) 40:28–45. doi: 10.1016/j.biocel.2007.06.011
28. Chen J, Repunte-Canonigo V, Kawamura T, Lefebvre C, Shin W, Howell LL, et al. Hypothalamic proteoglycan syndecan-3 is a novel cocaine addiction resilience factor. *Nat Commun.* (2013) 4:1955. doi: 10.1038/ncomms2955
29. Patterson AM, Gardner L, Shaw J, David G, Loreau E, Aguilar L, et al. Induction of a CXCL8 binding site on endothelial syndecan-3 in rheumatoid synovium. *Arthritis Rheum.* (2005) 52:2331–42. doi: 10.1002/art.21222
30. Patterson AM, Cartwright A, David G, Fitzgerald O, Bresnihan B, Ashton BA, et al. Differential expression of syndecans and glypicans in chronically inflamed synovium. *Ann Rheum Dis.* (2008) 67:592–601. doi: 10.1136/ard.2006.063875
31. Kehoe O, Kalia N, King S, Eustace A, Boyes C, Reizes O, et al. Syndecan-3 is selectively pro-inflammatory in the joint and contributes to antigen-induced arthritis in mice. *Arthritis Res Ther.* (2014) 16:R148. doi: 10.1186/ar4610
32. Eustace AD, McNaughton EF, King S, Kehoe O, Kungl A, Mattey D, et al. Soluble syndecan-3 binds chemokines, reduces leukocyte migration *in vitro* and ameliorates disease severity in models of rheumatoid arthritis. *Arthritis Res Ther.* (2019) 21:172. doi: 10.1186/s13075-019-1939-2
33. Krempel PG, Matsuda M, Marquezini MV, Seixas TG, Ventura GM, Sholl-Franco A, et al. Bevacizumab reduces neurocan content and gene expression

in newborn rat retina *in vitro*. *Invest Ophthalmol Vis Sci.* (2014) 55:5109–15. doi: 10.1167/iovs.14-14466
34. Vuong TT, Reine TM, Sudworth A, Jenssen TG, Kolset SO. Syndecan-4 is a major syndecan in primary human endothelial cells *in vitro*, modulated by inflammatory stimuli and involved in wound healing. *J Histochem Cytochem.* (2015) 63:280–92. doi: 10.1369/0022155415568995
35. Tinholt M, Stavik B, Louch W, Carlson CR, Sletten M, Ruf W, et al. Syndecan-3 and TFPI colocalize on the surface of endothelial-, smooth muscle-, and cancer cells. *PLoS ONE.* (2015) 10:e0117404. doi: 10.1371/journal.pone.0117404
36. Ashikari-Hada S, Habuchi H, Kariya Y, Kimata K. Heparin regulates vascular endothelial growth factor165-dependent mitogenic activity, tube formation, and its receptor phosphorylation of human endothelial cells. Comparison of the effects of heparin and modified heparins. *J Biol Chem.* (2005) 280:31508–15. doi: 10.1074/jbc.M414581200
37. Robinson CJ, Mulloy B, Gallagher JT, Stringer SE. VEGF165-binding sites within heparan sulfate encompass two highly sulfated domains and can be liberated by K5 lyase. *J Biol Chem.* (2006) 281:1731–40. doi: 10.1074/jbc.M510760200
38. De Rossi G, Whiteford JR. A novel role for syndecan-3 in angiogenesis. *F1000Research.* (2013) 2:270. doi: 10.12688/f1000research.2-270.v1
39. De Rossi G, Whiteford JR. Novel insight into the biological functions of syndecan ectodomain core proteins. *BioFactors.* (2013) 39:374–82. doi: 10.1002/biof.1104
40. De Rossi G, Whiteford JR. Syndecans in angiogenesis and endothelial cell biology. *Biochem Soc Trans.* (2014) 42:1643–6. doi: 10.1042/BST20140232
41. Beauvais DM, Ell BJ, McWhorter AR, Rapraeger AC. Syndecan-1 regulates alphavbeta3 and alphavbeta5 integrin activation during angiogenesis and is blocked by synstatin, a novel peptide inhibitor. *J Exp Med.* (2009) 206:691–705. doi: 10.1084/jem.20081278
42. De Rossi G, Evans AR, Kay E, Woodfin A, McKay TR, Nourshargh S, et al. Shed syndecan-2 inhibits angiogenesis. *Development.* (2014) 141:e2207. doi: 10.1242/dev.118901
43. Jannaway M, Yang X, Meegan JE, Coleman DC, Yuan SY. Thrombin-cleaved syndecan-3/-4 ectodomain fragments mediate endothelial barrier dysfunction. *PLoS ONE.* (2019) 14:e0214737. doi: 10.1371/journal.pone.0214737
44. Braun KR, DeWispelaere AM, Bressler SL, Fukai N, Kenagy RD, Chen L, et al. Inhibition of PDGF-B induction and cell growth by syndecan-1 involves the ubiquitin and SUMO-1 ligase, Topors. *PLoS ONE.* (2012) 7:e43701. doi: 10.1371/journal.pone.0043701
45. Gill SK, Loveday C, Gilson RJ. Transmission of HIV-1 infection by oroanal intercourse. *Genitourin Med.* (1992) 68:254–7. doi: 10.1136/sti.68.4.254
46. Sullivan AK, Atkins MC, Boag F. Factors facilitating the sexual transmission of HIV-1. *AIDS Patient Care STDs.* (1997) 11:167–77. doi: 10.1089/apc.1997.11.167
47. Cameron PU, Freudenthal PS, Barker JM, Gezelter S, Inaba K, Steinman RM. Dendritic cells exposed to human immunodeficiency virus type-1 transmit a vigorous cytopathic infection to CD4+ T cells. *Science.* (1992) 257:383–7. doi: 10.1126/science.1352913
48. Xu RH, Remakus S, Ma X, Roscoe F, Sigal LJ. Direct presentation is sufficient for an efficient anti-viral CD8+ T cell response. *PLoS Pathogens.* (2010) 6:e1000768. doi: 10.1371/journal.ppat.1000768
49. van Montfoort N, van der Aa E, Woltman AM. Understanding MHC class I presentation of viral antigens by human dendritic cells as a basis for rational design of therapeutic vaccines. *Front Immunol.* (2014) 5:182. doi: 10.3389/fimmu.2014.00182
50. Smed-Sorensen A, Lore K, Vasudevan J, Louder MK, Andersson J, Mascola JR, et al. Differential susceptibility to human immunodeficiency virus type 1 infection of myeloid and plasmacytoid dendritic cells. *J Virol.* (2005) 79:8861–9. doi: 10.1128/JVI.79.14.8861-8869.2005
51. Geijtenbeek TB, Kwon DS, Torensma R, van Vliet SJ, van Duijnhoven GC, Middel J, et al. DC-SIGN, a dendritic cell-specific HIV-1-binding protein that enhances trans-infection of T cells. *Cell.* (2000) 100:587–97. doi: 10.1016/S0092-8674(00)80694-7
52. Arrighi JF, Pion M, Wiznerowicz M, Geijtenbeek TB, Garcia E, Abraham S, et al. Lentivirus-mediated RNA interference of DC-SIGN expression inhibits human immunodeficiency virus transmission from dendritic cells to T cells. *J Virol.* (2004) 78:10848–55. doi: 10.1128/JVI.78.20.10848-10855.2004
53. Turville SG, Cameron PU, Handley A, Lin G, Pohlmann S, Doms RW, et al. Diversity of receptors binding HIV on dendritic cell subsets. *Nat Immunol.* (2002) 3:975–83. doi: 10.1038/ni841
54. de Witte L, Nabatov A, Pion M, Fluitsma D, de Jong MA, de Gruijl T, et al. Langerin is a natural barrier to HIV-1 transmission by Langerhans cells. *Nat Med.* (2007) 13:367–71. doi: 10.1038/nm1541
55. Granelli-Piperno A, Pritsker A, Pack M, Shimeliovich I, Arrighi JF, Park CG, et al. Dendritic cell-specific intercellular adhesion molecule 3-grabbing nonintegrin/CD209 is abundant on macrophages in the normal human lymph node and is not required for dendritic cell stimulation of the mixed leukocyte reaction. *J Immunol.* (2005) 175:4265–73. doi: 10.4049/jimmunol.175.7.4265
56. Gummuluru S, Rogel M, Stamatatos L, Emerman M. Binding of human immunodeficiency virus type 1 to immature dendritic cells can occur independently of DC-SIGN and mannose binding C-type lectin receptors via a cholesterol-dependent pathway. *J Virol.* (2003) 77:12865–74. doi: 10.1128/JVI.77.23.12865-12874.2003
57. Gurney KB, Elliott J, Nassanian H, Song C, Soilleux E, McGowan I, et al. Binding and transfer of human immunodeficiency virus by DC-SIGN+ cells in human rectal mucosa. *J Virol.* (2005) 79:5762–73. doi: 10.1128/JVI.79.9.5762-5773.2005
58. Geijtenbeek TB, Torensma R, van Vliet SJ, van Duijnhoven GC, Adema GJ, van Kooyk Y, et al. Identification of DC-SIGN, a novel dendritic cell-specific ICAM-3 receptor that supports primary immune responses. *Cell.* (2000) 100:575–85. doi: 10.1016/S0092-8674(00)80693-5
59. de Witte L, Bobardt M, Chatterji U, Degeest G, David G, Geijtenbeek TB, et al. Syndecan-3 is a dendritic cell-specific attachment receptor for HIV-1. *Proc Natl Acad Sci USA.* (2007) 104:19464–9. doi: 10.1073/pnas.0703747104
60. Hamimi C, David A, Versmisse P, Weiss L, Bruel T, Zucman D, et al. Dendritic cells from HIV controllers have low susceptibility to HIV-1 infection *in vitro* but high capacity to capture HIV-1 particles. *PLoS ONE.* (2016) 11:e0160251. doi: 10.1371/journal.pone.0160251
61. Beauvais DM, Burbach BJ, Rapraeger AC. The syndecan-1 ectodomain regulates alphavbeta3 integrin activity in human mammary carcinoma cells. *J Cell Biol.* (2004) 167:171–81. doi: 10.1083/jcb.200404171
62. Woods A, Longley RL, Tumova S, Couchman JR. Syndecan-4 binding to the high affinity heparin-binding domain of fibronectin drives focal adhesion formation in fibroblasts. *Archiv Biochem Biophys.* (2000) 374:66–72. doi: 10.1006/abbi.1999.1607
63. Corti F, Wang Y, Rhodes JM, Atri D, Archer-Hartmann S, Zhang J, et al. N-terminal syndecan-2 domain selectively enhances 6-O heparan sulfate chains sulfation and promotes VEGFA165-dependent neovascularization. *Nat Commun.* (2019) 10:1562. doi: 10.1038/s41467-019-10205-0

Conflict of Interest: The authors declare that the research was conducted in the absence of any commercial or financial relationships that could be construed as a potential conflict of interest.

International Journal of Biochemistry and Cell Biology 146 (2022) 106196

Contents lists available at ScienceDirect

International Journal of Biochemistry and Cell Biology

journal homepage: www.elsevier.com/locate/biocel

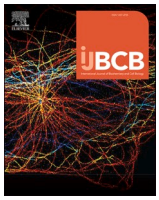

Roles of Syndecan-4 in cardiac injury and repair

Faheem Shaik, Michaela, J.M. Balderstone, Samantha Arokiasamy *, James R. Whiteford *

William Harvey Research Institute, Centre for Microvascular Research, Faculty of Medicine and Dentistry, Queen Mary University of London, Charterhouse Square, EC1M 6BQ, UK

ARTICLE INFO

Keywords:
Myocardial infarction
Cardiac remodeling
Angiogenesis
Syndecan
Cardiac fibrosis

ABSTRACT

The heparan sulphate proteoglycan Syndecan-4 belongs to a 4-member family of transmembrane receptors. Genetic deletion of Syndecan-4 in mice causes negligible developmental abnormalities however when challenged these animals show distinct phenotypes. Synedcan-4 is expressed in many cell types in the heart and its expression is elevated in response to cardiac injury and recent studies have suggested roles for Syndecan-4 in repair mechanisms within the damaged heart. The purpose of this review is to explore these biological insights into the role of Syndecan-4 in both the injured heart and later during cardiac repair and remodeling.

1. Introduction

The process of cardiac remodeling in response to injury is complex and multifactorial involving different cell types, chemokines and growth factors and leads to changes in the heart's size, shape and function, often with adverse outcomes for the patient. Insults such as those caused by myocardial infarction, pressure overload, myocarditis or valvular regurgitation all lead to the initiation of cardiac remodeling (Cohn et al., 2000). The loss or damage to cardiac myocytes in the immediate aftermath of a cardiac injury leads to a weakening of the heart wall meaning that the heart is unable to function properly particularly, with respect to withstanding pressure and load. Tissue repair responses repair the necrotic area which may lead to myocardial scarring, however, the damage promotes other cell types such as fibroblasts to proliferate, and produce extracellular matrix which contribute to the hypertrophy associated with cardiac remodeling. The underlying molecular mechanisms associated with cardiac remodeling involve a complex interplay between the extracellular matrix, cell-cell contacts and growth factor signaling, processes which are all intimately associated with cell surface heparan sulphate proteoglycans (HSPGs) (Gopal et al., 2021). The purpose of this review is to focus on the role of one such molecule, syndecan-4 (SDC4), and the roles it plays during this process.

1.1. Syndecan-4 structure and Interactions

The syndecan family of transmembrane HSPGs comprises 4 family members (SDC1–4) and have diverse functions in many different cell types such cell adhesion and migration, growth factor signaling and receptor trafficking (Gopal et al., 2021). All 4 family members have a similar molecular architecture consisting of a large extracellular domain which contains sites to which glycosaminoglycan side chains are covalently linked, a single pass transmembrane domain and a short cytoplasmic domain For reviews see (Couchman, 2010; Gondelaud and Ricard-Blum, 2019).

SDC4 has 3 glycosaminoglycan chain attachment sites (Ser $^{39, 61 \text{ and } 63}$ on human SDC4) towards the N-terminus of the extracellular core protein (Fig. 1A and B) consisting of conserved Ser-Gly motifs surrounded by acidic residues (Kojima et al., 1993; Shworak et al., 1994). Heparan sulphate (HS) chains are the principal GAGs associated with SDC4 and consist of repeating disaccharide units (50−200) consisting of glucuronic acid and N-acetyl glucosamine. Chains are covalently linked to serine residues via a linker sequence and during biosynthesis are modified by a variety of sulfotransferases (Nadanaka and Kitagawa, 2008). The resultant sugar chain is a highly acidic molecule with variable sulphation characteristics throughout. Analysis of sulphation characteristics of SDC HS chains shows that they may have a domain like

Abbreviations: CASK, Calcium/calmodulin-dependent serine protein kinase 3; CAVIN/PTRF, Polymerase I and transcript release factor; CCT5, T-complex protein 1 subunit epsilon; CDK9, Cyclin-dependent kinase 9; EIF2S1, Eukaryotic translation initiation factor 2 subunit 1; EIF4B, Eukaryotic translation initiation factor 4B; GIPC, GAIP interacting protein; HSPG, Heparan Sulphate Proteogylcan; IL1β, Interleukin 1 beta; MLP, Muscle LIM protein; MMP7, Matrix metalloproteinase 7; NFAT, Nuclear factor of activated T-cells; PARVB, Beta PARVIN; PFKM, 6-phosphofructokinase, muscle type; PKCα, Protein Kinase C alpha; RASIP, Ras-interacting protein; SDC, Syndecan; TNF, Tumour Necrosis Factor; VEGF, Vascular Endothelial Growth Factor.

* Corresponding authors.
E-mail addresses: s.arokiasamy@ucl.ac.uk (S. Arokiasamy), j.whiteford@qmul.ac.uk (J.R. Whiteford).

https://doi.org/10.1016/j.biocel.2022.106196
Received 17 January 2022; Received in revised form 17 March 2022; Accepted 18 March 2022
Available online 22 March 2022

structure consisting of low, intermediate and high sulphation. The exact sulphation characteristics of HS is likely to depend on both the cell type producing it, but also the syndecan core protein to which they it is attached. Numerous bioactive molecules such as growth factors, chemokines and cytokines and extracellular matrix molecules are known to bind heparan sulphate and these interactions are likely to play a role in SDC4 functionality in tissues (Häcker et al., 2005).

SDC4 is most likely an obligate dimer and this is mediated both by residues within its transmembrane domain as well as the cytoplasmic domain. Structural analysis on peptides corresponding to the 28 amino acid SDC4 cytoplasmic domain reveal a dimeric twisted clamp structure (Shin et al., 2001). In common with other syndecan family members. the SDC4 cytoplasmic domain shares a highly conserved C1 and C2 region flanking a variable (V) region, the sequence of which, is unique to SDC4 and is conserved across species (Fig. 1C) (Chakravarti and Adams, 2006; Whiteford et al., 2008). The cytoplasmic domain of SDC4 contains 3 lysine residues within the C1 domain and a further 4 within its V region. The lysine doublets within the V region are known to bind phospho-inositides, specifically phosphatidylinositol 4,5 bisphosphate ($PtdIns(4,5)P_2$) and this interaction further stabilizes dimer formation and forms a tertiary structure with PKCα (Lee et al., 1998; Oh et al., 1998). Evidence would also suggest that lysine residues within the V-region may also be sites of ubiquitination (Carvallo et al., 2010). SDC4 can also be phosphorylated at both Tyr^{180} and the adjacent Ser^{181} (Morgan et al., 2013; Koo et al., 2006). Both phosphorylation events would significantly alter the confirmation of the cytoplasmic domain and likely the entire molecule. The C2 domain of SDC4 (in common with SDC1,2 and 3) contains a Class II PDZ binding motif and interactions have been reported with synectin (GIPC), syntenin and CASK (Fig. 1C) (Grootjans et al., 1997; Hsueh et al., 1998; Gao et al., 2000).

Proteomic analysis of specific SDC4 interacting partners in both healthy and pressure overloaded heart lysates revealed a number of novel interactions which may provide an indication of SDC4′s role in cardiac injury and remodeling. Molecules such as CAVIN1/PTRF, CCT5, CDK9, EIF2S1, EIF4B, MPP7, PARVB, PFKM, and RASIP were all validated as SDC4 interactors within the heart. Notably another molecule, MLP (Muscle LIM protein) was shown not only to interact with the SDC4 cytoplasmic domain, but the binding between the two was increased in hearts subjected to pressure overload (Mathiesen et al., 2019). MLP is known to mediate hypertrophic gene expression in response to mechanical stress (Boateng et al., 2007) and this fits well with work demonstrating SDC4 is also a mechano-sensor (Bellin et al., 2009).

SDC4 is intimately associated with interactions between cells and the extracellular matrix, being both a component of focal adhesions and important for their formation under specific circumstances. Interactions between the V region of SDC4 and the actin bundling protein, α-actinin, have been reported and differentiation of SDC4 null fibroblasts to myofibroblasts is impaired (Okina et al., 2012; Greene et al., 2003). Of relevance, is the fact that SDC4 null fibroblasts do not form focal adhesions in response to stimulation with the heparin binding domain of fibronectin. Under normal circumstances, cells engage with fibronectin via the RGD containing integrin binding domain through α5β1 integrin and the heparin binding domain through interactions with the SDC4 HS chains leading to the formation of focal adhesions. This process involves an upregulation of PKCα activity via SDC4 and an increase in active RhoA levels and this is linked to integrin signaling via p190RhoGAP (Morgan et al., 2013; Bass et al., 2011, 2008). Clearly, further work is required to understand the molecular interactions described above and how they impact on heart pathology.

2. Syndecan-4 expression and roles in cardiac injury and repair in the Heart

SDC4 is expressed in cardiomyocytes and localizes to both costameres and focal complexes in vitro (VanWinkle et al., 2002). Of importance comparative studies of sham treated mice and a group in which MI was induced by ligation of the left coronary artery showed that both SDC4 and SDC3 gene expression was significantly upregulated in both infarcted and non-infarcted tissue (Finsen et al., 2004; Matsui et al., 2011). Serum SDC4 is also elevated in patients with acute myocardial infarction (Kojima et al., 2001). Cardiac fibroblasts also express SDC4 (Herum et al., 2015) and SDC4 is unique amongst the family in that it is

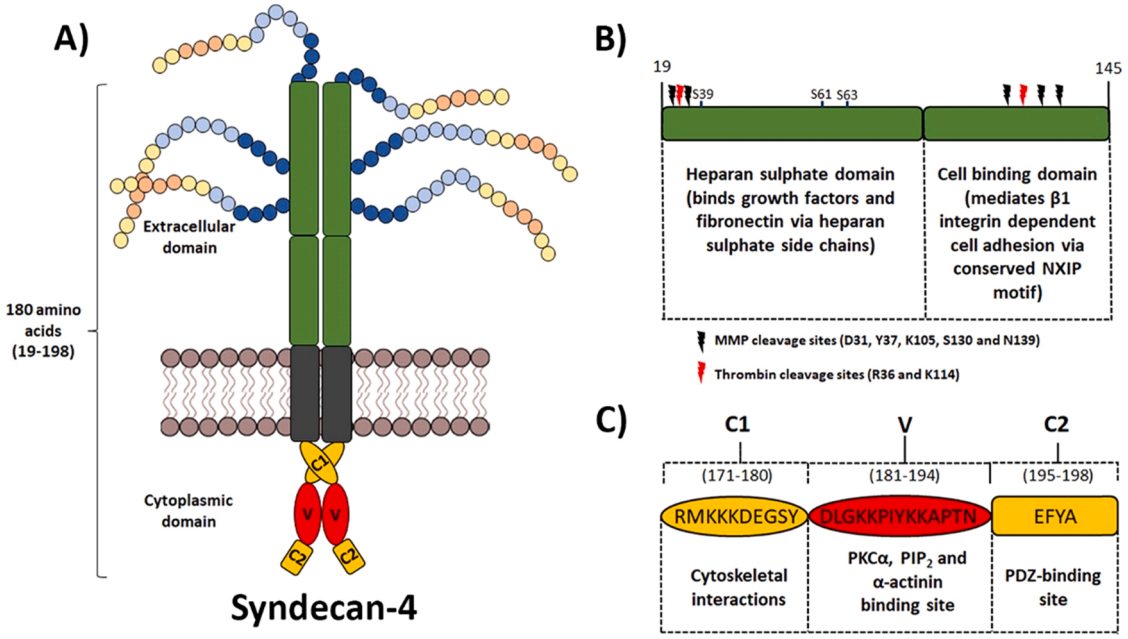

Fig. 1. Syndecan-4 structure. (A) Schematic representation of SDC4 dimer showing the extracellular domain with heparan sulphate chains, transmembrane domain and an intertwined cytoplasmic domain containing C1, V and C2 regions. Within this schematic the heterogenous nature of SDC4 HS chains are indicated as follows: the 4 saccharide GAG linker region is denoted by dark blue circles, low sulphated HS by light blue circles, intermediate sulphated HS by yellow circles and regions of highly sulphated HS by orange circles. **(B)** A schematic overview of SDC4 ectodomain showing three heparan sulphate side chain attachment sites (S31, S61 and S63) and protease cleavage sites. **(C)** Amino acid sequence of different subdomains of the SDC4 cytoplasmic domain and their interactions.

expressed on all types of leukocytes including neutrophils and macrophages (Gopal et al., 2021). Angiogenesis and lymphangiogenesis are also important components of cardiac remodeling and SDC4 is known to be expressed at low levels on both endothelial cells and also lymphatic endothelial cells (Johns et al., 2016). Interestingly, its expression seems to be upregulated after insult (De Rossi et al., 2021) and this is most likely due to the presence of both an NF-κB and hypoxia response elements within its promoter (Fujita et al., 2014; Okuyama et al., 2013).

2.1. The Syndecan-4 knockout mouse in models of cardiac injury and cardiac remodeling

Genetic deletion of SDC4 in mice leads to negligible gross developmental defects and specifically the heart and the vasculature are for the most part normal (Matsui et al., 2011) with the exception of a slight increase in arterial blood pressure (Partovian et al., 2008). However, the most profound phenotypes are observed when *Sdc4-/-* animals are challenged. Myocardial ischaemia with reperfusion injury initiated by ligation of the left coronary artery of *Sdc4-/-* animals leads to a greater infarct size, more myocardial damage and slower infarct healing times, and increased mortality compared to wild type littermates (Echtermeyer et al., 2011). Animals were also more prone to left ventricular rupture owing to impaired wound healing responses (Matsui et al., 2011). This correlated with a loss of normal function in cardiac fibroblasts, which exhibited defects in cell migration and differentiation. This wound healing phenotype is a feature of the SDC4 null mouse, for example dermal wound repair is also impaired in these animals (Echtermeyer et al., 2001). Overexpression of SDC4 immediately after LAD ligation in rats resulted in reduced mortality and improved cardiac function post MI with reduced cardiac hypertrophy. Other tissue repair processes such as angiogenesis were also enhanced when compared to animals transfected with the empty vector (Xie et al., 2012). Other studies highlight a role for SDC4 in the differentiation of cardiac fibroblasts driven by the calcineurin-dependent transcription factor nuclear factor of activated T-cells (NFAT). In common with other studies *Sdc4-/-* mice faired better than wildtype controls in response to aortic banding. Cardiac fibroblasts respond to mechanical stress by activating the NFAT pathway leading to increased ECM production and myofibroblasts differentiation and this was found to be SDC4 dependent (Herum et al., 2013). The models described above represent cardiac remodeling induced by pathological stimuli, but it is also evident that SDC4 is also involved in cardiac remodeling associated with physiological stimuli. For example, cardiac hypertrophy in *Sdc4-/-* mice is impaired in response to exercise, again suggesting a role for this molecule in promoting adverse tissue repair responses (Xie et al., 2016). Together these studies suggest protective roles for SDC4 in the early response phase to MI but potentially a more harmful role later when excessive cardiac hypertrophy occurs.

2.2. SDC4 shedding and cardiac remodeling

Like the other 3 syndecan family members, the entire extracellular core protein, or fragments thereof can be cleaved from cell surfaces by the action of matrix metalloproteinases in a tightly regulated process called shedding (for review see (Bertrand and Bollmann, 2019)). Inflammatory stimuli such as TNF and IL1β can promote SDC4 shedding in cardiac fibroblasts (Strand et al., 2013) and this can effect cellular processes in the cells that have shed SDC4, as well as the shed moiety acting as a paracrine effector of neighboring cellular responses (De Rossi et al., 2014). In mice that underwent cardiac pressure overload via stimulation by aortic banding, a significant increase in SDC4 gene expression was observed in conjunction with an upregulation of Osteopontin, which is both a marker and regulator of cardiac fibrosis (Herum et al., 2015). Osteopontin is cleaved by thrombin and it is this form which exerts a pro-fibrotic effect on cardiac fibroblasts (Uchinaka et al., 2015). Under basal conditions, osteopontin is thought to interact with SDC4 through its heparin binding domain and in this complex, it is protected from thrombin cleavage. Upon cardiac injury, elevated levels of serum SDC4 are observed indicating an increase in shedding. The model proposed is that upon shedding, osteopontin is no longer protected from thrombin cleavage and the pro-fibrotic fragment becomes greater in abundance (Fig. 2 A-D) (Herum et al., 2020). This situation is likely to be more complex since SDC4 can also be cleaved by thrombin and the resultant fragments have been shown to also affect tissue repair processes (Schmidt et al., 2005). For example, thrombin-cleaved fragments of both SDC3 and SDC4 increase vascular permeability in cultured endothelial cells (Jannaway et al., 2019). Owing to the complexity and variety of proteases which could potentially cleave both osteopontin and SDC4 in vivo there remains much to understand in relation to this. In addition, sequences within the SDC4 ectodomain are known to support fibroblast cell adhesion through an indirect interaction with β1 integrin, and this is also true of monocytic cell lines (Whiteford and Couchman, 2006; Whiteford et al., 2007). Shedding of SDC4 from heart tissue promotes recruitment of immune cells to the heart in rats treated with LPS (Strand et al., 2015). Additionally, overexpression of SDC4 in rat hearts also appears to attenuate both inflammation and fibrosis which is beneficial for infarct repair (Xie et al., 2012).

2.3. Syndecan-4 roles in angiogenesis

A key component of tissue repair is the re-establishment of blood supply to the wounded area. Angiogenesis is the formation of new blood vessels from the existing vasculature. It is essential for development and growth but can also be detrimental in disease states when the process becomes dysregulated leading to excessive or insufficient angiogenesis (Carmeliet and Jain, 2011). The global *Sdc4-/-* mouse develops a normal vasculature indicating that SDC4 does not play a significant role in developmental angiogenesis (De Rossi et al., 2021; Corti et al., 2019). However, in models where pathological angiogenesis is stimulated such as wound healing, hypoxia-induced ocular neovascularization and during tumor formation, angiogenesis is greatly impaired in these animals (De Rossi et al., 2021). This was found to be due to an impaired response to VEGFA in *Sdc4-/-* ECs. In this context, SDC4 has no role in VEFGA driven pro-angiogenic signaling, rather it is a down-stream effector of VEGFA stimulated responses having a critical role in EC junction disassembly, a necessary step in efficient angiogenesis. This is in contrast with its role in pathological lymphangiogenesis, where it has been found to be important for VEGFC/VEGFR3 driven responses (Johns et al., 2016). Given these roles in both new blood vessel and new lymphatic formation it seems likely that SDC4 would also perform a role in cardiac repair responses. Interestingly, when SDC4 is either overexpressed or applied exogenously, angiogenesis is enhanced in both models of ischemia and cardiac pressure overload (Xie et al., 2016; Jang et al., 2012; Das et al., 2016), again suggestive of a role in repair mechanisms.

2.4. Outlook

The collective studies described here identify several roles for SDC4 both during cardiac injury and in the remodeling phase thereafter. SDC4 clearly has an important role in wound healing processes, and this has dual implications. In the immediate aftermath of an injury to the heart SDC4 clearly has an important beneficial role to play in tissue repair processes. However, in the later remodeling phase the role of SDC4 is less beneficial. The question remains whether SDC4 is a viable therapeutic target in cardiac remodeling. The fact that SDC4 gene expression seems to be upregulated only during injury and pathological scenarios suggests that targeting it may not affect normal homeostasis. However more studies are required to understand what drives SDC4 gene expression in these situations. Additionally, SDC4 in its shed form may also be exploited to manipulate tissue remodeling processes but again more studies are required to determine how this entity affects different cell types involved in this process.

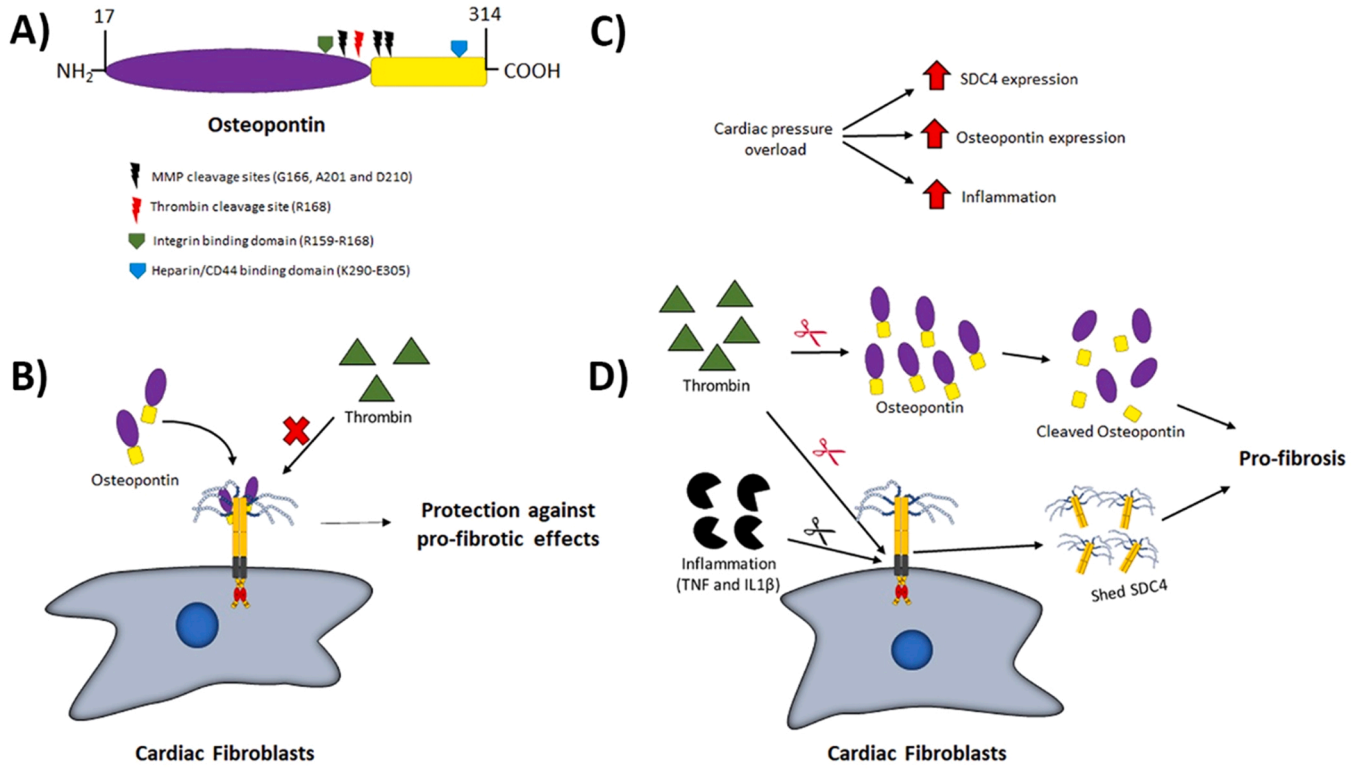

Fig. 2. Proposed model of regulation of anti-fibrotic and pro-fibrotic effects of osteopontin during cardiac pressure overload. (A) Schematic representation of osteopontin showing different cleavage sites, integrin and Heparan sulphate/CD44 binding domains. (B) Osteopontin binds to SDC4 HS via a heparan binding domain which overlaps with a thrombin cleavage site thereby masking it. This leads to inhibition of thrombin cleavage of osteopontin maintaining it in its non-active form, hence profibrotic pathways are not stimulated. (C) Cardiac injury or cardiac pressure overload leads to upregulation of SDC4 and osteopontin gene expression, and also inflammatory cytokines such as TNFα and IL1β. (D) This leads to SDC4 shedding by the action of MMPs and thrombin from cardiac fibroblasts. This unmasks the thrombin cleavage site on osteopontin and the subsequently cleaved fragment stimulates pro-fibrotic pathways.

Author contributions

JW, SA wrote the manuscript and FS and MB assembled the figures.

Acknowledgements

We gratefully acknowledge funding form the Dunhill Medical Trust (Grant No. RPGF1906\173) and The Macular Society.

Conflicts of interest

The authors declare no conflicts of interest.

References

Bass, M.D., Morgan, M.R., Roach, K.A., Settleman, J., Goryachev, A.B., Humphries, M.J., 2008. p190RhoGAP is the convergence point of adhesion signals from alpha 5 beta 1 integrin and syndecan-4. J. Cell Biol. 181 (6), 1013–1026.

Bass, M.D., Williamson, R.C., Nunan, R.D., Humphries, J.D., Byron, A., Morgan, M.R., Martin, P., Humphries, M.J., 2011. A syndecan-4 hair trigger initiates wound healing through caveolin- and RhoG-regulated integrin endocytosis. Dev. Cell 21 (4), 681–693.

Bellin, R.M., Kubicek, J.D., Frigault, M.J., Kamien, A.J., Steward Jr., R.L., Barnes, H.M., Digiacomo, M.B., Duncan, L.J., Edgerly, C.K., Morse, E.M., et al., 2009. Defining the role of syndecan-4 in mechanotransduction using surface-modification approaches. Proc. Natl. Acad. Sci. U.S.A. 106 (52), 22102–22107.

Bertrand, J., Bollmann, M., 2019. Soluble syndecans: biomarkers for diseases and therapeutic options. Br. J. Pharmacol. 176 (1), 67–81.

Boateng, S.Y., Belin, R.J., Geenen, D.L., Margulies, K.B., Martin, J.L., Hoshijima, M., de Tombe, P.P., Russell, B., 2007. Cardiac dysfunction and heart failure are associated with abnormalities in the subcellular distribution and amounts of oligomeric muscle LIM protein. Am. J. Physiol. Heart Circ. Physiol. 292 (1), H259–H269.

Carmeliet, P., Jain, R.K., 2011. Molecular mechanisms and clinical applications of angiogenesis. Nature 473 (7347), 298–307.

Carvallo, L., Muñoz, R., Bustos, F., Escobedo, N., Carrasco, H., Olivares, G., Larraín, J., 2010. Non-canonical Wnt signaling induces ubiquitination and degradation of Syndecan4. J. Biol. Chem. 285 (38), 29546–29555.

Chakravarti, R., Adams, J.C., 2006. Comparative genomics of the syndecans defines an ancestral genomic context associated with matrilins in vertebrates. BMC Genom. 7, 83.

Cohn, J.N., Ferrari, R., Sharpe, N., 2000. Cardiac remodeling–concepts and clinical implications: a consensus paper from an international forum on cardiac remodeling. Behalf of an International Forum on Cardiac Remodeling. J. Am. Coll. Cardiol. 35 (3), 569–582.

Corti, F., Wang, Y., Rhodes, J.M., Atri, D., Archer-Hartmann, S., Zhang, J., Zhuang, Z.W., Chen, D., Wang, T., Wang, Z., 2019. N-terminal syndecan-2 domain selectively enhances 6-O heparan sulfate chains sulfation and promotes VEGFA(165)-dependent neovascularization. Nat. Commun. 10 (1), 1562.

Couchman, J.R., 2010. Transmembrane signaling proteoglycans. Annu Rev. Cell Dev. Biol. 26, 89–114.

Das, S., Monteforte, A.J., Singh, G., Majid, M., Sherman, M.B., Dunn, A.K., Baker, A.B., 2016. Syndecan-4 enhances therapeutic angiogenesis after hind limb ischemia in mice with Type 2 diabetes. Adv. Health Mater. 5 (9), 1008–1013.

De Rossi, G., Evans, A.R., Kay, E., Woodfin, A., McKay, T.R., Nourshargh, S., Whiteford, J.R., 2014. Shed syndecan-2 inhibits angiogenesis. J. Cell Sci. 127 (Pt 21), 4788–4799.

De Rossi, G., Vähätupa, M., Cristante, E., Arokiasamy, S., Liyanage, S.E., May, U., Pellinen, L., Uusitalo-Järvinen, H., Bainbridge, J.W., Järvinen, T.A.H., et al., 2021. Pathological angiogenesis requires Syndecan-4 for efficient VEGFA-induced VE-cadherin internalization. Arterioscler. Thromb. Vasc. Biol. 41 (4), 1374–1389.

Echtermeyer, F., Streit, M., Wilcox-Adelman, S., Saoncella, S., Denhez, F., Detmar, M., Goetinck, P., 2001. Delayed wound repair and impaired angiogenesis in mice lacking syndecan-4. J. Clin. Investig. 107 (2), R9–r14.

Echtermeyer, F., Harendza, T., Hubrich, S., Lorenz, A., Herzog, C., Mueller, M., Schmitz, M., Grund, A., Larmann, J., Stypmann, J., et al., 2011. Syndecan-4 signalling inhibits apoptosis and controls NFAT activity during myocardial damage and remodelling. Cardiovasc. Res. 92 (1), 123–131.

Finsen, A.V., Woldbaek, P.R., Li, J., Wu, J., Lyberg, T., Tønnessen, T., Christensen, G., 2004. Increased syndecan expression following myocardial infarction indicates a role in cardiac remodeling. Physiol. Genom. 16 (3), 301–308.

Fujita, N., Hirose, Y., Tran, C.M., Chiba, K., Miyamoto, T., Toyama, Y., Shapiro, I.M., Risbud, M.V., 2014. HIF-1-PHD2 axis controls expression of syndecan 4 in nucleus pulposus cells. FASEB J. 28 (6), 2455–2465.

Gao, Y., Li, M., Chen, W., Simons, M., 2000. Synectin, syndecan-4 cytoplasmic domain binding PDZ protein, inhibits cell migration. J. Cell Physiol. 184 (3), 373–379.
Gondelaud, F., Ricard-Blum, S., 2019. Structures and interactions of syndecans. FEBS J. 286 (15), 2994–3007.
Gopal, S., Arokiasamy, S., Pataki, C., Whiteford, J.R., Couchman, J.R., 2021. Syndecan receptors: pericellular regulators in development and inflammatory disease. Open Biol. 11 (2), 200377.
Greene, D.K., Tumova, S., Couchman, J.R., Woods, A., 2003. Syndecan-4 associates with alpha-actinin. J. Biol. Chem. 278 (9), 7617–7623.
Grootjans, J.J., Zimmermann, P., Reekmans, G., Smets, A., Degeest, G., Dürr, J., David, G., 1997. Syntenin, a PDZ protein that binds syndecan cytoplasmic domains. Proc. Natl. Acad. Sci. U.S.A. 94 (25), 13683–13688.
Häcker, U., Nybakken, K., Perrimon, N., 2005. Heparan sulphate proteoglycans: the sweet side of development. Nat. Rev. Mol. Cell Biol. 6 (7), 530–541.
Herum, K.M., Lunde, I.G., Skrbic, B., Florholmen, G., Behmen, D., Sjaastad, I., Carlson, C. R., Gomez, M.F., Christensen, G., 2013. Syndecan-4 signaling via NFAT regulates extracellular matrix production and cardiac myofibroblast differentiation in response to mechanical stress. J. Mol. Cell Cardiol. 54, 73–81.
Herum, K.M., Lunde, I.G., Skrbic, B., Louch, W.E., Hasic, A., Boye, S., Unger, A., Brorson, S.H., Sjaastad, I., Tønnessen, T., et al., 2015. Syndecan-4 is a key determinant of collagen cross-linking and passive myocardial stiffness in the pressure-overloaded heart. Cardiovasc. Res. 106 (2), 217–226.
Herum, K.M., Romaine, A., Wang, A., Melleby, A.O., Strand, M.E., Pacheco, J., Braathen, B., Dunér, P., Tønnessen, T., Lunde, I.G., 2020. Syndecan-4 protects the heart from the profibrotic effects of thrombin-cleaved osteopontin. J. Am. Heart Assoc. 9 (3), e013518.
Hsueh, Y.P., Yang, F.C., Kharazia, V., Naisbitt, S., Cohen, A.R., Weinberg, R.J., Sheng, M., 1998. Direct interaction of CASK/LIN-2 and syndecan heparan sulfate proteoglycan and their overlapping distribution in neuronal synapses. J. Cell Biol. 142 (1), 139–151.
Jang, E., Albadawi, H., Watkins, M.T., Edelman, E.R., Baker, A.B., 2012. Syndecan-4 proteoliposomes enhance fibroblast growth factor-2 (FGF-2)-induced proliferation, migration, and neovascularization of ischemic muscle. Proc. Natl. Acad. Sci. U.S.A. 109 (5), 1679–1684.
Jannaway, M., Yang, X.Y., Meegan, J.E., Coleman, D.C., Yuari, S.Y., 2019. Thrombin-cleaved syndecan-3/-4 ectodomain fragments mediate endothelial barrier dysfunction. PLos One 14 (5).
Johns, S.C., Yin, X., Jeltsch, M., Bishop, J.R., Schuksz, M., El Ghazal, R., Wilcox-Adelman, S.A., Alitalo, K., Fuster, M.M., 2016. Functional importance of a proteoglycan coreceptor in pathologic lymphangiogenesis. Circ. Res. 119 (2), 210–221.
Kojima, T., Inazawa, J., Takamatsu, J., Rosenberg, R.D., Saito, H., 1993. Human ryudocan core protein: molecular cloning and characterization of the cDNA, and chromosomal localization of the gene. Biochem Biophys. Res. Commun. 190 (3), 814–822.
Kojima, T., Takagi, A., Maeda, M., Segawa, T., Shimizu, A., Yamamoto, K., Matsushita, T., Saito, H., 2001. Plasma levels of syndecan-4 (ryudocan) are elevated in patients with acute myocardial infarction. Thromb. Haemost. 85 (5), 793–799.
Koo, B.K., Jung, Y.S., Shin, J., Han, I., Mortier, E., Zimmermann, P., Whiteford, J.R., Couchman, J.R., Oh, E.S., Lee, W., 2006. Structural basis of syndecan-4 phosphorylation as a molecular switch to regulate signaling. J. Mol. Biol. 355 (4), 651–663.
Lee, D., Oh, E.S., Woods, A., Couchman, J.R., Lee, W., 1998. Solution structure of a syndecan-4 cytoplasmic domain and its interaction with phosphatidylinositol 4,5-bisphosphate. J. Biol. Chem. 273 (21), 13022–13029.
Mathiesen, S.B., Lunde, M., Aronsen, J.M., Romaine, A., Kaupang, A., Martinsen, M., de Souza, G.A., Nyman, T.A., Sjaastad, I., Christensen, G., et al., 2019. The cardiac syndecan-4 interactome reveals a role for syndecan-4 in nuclear translocation of muscle LIM protein (MLP). J. Biol. Chem. 294 (22), 8717–8731.
Matsui, Y., Ikesue, M., Danzaki, K., Morimoto, J., Sato, M., Tanaka, S., Kojima, T., Tsutsui, H., Uede, T., 2011. Syndecan-4 prevents cardiac rupture and dysfunction after myocardial infarction. Circ. Res. 108 (11), 1328–1339.
Morgan, M.R., Hamidi, H., Bass, M.D., Warwood, S., Ballestrem, C., Humphries, M.J., 2013. Syndecan-4 phosphorylation is a control point for integrin recycling. Dev. Cell 24 (5), 472–485.
Nadanaka, S., Kitagawa, H., 2008. Heparan sulphate biosynthesis and disease. J. Biochem. 144 (1), 7–14.
Oh, E.S., Woods, A., Lim, S.T., Theibert, A.W., Couchman, J.R., 1998. Syndecan-4 proteoglycan cytoplasmic domain and phosphatidylinositol 4,5-bisphosphate coordinately regulate protein kinase C activity. J. Biol. Chem. 273 (17), 10624–10629.
Okina, E., Grossi, A., Gopal, S., Multhaupt, H.A., Couchman, J.R., 2012. Alpha-actinin interactions with syndecan-4 are integral to fibroblast-matrix adhesion and regulate cytoskeletal architecture. Int. J. Biochem. Cell Biol. 44 (12), 2161–2174.
Okuyama, E., Suzuki, A., Murata, M., Ando, Y., Kato, I., Takagi, Y., Takagi, A., Murate, T., Saito, H., Kojima, T., 2013. Molecular mechanisms of syndecan-4 upregulation by TNF-α in the endothelium-like EAhy926 cells. J. Biochem. 154 (1), 41–50.
Partovian, C., Ju, R., Zhuang, Z.W., Martin, K.A., Simons, M., 2008. Syndecan-4 regulates subcellular localization of mTOR Complex2 and Akt activation in a PKCalpha-dependent manner in endothelial cells. Mol. Cell 32 (1), 140–149.
Schmidt, A., Echtermeyer, F., Alozie, A., Brands, K., Buddecke, E., 2005. Plasmin- and thrombin-accelerated shedding of syndecan-4 ectodomain generates cleavage sites at Lys(114)-Arg(115) and Lys(129)-Val(130) bonds. J. Biol. Chem. 280 (41), 34441–34446.
Shin, J., Lee, W., Lee, D., Koo, B.K., Han, I., Lim, Y., Woods, A., Couchman, J.R., Oh, E.S., 2001. Solution structure of the dimeric cytoplasmic domain of syndecan-4. Biochemistry 40 (29), 8471–8478.
Shworak, N.W., Shirakawa, M., Mulligan, R.C., Rosenberg, R.D., 1994. Characterization of ryudocan glycosaminoglycan acceptor sites. J. Biol. Chem. 269 (33), 21204–21214.
Strand, M.E., Herum, K.M., Rana, Z.A., Skrbic, B., Askevold, E.T., Dahl, C.P., Vistnes, M., Hasic, A., Kvaløy, H., Sjaastad, I., et al., 2013. Innate immune signaling induces expression and shedding of the heparan sulfate proteoglycan syndecan-4 in cardiac fibroblasts and myocytes, affecting inflammation in the pressure-overloaded heart. FEBS J. 280 (10), 2228–2247.
Strand, M.E., Aronsen, J.M., Braathen, B., Sjaastad, I., Kvaløy, H., Tønnessen, T., Christensen, G., Lunde, I.G., 2015. Shedding of syndecan-4 promotes immune cell recruitment and mitigates cardiac dysfunction after lipopolysaccharide challenge in mice. J. Mol. Cell Cardiol. 88, 133–144.
Uchinaka, A., Hamada, Y., Mori, S., Miyagawa, S., Saito, A., Sawa, Y., Matsuura, N., Yamamoto, H., Kawaguchi, N., 2015. SVVYGLR motif of the thrombin-cleaved N-terminal osteopontin fragment enhances the synthesis of collagen type III in myocardial fibrosis. Mol. Cell Biochem. 408 (1–2), 191–203.
VanWinkle, W.B., Snuggs, M.B., De Hostos, E.L., Buja, L.M., Woods, A., Couchman, J.R., 2002. Localization of the transmembrane proteoglycan syndecan-4 and its regulatory kinases in costameres of rat cardiomyocytes: a deconvolution microscopic study. Anat. Rec. 268 (1), 38–46.
Whiteford, J.R., Couchman, J.R., 2006. A conserved NXIP motif is required for cell adhesion properties of the syndecan-4 ectodomain. J. Biol. Chem. 281 (43), 32156–32163.
Whiteford, J.R., Behrends, V., Kirby, H., Kusche-Gullberg, M., Muramatsu, T., Couchman, J.R., 2007. Syndecans promote integrin-mediated adhesion of mesenchymal cells in two distinct pathways. Exp. Cell Res. 313 (18), 3902–3913.
Whiteford, J.R., Ko, S., Lee, W., Couchman, J.R., 2008. Structural and cell adhesion properties of zebrafish syndecan-4 are shared with higher vertebrates. J. Biol. Chem. 283 (43), 29322–29330.
Xie, J., Wang, J., Li, R., Dai, Q., Yong, Y., Zong, B., Xu, Y., Li, E., Ferro, A., Xu, B., 2012. Syndecan-4 over-expression preserves cardiac function in a rat model of myocardial infarction. J. Mol. Cell Cardiol. 53 (2), 250–258.
Xie, J., He, G., Chen, Q., Sun, J., Dai, Q., Lu, J., Li, G., Wu, H., Li, R., Chen, J., et al., 2016. Syndecan-4 signaling is required for exercise-induced cardiac hypertrophy. Mol. Med. 22, 192–201.